**The Dissertation Committee for Michael Brian Lowinger Certifies that this is the approved version of the following Dissertation:**

# Sustained Release Drug Delivery Applications of Poly(urethanes)

**Committee:**

Feng Zhang, Supervisor

Robert O. Williams III, Co-Supervisor

Hugh Smyth

Nathaniel Lynd

Stephanie Barrett

# Sustained Release Drug Delivery Applications of Poly(urethanes)

**by**

**Michael Brian Lowinger**

**Dissertation**

Presented to the Faculty of the Graduate School of

The University of Texas at Austin

in Partial Fulfillment

of the Requirements

for the Degree of

**Doctor of Philosophy**

**The University of Texas at Austin**

**December 2019**

# Dedication

To my partner, Alex, who has never stopped supporting me through this process.

To my family and friends, who encouraged me to pursue my doctoral dissertation long before I was ready to take the leap.

## Acknowledgements

The completion of my doctoral degree would not have been possible without the support of many people over the past several years. First I would like to recognize my partner Alex for supporting my decision to pursue this degree, for reminding me what's important during periods of high stress, and for keeping our house a home during my myriad trips to Austin. I owe a huge thank you to my parents, Jayne and Peter Lowinger, and my sister, Dr. Jennifer Baxter, who have instilled their hard working ethics in me and who have always encouraged me to go farther.

I will be forever grateful to Dr. Feng Zhang and Dr. Robert O. Williams III for taking chance on a guy they didn't really know who lives in New Jersey. Dr. Zhang, thank you for your constant scientific discussion and advice. Dr. Williams, thank you for helping me to clear my research obstacles and striving to ensure I communicate my research in the best possible way. I would also like to thank the rest of my committee members. Thank you to Dr. Hugh D.C. Smyth for your keen insight on the best way to compose my manuscripts. Thank you to Dr. Nathaniel Lynd for providing an orthogonal perspective to my polymer research. A big thank you to Dr. Stephanie Barrett, who mentored me at the same time she was leading amazing efforts at Merck.

I would like to thank my colleagues at Merck for their technical and emotional support. I am eternally grateful to Dr. Allen C. Templeton, who persistently encouraged me to pursue a doctoral degree over the years and who ultimately found a path for Merck to sponsor me in my pursuit of it. A big thank you to Dr. James C. DiNunzio, who originally connected me with Drs. Zhang and Williams, and without which my doctoral degree might have taken a completely different path. Thank you to my managers over

the past few years, Dr. Nancy Agrawal, Dr. Justin Pennington, Dr. Rubi Burlage, Dr. William Marinaro, and Dr. Craig A. McKelvey, who helped to sponsor and provide the space for me to tackle and complete my doctoral degree. A special thank you to Melanie Marota, Dr. Adam Procopio, Dr. Graciela Terife, Dr. Grace Okoh, Dr. Emily Gullotti, Dr. Gary Chia, Dr. Abbe Haser, Seth Forster, and Varsha Biyyala for providing support, feedback, and simply asking how I was doing whenever it was needed. Also to my MPDD department colleagues, who have all provided their support and encouragement.

Thank you to Dr. Eleni Dokou, who has been pushing me to pursue a doctoral degree since circa 2004. And thank you to Dr. Lynne Taylor, who provided indelible advice to me at a critical time in my life that ultimately drove me to pursue this degree.

I would like to acknowledge James Ormes, Dr. Yongchao Su, Dr. James Small, Dr. Xingyu Lu, and Dr. Esther Maier who all made substantial contributions to the research described in this dissertation and are co-authors of the various publications. I am grateful for the support and assistance of Charlie Martin, Augie Machado, and Brian Haight from the American Leistritz Extruder Corporation for providing the facilities and troubleshooting support to manufacture polymer films. I wish to thank Dr. Ryan Teller, Dr. Gregory Johnson, Dr. Gregory Troup, Sean Bowen, Dr. Matthew Lamm, Dr. Craig A. McKelvey, Candice Alleyne, Melanie Marota, Dr. Filippos Kesisoglou, Cassie Megna, Dr. Adam Procopio, and Jennie DeVore for their assistance and advice in executing the studies described in this dissertation.

# Abstract

## Sustained Release Drug Delivery Applications of Poly(urethanes)

Michael Brian Lowinger, Ph.D.

The University of Texas at Austin, 2019

Supervisor: Feng Zhang

Co-Supervisor: Robert O. Williams III

Patient adherence to drug therapies remains an obstacle to realizing their full therapeutic benefit. Sustained release formulations may decrease frequency of administration, potentially improving patient adherence.

Implants may decrease dosing frequency to once every 5 years. However, most polymers used today are hydrophobic, limiting drug properties suitable for development. Thermoplastic poly(urethanes) (TPUs) form pores upon hydration, offering a different release mechanism. We sought to assess the range of drug diffusion rates achieved by varying hydrophilic-to-hydrophobic TPU ratio compared with poly(ethylene-co-vinyl acetate) (EVA) crystallinity; investigate the effect of drug physicochemical properties on permeability through membranes of varying TPU composition; visualize microstructural changes to the membrane across the TPU composition range; and characterize the membrane microstructure.

Emtricitabine exhibited a >200-fold broader permeability range across the TPU blends than EVA grades. Varying hydrophilic content of the TPU mixture between 0-25% (w/w) led to a negligible permeability change, whereas a >100-fold permeability

change occurred between 50-55% (w/w). We observed a correlation between drug hydrophobicity and its permeability through hydrophobic-rich TPU. Conversely, drugs diffused through hydrophilic-rich TPU at similar rates, regardless of properties. Imaging revealed significant microstructure differences between hydrophobic-rich and hydrophilic-rich TPU, supporting that hydrophilic polymer domains form a continuous network above 55% (w/w) hydrophilic TPU. The large hydrophilic TPU equivalent pore radius suggests that it may modify the release of small molecular weight drugs and macromolecules.

Gastroretentive formulations may reduce dosing frequency of medications otherwise taken up to 5 times per day. Acyclovir is a short half-life drug with poor colonic absorption, and conventional controlled release formulations are unable to decrease dosing frequency. We developed a modified-release acyclovir matrix tablet and surrounded it with a hydrophilic poly(urethane) layer. When hydrated, the poly(urethane) swells to a size near to or beyond the relaxed pylorus diameter, without affecting drug release rate.

We demonstrated that the formulation is retained in the stomach for extended durations as it slowly releases drug, allowing for similar AUC but delayed $t_{max}$ relative to a control tablet. Unlike other gastroretentive formulations, this design decouples drug release rate from gastric retention time and effectively retains in the stomach regardless of prandial state.

# Table of Contents

## List of Tables

## List of Figures

# Chapter 1: Drug Delivery Applications of Poly(urethanes)[1]

## 1.1 ABSTRACT

Since their introduction over 50 years ago, poly(urethanes) have been applied to nearly every industry. This review describes applications of poly(urethanes) to the development of modified release drug delivery. Although drug delivery research leveraging poly(urethanes) has been ongoing for decades, there has been renewed and substantial interest in the field in recent years. The chemistry of poly(urethanes) and the mechanisms of drug release from sustained release dosage forms are briefly reviewed. Studies to assess the impact of intrinsic drug properties on release from poly(urethane)-based formulations are considered. The impact of hydrophilic water swelling poly(urethanes) on drug diffusivity and release rate is discussed. The role of pore formers in modulating drug release rate is examined. Finally, the value of assessing mechanical properties of the dosage form and approaches taken in the literature are described.

## 1.2 INTRODUCTION

Poly(urethanes) are among the most ubiquitous of materials found in society, owing to their versatile properties. They can be found in automobiles, chairs, beds, refrigerators, and many other household items [1]. Early research into the chemistry of poly(urethanes) can be found as early as 1947 [2]. By varying different substituents and their ratios, different poly(urethanes) with a wide range of physicochemical properties can be synthesized at large scales.

---

[1] Published in: M.B. Lowinger, S.E. Barrett, F. Zhang, R.O. Williams, Sustained release drug delivery applications of polyurethanes, Pharmaceutics. 10 (2018). doi:10.3390/pharmaceutics10020055. Michael Lowinger performed the literature review and wrote the manuscript.

This review presents an overview of recent applications of poly(urethanes) to sustained release drug delivery. Previous review publications generally focused on the chemistry, synthesis, and properties of poly(urethanes). Cherng et al. authored an extensive review of poly(urethane)-based drug delivery systems, however it was published over five years ago [3]. Since that time, there has been significant advancement in the research area of poly(urethanes), particularly as applied to parenteral sustained release dosage forms.

Poly(urethanes) have been applied to drug products in nearly every conceivable configuration. Seo and Na explored modifications to poly(urethane) membrane porosity from a non-erodible drug eluting stent [4]. Guo et al. developed biodegradable poly(urethane) stent coatings enabling adjustable drug release [5]. Chen et al. explored the use of poly(urethane) pressure-sensitive adhesives for transdermal drug delivery [6]. Several studies have explored the controlled release of antibiotics from poly(urethane) matrices through tissue scaffolds [7], bone grafts [8], microspheres [9], and nanoparticles [10]. Temperature- and pH-responsive poly(urethane) nanoparticles have been developed to deliver doxorubicin to the tumor microenvironment [11]. Drug loaded poly(urethane) implants have been studied for the treatment of bacterial infection [12] and inflammation [13]. The polymers have been extensively applied in the development of intravaginal rings [14–25]. Poly(urethanes) have also been applied to modulate the release characteristics of orally administered tablets [26].

Experimental work exploring monolithic mixtures of a polymer (ethylene vinyl acetate) with model drug compounds has been documented as early as 1964 [27] and the use of poly(urethanes) in medical devices has been well documented since 1968 [28–34].

Both biodegradable and biostable sub-dermal implant poly(urethane) formulations have been of more recent interest [3].

## 1.3 CHEMISTRY OF POLY(URETHANES)

Poly(urethanes) are a group of condensation polymers that include the urethane (–NHCOO–) group in the chemical structure (Figure 1.1). They are typically synthesized by a step-growth polymerization reaction between isocyanates and polyols in the presence of a suitable catalyst. Poly(urethanes) synthesized solely from isocyanates and polyols generally have poor mechanical properties. Therefore, chain extenders are added to the structure in order to induce microphase separation between the two thermodynamically incompatible segments. The two segments are commonly described as hard segments (composed of the isocyanate and chain extender components) and soft segments (composed of the polyol component). The hard segments impart mechanical strength, whereas the soft domains provide flexibility (Figure 1.1).

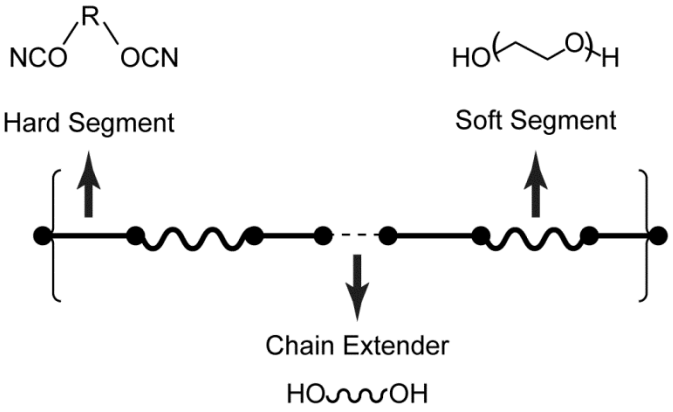


Figure 1.1: General chemical structure of poly(urethanes).

### 1.3.2 Isocyanates

Diisocyanates are commonly employed in the synthesis of poly(urethanes), which can be divided into aliphatic and aromatic diisocyanates. In general, aromatic diisocyanates are more reactive than aliphatic species. For example, poly(urethanes) made from aliphatic diisocyanates demonstrated more resistance to ultraviolet radiation, whereas those made from aromatic diisocyanates have been shown to undergo photodegradation [35,36]. Poly(urethanes) based on aromatic diisocyanates have also been shown to exhibit less biocompatibility than those synthesized from aliphatic diisocyanates, caused by toxic degradation products. Poly(urethanes) prepared with toluene diisocyanate have been shown to degrade under physiological conditions to yield 2,4-toluene diamine, which has known toxicity [37]. Kääriä et al. conducted an *in vivo* study using a poly(urethane) prepared from the aromatic 4,4'-methylenediphenyl diisocyanate and observed cytotoxicity attributed to the aromatic amine 4,4'-methylenedianiline produced as a degradation product of the polymer [38].

### 1.3.3 Chain Extenders

Chain extenders are typically low molecular weight (<400 Da) bisamines or diols, such as 1,4-butandiol, 1,3-propanediol, and ethylene diamine. The physical and mechanical properties of poly(urethanes), including hardness and crystallinity, are dependent on the extent of phase separation between the hard and soft segments. The extent of phase separation is, in part, a function of the type and number of chain extenders used for polymerization. Jabbari and Khakpour investigated the impact of changes to the mole fraction of poly(urethane) chain extruder to the porosity of prepared microspheres [39]. They observed that the pores in poly(urethane) microspheres decreased as the content of chain extruder increased from 0 to 50 mol%. When they

increased the chain extruder content to 67 mol%, the polymer stiffness increased and formation of pores was inhibited.

### 1.3.4 Polyols

Polyols are generally di-hydroxyl terminated macroglycols of poly(esters), poly(ethers), and poly(carbonates) in the molecular weight range of 1000 to 5000 Da. The molecular weight and type of polyol plays a significant role in the physicochemical and mechanical properties of the poly(urethane). Poly(ester)-based poly(urethanes) often have good mechanical strength and thermal stability, however they are susceptible to hydrolysis [40]. Biodegradable poly(ester urethanes) have been prepared from lysine diisocyanate with D,L-lactide, ε-caprolactone, and other monomers [41]. Kaur et al. developed a biodegradable intravaginal ring composed of a poly(ester urethane) prepared from bis(4-isocynaatocyclohexyl)methane with poly(tetramethylene ether)glycol and ε-caprolactone which released the antiretroviral dapivirine at target levels for one month [42]. Yu et al. developed biodegradable poly(urethanes) based on L-phenylalanine that possess tunable mechanical properties and degradation rates over a wider range than was achievable with poly(lactic acid) [43].

Poly(ether)-based poly(urethanes) tend to be more hydrolytically stable and exhibit more elasticity at lower temperatures. However, they can be more susceptible to oxidative and thermal lability [44,45]. It was found that poly(ether urethane) used as pacemaker lead insulation suffered from stress cracking due to oxidation after being placed in humans for long periods of time [46]. However, antioxidants have been used to stabilize poly(ether urethanes) to prevent oxidation and prolong the life of the polymer [47]. A polyether-based polyol particularly relevant to pharmaceutical applications is

polyethylene oxide (PEO). PEO-based poly(urethanes) exhibit sensitivity to water due to the hydrophilicity and water-absorbing capacity of the ethylene oxide units [3]. Ikeda et al. demonstrated that the larger the PEO content, the higher the degree of swelling which increased the drug release rate of slowly releasing model compounds [48].

Poly(carbonate)-based poly(urethanes) were developed in response to the disadvantages of poly(ester) and poly(ether) based poly(urethanes). They exhibit good mechanical properties, heat stability, and hydrolytic stability, but they have been shown to undergo enzymatic hydrolysis and oxidative degradation by inflammatory cells in long-term *in vivo* studies [49].

### 1.3.5 Synthesis

Poly(urethanes) are generally synthesized by reacting the isocyanate, polyol, and chain extender together at temperatures above 80°C [50]. The central reaction is the formation of a urethane linkage that occurs when an isocyanate reacts with an alcohol group of the polyol. The exothermic polymerization reaction is generally carried out in one of two ways. The "one-shot method" involves mixing all of the ingredients together, while the "prepolymer method" features the reaction of the polyol with an excess of isocyanate, followed by a subsequent reaction with the chain extender to form a linear block copolymer with alternating blocks of hard segment and soft segment [29]. The prepolymer method has been shown to yield more ordered structure with better control of polymer properties [51].

Two manufacturing methods are typically employed for industrial production: the belt process and the reaction extruder process. During the belt process, all components are mixed using a high efficiency mixing head and the reacting liquid mixture is poured

onto a belt, where it solidifies. The solid material is then granulated and may be blended with other components and extruded into pellets. Utilization of a reaction extruder allows for the mixing of prepolymers or all components inside of the extruder, where screw design and temperature can be modified to suit the desired product properties. The urethane reaction is nearly complete by the time the material exits the extruder and uniform pellets may be formed by the use of underwater or strand pelletizers [50].

Since phase separation of poly(urethanes) is dependent on the temperature and shear conditions during polymerization, the process may have a significant influence on the product properties. Consequently, although two poly(urethane) batches may start from the same raw materials, their physical properties can be very different [50].

## 1.4 DRUG RELEASE MECHANISMS

Solute diffusion, polymer swelling, and polymer erosion or degradation are generally considered to be the main driving forces for drug transport from a polymeric matrix [52]. However, other phenomena may be involved in the control of drug release and are discussed in more detail in other publications [53].

### 1.4.1 Solute Diffusion

Fick's law of diffusion is the fundamental basis for the mechanism describing drug transport from a polymer matrix. Fickian diffusion refers to a solute transport process in which the polymer relaxation time is much greater than the solvent diffusion time. When polymer swelling occurs, changes to diffusivity with time result in non-Fickian drug release. Drug release from poly(urethane) formulations can be categorized into two groups: (i) monolithic systems, where drug is dissolved or dispersed in a poly(urethane) matrix, and (ii) reservoir systems, where a drug depot is surrounded by a

rate controlling membrane [53]. Table 1.1 describes the categories of solute diffusion from poly(urethane)-based sustained release dosage forms.

In each of those categories, drug release kinetics will be dependent on whether the drug concentration is above or below its solubility in the system. In the case of a reservoir system where the initial drug concentration is below its solubility, those drug molecules that diffuse out of the system will not be replaced by undissolved drug and the drug activity at the rate controlling membrane's surface decreases with time, resulting in first order release kinetics. Models have also been developed which describe first order release kinetics from a cylindrical intravaginal ring [54,55]. However, a reservoir system where the drug concentration exceeds its solubility will feature a saturated solution at the membrane surface, resulting in zero order release kinetics. Over time, drug release kinetics from such a system will approach those of a dosage form with drug concentration below its solubility in the polymer [56].

In the case of monolithic systems, the device geometry and drug loading will significantly affect the drug release kinetics. For a monolithic system where the initial drug concentration is below its solubility in the system, models have been derived to describe the drug release of thin films, spheres, and cylinders, many of which assume an exponential function of release rate with time [57,58]. In the case of a monolithic dispersion where the drug is above its solubility in the system, Higuchi described a square root of time relationship between the amount of drug released from a thin film with a large excess of drug [59].

Table 1.1: Categories of Solute Diffusion from Poly(urethane)-based Sustained Release Dosage Forms.

| Dosage Form Type | Drug Concentration in Polymer | Release Kinetics | Examples |
|---|---|---|---|
| Monolithic | $C_{drug} \leq C_{solubility}$ | Geometry and drug load dependent | [57,58] |
| | $C_{drug} > C_{solubility}$ | Geometry and drug load dependent | [59] |
| Reservoir | $C_{drug} \leq C_{solubility}$ | First order | [54,55] |
| | $C_{drug} > C_{solubility}$ | Zero order | [56] |

### 1.4.2 Polymer Swelling

Depending on the polyol used, poly(urethanes) may exhibit substantial polymer swelling which can impact drug release kinetics in several ways. When a polymer swells, the length of the diffusion pathways increases. This can result in decreasing drug concentration gradients, which may decrease drug release rates. Guo et al. observed that the swelling of a synthesized poly(urethane) matrix slowed down the drug release rate, which was attributed to increased diffusion length [5].

Polymer swelling also increases the mobility of the polymer chains, which increases drug mobility and, potentially, increases drug release rates. Once a water content specific to each polymer is reached, the polymer mobility steeply increases in a phenomenon called “polymer chain relaxation” or “glassy-to-rubbery phase transition” [53]. However, poly(urethanes) commonly employed for pharmaceutical applications exhibit glass transition temperatures below room temperature, so the transition of poly(urethanes) from the glassy to the rubbery state is generally not of practical

significance to drug release [60]. Clark et al. applied similar pseudo-steady state approach as Higuchi's diffusion model to effectively predict the release of tenofovir from an intravaginal ring composed of hydrophilic poly(urethane) [54]. They argued that polymer swelling had minimal impact on the long-term drug release kinetics since the polymers reach equilibrium swelling at early time points and it was thus unnecessary to account for it in the model.

Beyond polymer chain mobility itself, water swelling increases free volume for diffusion, thereby increasing diffusivity of drugs [61]. Dapivirine, when released from an intravaginal ring composed of a water-swelling poly(urethane) grade, exhibited faster release than from a ring composed of non-swelling poly(urethane) (Figure 1.2) [14]. Given the wide variety of PEO-based poly(urethanes) available commercially, polymer swelling has the potential to dramatically impact drug release kinetics from dosage forms.

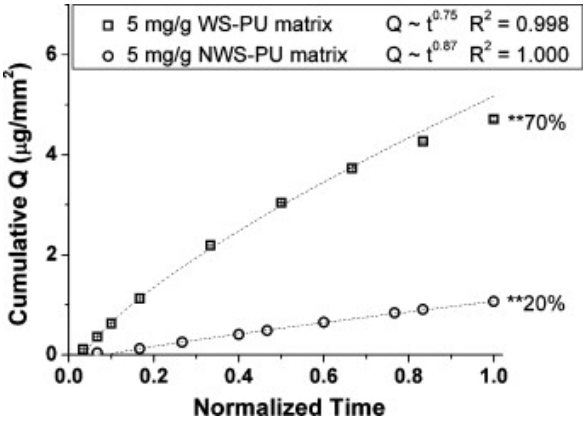


Figure 1.2: Cumulative flux (Q) of dapivirine as a function of time from a water swelling (WS-PU) and non-water swelling (NWS-PU) poly(urethane) matrix. ** denotes wt% cumulative release of dapivirine over 30 days. Adapted from reference [14], Elsevier, 2010 with permission.

### 1.4.3 Polymer Erosion and Degradation

The erosion and degradation of polymers to facilitate drug release are often confounded; however, they will be separated for the purpose of this review. Goepferich and Langer differentiated the two processes by defining degradation as involving cleavage of polymer chains into oligomers and monomers, while erosion can be defined as a general loss of weight from the polymer [62]. Consequently, although degradation of water-insoluble polymers is a step in its erosion process, the degradation of the polymer itself is not erosion.

Langer and Peppas defined two extremes of erosion: heterogeneous and homogeneous [63]. Heterogeneous erosion describes a physical situation where water penetration into the polymer is slow relative to polymer degradation rate. Under this scenario, polymer degradation is restricted to the outermost layers and erosion predominantly occurs at the surface of the dosage form. In the case of homogeneous erosion, water penetration occurs rapidly, degradation occurs throughout the device, and bulk erosion follows. Although all bioerodible polymers are likely to undergo some combination of the two extremes, surface erosion may be most often observed with hydrophobic poly(urethanes) and those with highly reactive bonds in their backbone structure, whereas hydrophilic poly(urethanes) and those with less reactive ester linkages are more likely to undergo bulk erosion [53]. Additionally, the water penetration rate may vary depending on the geometry of the delivery system [64].

Hafeman et al. synthesized hydrophilic poly(ester)-based poly(urethanes) from ε-caprolactone and observed rapid swelling followed by bulk erosion with approximately 50-80% mass remaining after 36 weeks [65] (Figure 1.3). In a subsequent study investigating the use of one of these polymers to deliver the antibiotic tobramycin, the

authors found that the hydrophilic drug released from the poly(urethane) scaffold over the course of approximately 30 days. Given the difference in time scales between the drug release and polymer degradation rates, the investigators concluded that tobramycin release was independent of polymer degradation [66]. The study demonstrates the ability to develop biodegradable sustained release dosage forms in which drug release kinetics are not dependent on polymer degradation kinetics.

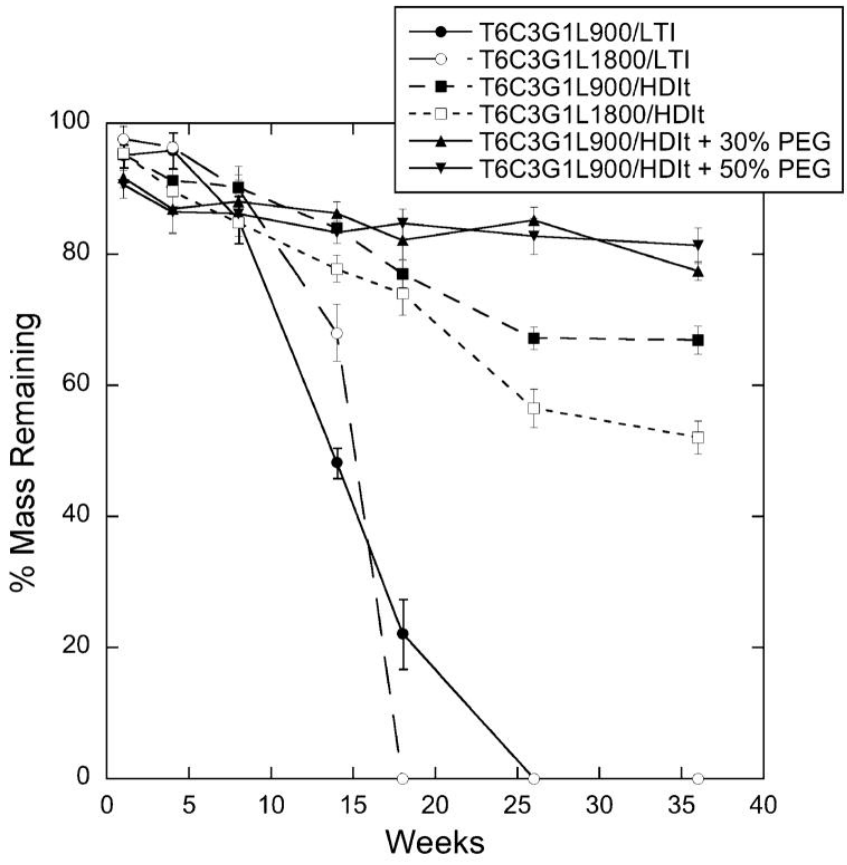


Figure 1.3: *In vitro* degradation of poly(urethane) scaffolds. By 36 weeks, polymers from prepared from lysine triisocyanate (LTI) had completely degraded, while the poly(urethanes) prepared from hexamethylene diisocyanate trimer remained at 52-81% of their original masses. Adapted from reference [65], Springer Nature, 2008 with permission.

## 1.5 Approaches to Modulate Drug Release Kinetics

Hombreiro-Pérez et al. described the key mass transport phenomena governing drug release through a polymer, including drug dissolution in the polymer; drug diffusion through the polymer matrix and/or through water-filled pores; drug diffusion through the unstirred liquid boundary layer on the surface of the dosage form; and diffusional and convective transport within the release medium [67]. Through deliberate polymer and formulation selection, the release kinetics of a particular drug may be modulated to achieve a target dose. Table 1.2 summarizes the approaches that may be taken to modulate drug release kinetics from a poly(urethane)-based reservoir sustained release dosage form.

Table 1.2: Approaches to Modulate Drug Release Kinetics from a Poly(urethane)-based Reservoir Sustained Release Dosage Form.

| Driver | Approach | Examples |
|---|---|---|
| Drug Solubility in Polymer | Polymer selection to increase or reduce drug solubility | [14,19,54,56] |
| Drug Diffusivity Through Polymer | Polymer selection to increase or reduce polymer crystallinity | [68–70] |
| | Polymer selection to increase or reduce polymer molecular weight | [71,72] |
| | Polymer selection to increase or reduce soft segment to hard segment ratio | [73,74] |
| Drug Diffusion Through Water-filled Channels | Polymer selection to increase or reduce soft segment to hard segment ratio | [73,74] |
| | Incorporation of additional component as pore former | [75–77] |

### 1.5.2 Intrinsic Drivers of Drug Release Through a Polymer

#### *1.5.2.1 Drug Solubility in Polymer*

In matrix systems where the drug is above its percolation threshold, it is conceivable for drug release to occur by diffusion through drug-rich channels [27,78]. However, for matrix systems where drug load is below its percolation threshold and for all reservoir systems, drug must first dissolve in the polymer in order to diffuse through it. For those formulations, drug solubility in the polymer is an important phenomenon. Johnson et al. found that release of hydrophilic tenofovir with a calculated logP of -2.3 was barely detectable from the hydrophobic poly(urethane) Tecoflex EG-85A, attributed to poor solubility in the polymer [14]. However, dapivirine with a calculated logP of 6.3 exhibited near zero order release from a similarly hydrophobic poly(urethane) Tecoflex EG-80A [19]. Van Laarhoven et al. measured the solubility of etonogestrel and ethinyl estradiol in ethylene vinyl acetate copolymers and found that the two hydrophobic drugs were sufficiently soluble in the hydrophobic polymer that they were present in the finished product in a molecularly dissolved state [56]. Clark et al. determined the solubility of tenofovir in a hydrophilic poly(urethane) and observed that its solubility was 100 to 1000 times lower than the drug loading explored in their studies [54].

#### *1.5.2.2 Drug Diffusivity Through Polymer*

The phase state of the polymer has been shown to impact diffusivity of drug through it. Almeida et al. studied the impact of vinyl acetate content on the release rate of metoprolol tartrate from melt extruded ethylene vinyl acetate matrices in the presence of varying levels of poly(ethylene) oxide. Lower vinyl acetate content results in greater crystallinity of the polymer. They found that matrices extruded with lower vinyl acetate

content polymers exhibited slower drug release rates than those extruded with higher vinyl acetate content polymers. By fitting the experimental data to an analytical model of Fick's second law of diffusion, they were able to show that release rate differences between polymers could be explained by changes to the apparent diffusion coefficient (Figure 1.4) [68]. Tallury et al. explored the impact of ethylene vinyl acetate copolymer composition on the release of chlorhexidine and acyclovir from polymer matrices. They observed a strong relationship between vinyl acetate content and drug release for both systems, where higher vinyl acetate content exhibited faster drug release [69]. Although the effect of polymer crystallinity on drug release from nonerodible poly(urethane)-based dosage forms has not been extensively studied, several investigators correlated the crystallinity of the soft segment to degradation rate of poly(ester urethanes). Reddy et al. proposed that higher crystallinity of the poly(caprolactone) soft segment resulted in reduced polymer degradation rates, which slowed the release of the model drug theophylline [70].

The molecular weight of the polymer may also impact the diffusion of drug through the dosage form. Hsu and Langer investigated the impact of changes to ethylene vinyl acetate molecular weight on the release rate of bovine serum albumin (BSA). They observed a substantial decrease in BSA release rate with relatively small increases in ethylene vinyl acetate molecular weight [71]. Skarja and Woodhouse investigated the effect of molecular weight on the properties of poly(urethanes) composed of either poly(caprolactone) or poly(ethylene oxide) as the soft segment. They found that phase separation between the hard and soft segments and crystallinity of the soft segment increases with soft segment molecular weight. For poly(urethanes) based on hydrophobic poly(caprolactone), one might expect reduced drug release rates from a higher molecular

weight polymer, however those based on hydrophilic poly(ethylene oxide) might be expected to release drug at faster rates [72].

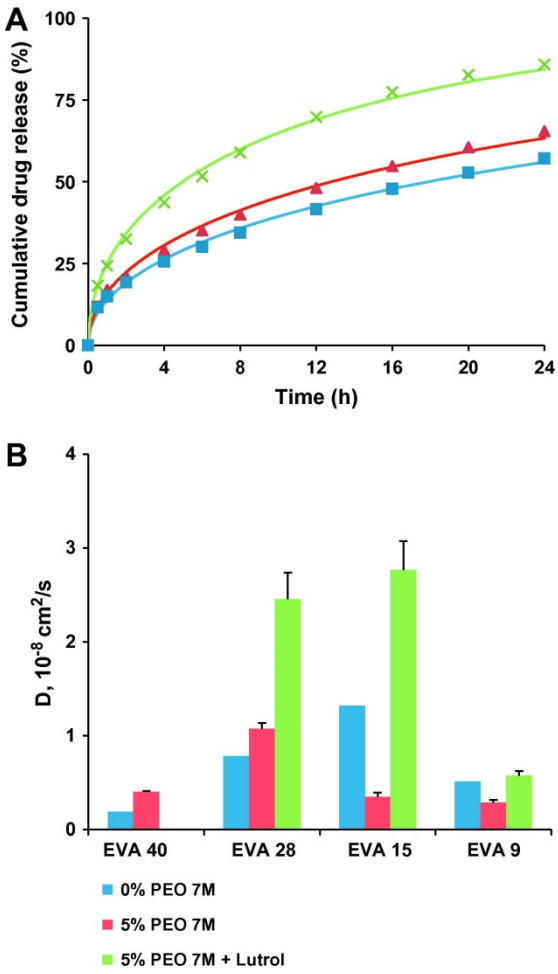


Figure 1.4: (A) Theory (curves) and experiments (symbols): metoprolol tartrate release from EVA 28-based matrices containing 0% PEO 7M (■), 5% PEO 7 M (▲), or 5% PEG 7M/Lutrol (9/1, w/w) (×). (B) Apparent diffusion coefficients of metoprolol tartrate in EVA-based matrices, containing 0% PEO 7M, 5% PEO 7M, or 5% PEO 7M/Lutrol (9/1, w/w). Adapted from reference [68], Elsevier, 2012 with permission.

For poly(urethanes), the ratio between soft segment and hard segment has also been shown to affect drug release kinetics. Shoaib et al. explored the effect of soft

segment to hard segment ratio on the release of ciprofloxacin. The poly(urethane)-urea elastomers were synthesized from the aromatic toluene diisocyanate and the hydrophilic poly(ethylene glycol). As soft segment to hard segment ratio was decreased, the investigators observed a decrease in ciprofloxacin release rate from drug/polymer films. The authors attributed the slower drug release to increased cross-linking of the hard segments in polymers featuring a higher concentration of hard segment. They speculated that increased cross-linking would reduce water penetration into the matrix and drug diffusion out of the matrix [73].

Verstraete et al. investigated the impact of soft segment to hard segment ratio on the release rates of diprophylline, theophylline, and acetaminophen for hydrophilic thermoplastic poly(urethanes) for which the soft segment is composed of poly(ethylene oxide). As the soft segment to hard segment ratio increased, the fraction of poly(ethylene oxide) in the polymer structure increased. The authors observed an increase in swelling for the polymers Tecophilic SP60D60, SP93A100, and TG2000 ranging from 60% to 900% weight gain. When investigating the drug release kinetics of the three drug compounds from matrices of each polymer, they found that all drugs followed the same trend with the TG2000-based matrix releasing fastest and the SP60D60-based matrix releasing slowest (Figure 1.5) [74]. Increased water uptake and faster drug release may be due to the formation of a water-filled pore structure or due to higher free volume that increases diffusivity.

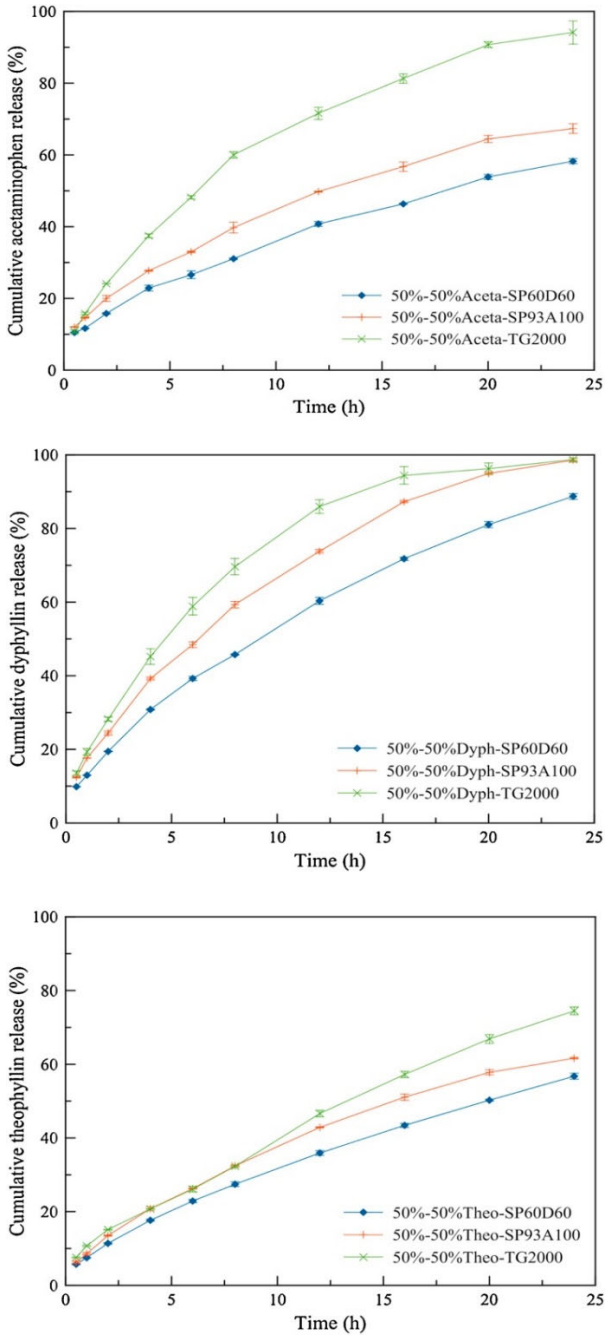


Figure 1.5: Influence of length of the poly(urethane) soft segment (polyethylene oxide) on the *in vitro* release kinetics of drugs with different aqueous solubility (acetaminophen, diprophylline, and theophylline) from poly(urethane)-based matrices (SP60D60, SP93A100, and TG2000). Adapted from reference [74], Elsevier, 2016 with permission.

### 1.5.3 The Use of Pore Formers

The incorporation of soluble components to an otherwise poorly soluble barrier has been utilized as an approach to modulate the release of drugs through film coated tablets for decades [79–83]. A similar approach has been applied to the development of drug/poly(urethane) dosage forms in order to optimize the drug release rate. Kim et al. evaluated the effect of poly(ethylene glycol), D-mannitol, and bovine serum albumin on the release of the antibiotic cefadroxil from a poly(urethane) matrix [75]. They observed that matrices utilizing bovine serum albumin as the pore former exhibited the fastest drug release. The authors proposed that immiscibility of the pore former with the poly(urethane) could facilitate channel formation and thus increase drug release rate.

Donelli et al. investigated the utility of incorporating poly(ethylene glycol) and bovine serum albumin into a poly(urethane) matrix to modify the release rate of the antifungal drug fluconazole [76]. They found that matrices incorporating poly(ethylene glycol) exhibited increased drug release relative to a control without pore former, whereas matrices incorporating bovine serum albumin exhibited sustained drug release relative to the control. Sreenivasan observed an increased release rate of the anti-inflammatory drug hydrocortisone when adding methyl β-cyclodextrin to poly(urethane) [77]. Claeys et al. explored the impact of poly(ethylene glycol), polysorbate 80, and the dicarboxylic acids malonic, succinic, maleic, and glutaric acid on the release of diprophylline from a poly(urethane) matrix (Figure 1.6) [26,60].

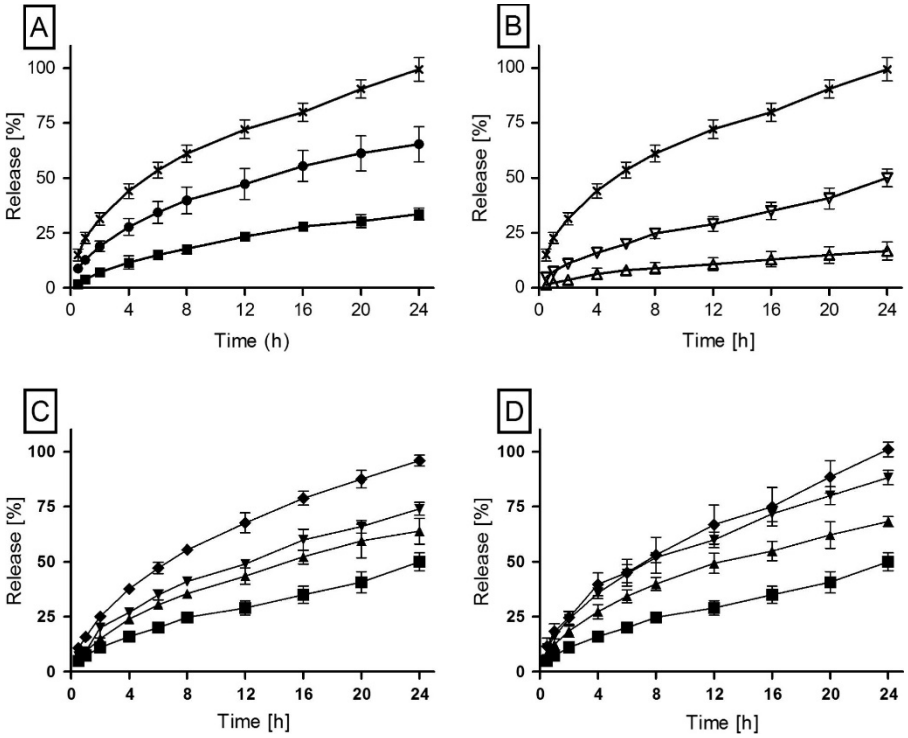


Figure 1.6: Mean dissolution profiles (± SD) of polyester-based poly(urethane) (Pearlbond) matrices as a function of (A) drug load: 50% (■), 60% (●), and 65% (×) metoprolol tartrate; (B) drug solubility: 65 wt% theophylline (△), diprophylline (▽), and metoprolol tartrate (×); pore former (C) PEG 4000 or (D) Polysorbate 80; 65 wt% diprophylline with 0% (■), 2% (▲), 5% (▼), and 10% (◆) of pore former, respectively. Adapted from reference [60], Elsevier, 2015 with permission.

## 1.6 MECHANICAL PROPERTIES OF POLY(URETHANE)-BASED DOSAGE FORMS

Since many poly(urethane)-based sustained release dosage forms are intended to remain *in vivo* for extended periods of time, their mechanical properties are critical to ensure consistent drug release kinetics and good patient adherence. The dosage forms must exhibit enough elasticity to deform seamlessly without causing discomfort to patients during routine daily activities and without causing tissue damage or inflammation [84]. On the other hand, the dosage forms must have sufficient strength to

prevent fracture, which would alter geometry and potentially affect drug release rate. For example, intravaginal rings that are too soft may not be effectively retained and could be expelled from the vagina [85].

### 1.6.1 Patient Perceptions

Given that many of the mechanical properties are driven by patient perceptions, it can be difficult to determine an appropriate target for a dosage form under development. The target mechanical properties of each dosage form may be dependent on the route of administration and duration of the product. However, patients are likely to have more interaction with intravaginal rings than most other parenteral formulations and therefore investigators have evaluated the mechanical performance of intravaginal rings more extensively than most other presentations.

Morrow Guthrie et al. conducted a clinical study to understand the relationship between user perceptions and mechanical properties of intravaginal rings composed of poly(urethane) [86]. Users perceived a ring with a matte and textured surface to be easier to manipulate during insertion, whereas they perceived a ring with a glossy and smooth surface to be more slick and challenging to insert. The study participants also expected rings composed of softer materials to be more comfortable to use. Although the participants preferred a small diameter ring, it conflicted with their general desire for a more pliable dosage form. For a given material at a defined cylinder diameter, a smaller diameter ring will be more difficult to squeeze. Faced with these tradeoffs, users were more comfortable with using softer materials and smaller diameter cylinders, even if the ring diameter were larger.

### 1.6.2 Mechanical Testing of Finished Product

Since most investigators lack the clinical data necessary to quantify patient preferences, studies describing the assessment of an investigational dosage form's mechanical properties typically reference their findings back to a marketed product. Baum et al. proposed several techniques to evaluate the mechanical properties of an experimental silicone-based intravaginal ring, comparing it to the commercially available Estring® [87]. The tensile strength, elongation, and compression strength were determined using methods adapted from ASTM D2240 and ISO 8009 standards [88,89].

Verstraete et al. built on Baum's efforts by applying those techniques to poly(urethane)-based intravaginal dosage forms and comparing back to the marketed product Nuvaring® [15]. Shore durometer hardness was measured using an indentation test on the surface of the ring. Elongation and force at maximum extension were measured using an extension testing system. To evaluate elongation, a sample was fixed between two hooks and its axial length was measured after applying a defined force. In order to assess maximum elongation, the sample was stretched at a defined rate until breakage. The researchers sought to evaluate resistance to compression by subjecting a sample to repeated compression cycles at a defined speed and amplitude and assessing changes to the diameter along the axis of compression and orthogonal to it. Table 1.3 provides a summary of the measured intravaginal ring mechanical properties in comparison to the marketed product. By performing a variety of compression, elongation, and indentation tests, the investigators were able to assess the mechanical properties of the dosage form under a variety of circumstances.

Table 1.3: Overview of intravaginal ring properties (mean ± SD, n = 3). Devices that featured similar mechanical properties to reference were highlighted in grey. Adapted from reference [15].

| Formulation | Hardness[a] (shore A) | Maximum load[a] (N) | Maximum elongation[b] (%) | $\frac{OD_1'}{OD_1}$ (%) | $\frac{OD_2'}{OD_2}$ (%) |
|---|---|---|---|---|---|
| **Reference** | | | | | |
| Nuvaring™ | 75 ± 4 | 102.4 ± 12.7 | 650.1 ± 11.8 | 92.1 | 107.5 |
| | | | | | |
| **Treatment** | | | | | |
| 25/75 metronidazole/SP-93-100 | 72 ± 3 | 82.8 ± 13.7 | 587.9 ± 117.4 | 94.6 | 104.6 |
| 50/50 metronidazole/SP-93-100 | 91 ± 2 | 68.1 ± 10.2 | 51.7 ± 21.4 | 88.3 | 110.2 |
| | | | | | |
| **Prophylaxis** | | | | | |
| 20/80 Lactic Acid/EG-80A | 51 ± 1 | 49.7 ± 12.4 | 517.0 ± 4.9 | 98.0 | 101.7 |
| 20/80 Lactic Acid/EG-85A | 62 ± 2 | 68.6 ± 22.7 | 389.4 ± 34.3 | 98.2 | 101.3 |
| 20/80 Lactic Acid/EG-93A | 71 ± 2 | 87.7 ± 8.15 | 336.7 ± 24.9 | 96.0 | 103.8 |
| 20/80 Lactic Acid/EG-100A | 80 ± 2 | 98.6 ± 11.6 | 244.6 ± 37.4 | 94.3 | 105.1 |
| 20/80 Lactic Acid/EG-60D | 80 ± 4 | 105.4 ± 13.8 | 173.8 ± 22.2 | 93.7 | 107.2 |
| 20/80 Lactic Acid/EG-72D | 86.3 ± 3 | 129.3 ± 14.1 | 125.7 ± 13.9 | 89.5 | 110.0 |

[a] Hardness and maximum load should be similar to the Nuvaring™ reference values.
[b] Mean elongation at break should not be less than 300%.
[c] After compression experiments, the diameter along the axis of compression ($OD_1'$) and the diameter orthogonal to the axis of compression ($OD_2'$) should be at least 90% of their initial values.

Clark et al. performed a destructive extension test on their segmented intravaginal ring samples both before and after 31 day *in vitro* release testing. Samples were stretched at a defined rate until failure was observed at which point the net extension and net load

were recorded [90]. The investigators did not compare measured properties back to a marketed product. Without a benchmark, it can be difficult to interpret the outcome as to whether the failure conditions were beyond what is reasonably expected during normal handling.

Young's modulus measures a material's resistance to being deformed elastically when a stress is applied to it. A stiffer material will have a higher Young's modulus. Ugaonkar et al. leveraged the Young's modulus as a measure of flexibility by subjecting a 25 mm long cylindrical segment to a defined elongation at a specified rate and again compared the measured value for their experimental dosage form to that of the marketed product Nuvaring® [55]. Clark et al. developed a model to predict the force necessary to compress an intravaginal ring material a given distance based on the Young's modulus [54]. Although Young's modulus is an effective measure of stiffness, it does not provide information on elongation and compression properties.

Crnich et al. were interested in understanding the effect of ethanol exposure on the mechanical properties of poly(urethane) stents. They performed tensile strength testing, including force-at-break, failure stress, elongation at failure, maximum strain, and modulus of elasticity in accordance with ISO standard 10555-1 [91]. The investigators concluded that exposure to ethanol had a minimal effect on the mechanical properties of poly(urethane) catheters.

Johnson et al. performed a tensile strength test on their intravaginal ring samples in a similar fashion to others [14]. Rings were stretched to a defined force at a specific rate and any evidence of failure or changes to diameter were assessed. The investigators also performed compression/retraction force tests in which the rings were compressed at a defined rate to 50% of their initial diameter and force was recorded throughout the

experiment (Figure 1.7). They benchmarked to a marketed product and observed that their hydrophilic poly(urethane)-based intravaginal ring exhibited similar mechanical properties to the Nuvaring® reference ("EVA-R") when kept dry. However, the hydrated poly(urethane)-based ring exhibited faster recoil than the reference, which the authors pointed out could improve retention in the vaginal tract.

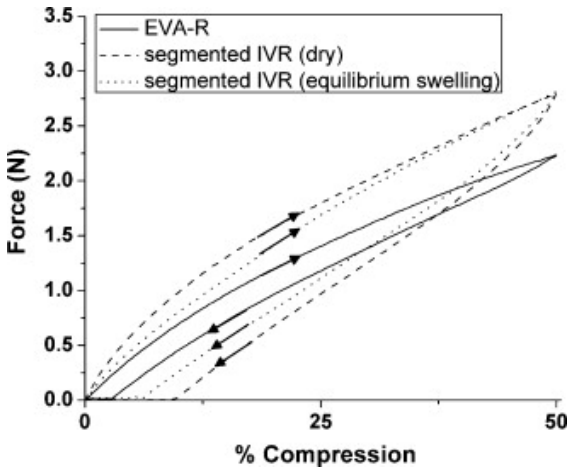


Figure 1.7: Force versus percent ring compression for experimental (segmented IVR) and Nuvaring® (EVA-R) intravaginal rings. Equilibrium swelling, as determined by mass change, was achieved after 3 days in water. Each ring was brought to 50% compression and subsequently allowed to recover to its original diameter as indicated by the direction of arrows. Adapted from reference [14], Elsevier, 2010 with permission.

### 1.6.3 Gamma Irradiation

Gamma irradiation is an established approach to sterilize materials for biomedical application. However, polymer irradiation may result in crosslinking or chain scission, resulting in physical and mechanical changes to the polymer. It has been generally reported that medical poly(urethane) products are able to withstand multiple exposures to gamma irradiation without change to physical or mechanical properties [92]. For example, Abraham et al. studied the effect of gamma irradiation on the mechanical

properties of an aromatic poly(ether urethane urea) and an aliphatic poly(carbonate)-based poly(urethane) [93]. The investigators assessed tensile properties with uniaxial stress-strain data following ASTM D638 methods and elongation properties using a stress hysteresis test. Although they observed a change in molecular weight distribution and soft segment glass transition temperature for both polymers, they found no significant effect of irradiation on the tensile properties and a small increase in hysteresis stress values.

In a separate study, Simmons et al. examined the effect of gamma irradiation on the mechanical properties of an aromatic poly(ether urethane) and an aromatic poly(urethane) based on both poly(ether) and poly(siloxane) in the soft segment [94]. They determined the ultimate tensile strength, ultimate elongation, and Young's modulus prior to and following sterilization. Gamma irradiation appeared to stiffen the poly(ether)/poly(siloxane)-based material, with an approximate 20% increase in Young's modulus, while tensile strength and elongation remained largely unchanged. There was no significant effect of irradiation on the measured mechanical properties of the poly(ether)-based poly(urethane).

Gorna et al. noted that previous studies had focused on the impact of gamma irradiation on the properties of non-erodible poly(urethanes). Therefore, they investigated the effect of gamma irradiation on the mechanical properties of biodegradable poly(urethanes) based on poly(ethylene oxide) and poly(ε-caprolactone), used for medical implants and scaffolds [95]. They measured the tensile strength, Young's modulus, and elongation at break before and after gamma irradiation. The investigators observed a decrease in mechanical strength following gamma irradiation,

with the poly(urethane) based on poly(ethylene oxide) exhibiting a substantial 50% decrease in tensile strength.

However, Ahmed et al. studied the effect of gamma irradiation on the mechanical properties of a non-erodible aromatic poly(carbonate urea) based poly(urethane) alongside a biodegradable aliphatic poly(caprolactone) based poly(urethane) [96]. They observed an approximate 25% decrease in Young's modulus and ultimate tensile strength for both polymers following irradiation. Consequently, no generalized conclusions can be made with regard to the effect of gamma irradiation on the mechanical properties of varying types of poly(urethanes), underscoring the importance of verifying mechanical properties of the drug product during development.

## 1.7 CONCLUSION

Owing to their chemical diversity, poly(urethanes) can be tailored to exhibit a wide variety of physical properties. Crystallinity, hydrophilicity, hydrated porosity, mechanical strength, and bioerodibility can be tuned to achieve the desired dosage form characteristics and release rate for a diverse array of treatment duration and route of administration. The diversity of poly(urethane) chemistry suggests that one may have substantially more degrees of freedom to select a polymer exhibiting good or poor drug solubility than with silicone or poly(ethylene-co-vinyl acetate) elastomers. The ability to tune the extent of water swelling by changing the soft segment to hard segment ratio of poly(urethanes) presents an exciting route to modulate drug release kinetics independent of drug solubility in polymer. Despite the available opportunities, few commercialized drug products leverage poly(urethanes), suggesting that it remains a nascent field with much to be understood before it can be routinely reduced to practice. Poly(urethane)-

based parenteral sustained release dosage forms are well suited toward therapies where high adherence to a consistent dose over a long duration is critical, particularly infectious and neurodegenerative diseases.

## 1.8 REFERENCES


[1] H.-W. Engels, H.-G. Pirkl, R. Albers, R.W. Albach, J. Krause, A. Hoffmann, H. Casselmann, J. Dormish, Polyurethanes: Versatile Materials and Sustainable Problem Solvers for Today's Challenges, Angew. Chemie Int. Ed. 52 (2013) 9422–9441. doi:10.1002/anie.201302766.

[2] O. Bayer, Das Di-Isocyanat-Polyadditionsverfahren (Polyurethane), Angew. Chemie. 59 (1947) 257–272. doi:10.1002/ange.19470590901.

[3] J.Y. Cherng, T.Y. Hou, M.F. Shih, H. Talsma, W.E. Hennink, Polyurethane-based drug delivery systems, Int. J. Pharm. 450 (2013) 145–162. doi:10.1016/j.ijpharm.2013.04.063.

[4] E. Seo, K. Na, Polyurethane membrane with porous surface for controlled drug release in drug eluting stent, Biomater. Res. 18 (2014) 15. doi:10.1186/2055-7124-18-15.

[5] Q. Guo, P.T. Knight, P.T. Mather, Tailored drug release from biodegradable stent coatings based on hybrid polyurethanes, J. Control. Release. 137 (2009) 224–233. doi:10.1016/J.JCONREL.2009.04.016.

[6] X. Chen, W. Liu, Y. Zhao, L. Jiang, H. Xu, X. Yang, Preparation and characterization of PEG-modified polyurethane pressure-sensitive adhesives for transdermal drug delivery, Drug Dev. Ind. Pharm. 35 (2009) 704–711. doi:10.1080/03639040802512235.

[7] B. Li, K. V. Brown, J.C. Wenke, S.A. Guelcher, Sustained release of vancomycin from polyurethane scaffolds inhibits infection of bone wounds in a rat femoral segmental defect model, J. Control. Release. 145 (2010) 221–230. doi:10.1016/J.JCONREL.2010.04.002.

[8] K. Gorna, S. Gogolewski, Preparation, degradation, and calcification of biodegradable polyurethane foams for bone graft substitutes, J. Biomed. Mater. Res. 67A (2003) 813–827. doi:10.1002/jbm.a.10148.

[9] B. Li, T. Yoshii, A.E. Hafeman, J.S. Nyman, J.C. Wenke, S.A. Guelcher, The effects of rhBMP-2 released from biodegradable polyurethane/microsphere composite scaffolds on new bone formation in rat femora, Biomaterials. 30 (2009)

6768–6779. doi:10.1016/J.BIOMATERIALS.2009.08.038.

[10] A. Martinelli, L. D'Ilario, I. Francolini, A. Piozzi, Water state effect on drug release from an antibiotic loaded polyurethane matrix containing albumin nanoparticles, Int. J. Pharm. 407 (2011) 197–206. doi:10.1016/J.IJPHARM.2011.01.029.

[11] A. Wang, H. Gao, Y. Sun, Y. Sun, Y.-W. Yang, G. Wu, Y. Wang, Y. Fan, J. Ma, Temperature- and pH-responsive nanoparticles of biocompatible polyurethanes for doxorubicin delivery, Int. J. Pharm. 441 (2013) 30–39. doi:10.1016/J.IJPHARM.2012.12.021.

[12] P. Basak, B. Adhikari, I. Banerjee, T.K. Maiti, Sustained release of antibiotic from polyurethane coated implant materials, J. Mater. Sci. Mater. Med. 20 (2009) 213–221. doi:10.1007/s10856-008-3521-3.

[13] S.A.L. Moura, L.D.C. Lima, S.P. Andrade, A. Da Silva-Cunha Junior, R.L. Órefice, E. Ayres, G.R. Da Silva, Local Drug Delivery System: Inhibition of Inflammatory Angiogenesis in a Murine Sponge Model by Dexamethasone-Loaded Polyurethane Implants, J. Pharm. Sci. 100 (2011) 2886–2895. doi:10.1002/jps.22497.

[14] T.J. Johnson, K.M. Gupta, J. Fabian, T.H. Albright, P.F. Kiser, Segmented polyurethane intravaginal rings for the sustained combined delivery of antiretroviral agents dapivirine and tenofovir, Eur. J. Pharm. Sci. 39 (2010) 203–212. doi:10.1016/J.EJPS.2009.11.007.

[15] G. Verstraete, L. Vandenbussche, S. Kasmi, L. Nuhn, D. Brouckaert, J. Van Renterghem, W. Grymonpré, V. Vanhoorne, T. Coenye, B.G. De Geest, T. De Beer, J.P. Remon, C. Vervaet, Thermoplastic polyurethane-based intravaginal rings for prophylaxis and treatment of (recurrent) bacterial vaginosis, Int. J. Pharm. 529 (2017) 218–226. doi:10.1016/J.IJPHARM.2017.06.076.

[16] M.R. Clark, T.J. Johnson, R.T. McCabe, J.T. Clark, A. Tuitupou, H. Elgendy, D.R. Friend, P.F. Kiser, A hot-melt extruded intravaginal ring for the sustained delivery of the antiretroviral microbicide UC781., J. Pharm. Sci. 101 (2012) 576–87. doi:10.1002/jps.22781.

[17] D.R. Friend, J.T. Clark, P.F. Kiser, M.R. Clark, Multipurpose prevention technologies: Products in development, Antiviral Res. 100 (2013) S39–S47. doi:10.1016/J.ANTIVIRAL.2013.09.030.

[18] P.M.M. Mesquita, R. Rastogi, T.J. Segarra, R.S. Teller, N.M. Torres, A.M. Huber, P.F. Kiser, B.C. Herold, Intravaginal ring delivery of tenofovir disoproxil fumarate for prevention of HIV and herpes simplex virus infection, J. Antimicrob. Chemother. 67 (2012) 1730–1738. doi:10.1093/jac/dks097.

[19] K.M. Gupta, S.M. Pearce, A.E. Poursaid, H.A. Aliyar, P.A. Tresco, M.A.

Mitchnik, P.F. Kiser, Polyurethane Intravaginal Ring for Controlled Delivery of Dapivirine, a Nonnucleoside Reverse Transcriptase Inhibitor of HIV-1, J. Pharm. Sci. 97 (2008) 4228–4239. doi:10.1002/jps.21331.

[20] Y.L. Traore, Y. Chen, A.-M. Bernier, E.A. Ho, Impact of Hydroxychloroquine-Loaded Polyurethane Intravaginal Rings on Lactobacilli., Antimicrob. Agents Chemother. 59 (2015) 7680–6. doi:10.1128/AAC.01819-15.

[21] J.M. Smith, R. Rastogi, R.S. Teller, P. Srinivasan, P.M.M. Mesquita, U. Nagaraja, J.M. McNicholl, R.M. Hendry, C.T. Dinh, A. Martin, B.C. Herold, P.F. Kiser, Intravaginal ring eluting tenofovir disoproxil fumarate completely protects macaques from multiple vaginal simian-HIV challenges., Proc. Natl. Acad. Sci. U. S. A. 110 (2013) 16145–50. doi:10.1073/pnas.1311355110.

[22] T.J. Johnson, M.R. Clark, T.H. Albright, J.S. Nebeker, A.L. Tuitupou, J.T. Clark, J. Fabian, R.T. McCabe, N. Chandra, G.F. Doncel, D.R. Friend, P.F. Kiser, A 90-day tenofovir reservoir intravaginal ring for mucosal HIV prophylaxis., Antimicrob. Agents Chemother. 56 (2012) 6272–83. doi:10.1128/AAC.01431-12.

[23] M.J. Keller, P.M. Mesquita, M.A. Marzinke, R. Teller, L. Espinoza, J.M. Atrio, Y. Lo, B. Frank, S. Srinivasan, D.N. Fredricks, L. Rabe, P.L. Anderson, C.W. Hendrix, P.F. Kiser, B.C. Herold, A phase 1 randomized placebo-controlled safety and pharmacokinetic trial of a tenofovir disoproxil fumarate vaginal ring., AIDS. 30 (2016) 743–51. doi:10.1097/QAD.0000000000000979.

[24] R.S. Teller, D.C. Malaspina, R. Rastogi, J.T. Clark, I. Szleifer, P.F. Kiser, Controlling the hydration rate of a hydrophilic matrix in the core of an intravaginal ring determines antiretroviral release, J. Control. Release. 224 (2016) 176–183. doi:10.1016/J.JCONREL.2015.12.035.

[25] J.M. Smith, P. Srinivasan, R.S. Teller, Y. Lo, C.T. Dinh, P.F. Kiser, B.C. Herold, Tenofovir disoproxil fumarate intravaginal ring protects high-dose depot medroxyprogesterone acetate-treated macaques from multiple SHIV exposures., J. Acquir. Immune Defic. Syndr. 68 (2015) 1–5. doi:10.1097/QAI.0000000000000402.

[26] B. Claeys, S. De Bruyn, L. Hansen, T. De Beer, J.P. Remon, C. Vervaet, Release characteristics of polyurethane tablets containing dicarboxylic acids as release modifiers – a case study with diprophylline, Int. J. Pharm. 477 (2014) 244–250. doi:10.1016/J.IJPHARM.2014.10.046.

[27] J. Lazarus, M. Pagliery, L. Lachman, Factors Influencing the Release of a Drug from a Prolonged-Action Matrix, J. Pharm. Sci. 53 (1964) 798–802. doi:10.1002/jps.2600530722.

[28] J.M. Anderson, A. Hiltner, M.J. Wiggins, M.A. Schubert, T.O. Collier, W.J. Kao, A.B. Mathur, Recent advances in biomedical polyurethane biostability and

biodegradation, Polym. Int. 46 (1998) 163–171. doi:10.1002/(SICI)1097-0126(199807)46:3<163::AID-PI972>3.0.CO;2-9.

[29] S.L. Cooper, J. Guan, Advances in Polyurethane Biomaterials, Woodhead Publishing, Cambridge, MA, USA, 2016. doi:10.1016/C2014-0-04143-3.

[30] J.W. Boretos, W.S. Pierce, Segmented polyurethane: A polyether polymer. An initial evalution for biomedical applications, J. Biomed. Mater. Res. 2 (1968) 121–130. doi:10.1002/jbm.820020109.

[31] S. Gogolewski, Selected topics in biomedical polyurethanes. A review, Colloid Polym. Sci. 267 (1989) 757–785. doi:10.1007/BF01410115.

[32] P.A. Gunatillake, D.J. Martin, G.F. Meijs, S.J. McCarthy, R. Adhikari, Designing Biostable Polyurethane Elastomers for Biomedical Implants, Aust. J. Chem. 56 (2003) 545–557. doi:10.1071/ch02168.

[33] N.M.K. Lamba, K.A. Woodhouse, S.L. Cooper, Polyurethanes in biomedical applications, CRC press, Boca Raton, FL, USA, 1997.

[34] P. Vermette, H.J. Griesser, G. Laroche, R. editors Guidoin, Biomedical applications of polyurethanes, Landes Bioscience, Georgetown, TX, USA, 2001. https://publications.csiro.au/rpr/pub?list=BRO&pid=procite:fb236b1d-fec9-46ef-a84d-6b9f75888af5 (accessed February 20, 2018).

[35] L. Irusta, M.J. Fernandez-Berridi, Aromatic poly(ester–urethanes): effect of the polyol molecular weight on the photochemical behaviour, Polymer (Guildf). 41 (2000) 3297–3302. doi:10.1016/S0032-3861(99)00548-0.

[36] G. DiBattista, H.W.I. Peerlings, W. Kaufhold, Aliphatic TPUs for light-stable applications, Rubber World. 227 (2003) 39–42.

[37] M. Szycher, A.A. Siciliano, An Assessment of 2,4 TDA Formation from Surgitek Polyurethane Foam under Simulated Physiological Conditions, J. Biomater. Appl. 5 (1991) 323–336. doi:10.1177/088532829100500404.

[38] K. Kääriä, A. Hirvonen, H. Norppa, P. Piirilä, H. Vainio, C. Rosenberg, Exposure to 4,4′-methylenediphenyl diisocyanate (MDI) during moulding of rigid polyurethane foam: determination of airborne MDI and urinary 4,4′-methylenedianiline (MDA), Analyst. 126 (2001) 476–479. doi:10.1039/B009549O.

[39] E. Jabbari, M. Khakpour, Morphology of and release behavior from porous polyurethane microspheres, Biomaterials. 21 (2000) 2073–2079. doi:10.1016/S0142-9612(00)00135-6.

[40] D.G. Thompson, J.C. Osborn, E.M. Kober, J.R. Schoonover, Effects of hydrolysis-induced molecular weight changes on the phase separation of a polyester polyurethane, Polym. Degrad. Stab. 91 (2006) 3360–3370.

doi:10.1016/j.polymdegradstab.2006.05.019.

[41] B. Saad, T.D. Hirt, M. Welti, G.K. Uhlschmid, P. Neuenschwander, U.W. Suter, Development of degradable polyesterurethanes for medical applications: In vitro and in vivo evaluations, J. Biomed. Mater. Res. 36 (1997) 65–74. doi:10.1002/(SICI)1097-4636(199707)36:1<65::AID-JBM8>3.0.CO;2-J.

[42] M. Kaur, K.M. Gupta, A.E. Poursaid, P. Karra, A. Mahalingam, H.A. Aliyar, P.F. Kiser, Engineering a degradable polyurethane intravaginal ring for sustained delivery of dapivirine, Drug Deliv. Transl. Res. 1 (2011) 223–237. doi:10.1007/s13346-011-0027-1.

[43] J. Yu, F. Lin, P. Lin, Y. Gao, M.L. Becker, Phenylalanine-Based Poly(ester urea): Synthesis, Characterization, and *in vitro* Degradation, Macromolecules. 47 (2014) 121–129. doi:10.1021/ma401752b.

[44] J. Rychlý, A. Lattuati-Derieux, B. Lavédrine, L. Matisová-Rychlá, M. Malíková, K. Csomorová, I. Janigová, Assessing the progress of degradation in polyurethanes by chemiluminescence and thermal analysis. II. Flexible polyether- and polyester-type polyurethane foams, Polym. Degrad. Stab. 96 (2011) 462–469. doi:10.1016/j.polymdegradstab.2011.01.012.

[45] E. Yilgör, E. Burgaz, E. Yurtsever, İ. Yilgör, Comparison of hydrogen bonding in polydimethylsiloxane and polyether based urethane and urea copolymers, Polymer (Guildf). 41 (2000) 849–857. doi:10.1016/S0032-3861(99)00245-1.

[46] M.J. Wiggins, B. Wilkoff, J.M. Anderson, A. Hiltner, Biodegradation of polyether polyurethane inner insulation in bipolar pacemaker leads, J. Biomed. Mater. Res. 58 (2001) 302–307. doi:10.1002/1097-4636(2001)58:3<302::AID-JBM1021>3.0.CO;2-Y.

[47] E.M. Christenson, M. Dadsetan, M. Wiggins, J.M. Anderson, A. Hiltner, Poly(carbonate urethane) and poly(ether urethane) biodegradation: In vivo studies, J. Biomed. Mater. Res. Part A. 69A (2004) 407–416. doi:10.1002/jbm.a.30002.

[48] Y. Ikeda, S. Kohjiya, S. Takesako, S. Yamashita, Polyurethane elastomer with PEO-PTMO-PEO soft segment for sustained release of drugs, Biomaterials. 11 (1990) 553–560. doi:10.1016/0142-9612(90)90077-4.

[49] J.M. Anderson, A. Rodriguez, D.T. Chang, Foreign body reaction to biomaterials, Semin. Immunol. 20 (2008) 86–100. doi:10.1016/j.smim.2007.11.004.

[50] H.R. Kricheldorf, R.P. Quirk, G. Holden, Thermoplastic elastomers, Hanser Gardner Publications, Munich, Germany, 2004.

[51] T.O. Ahn, I.S. Choi, H.M. Jeong, K. Cho, Thermal and mechanical properties of thermoplastic polyurethane elastomers from different polymerization methods, Polym. Int. 31 (1993) 329–333. doi:10.1002/pi.4990310404.

[52] D.Y. Arifin, L.Y. Lee, C.-H. Wang, Mathematical modeling and simulation of drug release from microspheres: Implications to drug delivery systems, Adv. Drug Deliv. Rev. 58 (2006) 1274–1325. doi:10.1016/j.addr.2006.09.007.

[53] J. Siepmann, F. Siepmann, Mathematical modeling of drug delivery, Int. J. Pharm. 364 (2008) 328–343. doi:10.1016/j.ijpharm.2008.09.004.

[54] J.T. Clark, T.J. Johnson, M.R. Clark, J.S. Nebeker, J. Fabian, A.L. Tuitupou, S. Ponnapalli, E.M. Smith, D.R. Friend, P.F. Kiser, Quantitative evaluation of a hydrophilic matrix intravaginal ring for the sustained delivery of tenofovir, J. Control. Release. 163 (2012) 240–248. doi:10.1016/J.JCONREL.2012.08.033.

[55] S.R. Ugaonkar, J.T. Clark, L.B. English, T.J. Johnson, K.W. Buckheit, R.J. Bahde, D.H. Appella, R.W. Buckheit, P.F. Kiser, An Intravaginal Ring for the Simultaneous Delivery of an HIV-1 Maturation Inhibitor and Reverse-Transcriptase Inhibitor for Prophylaxis of HIV Transmission., J. Pharm. Sci. 104 (2015) 3426–39. doi:10.1002/jps.24551.

[56] J.A.. van Laarhoven, M.A.. Kruft, H. Vromans, In vitro release properties of etonogestrel and ethinyl estradiol from a contraceptive vaginal ring, Int. J. Pharm. 232 (2002) 163–173. doi:10.1016/S0378-5173(01)00900-0.

[57] J. Crank, The mathematics of diffusion, 2d ed, Clarendon Press, Oxford, [Eng], 1979.

[58] J.-M. Vergnaud, Controlled drug release of oral dosage forms, CRC Press, Boca Raton, FL, USA, 1993.

[59] T. Higuchi, Mechanism of sustained-action medication. Theoretical analysis of rate of release of solid drugs dispersed in solid matrices, J. Pharm. Sci. 52 (1963) 1145–1149. doi:10.1002/jps.2600521210.

[60] B. Claeys, A. Vervaeck, X.K.D. Hillewaere, S. Possemiers, L. Hansen, T. De Beer, J.P. Remon, C. Vervaet, Thermoplastic polyurethanes for the manufacturing of highly dosed oral sustained release matrices via hot melt extrusion and injection molding, Eur. J. Pharm. Biopharm. 90 (2015) 44–52. doi:10.1016/J.EJPB.2014.11.003.

[61] H. Yasuda, C.E. Lamaze, L.D. Ikenberry, Permeability of solutes through hydrated polymer membranes. Part I. Diffusion of sodium chloride, Die Makromol. Chemie. 118 (1968) 19–35. doi:10.1002/macp.1968.021180102.

[62] A. Go¨pferich, R. Langer, Modeling monomer release from bioerodible polymers, J. Control. Release. 33 (1995) 55–69. doi:10.1016/0168-3659(94)00064-2.

[63] R. Langer, N. Peppas, Chemical and Physical Structure of Polymers as Carriers for Controlled Release of Bioactive Agents: A Review, J. Macromol. Sci. Part C. 23 (1983) 61–126. doi:10.1080/07366578308079439.

[64] P.L. Ritger, N.A. Peppas, A simple equation for description of solute release II. Fickian and anomalous release from swellable devices, J. Control. Release. 5 (1987) 37–42. doi:10.1016/0168-3659(87)90035-6.

[65] A.E. Hafeman, B. Li, T. Yoshii, K. Zienkiewicz, J.M. Davidson, S.A. Guelcher, Injectable Biodegradable Polyurethane Scaffolds with Release of Platelet-derived Growth Factor for Tissue Repair and Regeneration, Pharm. Res. 25 (2008) 2387–2399. doi:10.1007/s11095-008-9618-z.

[66] A.E. Hafeman, K.J. Zienkiewicz, E. Carney, B. Litzner, C. Stratton, J.C. Wenke, S.A. Guelcher, Local Delivery of Tobramycin from Injectable Biodegradable Polyurethane Scaffolds, J. Biomater. Sci. Polym. Ed. 21 (2010) 95–112. doi:10.1163/156856209X410256.

[67] M. Hombreiro-Pérez, J. Siepmann, C. Zinutti, A. Lamprecht, N. Ubrich, M. Hoffman, R. Bodmeier, P. Maincent, Non-degradable microparticles containing a hydrophilic and/or a lipophilic drug: preparation, characterization and drug release modeling, J. Control. Release. 88 (2003) 413–428. doi:10.1016/S0168-3659(03)00030-0.

[68] A. Almeida, L. Brabant, F. Siepmann, T. De Beer, W. Bouquet, L. Van Hoorebeke, J. Siepmann, J.P. Remon, C. Vervaet, Sustained release from hot-melt extruded matrices based on ethylene vinyl acetate and polyethylene oxide, Eur. J. Pharm. Biopharm. 82 (2012) 526–533. doi:10.1016/J.EJPB.2012.08.008.

[69] P. Tallury, N. Alimohammadi, S. Kalachandra, Poly(ethylene-co-vinyl acetate) copolymer matrix for delivery of chlorhexidine and acyclovir drugs for use in the oral environment: effect of drug combination, copolymer composition and coating on the drug release rate., Dent. Mater. 23 (2007) 404–9. doi:10.1016/j.dental.2006.02.011.

[70] T.T. Reddy, M. Hadano, A. Takahara, Controlled Release of Model Drug from Biodegradable Segmented Polyurethane Ureas: Morphological and Structural Features, Macromol. Symp. 242 (2006) 241–249. doi:10.1002/masy.200651033.

[71] T.T.-P. Hsu, R. Langer, Polymers for the controlled release of macromolecules: Effect of molecular weight of ethylene-vinyl acetate copolymer, J. Biomed. Mater. Res. 19 (1985) 445–460. doi:10.1002/jbm.820190409.

[72] L. Zhou, D. Liang, X. He, J. Li, H. Tan, J. Li, Q. Fu, Q. Gu, The degradation and biocompatibility of pH-sensitive biodegradable polyurethanes for intracellular multifunctional antitumor drug delivery, Biomaterials. 33 (2012) 2734–2745. doi:10.1016/J.BIOMATERIALS.2011.11.009.

[73] M. Shoaib, A. Bahadur, S. Iqbal, M.S.U. Rahman, S. Ahmed, G. Shabir, M.A. Javaid, Relationship of hard segment concentration in polyurethane-urea elastomers with mechanical, thermal and drug release properties, J. Drug Deliv.

Sci. Technol. 37 (2017) 88–96. doi:10.1016/J.JDDST.2016.12.003.

[74] G. Verstraete, J. Van Renterghem, P.J. Van Bockstal, S. Kasmi, B.G. De Geest, T. De Beer, J.P. Remon, C. Vervaet, Hydrophilic thermoplastic polyurethanes for the manufacturing of highly dosed oral sustained release matrices via hot melt extrusion and injection molding, Int. J. Pharm. 506 (2016) 214–221. doi:10.1016/J.IJPHARM.2016.04.057.

[75] J.-E. Kim, S.-R. Kim, S.-H. Lee, C.-H. Lee, D.-D. Kim, The effect of pore formers on the controlled release of cefadroxil from a polyurethane matrix, Int. J. Pharm. 201 (2000) 29–36. doi:10.1016/S0378-5173(00)00388-4.

[76] G. Donelli, I. Francolini, V. Ruggeri, E. Guaglianone, L. D'Ilario, A. Piozzi, Pore formers promoted release of an antifungal drug from functionalized polyurethanes to inhibit Candida colonization, J. Appl. Microbiol. 100 (2006) 615–622. doi:10.1111/j.1365-2672.2005.02801.x.

[77] K. Sreenivasan, Effect of blending methyl ?-cyclodextrin on the release of hydrophobic hydrocortisone into water from polyurethane, J. Appl. Polym. Sci. 81 (2001) 520–522. doi:10.1002/app.1466.

[78] R. LANGER, J. FOLKMAN, Polymers for the sustained release of proteins and other macromolecules, Nature. 263 (1976) 797–800. doi:10.1038/263797a0.

[79] T. Lindholm, B.-Å. Lindholm, M. Niskanen, J. Koskiniemi, Polysorbate 20 as a drug release regulator in ethyl cellulose film coatings, J. Pharm. Pharmacol. 38 (1986) 686–688. doi:10.1111/j.2042-7158.1986.tb03110.x.

[80] R. Bodmeier, O. Paeratakul, Theophylline Tablets Coated with Aqueous Latexes Containing Dispersed Pore Formers, J. Pharm. Sci. 79 (1990) 925–928. doi:10.1002/jps.2600791017.

[81] M.A. Frohoff-Hülsmann, A. Schmitz, B.C. Lippold, Aqueous ethyl cellulose dispersions containing plasticizers of different water solubility and hydroxypropyl methylcellulose as coating material for diffusion pellets: I. Drug release rates from coated pellets, Int. J. Pharm. 177 (1999) 69–82. doi:10.1016/S0378-5173(98)00327-5.

[82] D. Sauer, A.B. Watts, L.B. Coots, W.C. Zheng, J.W. McGinity, Influence of polymeric subcoats on the drug release properties of tablets powder-coated with pre-plasticized Eudragit® L 100-55, Int. J. Pharm. 367 (2009) 20–28. doi:10.1016/J.IJPHARM.2008.09.020.

[83] M. Irfan, A.R. Ahmed, K. Kolter, R. Bodmeier, A. Dashevskiy, Curing mechanism of flexible aqueous polymeric coatings, Eur. J. Pharm. Biopharm. 115 (2017) 186–196. doi:10.1016/J.EJPB.2017.02.012.

[84] W. Bounds, A. Szarewski, D. Lowe, J. Guillebaud, Preliminary report of

unexpected local reactions to a progestogen-releasing contraceptive vaginal ring, Eur. J. Obstet. Gynecol. Reprod. Biol. 48 (1993) 123–125. doi:10.1016/0028-2243(93)90252-8.

[85] S. Koetsawang, J. Gao, U. Krishna, A. Cuadros, G.I. Dhall, R. Wyss, J.R. la Puenta, A.T.L. Andrade, T. Khan, E.S. Kononova, J.P. Lawson, U. Parekh, M. Elstein, V. Hingorani, N. Wang, Z. Yao, B.-M. Landgren, R. Boukhris, L. Lo, S. Boccard, D. Machin, A. Pinol, P.J. Rowe, Microdose intravaginal levonorgestrel contraception: A multicentre clinical trial, Contraception. 41 (1990) 125–141. doi:10.1016/0010-7824(90)90142-I.

[86] K. Morrow Guthrie, S. Vargas, J.G. Shaw, R.K. Rosen, J.J. van den Berg, P.F. Kiser, K. Buckheit, D. Bregman, L. Thompson, K. Jensen, T. Johnson, R.W. Buckheit, The Promise of Intravaginal Rings for Prevention: User Perceptions of Biomechanical Properties and Implications for Prevention Product Development, PLoS One. 10 (2015) e0145642. doi:10.1371/journal.pone.0145642.

[87] M.M. Baum, I. Butkyavichene, J. Gilman, S. Kennedy, E. Kopin, A.M. Malone, C. Nguyen, T.J. Smith, D.R. Friend, M.R. Clark, J.A. Moss, An intravaginal ring for the simultaneous delivery of multiple drugs., J. Pharm. Sci. 101 (2012) 2833–43. doi:10.1002/jps.23208.

[88] ASTM International, ASTM D2240-15e1, Standard Test Method for Rubber Property—Durometer Hardness, in: ASTM Stand., West Conshohocken, PA, 2015. doi:10.1520/D2240-15E01.

[89] ISO, ISO 8009 Mechanical contraceptives — Reusable natural and silicone rubber contraceptive diaphragms — Requirements and tests, ISO Stand. 2014 (2014). www.iso.org (accessed February 27, 2018).

[90] J.T. Clark, M.R. Clark, N.B. Shelke, T.J. Johnson, E.M. Smith, A.K. Andreasen, J.S. Nebeker, J. Fabian, D.R. Friend, P.F. Kiser, Engineering a Segmented Dual-Reservoir Polyurethane Intravaginal Ring for Simultaneous Prevention of HIV Transmission and Unwanted Pregnancy, PLoS One. 9 (2014) e88509. doi:10.1371/journal.pone.0088509.

[91] C.J. Crnich, J.A. Halfmann, W.C. Crone, D.G. Maki, BS, W.C. Crone, P. and D.G. Maki, MD, The Effects of Prolonged Ethanol Exposure on the Mechanical Properties of Polyurethane and Silicone Catheters Used for Intravascular Access, Infect. Control Hosp. Epidemiol. 26 (2005) 708–714. doi:10.1086/502607.

[92] L.K. Massey, The effects of sterilization methods on plastics and elastomers : the definitive user's guide and databook, William Andrew Pub, Norwich, NY, USA, 2005.

[93] G.A. Abraham, P.M. Frontini, T.R. Cuadrado, Physical and mechanical behavior of sterilized biomedical segmented polyurethanes, J. Appl. Polym. Sci. 65 (1997)

1193–1203. doi:10.1002/(SICI)1097-4628(19970808)65:6<1193::AID-APP15>3.0.CO;2-V.

[94] A. Simmons, J. Hyvarinen, L. Poole-Warren, The effect of sterilisation on a poly(dimethylsiloxane)/poly(hexamethylene oxide) mixed macrodiol-based polyurethane elastomer, Biomaterials. 27 (2006) 4484–4497. doi:10.1016/J.BIOMATERIALS.2006.04.017.

[95] K. Gorna, S. Gogolewski, The effect of gamma radiation on molecular stability and mechanical properties of biodegradable polyurethanes for medical applications, Polym. Degrad. Stab. 79 (2003) 465–474. doi:10.1016/S0141-3910(02)00362-2.

[96] M. Ahmed, G. Punshon, A. Darbyshire, A.M. Seifalian, Effects of sterilization treatments on bulk and surface properties of nanocomposite biomaterials, J. Biomed. Mater. Res. Part B Appl. Biomater. 101 (2013) 1182–1190. doi:10.1002/jbm.b.32928.

# Chapter 2: Can Drug Release Rate from Implants Be Tailored Using Poly(urethane) Mixtures?[2]

## 2.1 ABSTRACT

Hydrophobic and hydrophilic thermoplastic poly(urethane) (TPU) mixtures offer the opportunity to tune water swelling capacity and diffusion rate for drugs exhibiting broadly different properties. We sought to (1) assess the range of drug diffusion rates achieved by varying hydrophilic-to-hydrophobic TPU ratio relative to varying ethylene vinyl acetate (EVA) crystallinity; (2) investigate the effect of mixture ratio on permeability of emtricitabine; and (3) investigate the impact of the extrusion process on mixing of the two TPUs and the resulting impact on drug diffusion. The permeability of water-soluble emtricitabine exhibited a 736-fold range across the blends of TPU, but only a 3.4-fold range across the EVA grades investigated. Varying hydrophilic content of the TPU mixture from 0% to 25% (w/w) led to a negligible permeability change, while changing hydrophilic content from 55% to 100% resulted in a linear 3-fold increase in drug permeability. Interestingly, an 123-fold permeability change occurred between 50% and 55% hydrophilic polymer. Extrusion process parameters exhibited minimal impact on homogeneity and drug diffusion. These findings suggest that hydrophilic polymer domains form a continuous network at levels above 55% hydrophilic TPU, thus facilitating a water-filled porous network when exposed to water that provides a mechanism for accelerated drug diffusion.

---

[2] Published in: M.B. Lowinger, Y. Su, X. Lu, R.O. Williams, F. Zhang, Can drug release rate from implants be tailored using poly(urethane) mixtures?, Int. J. Pharm. 557 (2019) 390–401. doi:10.1016/j.ijpharm.2018.11.067. Michael Lowinger designed, executed, and performed the experiments, and wrote the manuscript.

## 2.2 INTRODUCTION

Patient adherence, or the extent to which patients follow the recommendations of their healthcare providers, has a substantial impact on health outcomes [1]. A meta-analysis of 85 reports with electronic adherence monitoring across a variety of therapeutic areas found an overall rate of adherence of 71%, with some studies as low as 34% [2]. Poor adherence to therapy can reduce the real-world efficacy of treatments. Nachega et al. identified a strong correlation between adherence to a class of human immunodeficiency virus (HIV) antiretrovirals and suppression of the virus [3]. Although the well-established heuristic that "drugs don't work in patients who don't take them" applies to all therapeutic areas, infectious disease patients are at particular risk. For example, those individuals infected with human immunodeficiency virus (HIV) who exhibit poor adherence to therapy may inadvertently encourage the proliferation of mutant variants that are resistant to the medication [4]. Consequently, significant effort has been spent in recent years focused on products intended to improve adherence to HIV therapy [5–10].

Among other interventions, decreasing the frequency of administration is an effective way to improve patient adherence [2]. Development scientists have increased duration of treatment by increasing drug half-life [11], designing novel oral sustained release formulations [12], and developing subcutaneous or intramuscular injections [13,14]. Although these approaches have been successful at enhancing treatment duration, they are limited to once quarterly administration. Intravaginal rings and subdermal implants have been demonstrated to decrease administration frequency to as little as once every five years [15,16]. Subdermal implants, in particular, have the

potential to substantially improve patient adherence by mitigating the burden to take medication daily or more frequently.

Implants may be designed as a reservoir system, with a core composed of drug and polymer surrounded by a rate-controlling membrane. Drug release rate from reservoir systems is much less driven by drug load and dosage form geometry, compared with matrix systems composed of a drug and polymer mixture with no membrane. Consequently, reservoir systems are able to decouple drug release rate and treatment duration, facilitating longer acting formulations [17]. Because the membrane determines release rate, the composition of the core may be selected in a manner that is largely independent from release kinetics considerations. We speculate that, to some extent, reservoir systems also decouple release rate from the mechanical properties of the dosage form in contrast to matrix systems.

The vast majority of marketed implants and vaginal rings are composed of either silicone or ethylene vinyl acetate copolymer (EVA), with EVA playing a particularly prominent role as the rate controlling membrane polymer. NuvaRing® is an intravaginal ring inserted once monthly, composed of EVA and intended to release etonogestrel and ethinylestradiol for contraception [18]. Nexplanon® is a subdermal implant consisting of a single rod administered once every 3 years, composed of EVA and intended to release etonogestrel for contraception [19]. Probuphine® is a subdermal implant consisting of 4 rods administered once every 6 months, composed of EVA and intended to release buprenorphine for opioid dependence [20]. NuvaRing® and Nexplanon® are reservoir systems with an EVA polymer membrane surrounding a core. In those cases, the drug diffusion rate through the EVA polymer is strongly influenced by varying the vinyl acetate content of the polymer in both the core and the membrane. For a given drug

molecule, lower vinyl acetate content of the EVA copolymer results in greater polymer crystallinity and slower drug diffusion [21,22].

Although EVA has been used in multiple commercial products with established biocompatibility and suitability to extrusion processing due to its shear-thinning thermoplastic behavior, it has several disadvantages [23]. Firstly, a relatively narrow range of vinyl acetate content is achievable that retains mechanical properties suitable for a long-term implant product, thereby limiting the ability to tune drug release rate. Additionally, the inherent nature of crystallinity in a polymer is variable, dependent on the crystallization conditions, storage conditions, and precise composition of a given polymer chain [24]. Moreover, polymer crystallinity can be difficult to accurately measure [25]. Finally, drug solubility in the polymer is a critical factor of diffusion through the membrane [26]. It may be expected that hydrophilic drugs with poor polymer solubility would have limited drug release rate, regardless of EVA crystallinity [27]. Moreover, it is possible that the drug diffusion necessary for release could also occur over time on the shelf, resulting in burst release at early time points for products that have sat on the shelf over long time periods. Probuphine® implants are washed to remove surface buprenorphine to reduce the initial burst [28,29].

Thermoplastic poly(urethanes) (TPU; poly(urethanes)) have been used for parenteral administration of medical devices with good demonstrated biocompatibility [30–32]. Poly(urethane) chemistry has been extensively covered in prior publications [26,33,34]. Hydrophilic poly(urethanes), in which the soft segment is polyethylene oxide (PEO), have been demonstrated to swell when immersed in water in proportion to the ratio of soft segment in the polymer [35]. Drug release rate through these TPU polymers has also been shown to increase with increasing soft segment ratio [35,36].

The extent of hydrophilicity of the TPUs presents an opportunity to define an appropriate drug release profile. In contrast to the relatively narrow range of vinyl acetate content practically achievable to tune drug release, hydrophilic TPUs have been synthesized covering a wide range of swelling extent [35]. The extent of water swelling is also easily measured, in contrast to polymer crystallinity, allowing for good quality control. Finally, diffusion through water-filled pores is likely to be the major drug release pathway, making drug solubility in the non-swollen polymer a substantially less relevant parameter governing release kinetics [37].

The ability to tune the water-swelling properties of poly(urethanes) as the rate controlling membrane polymer provides an opportunity to modulate release rate independent of drug solubility in the non-swollen membrane polymer. Johnson et al. described findings of a prototype intravaginal ring composed of hydrophilic TPU tubing filled with a semisolid paste of tenofovir (a hydrophilic drug), glycerol, and water [27]. The mechanism of drug release through the membrane polymer was proposed to be the creation of a pore structure driven by swelling upon contact with water. Notably, the *in vitro* release data showed no measurable burst effect and a zero-order release rate determined by their relative propensity to uptake water. A subsequent publication by Clark et al. detailed their effort to develop a single intravaginal ring capable of delivering tenofovir (a hydrophilic drug) and levonogestrel (a hydrophobic drug) [38]. They noted that their approximately 7-log difference in their partition/distribution coefficients precluded release from the same polymer system. Consequently, they developed a ring composed of one segment containing levonogestrel surrounded by a hydrophobic, non-swelling TPU and the other segment consisting of tenofovir surrounded by a hydrophilic, water-swelling TPU.

Drugs vary widely in physicochemical properties and dose, however there are a limited number of hydrophilic TPUs readily available to be used in pharmaceutical formulations. Blends of water insoluble polymers of varying hydrophilicity have been extensively leveraged to modulate drug diffusion through membranes in the tablet film coating and multiparticulate oral controlled release fields. Amighi and Moës investigated different ratios of Eudragit® RS and RL as a coating to theophylline-containing pellets [39]. Eudragit® RS and RL are water insoluble acrylate/methacrylate copolymers containing different amounts of quaternary ammonium. They demonstrated the ability to achieve a broad range of release rates in an approximately proportional relationship to the polymer mixture composition. Lecomte et al. studied ratios of ethylcellulose and Eudragit® L as a coating to propranolol-containing pellets [40]. Ethylcellulose is insoluble in water, while Eudragit® L is an anionic poly(methacrylate) soluble in aqueous media at pH > 6. The investigators were able to modulate the drug release kinetics in approximate proportion to the polymer mixture composition. Consequently, we expect that mixtures of a hydrophobic and hydrophilic TPU in different ratios will allow us to broadly tune the diffusion rate of a model hydrophilic drug through a membrane as a function of membrane composition.

We hypothesize that using mixtures of hydrophilic and hydrophobic TPUs as the rate controlling membrane polymer allows for a wider range of release rates for a hydrophilic drug than varying the vinyl acetate content of EVA. This approach has not been extensively studied in the literature and offers the opportunity to mitigate the effect of drug/polymer interactions on drug release rate. Several patents and patent applications have described the use of TPU blends and found that there was a change in diffusion rate over a narrow range of blended ratios [41–43]. We further hypothesize that drug release

rate can be broadly modulated by varying the ratio of hydrophilic to hydrophobic TPU in the membrane. Since each TPU exhibits phase separation between the hard and soft segments of the copolymer, we expect that the hydrophilic and hydrophobic TPUs will be partially immiscible. Therefore, we hypothesize that extrusion process parameters will impact the homogeneity of the two components, potentially impacting the diffusion behavior of drugs through the membrane.

In order to interrogate our hypotheses, we manufactured films composed of binary mixtures of varying composition of a hydrophilic and hydrophobic TPU using a melt extrusion process coupled with a roll stack to directly form thin films. The films are intended to represent the rate controlling membrane in a reservoir implant system. At a given composition, we varied extrusion process parameters to investigate the effect of process on key response attributes. Finally, we characterized extent of polymer mixing using a spectroscopic technique and drug permeability using a diffusion cell.

## 2.3 MATERIALS AND METHODS

### 2.3.1 Materials

Ethylene vinyl acetate copolymer was obtained from Sigma-Aldrich (St. Louis, MO). EVA grades containing target vinyl acetate content of 12% (w/w), 25% (w/w), and 40% (w/w) were purchased and are subsequently described as EVA 12, EVA 25, and EVA 40, respectively (Figure 2.1). We varied the vinyl acetate content of the copolymer in order to modulate the extent of crystallinity.

Non-swelling thermoplastic poly(urethane) Pathway™ PY-PT60DE was obtained from Lubrizol (Cleveland, OH) and is described as hydrophobic TPU. Water-swelling thermoplastic poly(urethane) Pathway™ PY-PT60DE500 was also obtained from

Lubrizol (Cleveland, OH) and is described as hydrophilic TPU. The structures of the two poly(urethanes) were previously identified by $^{1}H$ nuclear magnetic resonance (NMR) [35]. As seen in Figure 2.1, both poly(urethanes) contain hexamethylene diisocyanate as the hard segment and their soft segment monomer differs by two carbons. Hydrophobic TPU contains poly(tetrahydrofuran) as its soft segment, while hydrophilic TPU contains PEO as its soft segment.

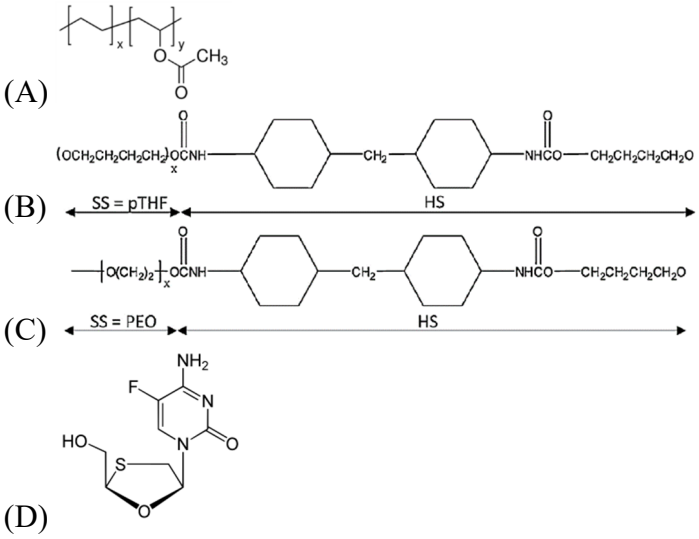


Figure 2.1: Chemical structures of (A) ethylene vinyl acetate, (B) hydrophobic TPU Pathway PY-PT60DE, (C) hydrophilic TPU Pathway PY-PT60DE500, and (D) emtricitabine.

Emtricitabine (FTC), an HIV nucleoside reverse transcriptase inhibitor, was obtained from Laurus Labs (Hyderabad, India). As shown in Figure 2.1, it has a molecular weight of 247 Da, a calculated octanol/water partition coefficient (clogP) of -1.3, and a water solubility of 112 mg/mL. As described previously, long-acting treatments are currently under development for multiple HIV antiretrovirals in order to

address the unmet need of improved patient adherence. Although emtricitabine's potency is likely insufficient to be in the realm necessary to extend the duration over a significant length of time (e.g., ≥ 6 months), it represents a class of drugs with certain physicochemical properties (small, hydrophilic, water soluble) that are relevant for current efforts to develop implants and other sustained release formulations of HIV drugs.

### 2.3.2 Methods

#### *2.3.2.1 Film Preparation*

Films were prepared using a Leistritz ZSE 18 twin-screw extruder (Somerville, NJ). Figure 2.2 shows the screw and barrel configurations used to manufacture the polymer films. The barrels were configured with a 40:1 length:diameter ratio. In the case of TPU film manufacture, the two polymers were charged into separate K-Tron KT20 loss-in-weight gravimetric feeders (Sewell, NJ), which were configured to feed into a single port. In the case of EVA film manufacture, a single polymer was charged into a single K-Tron gravimetric feeder. The vent zone was connected to a vacuum, set to 1000 mbar vacuum pressure. Table 2.1 describes the barrel configuration and temperature profile used to manufacture the polymer films. The barrel temperature profiles were selected to maximize the temperature difference between the two profiles without approaching the torque limit of the equipment. The extruder was connected to a Baldor gear pump (Mount Laurel, NJ) to dampen oscillations in flow. The end of the extruder featured a 0.02 x 6 inch sheet die. The extrudate was fed into a Leistritz 3-roll film stack (Somerville, NJ). The temperature of the rolls was controlled to 15°C.

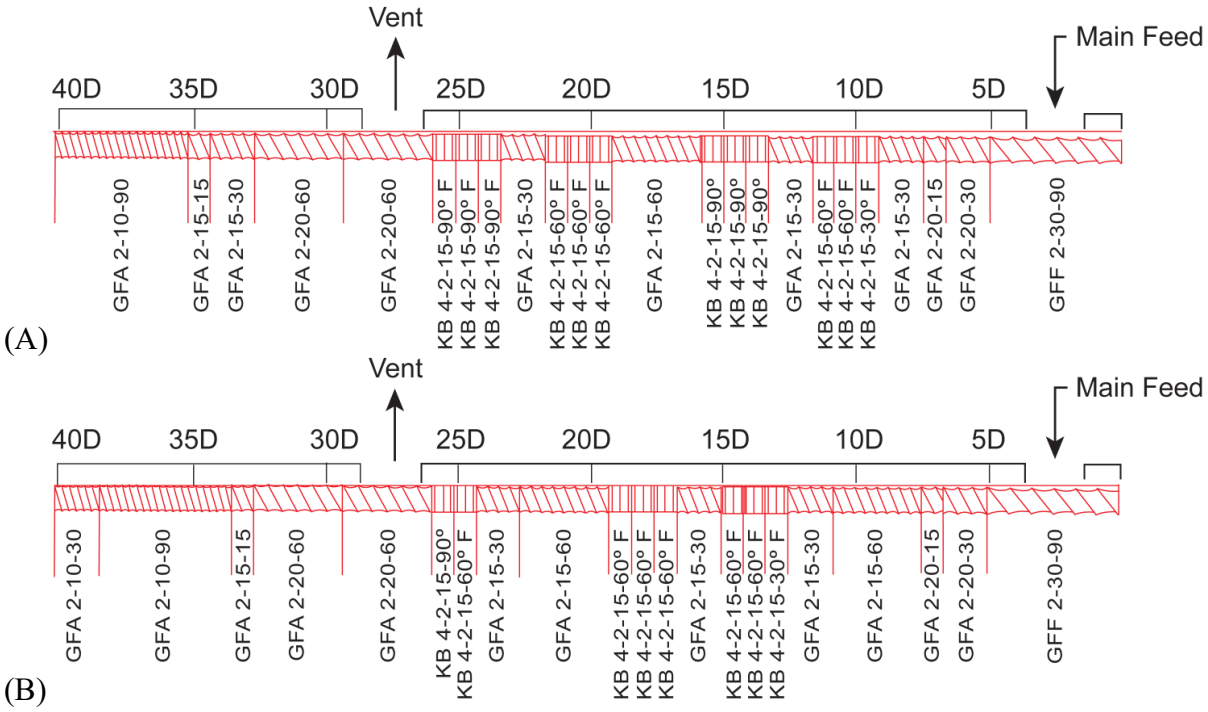


Figure 2.2: Screw profiles used to manufacture polymer films on Leistritz 18 mm twin-screw extruder. In the diagram, GFF denotes a co-rotating, non-self-wiping, conveying element; GFA denotes a co-rotating, intermeshing, conveying element; and KB denotes a kneading block. For conveying elements, the first number indicates the number of screw flights, the second number indicates the screw pitch in mm, and the third number indicates the screw length in mm. For the kneading blocks, the first number is the number of kneading segments, the second number is the number of screw flights, the third number is the length in mm, and the four number is the offset angle of the individual kneading segments. Screw profile A (A) has significantly more mixing elements with a higher degree of offset than screw profile B (B).

Polymer film composition (ratio of the two polymers) was varied by changing the ratio of the feed rates of each polymer into the extruder. Extruder processing conditions were varied at a given polymer composition by changing barrel temperature, screw speed, total feed rate, and screw design. Samples and measurements were not taken for 10 minutes after each process condition change to ensure steady state had been achieved.

Samples were collected and measurements recorded for 5 minutes once steady state was reached.

Table 2.1: Barrel configuration and temperature profiles used to manufacture polymer films on Leistritz 18 mm twin-screw extruder.

| **Zone** | **0** | **1** | **2** | **3** | **4** | **5** | **6** | **7** | **8** | **9** | **10** |
|---|---|---|---|---|---|---|---|---|---|---|---|
| **Unit Operation** | Feed Port | Closed Port | Closed Port | Closed Port | Closed Port | Vent | Closed Port | Closed Port | Die Adapter | Gear Pump Adapter | Die |
| **Temperature Profile A (°C)** | Always Cool | 150 | 180 | 200 | 200 | 200 | 200 | 200 | 200 | 200 | 200 |
| **Temperature Profile B (°C)** | Always Cool | 150 | 160 | 160 | 160 | 160 | 160 | 160 | 160 | 160 | 160 |

### *2.3.2.2 Assessment of Polymer Film Homogeneity*

Solid-state NMR (ssNMR) experiments were carried out on a 400 MHz Bruker (Billerica, MA) Avance III HD spectrometer (9.4 T). Polymer samples were packed into 4 mm zirconia rotors. All spectra were acquired under a magic angle spinning (MAS) frequency of 12 kHz at ambient temperature and using a Bruker H/F/X probe tuned to $^{1}H/^{13}C$ double resonance mode.

The $^{1}H$ spin-lattice relaxation time ($T_1$) and spin-lattice relaxation time in the rotating frame ($T_{1\rho}$) values of polymer samples were measured to evaluate the homogeneity of hydrophilic and hydrophobic TPU. In studies of amorphous solid dispersions, drug and polymer often have resolved peaks in $^{13}C$ spectra. Therefore, $^{13}C$-

detected relaxation measurements have been often utilized to extract relaxation values of drug and polymer components to evaluate their heterogeneity [44–50]. In this study however, we utilized a $^{1}$H-direct-detected relaxation measurement and double-component fitting to measure $^{1}$H $T_1$ and $T_{1\rho}$. Compared to $^{13}$C-detected experiments, a direct detection of $^{1}$H has much better sensitivity and thus significantly shorter acquisition time. The $^{1}$H spectra of the pure polymers extruded into films under similar conditions were measured as references. These reference spectra were utilized to quantify the hydrophilic and hydrophobic components. We found that the NMR quantified weight ratio of the two polymers matches well with the actual percentages of the two polymers in their extruded mixture, underscoring the quantitative nature of the $^{1}$H ssNMR method. Therefore, we utilized a double-component decay to fit all $T_1$ and $T_{1\rho}$ curves. The ratio of the two components comes from the weight ratio of hydrophilic and hydrophobic polymers.

For example, the peak areas $I(\tau)$ in $^{1}$H $T_1$ and $T_{1\rho}$ measurements were integrated in Bruker Topspin software and fitted by the following equations:

$$\boldsymbol{I(\tau) = S_0\left\{S_1\left[1 - e^{\left(-\tau/T_{1,1}\right)}\right] + S_2\left[1 - e^{\left(-\tau/T_{1,2}\right)}\right] + I_0\right\}} \quad (2.1)$$

$$\boldsymbol{I(\tau) = S_0\left\{S_1\left[1 - e^{\left(-\tau/T_{1\rho,1}\right)}\right] + S_2\left[1 - e^{\left(-\tau/T_{1\rho,2}\right)}\right] + I_0\right\}} \quad (2.2)$$

Where $\tau$ is the relaxation time interval, utilizing 32 time points from 0.01 to 8 s for the $^{1}$H $T_1$ and 1 to 50 ms for the $^{1}$H $T_{1\rho}$ measurement, respectively; $S_0$ is the global scaling factor of integration; $S_1$ and $S_2$ are the corresponding weight fractions of the two

components in the extruded samples, respectively. $T_{1,1}$ and $T_{1,2}$ for $T_1$ and $T_{1\rho,1}$ and $T_{1\rho,2}$ for $T_{1\rho}$ are the fitted relaxation times of the two polymer components.

#### *2.3.2.3 Assessment of Emtricitabine Permeability Through Polymer Films*

In order to assess changes in drug diffusion behavior through polymer films of different composition, apparent permeability was measured using a diffusion cell. A polymer film of each sample was cut using a hammer-driven hole punch and placed into a membrane holder. The membrane holder was spaced between two identical donor and acceptor chambers. Cross-type magnetic stir bars were added to each chamber. The drug solution was intended to model the core of a reservoir implant system, while the polymer film was intended to model the rate controlling membrane of the implant. A 1 mg/mL solution of emtricitabine in deionized water was added to the donor chamber, while pure deionized water was added to the acceptor chamber. The saturation solubility of emtricitabine in water is >100 mg/mL. A concentration of 1 mg/mL was selected to ensure sink conditions at early time points, such that there were sufficient time points to obtain an initial slope of the diffusion curve. The stirring speed was set at 400 rpm to minimize the boundary layer around the polymer membrane. Ultraviolet (UV) absorbance was measured in the acceptor chamber used a Pion Rainbow fiber optic system (Billerica, MA) equipped with a deuterium lamp and UV dip probes with 10 mm path length tips.

In order to calculate apparent permeability, a line was fit to the linear portion of the concentration-time curve. The average concentration over the first 12 hours of concentration data, assumed to be within the lag time where no drug has diffused into the acceptor chamber, was taken as effectively zero concentration. The time point where

these two lines intersect represented the start of steady state and was the earliest time point used to conduct a linear regression. The slope of the fitted line can be described as $\frac{dc}{dt}$ and was used to determine the apparent permeability ($P_{app}$) using Fick's first law of diffusion as shown in equation 2.3.

$$\boldsymbol{P_{app} = \frac{D}{h} = \frac{V\left(\frac{dc}{dt}\right)}{A(c_2 - c_1)}} \tag{2.3}$$

Where $V$ is the volume of the acceptor compartment (23 mL), $A$ is the exposed surface area of the membrane (1.54 $cm^2$), $c_2$ is the concentration in the donor compartment (1 mg/mL), and $c_1$ is the concentration is the acceptor compartment (0 mg/mL). The concentrations for the donor and acceptor compartments used in the calculation are good assumptions at early time points. The diffusion study was replicated three times for each polymer film sample.

#### *2.3.2.4 Impact of Water Swelling to Polymer Film Weight and Volume*

The impact of water on polymer film geometry was investigated by assessing changes to both the weight and volume of the film upon exposure to water. In order to assess the weight gain upon swelling, we measured a dynamic vapor sorption isotherm using a TA Instruments Q5000 thermogravimetric analyzer (New Castle, DE). The polymer film sample was dried at 60°C under nitrogen purge for 3 hours or until <0.001% weight change over 5 minutes was observed. The sample was then equilibrated to 21°C and 94% RH, 96% RH, and 98% RH each for 3 days or until <0.0005% weight change over 5 minutes was observed. After determining the equilibrium moisture content of the polymer film at each condition, we ran a linear regression on the data points and

extrapolated to 100% RH to obtain the water content in the polymer film when immersed in water.

To assess the volume change upon swelling, we cut thin cylindrical slabs of polymer film and measured diameter and thickness prior to hydration using a caliper and thickness gauge. Each film sample was placed into a separate beaker and filled with approximately 20 mL of deionized water. At each time point, we removed the polymer film from the beaker and measured its diameter and thickness. Initial and hydrated volumes were determined using the measured diameter ($d$) and thickness ($h$) and equation 4. The volume change was replicated three times for each polymer film sample.

$$\boldsymbol{V = \pi \left(\frac{d}{2}\right)^2 h} \tag{2.4}$$

#### *2.3.2.5 Statistical Analysis*

Statistical analysis was used to assess the impact of polymer mixture composition and extrusion process parameters on emtricitabine apparent permeability. Analysis of Variance (ANOVA) was conducted with bivariate fits of each parameter (composition, melt temperature, breakthrough time, and specific mechanical energy) on apparent permeability using JMP software by SAS Institute (Cary, NC). We grouped the data set into low and high hydrophilic polymer concentration cohorts and performed statistics separately for each group.

## 2.4 RESULTS

### 2.4.1 Film Fabrication

We varied the independent extrusion parameters (barrel temperature profile, screw speed, screw profile, and feed rates) in order to affect dependent process parameters as shown in Table A.1. Mixture composition was calculated by dividing the feed rate of the hydrophilic TPU by the total feed rate. Melt temperature was measured directly by a flush-mounted thermocouple at the die adapter. Specific mechanical energy was calculated by dividing the measured screw motor power draw by the total feed rate. Estimated breakthrough time is a measure of residence time. Briefly, we added color-dyed poly(ethylene) pellets to the extruder feed port while the process was running at steady state and recorded the time until the appearance of color was observed at the die. Thus, breakthrough time represents the leading edge of the residence time distribution. Breakthrough time was measured at several key runs. It was found to vary only with screw profile and total feed rate (not temperature or screw speed). Therefore, breakthrough time for most runs was estimated based on measurements of other runs using the same screw profile and total feed rate.

By varying the extrusion process parameters, we were able to achieve a wide range of dependent process parameters. Over the course of the 34-run composition range, we were able to vary the melt temperature from 164°C to 213°C. Lower melt temperatures could not be obtained due to equipment torque limitations. We varied the breakthrough time from 46 to 127 seconds, representing a nearly three-fold range of residence time. Specific mechanical energy ranged from 0.17 to 0.77 kW*hr/kg, with lower values also constrained by equipment torque limitations.

### 2.4.2 Emtricitabine Apparent Permeability Range Through TPU Mixtures and EVA Grades

We sought to investigate whether mixtures of hydrophilic and hydrophobic poly(urethane) would provide a broader range of apparent permeability of a hydrophilic drug compared with varying the vinyl acetate content of EVA. Figure 2.3 shows the range of emtricitabine apparent permeability achieved by either varying the poly(urethane) mixture composition or by varying the vinyl acetate content of the EVA copolymer. Varying the mixture composition between hydrophilic and hydrophobic poly(urethanes) offers a 736-fold range in emtricitabine apparent permeability, as opposed to a 3.4-fold apparent permeability range achieved by varying the vinyl acetate content.

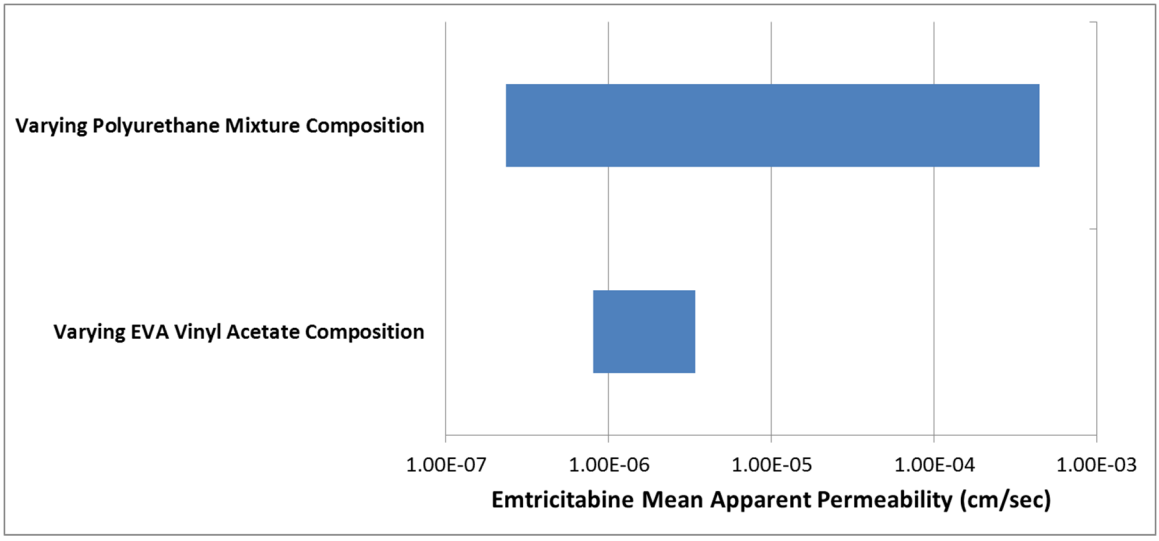


Figure 2.3: Range of emtricitabine mean apparent permeability achieved by varying hydrophobic/hydrophilic TPU ratio compared with that achieved by varying EVA vinyl acetate content. Film thickness varied between 50 and 200 μm.

### 2.4.3 Effect of Poly(urethane) Mixture Composition on Emtricitabine Apparent Permeability with a "Well Mixed" Process

In an effort to decouple our analysis of mixture composition and extrusion process impacts on permeability, we investigated the effect of poly(urethane) mixture composition on emtrictabine apparent permeability using only the extrusion process runs assumed to be "well mixed". In other words, we selected runs extruded with high breakthrough time, high specific mechanical energy, and high melt temperature. As shown in Figure 2.4, there is a negligible change in apparent permeability over polymer mixture compositions between 0% and 25% (w/w) hydrophilic TPU. Between 25% and 50% (w/w) hydrophilic TPU, there is an approximate 7-fold increase in apparent permeability. We observe a significant 123-fold jump in apparent permeability between 50% and 55% (w/w) hydrophilic TPU. Finally, there is a linear increase in the drug's apparent permeability through TPU membranes as the membrane composition changes from 55% to 100% (w/w) hydrophilic TPU.

(A)

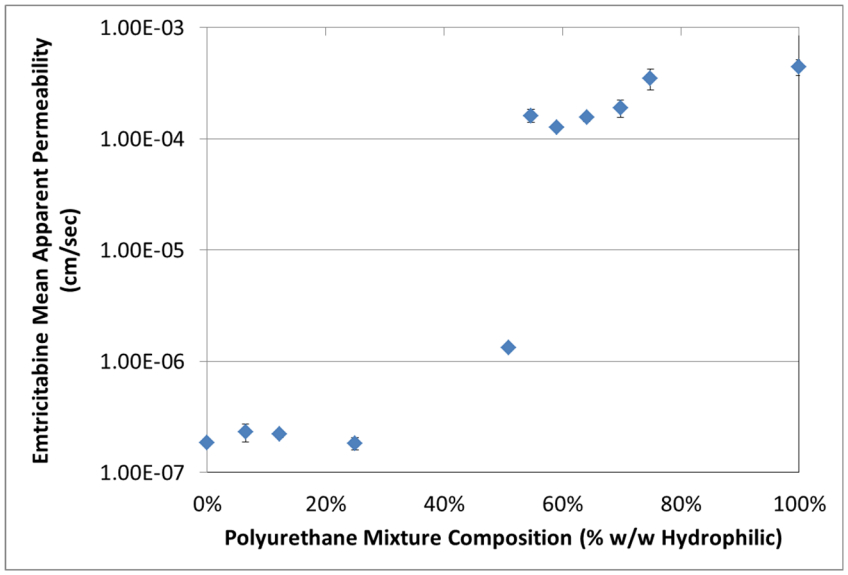


(B)

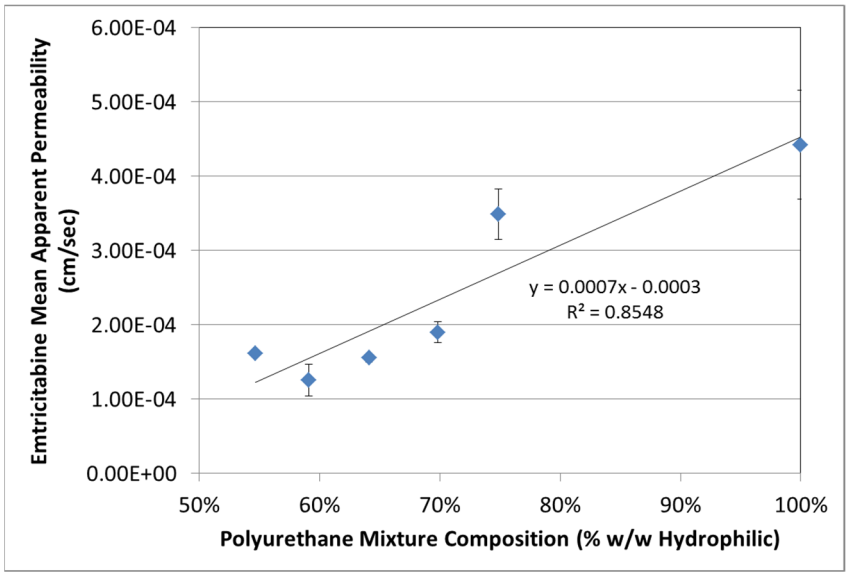


Figure 2.4: Mean apparent permeability of emtricitabine as a function of mixture composition for a "well mixed" extrusion process on a log-linear scale (A) and a higher hydrophilic TPU concentration samples on a rectilinear scale (B). Film thickness varied between 50 and 200 μm.

### 2.4.4 Effect of the Extrusion Process on Emtricitabine Apparent Permeability

In order to better assess the impact of extrusion process parameters on mean apparent permeability, the data were separated into low and high hydrophilic TPU concentration cohorts. Figure 2.5 offers a visual assessment of the relationship between the factors and the drug's permeability. Within the low hydrophilic TPU concentration group, there is no significant linear relationship between composition, melt temperature, breakthrough time, and specific mechanical energy on emtricitabine mean apparent permeability. Within the high hydrophilic TPU concentration group, there is a clear linear relationship of apparent permeability with polymer composition. However, there is no apparent relationship between any of the investigated process parameters used to manufacture the polymer film and permeability.

Bivariate ANOVA was performed to investigate the effect of TPU polymer composition and extrusion process parameters on emtricitabine apparent permeability. As described in Table 2.2, there was a statistically significant ($p < 0.05$) relationship observed between polymer composition and drug apparent permeability in the high hydrophilic TPU concentration group (>50% w/w hydrophilic TPU). However, there was no statistically significant effect of polymer composition on drug apparent permeability in the low hydrophilic TPU concentration group. Additionally, there was no statistically significant effect of any extrusion process parameter on emtricitabine apparent permeability across the polymer composition range.

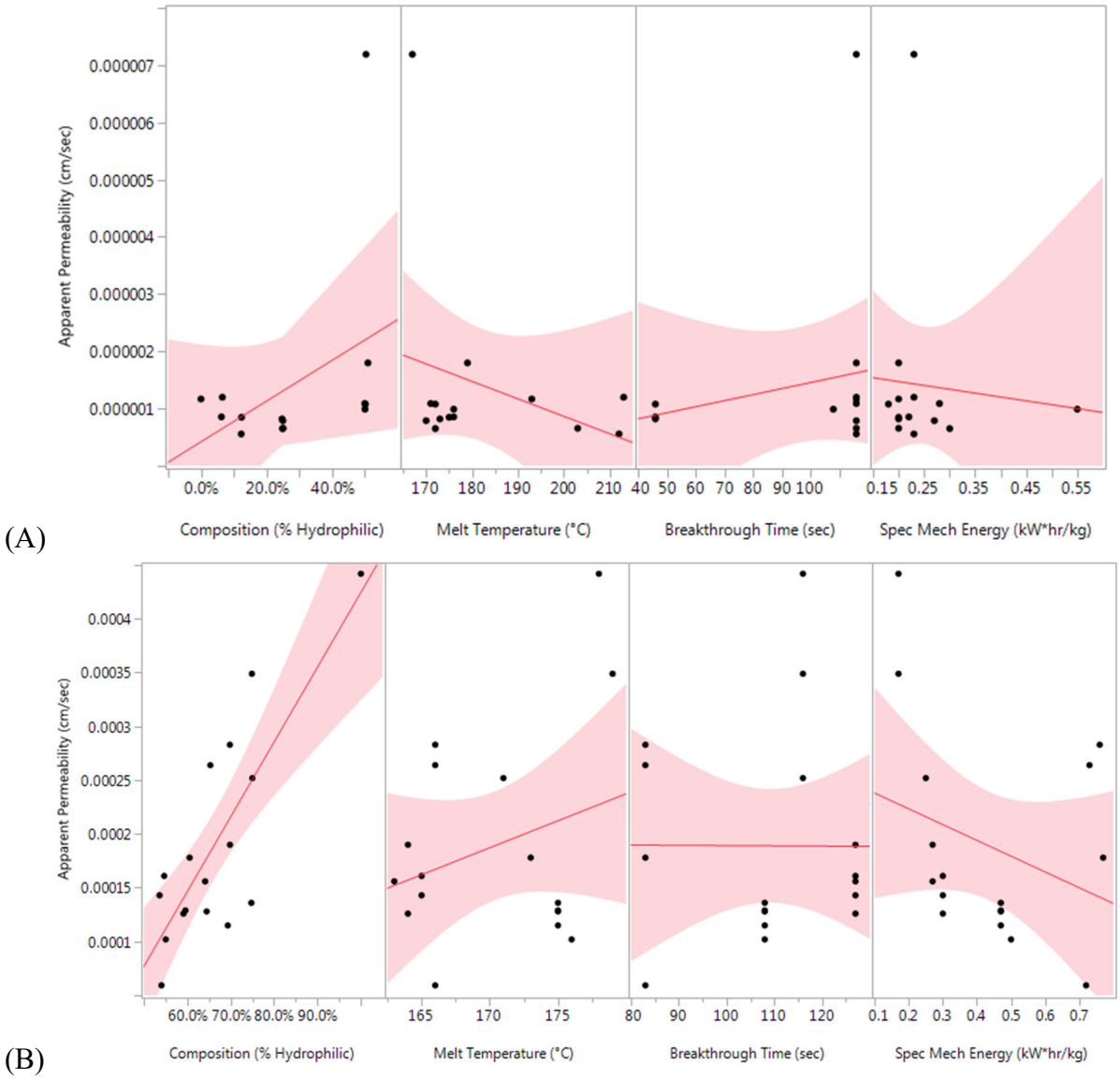


Figure 2.5: Effect of composition and extrusion dependent process parameters on emtricitabine mean apparent permeability for (A) mixtures ≤50% w/w hydrophilic TPU and (B) mixtures >50% w/w hydrophilic TPU. Black points represent actual data points. Red line represents regression line of the bivariate fit of apparent permeability with each factor. Red shaded region represents 95% confidence interval. Linear relationship between polymer composition and emtricitabine apparent permeability at higher hydrophilic TPU concentration is evident, however there is no apparent relationship between polymer composition and extrusion process parameters over the entire composition range.

Table 2.2: Summary of Analysis of Variance (ANOVA) statistics assessing the relationship between composition and extrusion process parameters on emtricitabine apparent permeability. Statistically significant ($p < 0.05$) relationship observed between TPU mixture composition and emtricitabine apparent permeability in the high hydrophilic TPU concentration group. All other factors were not statistically significant.

| Analysis Group | Factor | Coefficient of Determination, $r^2$ | F Ratio | P Value |
|---|---|---|---|---|
| **Low Hydrophilic TPU Concentration** | Composition | 0.188 | 2.78 | 0.122 |
| | Melt Temperature | 0.103 | 1.37 | 0.264 |
| | Breakthrough Time | 0.0375 | 0.467 | 0.507 |
| | Specific Mechanical Energy | 0.0049 | 0.0594 | 0.812 |
| **High Hydrophilic TPU Concentration** | Composition | 0.625 | 25.0 | 0.0002 |
| | Melt Temperature | 0.0702 | 1.13 | 0.304 |
| | Breakthrough Time | 0.0013 | 0.0196 | 0.891 |
| | Specific Mechanical Energy | 0.0724 | 1.17 | 0.296 |

### 2.4.5 Effect of Polymer Composition and Extrusion Process on Polymer Film Homogeneity

ssNMR relaxation measurements have been utilized to evaluate the heterogeneity of binary systems including polymer mixtures and drug-polymer amorphous solid dispersions [44–50]. Most previous studies of pharmaceutical dispersions have used $^{13}C$-detected relaxation time measurements for making use of the resolved carbon peak of API and polymer. In this study, the hydrophilic and hydrophobic TPU polymers exhibit fully overlapped carbon peaks as shown in Figure A.1. Therefore, we established a $^{1}H$-detected method for efficiently evaluating the miscibility of the two polymer components, as described in section 2.3.2.2. An example is illustrated in Figure A.2. $^{1}H$ ssNMR spectra of extruded pure hydrophobic TPU, pure hydrophilic TPU, and a mixture (50.11% hydrophilic contents) are shown in the left column of A, B, and C, respectively. The $^{1}H$ spectrum of the TPU mixture sample can be deconvoluted to two components by

utilizing the weight percentages (i.e., 49.89% and 50.11% for hydrophobic and hydrophilic TPUs, respectively).

Single component fitting was utilized for relaxation measurement of single component samples (i.e., pure hydrophobic and hydrophilic TPU references). Double component fitting for both $T_1$ and $T_{1\square}$ curves was utilized for the polymer mixture samples. In the double component fitting (equations 2.1 and 2.2), the weight fractions $S_1$ and $S_2$ of the two components in the extruded samples are the corresponding weight percentages. A single $T_1$ value (0.821 s) and two $T_{1\rho}$ values (1.79 ms and 8.86 ms) were identified. Interestingly, the $T_1$ fittings gave a single value for both hydrophilic and hydrophobic TPU components in each TPU sample. Previous studies have determined that a single $T_1$ value for a multicomponent system suggests that system is homogeneous at approximately 100 nm domain size [46,50].

Table 2.3 shows the $T_{1\rho}$ relaxation values fitted using double-component decay by taking into account the weight fraction of the two polymer components. At a given polymer mixture composition, there is no significant change to $T_{1\rho}$ for each polymer or to the difference in $T_{1\rho}$ between the two polymers. Since $T_{1\rho}$ is expected to correlate with the domain size of each polymer in the mixture, we conclude that there is no effect of the extrusion process parameters on polymer mixture homogeneity. We observe a decrease in the difference in $T_{1\rho}$ between the two TPU polymers with increasing hydrophilic TPU concentration, suggesting smaller domain size and better mixing at these concentrations.

Table 2.3: Homogeneity of poly(urethane) mixtures inferred by solid-state NMR using $T_{1\rho}$ by $^{1}H$ relaxation time. All $T_{1\rho}$ curves are fitted well using double-component decay by taking weight percent of the two polymer components into account.

| **Hydrophobic TPU** | | **Hydrophilic TPU** | | **$\Delta T_{1\rho}$ (ms)** | **Average $\Delta T_{1\rho}$ (ms)** |
|---|---|---|---|---|---|
| **Composition (% w/w)** | **$T_{1\rho}$ (ms)** | **Composition (% w/w)** | **$T_{1\rho}$ (ms)** | | |
| 100 | 4.04 | 0 | - | - | - |
| 0 | - | 100 | 16.50 | - | - |
| | | | | | |
| 75.31 | 3.03 | 24.69 | 14.85 | 11.82 | 11.26 |
| 75.05 | 3.04 | 24.95 | 14.68 | 11.64 | |
| 75.14 | 2.96 | 24.86 | 13.95 | 10.99 | |
| 75.00 | 3.07 | 25 | 13.64 | 10.57 | |
| | | | | | |
| 49.89 | 1.79 | 50.11 | 8.86 | 7.07 | 6.77 |
| 49.70 | 1.78 | 50.3 | 8.66 | 6.88 | |
| 50.08 | 1.78 | 49.92 | 8.45 | 6.67 | |
| 49.12 | 1.73 | 50.88 | 8.20 | 6.47 | |
| | | | | | |
| 45.31 | 1.62 | 54.69 | 8.09 | 6.47 | 6.31 |
| 45.94 | 1.62 | 54.06 | 7.98 | 6.36 | |
| 44.97 | 1.57 | 55.03 | 7.66 | 6.09 | |
| | | | | | |
| 35.88 | 1.37 | 64.12 | 6.77 | 5.40 | 5.26 |
| 34.69 | 1.33 | 65.31 | 6.65 | 5.32 | |
| 35.54 | 1.31 | 64.46 | 6.37 | 5.06 | |

### 2.4.6 Impact of Water Swelling to Polymer Film Weight and Volume

Figure 2.6 depicts the change in weight and volume to polymer films when they are immersed in water. The films exhibit a proportional increase in weight and volume with hydrophilic TPU concentration at equilibrium time points. However, kinetic studies

of volume change over time reveal a relatively slow rate of water transport into the films over the course of the first day.

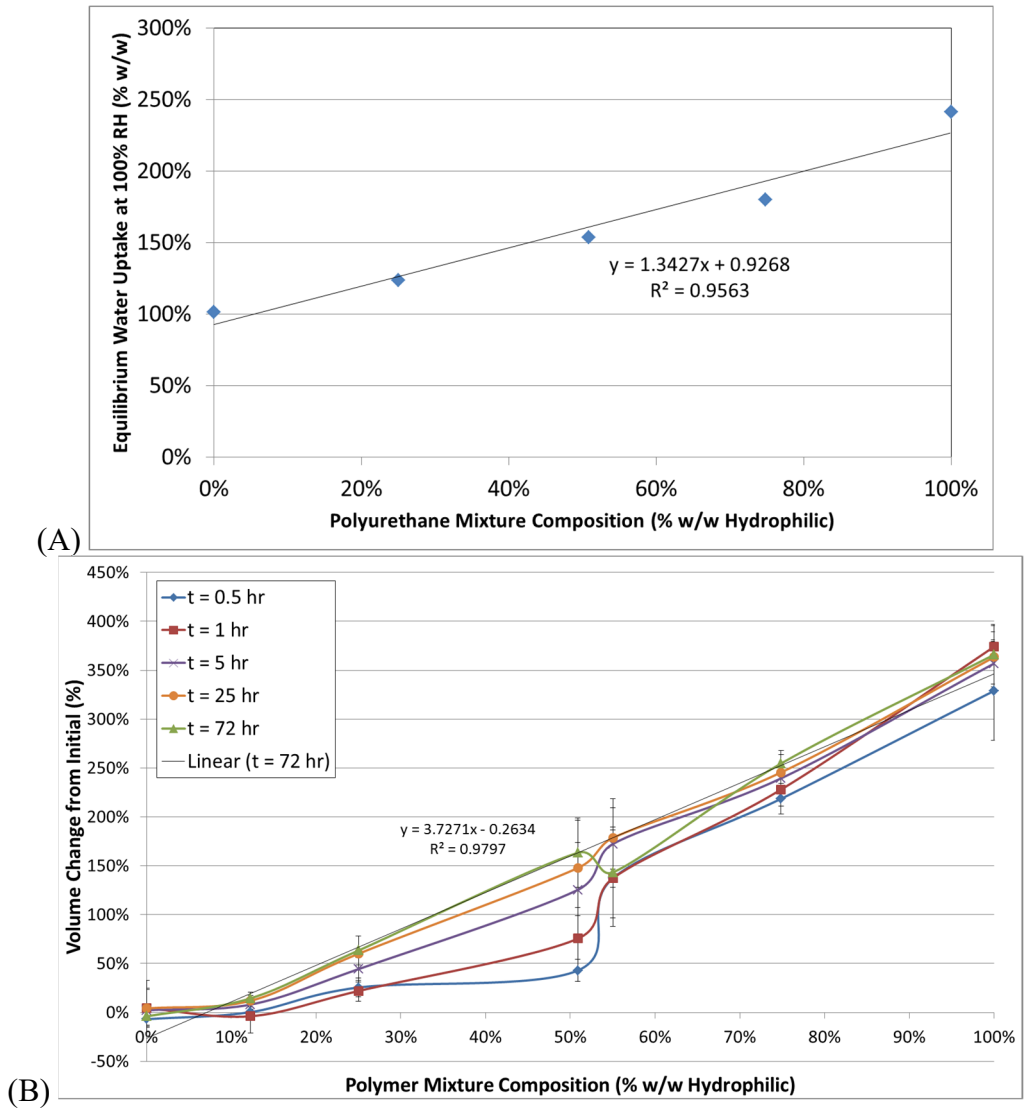


Figure 2.6: (A) Equilibrium weight change at 100% RH of poly(urethane) films of varying mixture composition; (B) volume change in poly(urethane) films over time from the initial dry state. Both plots depict a proportional relationship between water uptake and hydrophilic TPU concentration at equilibrium. However, the volume change plot describes a relatively slow rate of water transport into the polymer film over the course of 24 hours.

## 2.5 DISCUSSION

### 2.5.1 Emtricitabine Apparent Permeability Range Through TPU Mixtures and EVA Grades

As demonstrated in Figure 2.3, varying the TPU grade from hydrophobic to hydrophilic resulted in a nearly three order of magnitude range of apparent permeability, compared with an approximate three-fold change in apparent permeability when varying the EVA grade from 12% vinyl acetate to 40% vinyl acetate. We hypothesize that the difference in ranges between the two polymer systems is exacerbated by the use of emtricitabine as the model drug. As a hydrophilic, water soluble compound, emtricitabine is expected to have better solubility in the water-swollen systems relative to the non-swollen polymers. Drug dissolution in the polymer is a prerequisite for its diffusion through the polymer membrane.

The same phenomenon was reported by Clark et al. in their endeavor to create a single intravaginal ring capable of releasing two drugs of divergent physicochemical properties: tenofovir, a hydrophilic molecule and levonorgestrel, a hydrophobic compound [38]. In order to deliver each drug molecule at its target release rate, they developed a segmented ring with each component composed of a different polymer. Consequently, a more hydrophobic drug may exhibit a wider range of apparent permeability between the different EVA grades.

### 2.5.2 Effect of Extrusion Process on TPU Mixture Homogeneity and Emtricitabine Apparent Permeability

The extrusion process parameters were ranged to the limits of the equipment, resulting in a 50°C range of melt temperature, a nearly 3-fold range of breakthrough time, and a nearly 5-fold range of specific mechanical energy. Across this range, however we

observed no statistically significant changes in the polymer film properties as determined by ssNMR relaxation measurements and emtricitabine apparent permeability. The analysis suggests that the critical quality attributes of the polymer mixture are robust to broad changes in manufacturing process parameters.

These findings are somewhat in contrast to prior work with aqueous coatings demonstrating an effect of particle size of the dispersed polymer on drug release kinetics [51,52]. Those studies linked the particle size of components used in mixed polymer membranes to a critical volume fraction necessary to form a continuous phase. Although our study did not explicitly vary polymer particle size, extrusion process parameters have been routinely correlated to extent of mixing [53–55] and may be expected to affect volume fraction of each component. Therefore, it was surprising to find no significant relationship between process parameters and homogeneity or permeability.

The consistent homogeneity of the polymer mixture may be explained by an examination of the chemical structures of the two polymers (Figure 2.1). The polymers have identical hard segments and their soft segment monomers differ only by a length of two carbons [56]. Although the polymers exhibit dramatically different behavior in water, their similar chemistries imply good miscibility between them. Although it was not explicitly studied in the previously described studies identifying an effect of particle size on extent of mixing, we speculate that the components in those studied are immiscible.

### 2.5.3 Effect of TPU Mixture Composition on Emtricitabine Apparent Permeability

Despite the preponderance of published studies showing tablet film coats facilitating a range of drug release rates by varying the ratio of hydrophobic and hydrophilic components in the mixture [39,40,57–61], we did not observe a proportional

change in drug apparent permeability with changes in the polymer mixture composition. As shown in Figure 2.4, we observed minimal effect of increasing hydrophilic TPU content in the mixture on emtricitabine apparent permeability at concentrations ≤50% (w/w) hydrophilic TPU. A statistical analysis also revealed no significant ($p < 0.05$) effect of polymer composition on emtricitabine apparent permeability at concentrations ≤50% (w/w) hydrophilic TPU (Table 2.2). Notably, there was a proportional increase in polymer film weight and volume with increased hydrophilic TPU content when the samples were soaked in water to equilibrium time points (Figure 2.6). In other words, the data initially suggested that emtricitabine apparent permeability through the polymer is not affected by hydrophilic TPU content over this composition range, while water apparent permeability appears to change proportionally.

At hydrophilic TPU concentrations ≥55% (w/w), the apparent permeability of emtricitabine through the polymer membrane increases in a linear relationship ($r^2 = 0.85$) with polymer composition. An ANOVA analysis verified the statistical significance ($p < 0.05$) of the relationship between drug permeability and polymer content over this composition range. This experimental observation is also in line with data showing a proportional change in polymer weight and volume with polymer mixture composition (Figure 2.6). It has been previously shown that drug permeability through a polymer system is dependent on extent of water penetration into it [62]. As described by Siepmann and Peppas, water swelling results in two substantial impacts: (1) volume changes to the system, resulting in drug concentration changes, and (2) mobility changes to the polymers, leading to increased diffusivity of both water and drug.

Most significantly, we observed an approximate 123-fold increase in emtricitabine apparent permeability through the polymer films when the hydrophilic TPU

concentration was increased from 50% to 55% (w/w). Although this mixed system of hydrophilic and hydrophobic TPUs has not been well studied in the literature, a patent by Kleiner et al. describes blending a hydrophilic TPU with a hydrophobic TPU to achieve a target water swelling extent and drug permeability [41]. However, the authors examined a single composition of 65% (w/w) hydrophilic TPU which is within the linear region of our data set. Consequently, although the publication might imply a broader ability to blend TPUs to achieve a target drug release rate, their data set was insufficient to comprehensively conclude such a possibility.

In order to better understand the physical relevance of this apparent step change, we calculated the free diffusion coefficient of emtricitabine in water. We assumed that the viscosity of the solvent was slightly higher than pure water because the polymer's PEO groups are likely hydrated when the polymer is immersed in water, thus increasing the local viscosity. In order to compare this calculation to our measured permeability values, we then converted the diffusion coefficient to an effective permeability by assuming diffusion path length through water.

The free diffusion coefficient of emtricitabine in water can be determined using the Wilke and Chang equation [63] as described in equation 2.5.

$$\boldsymbol{D = 7.4 \times 10^{-8} \frac{(xM)^{0.5} T}{\eta V^{0.6}}} \qquad (2.5)$$

The temperature (T) was assumed to be 294.15 K, the association constant ($x$) was assumed to be 2.6 for the solvent water, and the molecular weight of the solvent water (M) was assumed to be 18.02 Da. The viscosity of the solvent (η) was assumed to be 10 cP, based on previously published data measuring the viscosity of a 20% polyethylene

glycol 3350 aqueous solution [64]. The atomic volume of emtricitabine (V) was calculated to be 26.9 cc/mol [65].

Using equation 2.5, the diffusivity of emtricitabine in water was calculated to be 2.07 x $10^{-6}$ $cm^2$/sec. Throughout this chapter, we have reported apparent permeability instead of diffusivity in order to account for film thickness variability and boundary layer differences between samples. In order to compare this value to our measured permeability values, we have calculated an effective permeability of emtricitabine through water of an assumed thickness. We achieve this conversion using equation 2.6 [66]:

$$\boldsymbol{P_{FTC,water}} = \frac{\boldsymbol{D_{FTC,water}}}{\boldsymbol{h}} \tag{2.6}$$

Where $D_{FTC,water}$ is the calculated diffusion coefficient of emtricitabine in water and $h$ is the assumed thickness of the diffusion layer. The extruded polymer film thickness varied from 50 to 200 μm. Assuming diffusion path lengths of 50 μm and 200 μm, we estimate the permeability of emtricitabine through water of a similar thickness to the TPU membranes to be in the range of 1.03 x $10^{-4}$ to 4.13 x $10^{-4}$ cm/sec.

It is noteworthy that the estimated permeability of emtricitabine through water is comparable to the measured permeability of emtricitabine through the polymer membranes at hydrophilic TPU content ≥55% (w/w). This finding suggests that the primary path of drug diffusion through the polymer membrane over this composition range is through a viscous aqueous phase.

Percolation theory may be used to explain the drug permeability behavior in the TPU mixture system. As described by Mohanty et al., percolation theory applies to

multicomponent, multiphase systems involving interspersions of complicated morphology [67]. They illustrated the concept of a percolation threshold by describing a hypothetical composite in which material *i* can exist as either isolated clusters surrounded by other materials or in regions that allow passage through material *i* from one side of the sample to the other without leaving material *i*. In this illustration, the volume fraction of material *i,* $\varphi_i$, can be split into the following:

$$\boldsymbol{\varphi_i = \varphi_i^I + \varphi_i^A} \tag{2.7}$$

Where $\varphi_i^I$ is the total volume fraction of material *i* existing as isolated clusters, while $\varphi_i^A$ represents the total volume fraction of *i* that is accessible to solutes. According to percolation theory, if $\varphi_i$ is below a critical value, known as the percolation threshold, then $\varphi_i^A$ is zero and all of material *i* exists in the sample as isolated clusters.

We propose that a percolation threshold is achieved in the system between 50 and 55% (w/w) hydrophilic TPU [68,69]. There is insufficient hydrophilic TPU in the mixture to form a continuous network at concentrations ≤50% hydrophilic TPU. Figure 2.7 depicts a two-dimensional cartoon of the proposed three-dimensional mechanism of drug diffusion through the TPU mixture below and above the percolation threshold. It depicts the hydrophobic domains as the continuous phase and the hydrophilic domains as the discrete phase.

As illustrated in Figure 2.7, water diffuses into the polymer and causes hydrophilic domains to swell with the PEO domains of the poly(urethane) dissolved in the water. At concentrations below the percolation threshold, however, those hydrophilic regions are discrete. We have measured the permeability of emtricitabine through pure

hydrophobic TPU and pure hydrophilic TPU and observe diffusion through a hydrophobic TPU membrane to be approximately 1000-fold slower than a hydrophilic TPU (Figure 2.3). As drug diffuses through the polymer mixture, its transport is rate limited by the significantly slower rate associated with diffusivity of drug in the hydrophobic TPU, since a continuous hydrophilic TPU phase does not exist.

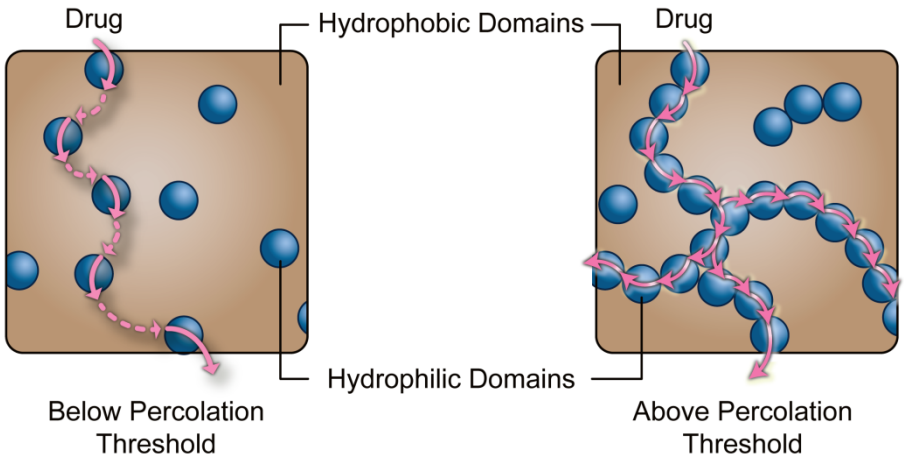


Figure 2.7: Conceptual illustration of mechanism of drug diffusion through polymer mixture below and above the percolation threshold. The cartoon depicts the hydrophobic domains as the continuous phase and the hydrophilic domains as the discrete phase. Above the percolation threshold, drug is able to diffuse within the polymer entirely through water-filled pores.

Between 50% and 55% (w/w) hydrophilic TPU content, we propose that there is sufficient hydrophilic polymer in the mixture to form a continuous network. Our studies assessing the rate and extent of water transport into the polymer mixtures (Figure 2.6) feature a clear differential between 50% and 55% (w/w) hydrophilic TPU compositions at early time points, but the difference in weight and volume increase of the 50% and 55% (w/w) films soaked in water is negligible by 24 hours. Water diffusion through the

continuous phase of hydrophobic TPU is significantly slower than its transport through hydrophilic TPU, but the slower rate is still sufficiently fast to come to equilibrium within one day. We expect this is driven by the low molecular weight of water (18 Da) compared with the comparatively larger drug molecule (247 Da).

The sigmoidal behavior we observe with this polymer system is more typically observed for mixed component systems where the discrete phase can be described as "porous aggregates". As articulated by Nielsen, this system is one in which the second component is highly permeable to the solute but poorly dispersed [70]. This behavior was observed by Siepmann et al. when they compared theophylline release from pellets coated with aqueous dispersions of ethylcellulose and either hydroxypropyl methylcellulose acetate succinate (HPMCAS) or Eudragit® L [52]. Ethylcellulose is insoluble in water, while both HPMCAS and Eudragit® L are anionic polymers soluble in aqueous media at approximately pH > 6. They observed a similar step change in the relationship between drug release rate and polymer mixture composition for the ethylcellulose/HPMCAS formulation and a relatively incremental change in drug release rate with polymer composition changes for the ethylcellulose/Eudragit® L system. They attributed the difference in behavior to the large particle size of HPMCAS, which they demonstrated did not disperse as well as Eudragit® L, resulting in large voids that are highly permeable to drug. However, our ssNMR data of the TPU system in this present work showing no effect of process parameters on polymer mixture homogeneity (Table 2.3), as well as a single $T_1$ relaxation value for all mixed TPU samples, would imply that the two polymers are well mixed.

One may envision voids formed by water soluble components that dissolve when the membrane is hydrated in the study described by Siepmann et al. In our studied

polymer system however, both polymers are water insoluble. Amighi et al. had previously studied the effect of polymer blend ratio on drug release from pellets coated with Eudragit® RL/Eudragit® RS mixtures [39]. The two polymers are insoluble in water and contain different amounts of quaternary ammonium groups, which result in differing mobility within the polymer networks [71]. They observed an incremental change in drug release rate with polymer mixture composition. Lyu et al. measured dexamethasone release rate from films composed of mixtures of two thermoplastic poly(urethanes) [61]. They observed a similar incremental change in drug release rate with changes in polymer mixture composition.

We propose that our studied mixture of two water insoluble thermoplastic poly(urethanes) behaves more like a porous aggregate system due to two consequences of the water-swelling behavior of the hydrophilic TPU. Firstly, although the hydrophilic polymer is finely dispersed throughout the mixture in the dry state, it swells to such a degree that its volume fraction changes substantially in the hydrated state. As we described in Figure 2.6, the pure hydrophilic TPU exhibited a 365% increase in volume from its initial dry state after 3 days soaking in water. Secondly, the hydrophilic TPU domains draw in so much water that hydrophilic emtricitabine is highly permeable through them.

Alternatively, one may hypothesize that increased drug permeability through the polymer mixture at higher hydrophilic content was simply due to increases in drug diffusivity driven by polymer swelling resulting in changes to free volume of diffusion [72]. Another potential explanation of the observed data relates to drug binding or a strong interaction with hydrophobic polymer domains. As hydrophilic TPU content in the polymer increases, the number of hydrophobic domains decreases resulting in a lower

extent of binding. However, if either of these phenomena were occurring, one would expect to observe a gradual increase in apparent permeability with increased hydrophilic TPU composition. Instead, we observe a large increase between 50% and 55% (w/w) hydrophilic TPU.

## 2.6 CONCLUSION

In this study, we sought to assess the feasibility of mixing hydrophobic and hydrophilic thermoplastic poly(urethanes) to tune the drug release rate from an implant in which the rate-controlling membrane was composed of the polymer mixture. We demonstrated the capability of varying TPU hydrophilicity to more broadly vary the diffusion rate of a hydrophilic model drug compared with varying the crystallinity of EVA. Although we showed that drug permeability through pure hydrophilic TPU was orders of magnitude higher than through hydrophobic TPU, we were unable to tailor drug release to intermediate rates. Consequently, our data suggest that the best way to tailor the drug release rate with thermoplastic poly(urethanes) is to select a hydrophilic TPU with the appropriate soft segment content to result in the desired drug diffusion rate. Verstraete et al. have previously demonstrated the ability to modulate the release rate of drugs with varying physicochemical properties by selecting thermoplastic poly(urethanes) of varying hydrophilicity [35]. Our proposed explanation for the observed behavior has not been verified with direct measurements and subsequent work is needed to experimentally support or refute the hypothesis.

## 2.7 REFERENCES


[1] K.B.H. Zolnierek, M.R. Dimatteo, Physician communication and patient adherence to treatment: a meta-analysis., Med. Care. 47 (2009) 826–34. doi:10.1097/MLR.0b013e31819a5acc.

[2] A.J. Claxton, J. Cramer, C. Pierce, A systematic review of the associations between dose regimens and medication compliance., Clin. Ther. 23 (2001) 1296–310. http://www.ncbi.nlm.nih.gov/pubmed/11558866 (accessed September 4, 2018).

[3] J.B. Nachega, M. Hislop, D.W. Dowdy, R.E. Chaisson, L. Regensberg, G. Maartens, Adherence to Nonnucleoside Reverse Transcriptase Inhibitor–Based HIV Therapy and Virologic Outcomes, Ann. Intern. Med. 146 (2007) 564. doi:10.7326/0003-4819-146-8-200704170-00007.

[4] J.B. Nachega, V.C. Marconi, G.U. van Zyl, E.M. Gardner, W. Preiser, S.Y. Hong, E.J. Mills, R. Gross, HIV treatment adherence, drug resistance, virologic failure: evolving concepts., Infect. Disord. Drug Targets. 11 (2011) 167–74. http://www.ncbi.nlm.nih.gov/pubmed/21406048 (accessed September 4, 2018).

[5] M. Gisslén, V. Svedhem, L. Lindborg, L. Flamholc, H. Norrgren, S. Wendahl, M. Axelsson, A. Sönnerborg, Sweden, the first country to achieve the Joint United Nations Programme on HIV/AIDS (UNAIDS)/World Health Organization (WHO) 90-90-90 continuum of HIV care targets, HIV Med. 18 (2017) 305–307. doi:10.1111/hiv.12431.

[6] L. Baert, G. van ‘t Klooster, W. Dries, M. François, A. Wouters, E. Basstanie, K. Iterbeke, F. Stappers, P. Stevens, L. Schueller, P. Van Remoortere, G. Kraus, P. Wigerinck, J. Rosier, Development of a long-acting injectable formulation with nanoparticles of rilpivirine (TMC278) for HIV treatment, Eur. J. Pharm. Biopharm. 72 (2009) 502–508. doi:10.1016/J.EJPB.2009.03.006.

[7] C. Trezza, S.L. Ford, W. Spreen, R. Pan, S. Piscitelli, Formulation and pharmacology of long-acting cabotegravir., Curr. Opin. HIV AIDS. 10 (2015) 239–45. doi:10.1097/COH.0000000000000168.

[8] J.M. Cortez, R. Quintero, J.A. Moss, M. Beliveau, T.J. Smith, M.M. Baum, Pharmacokinetics of injectable, long-acting nevirapine for HIV prophylaxis in breastfeeding infants., Antimicrob. Agents Chemother. 59 (2015) 59–66. doi:10.1128/AAC.03906-14.

[9] S.E. Barrett, R.S. Teller, S.P. Forster, L. Li, M.A. Mackey, D. Skomski, Z. Yang, K.L. Fillgrove, G.J. Doto, S.L. Wood, J. Lebron, J.A. Grobler, R.I. Sanchez, Z. Liu, B. Lu, T. Niu, L. Sun, M.E. Gindy, Extended Duration MK-8591-Eluting

Implant as a Candidate for HIV Treatment and Prevention., Antimicrob. Agents Chemother. (2018) AAC.01058-18. doi:10.1128/AAC.01058-18.

[10] M. Gunawardana, M. Remedios-Chan, C.S. Miller, R. Fanter, F. Yang, M.A. Marzinke, C.W. Hendrix, M. Beliveau, J.A. Moss, T.J. Smith, M.M. Baum, Pharmacokinetics of Long-Acting Tenofovir Alafenamide (GS-7340) Subdermal Implant for HIV Prophylaxis, Antimicrob. Agents Chemother. 59 (2015) 3913–3919. doi:10.1128/aac.00656-15.

[11] F. Bauss, R.G. Russell, Ibandronate in osteoporosis: preclinical data and rationale for intermittent dosing, Osteoporos. Int. 15 (2004) 423–433. doi:10.1007/s00198-004-1612-7.

[12] A.R. Kirtane, O. Abouzid, D. Minahan, T. Bensel, A.L. Hill, C. Selinger, A. Bershteyn, M. Craig, S.S. Mo, H. Mazdiyasni, C. Cleveland, J. Rogner, Y.-A.L. Lee, L. Booth, F. Javid, S.J. Wu, T. Grant, A.M. Bellinger, B. Nikolic, A. Hayward, L. Wood, P.A. Eckhoff, M.A. Nowak, R. Langer, G. Traverso, Development of an oral once-weekly drug delivery system for HIV antiretroviral therapy, Nat. Commun. 9 (2018) 2. doi:10.1038/s41467-017-02294-6.

[13] J.M. Kane, M. Eerdekens, J.-P. Lindenmayer, S.J. Keith, M. Lesem, K. Karcher, Long-Acting Injectable Risperidone: Efficacy and Safety of the First Long-Acting Atypical Antipsychotic, Am. J. Psychiatry. 160 (2003) 1125–1132. doi:10.1176/appi.ajp.160.6.1125.

[14] W.R. Spreen, D.A. Margolis, J.C. Pottage, Jr., Long-acting injectable antiretrovirals for HIV treatment and prevention., Curr. Opin. HIV AIDS. 8 (2013) 565–71. doi:10.1097/COH.0000000000000002.

[15] T.M.. Mulders, T.O.. Dieben, Use of the novel combined contraceptive vaginal ring NuvaRing for ovulation inhibition, Fertil. Steril. 75 (2001) 865–870. doi:10.1016/S0015-0282(01)01689-2.

[16] S.H. Perry, P. Swamy, G.A. Preidis, A. Mwanyumba, N. Motsa, H.N. Sarero, Implementing the Jadelle implant for women living with HIV in a resource-limited setting, AIDS. 28 (2014) 791–793. doi:10.1097/QAD.0000000000000177.

[17] J. Siepmann, F. Siepmann, Mathematical modeling of drug delivery, Int. J. Pharm. 364 (2008) 328–343. doi:10.1016/j.ijpharm.2008.09.004.

[18] C.J. Timmer, T.M.T. Mulders, Pharmacokinetics of Etonogestrel and Ethinylestradiol Released from a Combined Contraceptive Vaginal Ring, Clin. Pharmacokinet. 39 (2000) 233–242. doi:10.2165/00003088-200039030-00005.

[19] S. Palomba, A. Falbo, A. Di Cello, C. Materazzo, F. Zullo, Nexplanon: The new implant for long-term contraception. A comprehensive descriptive review, Gynecol. Endocrinol. 28 (2012) 710–721. doi:10.3109/09513590.2011.652247.

[20] J. White, J. Bell, J.B. Saunders, P. Williamson, M. Makowska, A. Farquharson, K.L. Beebe, Open-label dose-finding trial of buprenorphine implants (Probuphine)® for treatment of heroin dependence, Drug Alcohol Depend. 103 (2009) 37–43. doi:10.1016/J.DRUGALCDEP.2009.03.008.

[21] A. Almeida, L. Brabant, F. Siepmann, T. De Beer, W. Bouquet, L. Van Hoorebeke, J. Siepmann, J.P. Remon, C. Vervaet, Sustained release from hot-melt extruded matrices based on ethylene vinyl acetate and polyethylene oxide, Eur. J. Pharm. Biopharm. 82 (2012) 526–533. doi:10.1016/J.EJPB.2012.08.008.

[22] P. Tallury, N. Alimohammadi, S. Kalachandra, Poly(ethylene-co-vinyl acetate) copolymer matrix for delivery of chlorhexidine and acyclovir drugs for use in the oral environment: effect of drug combination, copolymer composition and coating on the drug release rate., Dent. Mater. 23 (2007) 404–9. doi:10.1016/j.dental.2006.02.011.

[23] C. Schneider, R. Langer, D. Loveday, D. Hair, Applications of ethylene vinyl acetate copolymers (EVA) in drug delivery systems, J. Control. Release. 262 (2017) 284–295. doi:10.1016/J.JCONREL.2017.08.004.

[24] S.J. Lue, D.-T. Lee, J.-Y. Chen, C.-H. Chiu, C.-C. Hu, Y.C. Jean, J.-Y. Lai, Diffusivity enhancement of water vapor in poly(vinyl alcohol)–fumed silica nano-composite membranes: Correlation with polymer crystallinity and free-volume properties, J. Memb. Sci. 325 (2008) 831–839. doi:10.1016/J.MEMSCI.2008.09.015.

[25] Y. Kong, J.N. Hay, The measurement of the crystallinity of polymers by DSC, Polymer (Guildf). 43 (2002) 3873–3878. doi:10.1016/S0032-3861(02)00235-5.

[26] M.B. Lowinger, S.E. Barrett, F. Zhang, R.O. Williams, Sustained Release Drug Delivery Applications of Polyurethanes, Pharmaceutics. 10 (2018) 55. doi:10.3390/pharmaceutics10020055.

[27] T.J. Johnson, K.M. Gupta, J. Fabian, T.H. Albright, P.F. Kiser, Segmented polyurethane intravaginal rings for the sustained combined delivery of antiretroviral agents dapivirine and tenofovir, Eur. J. Pharm. Sci. 39 (2010) 203–212. doi:10.1016/J.EJPS.2009.11.007.

[28] L.C. Costantini, The Development of ProNeura Technology for the Treatment of Addictions, in: Opiate Recept. Antagon., Humana Press, Totowa, NJ, 2009: pp. 689–708. doi:10.1007/978-1-59745-197-0_37.

[29] R.A. Patel, L.R. Bucalo, Implantable polymeric device for sustained release of buprenorphine, US7736665B2, 2002. https://patents.google.com/patent/US20040033250A1/en?assignee=titan+pharmaceuticals&oq=titan+pharmaceuticals (accessed September 17, 2018).

[30] A.J. Coury, P.C. Slaikeu, P.T. Cahalan, K.B. Stokes, C.M. Hobot, Factors and

Interactions Affecting the Performance of Polyurethane Elastomers in Medical Devices, J. Biomater. Appl. 3 (1988) 130–179. doi:10.1177/088532828800300202.

[31] M. Habash, G. Reid, Microbial Biofilms: Their Development and Significance for Medical Device-Related Infections, J. Clin. Pharmacol. 39 (1999) 887–898. doi:10.1177/00912709922008506.

[32] K. Stokes, R. McVenes, J.M. Anderson, Polyurethane Elastomer Biostability, J. Biomater. Appl. 9 (1995) 321–354. doi:10.1177/088532829500900402.

[33] J.Y. Cherng, T.Y. Hou, M.F. Shih, H. Talsma, W.E. Hennink, Polyurethane-based drug delivery systems, Int. J. Pharm. 450 (2013) 145–162. doi:10.1016/j.ijpharm.2013.04.063.

[34] S. Gogolewski, Selected topics in biomedical polyurethanes. A review, Colloid Polym. Sci. 267 (1989) 757–785. doi:10.1007/BF01410115.

[35] G. Verstraete, J. Van Renterghem, P.J. Van Bockstal, S. Kasmi, B.G. De Geest, T. De Beer, J.P. Remon, C. Vervaet, Hydrophilic thermoplastic polyurethanes for the manufacturing of highly dosed oral sustained release matrices via hot melt extrusion and injection molding, Int. J. Pharm. 506 (2016) 214–221. doi:10.1016/J.IJPHARM.2016.04.057.

[36] Y. Ikeda, S. Kohjiya, S. Takesako, S. Yamashita, Polyurethane elastomer with PEO-PTMO-PEO soft segment for sustained release of drugs, Biomaterials. 11 (1990) 553–560. doi:10.1016/0142-9612(90)90077-4.

[37] T. Higuchi, Mechanism of sustained-action medication. Theoretical analysis of rate of release of solid drugs dispersed in solid matrices, J. Pharm. Sci. 52 (1963) 1145–1149. doi:10.1002/jps.2600521210.

[38] J.T. Clark, M.R. Clark, N.B. Shelke, T.J. Johnson, E.M. Smith, A.K. Andreasen, J.S. Nebeker, J. Fabian, D.R. Friend, P.F. Kiser, Engineering a Segmented Dual-Reservoir Polyurethane Intravaginal Ring for Simultaneous Prevention of HIV Transmission and Unwanted Pregnancy, PLoS One. 9 (2014) e88509. doi:10.1371/journal.pone.0088509.

[39] K. Amighi, A.J. Moës, Evaluation of Thermal and Film Forming Properties of Acrylic Aqueous Polymer Dispersion Blends: Application to the Formulation of Sustained-Release Film Coated Theophylline Pellets, Drug Dev. Ind. Pharm. 21 (1995) 2355–2369. doi:10.3109/03639049509070874.

[40] F. Lecomte, J. Siepmann, M. Walther, R.. MacRae, R. Bodmeier, Blends of enteric and GIT-insoluble polymers used for film coating: physicochemical characterization and drug release patterns, J. Control. Release. 89 (2003) 457–471. doi:10.1016/S0168-3659(03)00155-X.

[41] L.W. Kleiner, R.M. Gale, R.G. Berggren, G.T. Tong, G. Chen, K.E. Dionne, P.R.

Houston, Rate controlling membranes for controlled drug delivery devices, US6375978B1, 1997. https://patents.google.com/patent/US6375978B1/en (accessed September 17, 2018).

[42] T. Dinh, R. Sparer, S. Lyu, K. Dang, C. Hobot, Active agent delivery systems including a miscible polymer blend, medical devices, and methods, US20050064005A1, 2003.

[43] J. Rosenblatt, I. Raad, Antimicrobial catheters, US20160074560A1, 2013. https://patents.google.com/patent/US20160074560A1/en?q=polyurethane&q=tecophilic&q=tecoflex&q=blends&oq=polyurethane+tecophilic+tecoflex+blends (accessed September 17, 2018).

[44] R.-R. Wu, H.-M. Kao, J.-C. Chiang, E.. Woo, Solid-state NMR studies on phase behavior and motional mobility in binary blends of polystyrene and poly(cyclohexyl methacrylate), Polymer (Guildf). 43 (2002) 171–176. doi:10.1016/S0032-3861(01)00570-5.

[45] Y. Aso, S. Yoshioka, T. Miyazaki, T. Kawanishi, K. Tanaka, S. Kitamura, A. Takakura, T. Hayashi, N. Muranushi, Miscibility of Nifedipine and Hydrophilic Polymers as Measured by 1H-NMR Spin–Lattice Relaxation, Chem. Pharm. Bull. (Tokyo). 55 (2007) 1227–1231. doi:10.1248/cpb.55.1227.

[46] X. Yuan, D. Sperger, E.J. Munson, Investigating Miscibility and Molecular Mobility of Nifedipine-PVP Amorphous Solid Dispersions Using Solid-State NMR Spectroscopy, Mol. Pharm. 11 (2014) 329–337. doi:10.1021/mp400498n.

[47] F. Yang, Y. Su, J. Zhang, J. DiNunzio, A. Leone, C. Huang, C.D. Brown, Rheology Guided Rational Selection of Processing Temperature To Prepare Copovidone–Nifedipine Amorphous Solid Dispersions via Hot Melt Extrusion (HME), Mol. Pharm. 13 (2016) 3494–3505. doi:10.1021/acs.molpharmaceut.6b00516.

[48] M.A. Mensink, M.J. Nethercott, W.L.J. Hinrichs, K. van der Voort Maarschalk, H.W. Frijlink, E.J. Munson, M.J. Pikal, Influence of Miscibility of Protein-Sugar Lyophilizates on Their Storage Stability, AAPS J. 18 (2016) 1225–1232. doi:10.1208/s12248-016-9937-7.

[49] H.S. Purohit, J.D. Ormes, S. Saboo, Y. Su, M.S. Lamm, A.K.P. Mann, L.S. Taylor, Insights into Nano- and Micron-Scale Phase Separation in Amorphous Solid Dispersions Using Fluorescence-Based Techniques in Combination with Solid State Nuclear Magnetic Resonance Spectroscopy, Pharm. Res. 34 (2017) 1364–1377. doi:10.1007/s11095-017-2145-z.

[50] M. Hanada, S. V. Jermain, X. Lu, Y. Su, R.O. Williams, Predicting physical stability of ternary amorphous solid dispersions using specific mechanical energy in a hot melt extrusion process, Int. J. Pharm. 548 (2018) 571–585.

doi:10.1016/J.IJPHARM.2018.07.029.

[51] R.P. Kusy, Influence of particle size ratio on the continuity of aggregates, J. Appl. Phys. 48 (1977) 5301–5305. doi:10.1063/1.323560.

[52] F. Siepmann, J. Siepmann, M. Walther, R.J. MacRae, R. Bodmeier, Blends of aqueous polymer dispersions used for pellet coating: Importance of the particle size, J. Control. Release. 105 (2005) 226–239. doi:10.1016/J.JCONREL.2005.03.028.

[53] H. Liu, P. Wang, X. Zhang, F. Shen, C.G. Gogos, Effects of extrusion process parameters on the dissolution behavior of indomethacin in Eudragit® E PO solid dispersions, Int. J. Pharm. 383 (2010) 161–169. doi:10.1016/J.IJPHARM.2009.09.003.

[54] J. Breitenbach, Melt extrusion: from process to drug delivery technology, Eur. J. Pharm. Biopharm. 54 (2002) 107–117. doi:10.1016/S0939-6411(02)00061-9.

[55] A.L. Sarode, H. Sandhu, N. Shah, W. Malick, H. Zia, Hot melt extrusion (HME) for amorphous solid dispersions: Predictive tools for processing and impact of drug–polymer interactions on supersaturation, Eur. J. Pharm. Sci. 48 (2013) 371–384. doi:10.1016/J.EJPS.2012.12.012.

[56] G. Verstraete, L. Vandenbussche, S. Kasmi, L. Nuhn, D. Brouckaert, J. Van Renterghem, W. Grymonpré, V. Vanhoorne, T. Coenye, B.G. De Geest, T. De Beer, J.P. Remon, C. Vervaet, Thermoplastic polyurethane-based intravaginal rings for prophylaxis and treatment of (recurrent) bacterial vaginosis, Int. J. Pharm. 529 (2017) 218–226. doi:10.1016/J.IJPHARM.2017.06.076.

[57] S. Narisawa, M. Nagata, C. Danyoshi, H. Yoshino, K. Murata, Y. Hirakawa, K. Noda, An Organic Acid-Induced Sigmoidal Release System for Oral Controlled-Release Preparations, Pharm. Res. 11 (1994) 111–116. doi:10.1023/A:1018910114436.

[58] F. Siepmann, A. Hoffmann, B. Leclercq, B. Carlin, J. Siepmann, How to adjust desired drug release patterns from ethylcellulose-coated dosage forms, J. Control. Release. 119 (2007) 182–189. doi:10.1016/J.JCONREL.2007.02.003.

[59] M.Z.I. Khan, Ž. Prebeg, N. Kurjaković, A pH-dependent colon targeted oral drug delivery system using methacrylic acid copolymers: I. Manipulation of drug release using Eudragit® L100-55 and Eudragit® S100 combinations, J. Control. Release. 58 (1999) 215–222. doi:10.1016/S0168-3659(98)00151-5.

[60] F. Lecomte, J. Siepmann, M. Walther, R.J. MacRae, R. Bodmeier, Polymer Blends Used for the Coating of Multiparticulates: Comparison of Aqueous and Organic Coating Techniques, Pharm. Res. 21 (2004) 882–890. doi:10.1023/B:PHAM.0000026443.71935.cb.

[61] S.-P. Lyu, R. Sparer, C. Hobot, K. Dang, Adjusting drug diffusivity using miscible polymer blends, J. Control. Release. 102 (2005) 679–687. doi:10.1016/J.JCONREL.2004.11.007.

[62] J. Siepmann, N.A. Peppas, Hydrophilic Matrices for Controlled Drug Delivery: An Improved Mathematical Model to Predict the Resulting Drug Release Kinetics (the "sequential Layer" Model), Pharm. Res. 17 (2000) 1290–1298. doi:10.1023/A:1026455822595.

[63] C.R. Wilke, P. Chang, Correlation of diffusion coefficients in dilute solutions, AIChE J. 1 (1955) 264–270. doi:10.1002/aic.690010222.

[64] P. Gonzalez-Tello, F. Camacho, G. Blazquez, Density and Viscosity of Concentrated Aqueous Solutions of Polyethylene Glycol, J. Chem. Eng. Data. 39 (1994) 611–614. doi:10.1021/je00015a050.

[65] G.L. Bas, The Molecular Volumes of Liquid Chemical Compounds, from the Point of View of Kopp, Longmans, Green, 1915. https://books.google.com/books?id=6FUuAQAAIAAJ.

[66] A. Avdeef, Physicochemical Profiling (Solubility, Permeability and Charge State), Curr. Top. Med. Chem. 1 (2001) 277–351. doi:10.2174/1568026013395100.

[67] K.K. Mohanty, J.M. Ottino, H.T. Davis, Reaction and transport in disordered composite media: Introduction of percolation concepts, Chem. Eng. Sci. 37 (1982) 905–924. doi:10.1016/0009-2509(82)80179-6.

[68] E.J. Garboczi, K.A. Snyder, J.F. Douglas, M.F. Thorpe, Geometrical percolation threshold of overlapping ellipsoids, Phys. Rev. E. 52 (1995) 819–828. doi:10.1103/PhysRevE.52.819.

[69] G. Di Colo, Controlled drug release from implantable matrices based on hydrophobia polymers, Biomaterials. 13 (1992) 850–856. doi:10.1016/0142-9612(92)90178-Q.

[70] L.E. Nielsen, Models for the Permeability of Filled Polymer Systems, J. Macromol. Sci. Part A - Chem. 1 (1967) 929–942. doi:10.1080/10601326708053745.

[71] F. Siepmann, J. Siepmann, M. Walther, R.J. MacRae, R. Bodmeier, Polymer blends for controlled release coatings, J. Control. Release. 125 (2008) 1–15. doi:10.1016/J.JCONREL.2007.09.012.

[72] J.S. Vrentas, J.L. Duda, Diffusion in polymer—solvent systems. I. Reexamination of the free-volume theory, J. Polym. Sci. Polym. Phys. Ed. 15 (1977) 403–416. doi:10.1002/pol.1977.180150302.

# Chapter 3: How broadly can poly(urethane)-based implants be applied to drugs of varied properties?[3]

## 3.1 ABSTRACT

Implants offer the opportunity to improve patient adherence and real-world outcomes. However, most polymers used today are hydrophobic and limit drug properties suitable for development. Thermoplastic poly(urethanes) (TPUs) form pores upon hydration and may facilitate the development of implants containing drugs exhibiting broadly different properties. We sought to investigate the effect of drug physicochemical properties on permeability through membranes of varying TPU mixture composition; leverage imaging to visualize microstructural changes to the membrane across the TPU mixture composition range; and quantitatively characterize the membrane microstructure using equivalent pore analysis. We observed a correlation between drug hydrophobicity and its permeability through hydrophobic-rich TPU membranes. Conversely, all compounds diffused through hydrophilic-rich TPU membranes at similar rates, regardless of drug properties. Imaging revealed significant microstructure differences between hydrophobic-rich and hydrophilic-rich TPU membranes, supporting hypotheses proposed in our previous study. The hydrated hydrophilic TPU membrane pore area was determined to be 0.583% and its equivalent pore radius was found to be 128 nm, suggesting that hydrophilic TPU membranes may be used to modify the release of small molecular weight drugs and macromolecules. These findings highlight the

[3] Published in: M.B. Lowinger, J.D. Ormes, Y. Su, J.H. Small, R.O. Williams, F. Zhang, How broadly can poly(urethane)-based implants be applied to drugs of varied properties?, Int. J. Pharm. 568 (2019) 118550. doi:10.1016/J.IJPHARM.2019.118550. Michael Lowinger designed, executed, and performed the experiments, and wrote the manuscript.

benefits of hydrophilic TPUs as rate-controlling membranes to modulate the release rate of drugs with varying physicochemical properties.

## 3.2 INTRODUCTION

Patient adherence to drug therapies remains a major obstacle to realizing the full therapeutic benefit of drug treatments in the real world [1]. Across a variety of therapeutic areas ranging from cardiovascular disease to alcoholism to infectious disease, studies have identified a correlation between adherence and health outcomes [2–6]. In response to this challenge, researchers have devoted substantial resources to develop products intended to improve adherence by leveraging technological capabilities or by changing their route of administration [7–12].

One promising avenue to improve patient compliance and persistence is the effort to decrease frequency of administration. An approach periodically used is to increase the drug half-life, resulting in dosing frequencies from a single dose significantly longer than once daily [13,14]. However, designing decreased administration frequency into the drug molecule itself is not always an option available to medicinal chemists. In such cases, oral and parenteral modified release formulations may be useful in extending the duration of action [15]. Subdermal implants, in particular, have been commercially demonstrated to reduce the frequency of administration to as little as once every 5 years [16]. The ability of implants to transform a drug's frequency of administration from once daily to once every 5 years has the potential to significantly enhance patient adherence by alleviating the patient's need to take their medication as frequently.

Implants may be designed as a matrix composed of drug and polymer, wherein the release behavior is driven by a pore network created by the distribution of drug in the

polymer [17]. In such a system, the drug release rate is strongly dependent on both the drug load and the dosage form geometry. Alternatively, implants can be designed as reservoir systems, wherein a core of drug and polymer is surrounded by a rate-controlling polymer membrane [18]. Since the drug release kinetics from reservoir implants are limited by diffusion through the rate-controlling membrane, they are capable of decoupling the treatment duration of a single implant from its release rate [19].

Most commercialized implants are composed of either silicone or ethylene vinyl acetate (EVA). Nexplanon® is a contraceptive reservoir implant, composed of EVA and designed to deliver etonogestrel, consisting of a single rod administered once every 3 years [20]. Jadelle® is another contraceptive reservoir implant, composed of silicone and designed to deliver levonorgestrel, consisting of two rods administered once every 5 years [21]. Probuphine® is a matrix implant for the treatment of opioid use disorder, consisting of four rods administered once every 6 months, composed of EVA and designed to deliver buprenorphine [17]. Researchers have also described the development of a subdermal implant of tenofovir alafenamide composed of silicone and a subdermal implant of MK-8591 composed of EVA, both designed to prevent human immunodeficiency virus (HIV) infection [22,23].

Since drug release from reservoir implants is driven by diffusion through the rate-controlling membrane and because there is a limited ability to tune the polymer properties to affect drug diffusion, drug properties or duration are substantially constrained to effectively deliver long-acting therapeutics using implants. For example, Nexplanon® provides efficacy from a single administration for up to 3 years, but etonogestrel is lipophilic (log P = 3.3) and highly potent (25-70 μg/day release rate) [24,25]. Jadelle® currently sets the record for longest-acting marketed implant with a 5

year duration from a single administration, but levonorgestrel is also lipophilic (log P = 3.9) and highly potent (25-80 μg/day release rate) [26,27]. Even so, it requires two rods to provide the desired release rate for the 5 year duration.

There are no commercially marketed reservoir implants composed of EVA or silicone intended to release a drug of substantially lower hydrophilicity than etonogestrel. In contrast, Supprelin® LA is a subcutaneous reservoir implant intended to deliver hestrelin acetate over the course of 12 months for the treatment of central precocious puberty [28]. The drug is hydrophilic (log P = -2.4) and the rate-controlling membrane is a polymethacrylate hydrogel, suggesting that it would not have diffused through rate-controlling membranes composed of the more common EVA or silicone at sufficient rates [29]. Clark et al., in describing their efforts to develop a single intravaginal ring to deliver both hydrophobic levonorgestrel and hydrophilic tenofovir, noted that the hydrophobic poly(urethane) they leveraged to deliver levonorgestrel at the desired rate was incapable of delivering tenofovir at the desired rate [30]. To achieve their goals, they created a segmented ring in which levonorgestrel eluted from a hydrophobic poly(urethane) and tenofovir eluted from a hydrophilic poly(urethane). These examples highlight the value of alternate polymer chemistry in facilitating the long-term delivery of medicines.

Thermoplastic poly(urethanes) (TPU) have been used in parenterally administered medical devices for decades with a good track record [31–33]. Hydrophilic TPUs, in which the soft segment is polyethylene oxide (PEO), have been shown to swell when exposed to water to an extent proportional to the PEO content in the copolymer [34]. Multiple studies have also demonstrated a correlation between drug release rate through these polymers and the soft segment content in the TPU [35,36].

Our previous study sought to understand how mixtures of a hydrophobic and hydrophilic TPU could be used to modulate the diffusion behavior of the hydrophilic drug emtricitabine, compared with its permeability through EVA membranes of varying vinyl acetate content [37]. We observed a sharp increase in drug apparent permeability as the membrane composition changed from 50% (w/w) to 55% (w/w) hydrophilic TPU. We hypothesized that a continuous network of water-filled pores was formed at concentrations ≥55% (w/w) hydrophilic TPU (referred to as "hydrophilic-rich TPU compositions"), facilitating drug diffusion through the membrane. At these hydrophilic-rich TPU mixture compositions, we observed a nearly 700-fold increase in drug permeability relative to EVA. At concentrations <50% (w/w) hydrophilic TPU (referred to as "hydrophobic-rich TPU compositions"), we observed the drug apparent permeability through the membrane to be similar to that of EVA.

The previous study did not investigate the impact of a drug's physicochemical properties on membrane permeability. Given that EVA membranes are likely to enable desired release rates only for drugs with certain properties, it is important to understand the range of drug attributes suitable for release through TPU membranes. The current study seeks to investigate the effect of drug hydrophobicity on its permeability through membranes of varying TPU mixture composition. We hypothesize that drug hydrophobicity has a substantial impact on its diffusion rate through the TPU membrane at hydrophobic-rich compositions, similar to what has been observed by others for hydrophobic membranes [30]. In contrast, we hypothesize that drug hydrophobicity has a minimal impact on its permeability through the TPU membrane at hydrophilic-rich compositions due to the presence of water-filled pores that facilitate drug diffusion through the membrane irrespective of its dissolution in the polymer itself.

The previous study also did not characterize the microstructure of the TPU membranes, instead relying on permeability data to form conclusions [37]. However, an analysis of the membrane microstructure would enable a better understanding of the observed permeability data, including its potential application to drugs of varying properties. A better understanding of the interplay between membrane microstructure and drug permeability may potentially aid in the rational selection or design of polymers for these applications. In this study, we sought to characterize the microstructure by imaging changes to the membrane structure across the TPU mixture composition range. We also sought to understand the pore size and pore area of the TPU membrane at compositions above the observed percolation threshold where we believe a pore network exists when the membrane is hydrated.

To assess the impact of drug lipophilicity on membrane permeability, we selected model drugs of similar molecular weight but different hydrophilicity. The drugs possess ionizable groups, allowing us to further vary the hydrophilicity (distribution coefficient, log D) by changing the ionization state of each drug. We then measured the steady-state diffusion rate of different drug compounds at varying pH through membranes of varying TPU mixture composition to establish a relationship between key drug properties and membrane permeability.

Atomic force microscopy (AFM) is a surface imaging technique with the demonstrated ability to detect changes in both topography and material properties with extremely high resolution. By using an ultramicrotome to create a flat cross section, we leveraged shifts in tip-sample interactions to infer changes in material properties likely attributed to different phases. By understanding the presence, extent, and morphology of

separation between the hydrophobic- and hydrophilic-rich TPU phases, we inferred conclusions about the microstructure of the membrane when it is hydrated.

Fluorescein isothiocyanate (FITC) dextrans are commercially available in multiple molecular weight distributions. By measuring the steady-state diffusion rate of different molecular weight dextrans through the polymer membrane, we leveraged equivalent pore analysis to determine the porosity attributes of the membrane, including equivalent pore size and equivalent number of pores.

## 3.3 MATERIALS AND METHODS

### 3.3.1 Materials

Emtricitabine, a human immunodeficiency virus nucleoside reverse transcriptase inhibitor, was obtained from Laurus Labs (Hyderabad, India). As shown in Table 3.1, it has a molecular weight of 247 Da, an octanol/water partition coefficient (log P) of -0.68, and a $pK_a$ of 2.6. Metoprolol tartrate, a beta blocker, was obtained from Sigma Aldrich (St. Louis, MO). The free base form of the drug has a molecular weight of 267 Da, a log P of 1.81, and a $pK_a$ of 9.7 (Table 3.1). Ibuprofen, a non-steroidal anti-inflammatory drug, was also obtained from Sigma Aldrich (St. Louis, MO). As described in Table 3.1, its molecular weight is 206 Da, its log P is 3.49, and it had a $pK_a$ at 4.9. Although the drugs themselves are likely to be insufficiently potent to formulate as an implant for a meaningful duration, they represent a range of drug physicochemical properties of interest to the study. As described previously, these drug compounds were selected to have similar molecular weight but significantly different hydrophilicity.

Table 3.1: Key physicochemical properties of emtricitabine, metoprolol, and ibuprofen. The listed molecular weight of metoprolol tartrate reflects the free form without the tartrate counterion.

| Compound | Chemical Structure | Molecular Weight (Da) | Octanol/water Partition Coefficient (log P) | Calculated $pK_a$ |
|---|---|---|---|---|
| Emtricitabine | 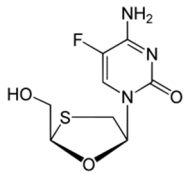 | 247 | -0.68 | 2.7 (basic) |
| Metoprolol Tartrate | 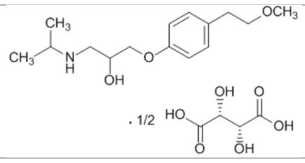 | 267 | 1.81 | 9.7 (basic) |
| Ibuprofen | 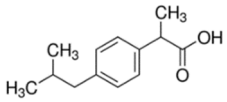 | 206 | 3.49 | 4.9 (acidic) |

Non-swelling thermoplastic poly(urethane) Pathway™ PY-PT60DE was obtained from Lubrizol (Cleveland, OH) and is described as hydrophobic TPU. Water-swelling thermoplastic poly(urethane) Pathway™ PY-PT60DE500 was also obtained from Lubrizol (Cleveland, OH) and is described as hydrophilic TPU. The structures of the two poly(urethanes) were previously identified using $^{1}H$ nuclear magnetic resonance (NMR) [36]. As shown in Figure 3.1, both poly(urethanes) exhibit a hard segment composed of hexamethylene diisocyanate. However, their soft segment monomers differ slightly with the hydrophobic TPU containing poly(tetrahydrofuran) as its soft segment and hydrophilic TPU containing PEO as its soft segment.

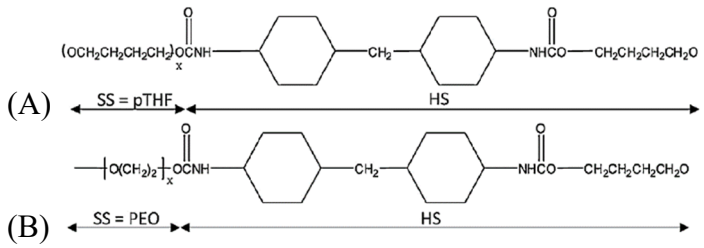


Figure 3.1: Chemical structures of (A) Pathway™ PY-PT60DE (hydrophobic TPU) and (B) Pathway™ PY-PT60DE500 (hydrophilic TPU).

Fluorescein isothiocyanate (FITC) dextrans of average molecular weight 20, 40, 250, 500, and 2000 kDa were obtained from Sigma Aldrich (St. Louis, MO). Different buffers were used to control pH during the permeability studies. We obtained 1 M pH 3.0 acetate buffer and 0.2 M pH 7.0 phosphate buffer from Alfa Aesar (Haverhill, MA). We acquired 0.1 M pH 10.0 carbonate-bicarbonate buffer from Fisher (Hampton, NH). To obtain aqueous media at pH 12.0, we titrated 1 N sodium hydroxide obtained from Fisher (Hampton, NH) into deionized water.

### 3.3.2 Methods

#### *3.3.2.1 Membrane Preparation*

This study leveraged the membranes composed of mixtures of hydrophobic and hydrophilic TPU described in our previous publication [37]. Briefly, films were manufactured using a Leistritz ZSE 18 twin-screw extruder (Somerville, NJ). The two polymers were charged into separate K-Tron KT20 loss-in-weight gravimetric feeders (Sewell, NJ), which were configured to feed into a single extruder feed port. The vent zone was connected to a vacuum pump to remove water and other volatiles from the system. The extruder was connected to a Baldor gear pump (Mount Laurel, NJ) to dampen oscillations in flow. The end of the extruder featured a 0.02 x 6 inch sheet die.

The extrudate was fed into a Leistritz 3-roll film stack (Somerville, NJ). The rolls were temperature controlled to 15°C. The polymer membrane composition (ratio of the two polymers) was determined by changing the ratio of the feed rates of each polymer into the extruder.

#### *3.3.2.2 Drug Distribution coefficient (log D) Determination*

The distribution coefficient (log D) of each drug at each pH was determined using the shake-flask method. A stock solution of each drug in methanol was added to a vial. Both aqueous buffer and octanol were added to the vial in equal proportions. The vial was then capped and allowed to mix overnight. The following day, the specimen was left to settle for at least one hour, followed by sampling of the octanol and aqueous phases. The samples were injected into a VMR Vydac® 218TP (Radnor, PA) $C_{18}$ reverse phase high performance liquid chromatography column with a 4.6 mm inner diameter, 150 mm length, and 5 µm silica particle size. The column was maintained at 40°C, the mobile phase flow rate was set at 3.0 mL/min and the detector monitored the 210 nm wavelength. The mobile phase consisted of a gradient with mixtures of 0.1% (v/v) phosphoric acid and acetonitrile. Over the course of the 5 minute run time, the mobile phase composition shifted from 5% acetonitrile to 95% acetonitrile.

#### *3.3.2.3 Drug Diffusivity Determination*

Two-dimensional (2D) Nuclear magnetic Resonance (NMR) Diffusion Ordered Spectroscopy (DOSY) was utilized to measure the diffusion coefficient of metoprolol in solution at different pH values. DOSY experiments were carried out on a Bruker 600 MHz NEO HD spectrometer equipped with a 5 mm TCI HCN helium cryoprobe with the standard gradient accessory providing a maximum gradient output of 65.7 G/cm. The

2D $^{1}$H DOSY spectra were collected using a standard Bruker DOSY pulse sequence (ledbpgp2ses) modified with the incorporation of excitation sculpting water suppression. The resulting diffusion coefficients were extracted from the resulting plots using the Bruker Dynamics Center software.

#### *3.3.2.4 Drug Apparent Permeability Measurement through Membranes*

This study used the same technique to measure drug apparent permeability through the polymer membrane as we described in our previous publication [37]. Briefly, a polymer membrane of each sample was cut using a hammer-driven hole punch and placed into a membrane holder. The membrane holder was positioned between identical donor and acceptor glass chambers. Cross-type magnetic stir bars were used to ensure good mixing within the chamber. The drug solution was intended to model the core of the reservoir implant, while the polymer film was intended to model the rate-controlling membrane of the implant. A drug solution in a buffer of defined pH was added to the donor chamber, while pure buffer was added to the acceptor chamber. Ultraviolet absorbance was measured in the acceptor chamber using a Pion Rainbow™ fiber optic system (Billerica, MA) equipped with a deuterium lamp and UV dip probes. Figure B.1, Figure B.2, and Figure B.3 in Appendix B: show representative concentration data as a function of time for emtricitabine, metoprolol, and ibuprofen, respectively.

In order to calculate the apparent permeability, a linear regression was performed on the steady-state portion of the diffusion curve. The slope of the fitted line is $\frac{dc}{dt}$. Using Fick's law of diffusion, the apparent permeability ($P_{app}$) can be calculated:

$$P_{app} = \frac{D}{h} = \frac{V\left(\frac{dc}{dt}\right)}{A(c_2 - c_1)} \quad (3.1)$$

where V is the volume of the acceptor compartment (23 mL), A is the exposed surface area of the membrane (1.54 $cm^2$), $c_2$ is the initial drug concentration in the donor compartment (different for each drug) and $c_1$ is the initial concentration in the acceptor compartment (0 mg/mL). Although the drug concentration changes in the chambers during the diffusion study, the initial concentration used in the calculation are good assumptions at early time points. Each diffusion study was replicated three times.

#### *3.3.2.5 Atomic Force Microscopy*

Each polymer membrane sample was placed vertically in a Leica Microsystems 0-2 mm specimen holder (Buffalo Grove, IL). The sample was submersed in liquid nitrogen for 5 minutes to harden and then quickly sectioned to be flush with the vice surface using a Leica Microsystems EM UC7 ultramicrotome (Buffalo Grove, IL). Glass knives from 400 x 25 x 6.4 mm Leica Microsystems glass strips (Buffalo Grove, IL) were used for sectioning and prepared with a Leica Microsystems EM KMR3 glass knife cutter (Buffalo Grove, IL). Each sample was then dried under nitrogen gas for 2 minutes to remove condensation associated with exposure to liquid nitrogen.

Samples were analyzed using an Asylum Cypher ES Scanning Probe Microscope (Oxford Instruments, Santa Barbara, CA). Ultra-high frequency NanoWorld Arrow™ UHFAuD silicon tips with gold coating on the detector side (Neuchâtel, Switzerland) were used for AFM sample analysis. Samples were analyzed in air, at ambient conditions, using alternating contact mode and photothermal actuation (BlueDrive™) of the cantilever. Cantilevers were driven at resonance, typically 1 MHz, and settings were

optimized to maintain net repulsive tip-sample scanning (i.e., phase <90°). Images were collected at 512 x 512 pixel resolution with scan rates at 6.3-6.7 Hz. A zero-order flattening algorithm was applied to height images. No correction was made for phase images.

#### *3.3.2.6 Membrane Microstructure Determination*

The apparent permeability of each dextran across the 75% (w/w) hydrophilic TPU membrane was determined using the method described in section 3.3.2.3 and FITC-dextrans of varying average molecular weight. The hydrodynamic radius of each FITC-dextran was previously determined by Armstrong et al. by measuring the viscosity of FITC-dextran solutions and leveraging the Einstein viscosity relation to model the hydrated polymer molecules in terms of equivalent hydrodynamic spheres that would increase the viscosity to the same extent as solid spherical particles of equivalent volume [38]. The free diffusivity (D) of each FITC-dextran in water was determined from the hydrodynamic radius using the Stokes-Einstein equation and the known viscosity of water:

$$\boldsymbol{D = \frac{k_B T}{6\pi\eta r_h}} \tag{3.2}$$

Where $k_B$ is the Boltzmann constant, T is the temperature, $\eta$ is the viscosity of water, and $r_h$ is the hydrodynamic radius.

To characterize the pore microstructure, we leveraged a method originally described by Durbin et al. to estimate pore radii, modified by assumptions developed by

Renkin to account for steric hindrance at the entrance to porous membranes and frictional resistance within the pores [39,40].

$$\frac{P_{app}}{D} = \left(\frac{A_p}{dx}\right)(1-u)^2\left(1 - 2.104u + 2.09u^3 - 0.95u^5\right) \quad (3.3)$$

Where $A_p$ is the total pore area, dx is the pore length, and u is equal to $\frac{r_h}{r_p}$ where $r_h$ is the hydrodynamic radius as described previously and $r_p$ is the pore radius.

The first term establishes the condition that a molecule must pass through a pore opening without striking the edge. The second term corrects for friction between the molecule moving within a pore and its walls. Examining equation 3.3, we find that there are several known and unknown terms. For each FITC-dextran, we have measured the apparent permeability through the membrane, others have determined the hydrodynamic radius, and we have determined free diffusivity using equation 3.2. We assume that the tortuosity of the pore is negligible, and the pore length is equivalent to the measured membrane thickness (0.1 mm). We utilized imaging data to assess whether our tortuosity assumption is reasonable, which is described in more detail in later sections. Both $A_p$ and $r_p$ are unknown and we leveraged the measured permeability data for each dextran to perform a non-linear fit. In an approach utilized by several other researchers, we performed a chi-squared test, minimizing the difference between the calculated apparent permeability and the observed apparent permeability to obtain an estimate of total pore area and pore radius [41–43]. The total pore area relative to total membrane area, a measure of porosity, can then be calculated by dividing the total pore area by the total membrane area (1.54 $cm^2$). Finally, the number of equivalent pores ($N_p$) can be determined using equation 3.4 and the number of pores can be divided by the total

membrane area to obtain the number of equivalent pores per unit area.

$$N_p = \frac{A_p}{\pi r_p^2} \tag{3.4}$$

## 3.4 RESULTS

### 3.4.1 Effect of drug physicochemical properties on apparent permeability through TPU membranes

We endeavored to investigate the impact of drug hydrophilicity on its permeability through TPU membranes of varying composition. In an effort to quantitatively relate drug physicochemical properties to their diffusion behavior through poly(urethane) membranes, we measured the octanol-water distribution coefficient (log D) of each drug compound as a function of buffer pH. Table 3.2 describes the octanol-water distribution coefficient of emtricitabine, metoprolol, and ibuprofen as a function of buffer pH. Based on the dissociation coefficient ($pK_a$) of each compound, we can work with fully unionized drug compounds by controlling the buffer pH to pH 7 for emtricitabine, pH 12 for metoprolol, and pH 3 for ibuprofen. The log D at a pH where the drug is in the unionized state is equivalent to the octanol-water partition coefficient (log P) of that compound. Consequently, the log P for emtricitabine, metoprolol, and ibuprofen was measured to be -0.68, 1.81, and 3.49, respectively. Compounds in this study span an approximately 10,000-fold range in partition coefficient.

By changing the buffer pH for each compound, we can alter the ionization state and thus affect the hydrophilicity of the species in the permeability study. As shown in Table 3.2, we observed no substantial change in the distribution coefficient of emtricitabine between pH 7 and pH 10. Given emtricitabine's $pK_a$ of 2.7, we would

expect no change in ionization state between pH 7 and 10. We measured a significant 2-log change in the log D of metoprolol in shifting from the fully ionized state at pH 7 to the fully unionized state at pH 12 (Table 3.2). We found a similar 100-fold change in the distribution coefficient of ibuprofen when the ionization state was shifted from fully unionized at pH 3 to fully ionized at pH 7 (Table 3.2). Thus, by varying the compound type and buffer pH, we can obtain a range of intermediate hydrophilicities, as measured by log D, over a 10,000-fold range.

Table 3.2: Shake-flask octanol-water distribution coefficient (log D) of each drug compound as a function of buffer pH. Boxes containing "N/M" indicates that the distribution coefficient was not measured at that pH.

| **Compound** | **Calculated $pK_a$** | **log $D_{pH\ 3}$** | **log $D_{pH\ 7}$** | **log $D_{pH\ 10}$** | **log $D_{pH\ 12}$** |
|---|---|---|---|---|---|
| Emtricitabine | 2.7 (basic) | N/M | -0.68 | -0.70 | N/M |
| Metoprolol | 9.7 (basic) | N/M | -0.67 | 1.73 | 1.81 |
| Ibuprofen | 4.9 (acidic) | 3.49 | 1.30 | N/M | N/M |

By comparing the apparent permeability of the three compounds in the unionized state across the TPU mixture range, we were able to assess the impact of drug hydrophilicity on its apparent permeability through TPU membranes both below and above the previously described percolation threshold [37]. Figure 3.2 describes the apparent permeability of unionized drug compounds as a function of TPU mixture composition. We observed a strong correlation between drug hydrophilicity and its apparent permeability through hydrophobic-rich TPU mixtures (≤50% (w/w) hydrophilic TPU), with more lipophilic drug compounds diffusing through the membranes at faster

rates over this TPU composition range. Conversely, we saw a negligible effect of drug physicochemical properties on its apparent permeability through hydrophilic-rich TPU mixtures (≥55% (w/w) hydrophilic TPU).

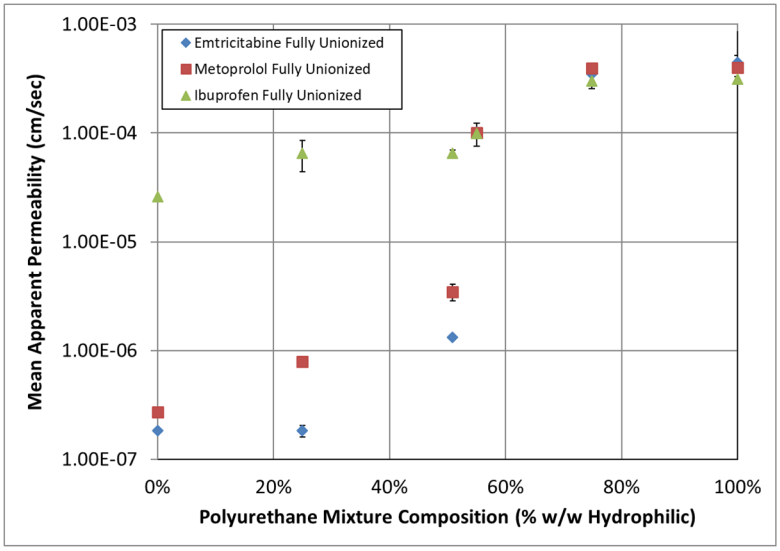


Figure 3.2: Mean apparent permeability (N = 3 ± SD) of unionized drug compounds (varying log P) as a function of TPU mixture composition. Buffer pH was selected for each compound to ensure it was fully unionized during the diffusion study. Emtricitabine study was conducted at pH 7, metoprolol study was conducted at pH 12, and ibuprofen study was conducted at pH 3.

As shown in Table 3.2, metoprolol tartrate has a $pK_a$ of 9.7. In the fully ionized state at pH 7, it exhibits a log D of -0.67 similar to emtricitabine. The compound is partially ionized at pH 10 and its log D was determined to be 1.73, while its log D in the fully unionized state (pH 12) was measured at 1.81. This nearly 100-fold change distribution coefficient offers an opportunity to examine the effect of hydrophilicity on apparent permeability while keeping most other physicochemical properties constant.

Figure 3.3a shows the apparent permeability of metoprolol in different ionization states as a function of TPU mixture composition. Similar to our finding when investigating the apparent permeability of different compounds of varying hydrophilicity (Figure 3.2), we observed a correlation between metoprolol log D and its apparent permeability through hydrophobic-rich TPU compositions. We again found a negligible effect of drug physicochemical properties on apparent permeability through hydrophilic-rich TPU compositions.

We also leveraged the $pK_a$ of ibuprofen to separately investigate the effect of hydrophilicity on apparent permeability while keeping most other physicochemical properties constant. As described in Table 3.2, ibuprofen is fully ionized at pH 7 with a measured log D of 1.30 and fully unionized at pH 3 with a distribution coefficient of 3.49. As illustrated by Figure 3.3b, we observed a similar phenomenon to the studies comparing different compounds of varying log P and comparing different ionization states of metoprolol, with a correlation between ibuprofen distribution coefficient and its apparent permeability through hydrophobic-rich TPU mixtures. For ibuprofen, there is an approximate 10-fold change in apparent permeability through a 25% (w/w) hydrophilic TPU membrane when varying ionization state. We again found a negligible effect of drug physicochemical properties on ibuprofen apparent permeability through hydrophilic-rich TPU compositions.

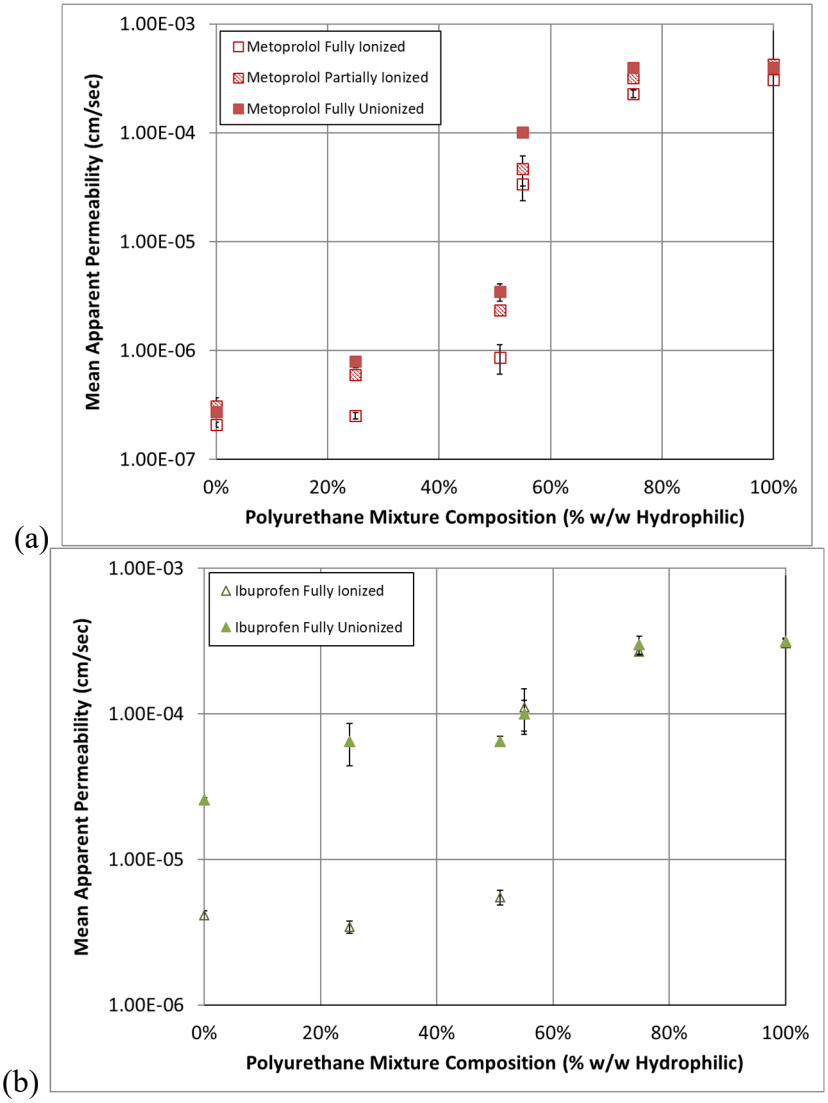


Figure 3.3: Mean apparent permeability (N = 3 ± SD) of metoprolol (a) and ibuprofen (b) at different ionization states as a function of TPU mixture composition. Buffer pH was varied to affect the drug's ionization state in each diffusion study. For metoprolol, fully ionized was conducted at pH 7, partially ionized was conducted at pH 10, and fully unionized was conducted at pH 12. For ibuprofen, fully ionized was conducted at pH 7 and fully unionized was conducted at pH 3.

The poly(urethanes) comprising the membrane do not contain ionizable groups. Therefore, we would not expect changes in pH to affect the microstructure of the

membrane in a way that would account for observed changes in drug apparent permeability. However, we investigated the effect of buffer pH on the apparent permeability of emtricitabine over a range where there is no change to the drug's ionization state as a control to ensure the observed apparent permeability changes are due to drug physicochemical properties. Figure 3.4 shows the apparent permeability of emtricitabine through TPU membranes of varying composition at pH 7 and 10. As is evident from Table 3.2, the distribution coefficient of emtricitabine does not change appreciably between pH 7 and 10, reflecting the fact that the compound is fully unionized in both environments. Consequently, there is negligible difference in the apparent permeability of the drug through TPU membranes as the buffer pH is changed.

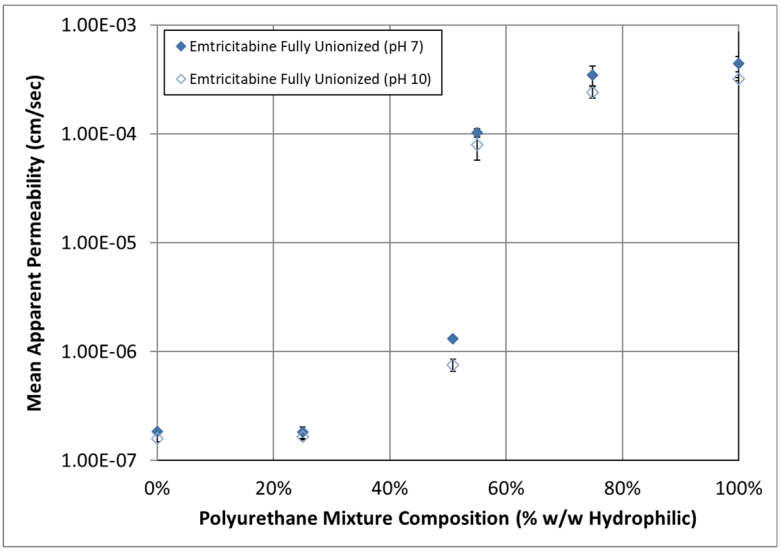


Figure 3.4: Mean apparent permeability (N = 3 ± SD) of emtricitabine at two different buffer pH values (pH 7 and 10) as a function of TPU mixture composition. Emtricitabine is fully unionized at both pH values. Buffer pH was varied as a negative control to ensure that variations in pH had no effect on the polymer membrane in a way that would impact drug permeability.

Although several factors may contribute to the diffusion rate of a solute (i.e., drug), we sought to assess whether distribution coefficient is an effective predictor of apparent permeability through hydrophobic-rich TPU membranes, agnostic to other differences between drug compounds. Figure 3.5 describes the mean apparent permeability of each compound at each studied pH through both a 25% (w/w) hydrophilic TPU membrane (hydrophobic-rich composition) and a 75% (w/w) hydrophilic TPU membrane (hydrophilic-rich composition) as a function of the compound's distribution coefficient (log D). We observed a good correlation between mean apparent permeability of a compound through a 25% (w/w) hydrophilic TPU membrane and its log D, regardless of the other physicochemical features of that drug. The fitted relationship was exponential due to the logarithmic transformation of the distribution coefficient and its correlation coefficient ($r^2$) was determined to be 0.78. Deviations from the fitted curve may be explained by other differences between the drugs. For example, ibuprofen is 61 Da smaller than metoprolol and it is well established that molecular weight plays a role in the diffusion of small molecule solutes through a polymer [44]. In contrast, we observed no change in the mean apparent permeability through a 75% (w/w) hydrophilic TPU membrane, regardless of API physicochemical property.

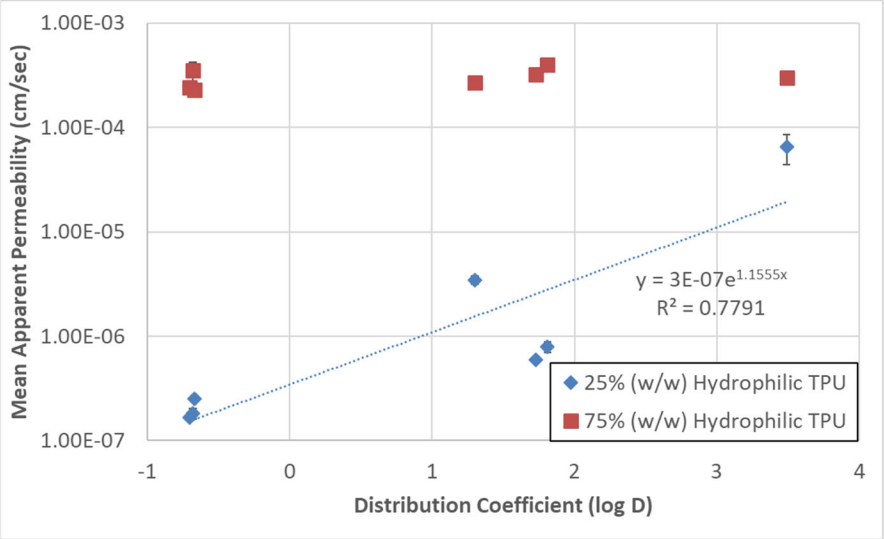


Figure 3.5: Mean apparent permeability (N = 3 ± SD) of all studied compounds through a 25% (w/w) hydrophilic TPU (blue diamonds) and a 75% (w/w) hydrophilic TPU (red squares) membrane as a function of octanol/water distribution coefficient (log D). We observe a correlation between log D and mean apparent permeability at a 25% (w/w) hydrophilic TPU membrane composition, with a curve representing an exponential regression fit with a correlation coefficient ($r^2$) value of 0.78. However, we observe no correlation between log D and mean apparent permeability at a 75% (w/w) hydrophilic TPU membrane composition.

We also sought to understand whether changes to a compound's ionization state were affecting its diffusivity, such that these diffusivity may explain the observed changes in diffusion behavior. As illustrated by equation 3.1, there is a direct relationship between the diffusivity of a compound and its apparent permeability through a membrane. Two-dimensional DOSY NMR was utilized to determine the diffusion coefficient of metoprolol in solution [45]. Table 3.3 shows the measured diffusivity of metoprolol at each pH studied. There is a negligible change in its diffusivity as buffer pH changes, suggesting that it cannot explain the observed changes in apparent permeability through the hydrophobic-rich TPU membranes.

Table 3.3: Diffusivity of metoprolol in relevant pH buffers, as measured using solution NMR.

| Buffer pH | Diffusivity ($cm^2/sec$) |
|---|---|
| 7.0 | $7.22 \times 10^{-6}$ |
| 10.0 | $7.19 \times 10^{-6}$ |
| 12.0 | $7.22 \times 10^{-6}$ |

### 3.4.2 Nanoscale Imaging of Dry TPU Membrane Microstructure

Atomic force microscopy enables high resolution imaging of a variety of surfaces and can be used to visualize the microstructure of the TPU membranes in the dry state. In addition to measuring changes in the height of the surface, AFM can be used to detect changes in material properties, such as modulus or adhesion, that may be indicative of phase separation. The change in material properties is most evident in the phase image, which represents offsets in the resonance frequency of the tip when it meets the polymer surface. However, changes in phase may also be caused by large changes in surface topography. To reduce this effect, we strive to create a surface as flat as possible using the ultramicrotome. Additionally, we verify that features we observe in the phase image that we believe to represent phase separation are not present in the height image.

As illustrated in Figure 3.6, the topographic (height) images show a relatively flat surface with roughness variation below 40 nm. Moreover, the height changes in the topographic images do not correspond to the contrast observed in the phase images, suggesting that the phase contrast is due to material property changes. The 25% (w/w) hydrophilic TPU phase contrast image suggests that at this composition there is a discrete phase of hydrophilic TPU well-dispersed in a continuous phase of hydrophobic TPU.

The hydrophilic TPU domain size appears to be in the range of 10-30 nm. On the other hand, the 75% (w/w) hydrophilic TPU phase contrast image suggests that at this composition there is a continuous phase of hydrophilic TPU as well as discrete phases of hydrophobic TPU. The hydrophilic TPU appears to be partially crystallized, forming microstructure consistent with lamellar crystals [46–48]. The darker regions may be hydrophobic TPU or amorphous phases of hydrophilic TPU. The crystalline lamellae appear to be in the range of 5-15 nm thick and are very close in proximity (<5 nm) to each other.

Figure 3.7 features the phase images of poly(urethane) membranes of varying mixture composition. Pure hydrophobic TPU (Figure 3.7a) has a surface with no well-defined features, whereas pure hydrophilic TPU (Figure 3.7f) exhibits features resembling crystalline lamellae. We observed a significant change in the membrane microstructure between 25% (w/w) hydrophilic TPU (Figure 3.7b) and 55% (w/w) hydrophilic TPU (Figure 3.7d), with 50% (w/w) hydrophilic TPU (Figure 3.7c) exhibiting an intermediate microstructure to the former two compositions. We were unable to discern a substantial structural difference between 55% (w/w) hydrophilic TPU (Figure 3.7d), 75% (w/w) hydrophilic TPU (Figure 3.7e), and 100% hydrophilic TPU (Figure 3.7f), although it is possible that the lamellar structures are more densely packed at higher hydrophilic TPU composition.

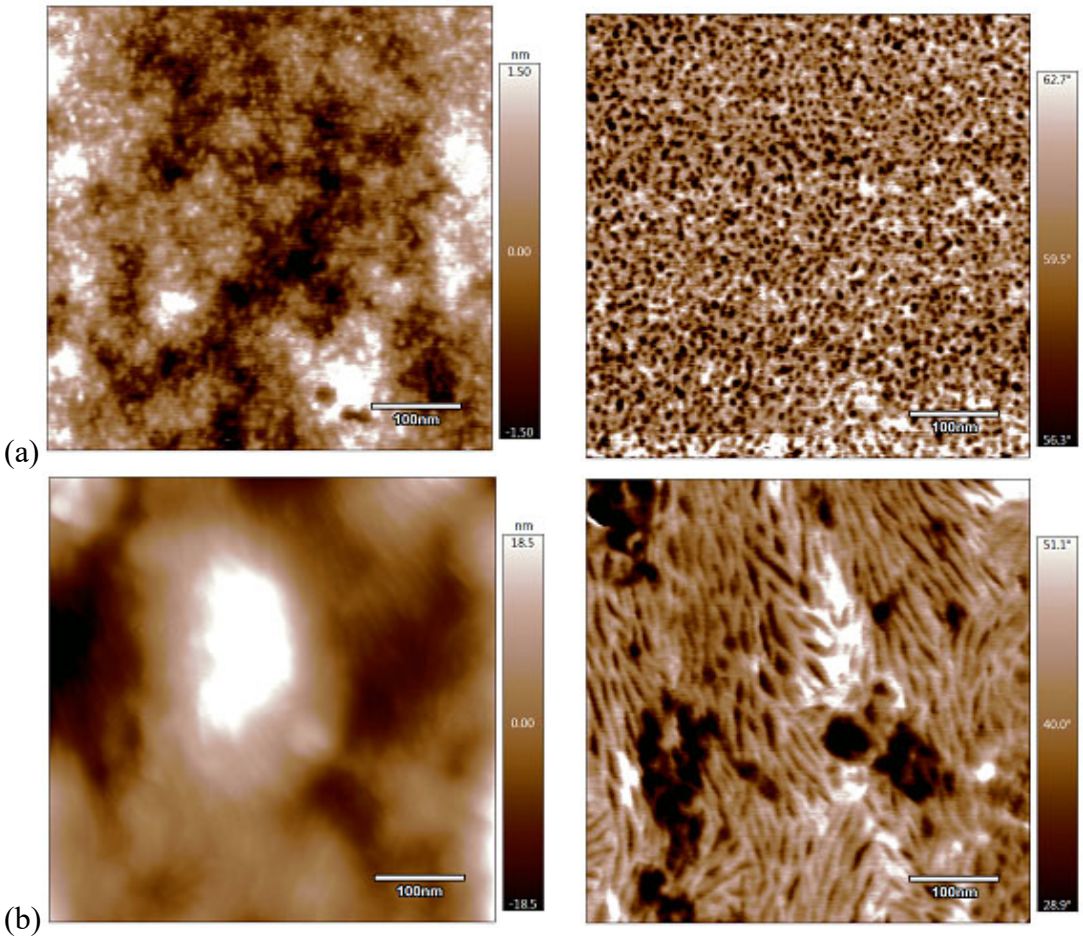


Figure 3.6: AFM height (left) and phase (right) images of (a) a dry 25% (w/w) hydrophilic TPU membrane, and (b) a dry 75% (w/w) hydrophilic TPU membrane.

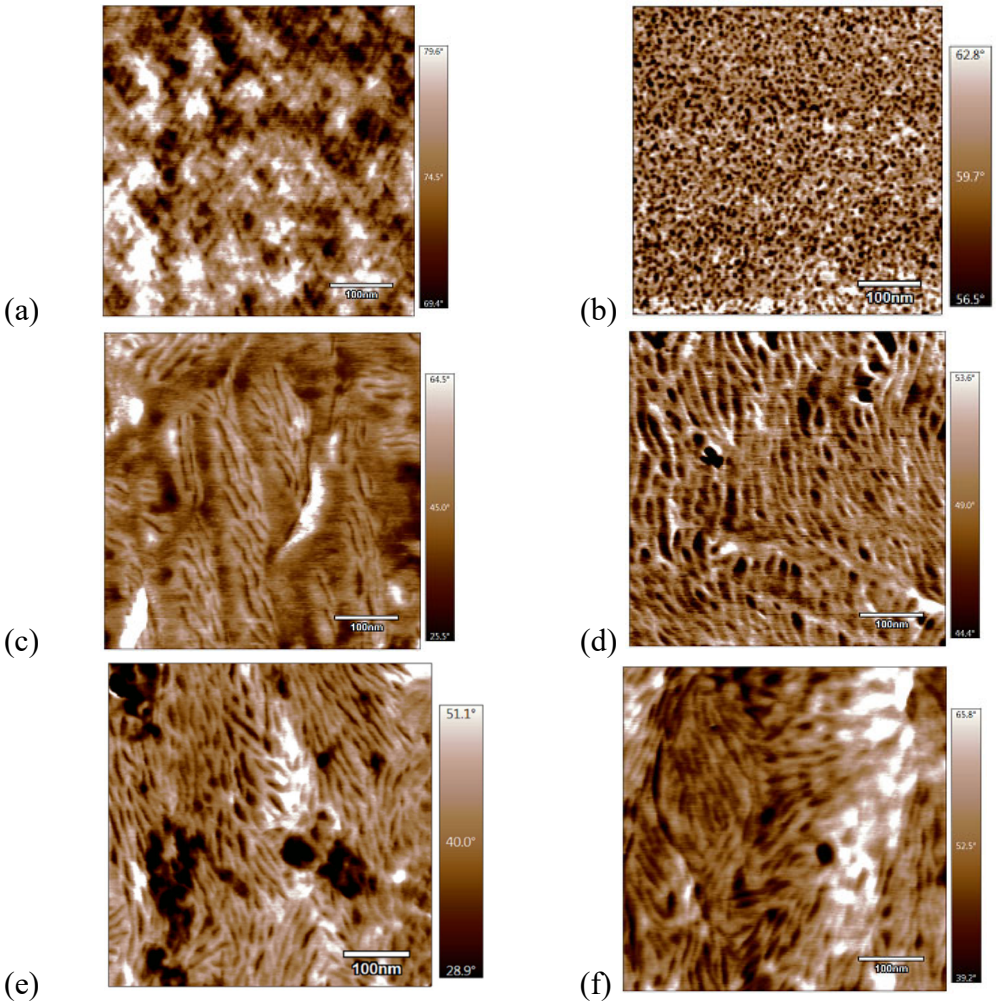


Figure 3.7: Phase images of dry TPU membranes of varying composition. Membrane composition is as follows: 0% (w/w) hydrophilic TPU (a); 25% (w/w) hydrophilic TPU (b); 50% (w/w) hydrophilic TPU (c); 55% (w/w) hydrophilic TPU (d); 75% (w/w) hydrophilic TPU (e); and 100% (w/w) hydrophilic TPU (f).

### 3.4.3 Hydrated Membrane Microstructure Characterization

By comparing our measured apparent permeability values of FITC-dextrans with varying average molecular weight and leveraging the previously determined hydrodynamic radius of FITC-dextrans, we were able to relate the hydrodynamic radius of each FITC-dextran to its mean apparent permeability. Table 3.4 describes the

comparison of our measured mean apparent permeability of each FITC-dextran of varying average molecular weight through a 75% (w/w) hydrophilic TPU membrane (hydrophilic-rich composition) and the previously determined hydrodynamic radius of that dextran. As expected, there is a clear downward trend in mean apparent permeability with increasing hydrodynamic radius.

Table 3.4: Comparison of the measured mean apparent permeability through a 75% (w/w) hydrophilic TPU membrane of FITC-dextrans of varying nominal molecular weight. Hydrodynamic radius of the FITC-dextrans was previously determined by Armstrong et al. [38].

| **FITC-dextran Nominal Molecular Weight (kDa)** | **Hydrodynamic Radius (nm)** | **Mean Apparent Permeability (cm/sec)** |
|---|---|---|
| 20 | 3.24 | $4.71 \times 10^{-7}$ |
| 40 | 4.78 | $3.26 \times 10^{-7}$ |
| 250 | 11.46 | $1.12 \times 10^{-7}$ |
| 500 | 15.9 | $7.03 \times 10^{-8}$ |
| 2000 | 26.89 | $2.54 \times 10^{-8}$ |

As we described in section 3.3.2.6, we performed a non-linear fit of equation 3.3 using the hydrodynamic radius and mean apparent permeability data listed in Table 3.4, solving for the equivalent pore radius ($r_p$) and the total pore area available for diffusion relative to the pore length ($A_p/dx$). As outlined in Table 3.2, our analysis found $A_p/dx$ to be 0.898 cm. Assuming minimal pore tortuosity such that the pore length is similar to the membrane thickness (100 μm), we determined the total pore area ($A_p$) to be 0.00898 $cm^2$.

Since the total membrane area was measured at 1.54 $cm^2$, we observed that the pore area was 0.583% relative to the total membrane area. The equivalent pore radius ($r_p$) was found to be 128 nm. By using equation 3.4, we determined the equivalent number of pores ($N_p$) to be 1.14 x $10^7$ pores/$cm^2$.

## 3.5 DISCUSSION

### 3.5.1 Effect of drug physicochemical properties on apparent permeability through TPU membranes

As in our previous study, we observed a clear bifurcation in the behavior of the mixed TPU membrane system across drugs of varying physicochemical properties [37]. As we proposed in that publication, for membranes composed of low hydrophilic TPU concentration, drug must diffuse through hydrophobic TPU polymer domains to move from the donor to the acceptor chamber. For the drug to diffuse through the polymer, it must dissolve into it [49]. Multiple previous studies have identified a drug's hydrophobicity, typically quantified by its octanol/water partition coefficient, as a significant contributor to its solubility [50,51]. Therefore, it is not surprising that the physicochemical properties of a drug compound would influence its ability to diffuse through the membrane.

We have shown that the drug's hydrophilicity, as quantified by its octanol/water distribution coefficient, correlates with its diffusion rate through the membrane at low hydrophilic TPU compositions (Figure 3.2 and Figure 3.3). This phenomenon is observed with compounds of different structural features that have inherently different polarity, as well as for a given drug as it transitions between different ionization states. It is remarkable how strongly the distribution coefficient is a determinant of membrane permeability below the percolation threshold, regardless of the drug compound studied

(Figure 3.5). Specifically, we observed that hydrophobic unionized ibuprofen (log D = 3.49, Table 3.2) exhibited similar apparent permeability through hydrophobic-rich TPU membranes as through water-filled pores of hydrophilic-rich TPU membranes (Figure 3.3b). We would envision that hydrophobic TPU is a broadly similar hydrophobic environment for the drug to EVA or silicone, although specific diffusion rates may vary. Compounds of a similar hydrophobic character would be expected to diffuse through the hydrophobic membrane at a reasonably fast rate to elute effective drug levels. Perhaps not coincidentally, both etonogestrel and levonorgestrel are available commercially as reservoir implants in which drug must diffuse through a hydrophobic EVA or silicone membrane and both compounds have octanol/water partition coefficients similar to or greater than ibuprofen [20,21].

Another possible explanation for the observed change in apparent permeability between different drug compounds and within a given drug compound at different ionization states is that the diffusivity of the compound may be changing. We deliberately selected drug molecules of similar molecular weight to minimize the effect of diffusivity differences on their membrane permeability. However, others have demonstrated a relationship between the ionization status of a solute and its diffusion coefficient [52]. Therefore, we measured the diffusivity of metoprolol for each pH at which we chose to conduct the permeability studies. Table 3.3 highlights the negligible change in diffusivity of the compound as a function of ionization state. Consequently, we conclude that shifts in the hydrophobicity of the drug species are the primary cause of the observed changes in membrane permeability.

We have also demonstrated that the change in apparent permeability of the drug compounds observed with changing the environmental pH is not caused by any changes

to the membrane itself. Figure 3.4 illustrates the measured apparent permeability of emtricitabine at pH 7 and pH 10. As shown in Table 3.2, there is no substantial difference in the log D of emtricitabine between pH 7 and 10, which is expected based on its $pK_a$ at 2.7. There was no observed difference in emtricitabine apparent permeability across the TPU composition range between pH 7 and 10, underscoring the relevance of drug physicochemical properties as the driver of permeability changes in our study. However, our conclusion that environmental pH does not cause changes to the membrane itself is driven by an assessment using a single drug.

For membranes composed of high hydrophilic TPU concentrations, above the percolation threshold that we proposed in which a continuous network of water-filled pores is formed, drug may diffuse through the pores to move from the donor to the acceptor chamber [37]. In this way, drug is largely able to avoid polymer interactions as a major determinant of its diffusion rate. Consequently, we observed minimal differences in apparent permeability through the TPU membranes at hydrophilic TPU compositions ≥55% (w/w) hydrophilic TPU, regardless of the drug compound or ionization state studied.

This finding has substantial implications for the development of implants and other pharmaceutical dosage forms where hydrophilic TPUs may be used as a rate-controlling membrane. We have demonstrated that diffusion rate through the membrane is not sensitive to drug physicochemical properties, suggesting that drug release rate may be controlled by modifying the microstructure of the TPU pore network, largely irrespective of the properties of the drug of interest. Our study suggests that modulating membrane microstructure by mixing TPUs of varying hydrophilicity has limitations. Drug permeability does not significantly change across the hydrophobic-rich TPU

composition range and it changes dramatically over the composition range representing the percolation threshold. Changing the TPU pore network microstructure can be achieved by varying the hard segment to soft segment ratio of the TPU. While the consequences of this behavior are exciting, it's important to acknowledge that we do expect some physicochemical properties of the drug to impact its diffusion through hydrophilic TPU membranes. For example, it is well established that molecular weight impacts a solute's diffusion rate through a polymer [53]. We observed this phenomenon in our study in comparing the apparent permeability of FITC-dextrans of varying average molecular weight through a TPU membrane (Table 3.4).

### 3.5.2 Nanoscale Imaging of Dry TPU Membrane Microstructure

We sought to leverage atomic force microscopy to visualize the microstructure of the TPU membranes and assess whether our proposed hypothesis could be supported by the imaging data. The observed microstructure of the dry membranes as a function of TPU mixture composition (Figure 3.7) is generally similar to the hypothesized structure represented by the cartoon depicted by Lowinger et al. (Figure 3.8a) [37]. The AFM images support the depiction of hydrophobic TPU domains as the continuous phase and hydrophilic TPU domains as the discrete phase below the percolation threshold. At low hydrophilic TPU compositions, we observed a discrete phase well-dispersed in a separate continuous phase. We propose that the discrete phase is amorphous hydrophilic TPU and the continuous phase is hydrophobic TPU. The hydrophilic TPU domain size is in the range of 10-30 nm, although we would expect the domain size to increase when the polymer is hydrated. We have previously shown that the hydrophilic TPU swells substantially when exposed to water [37].

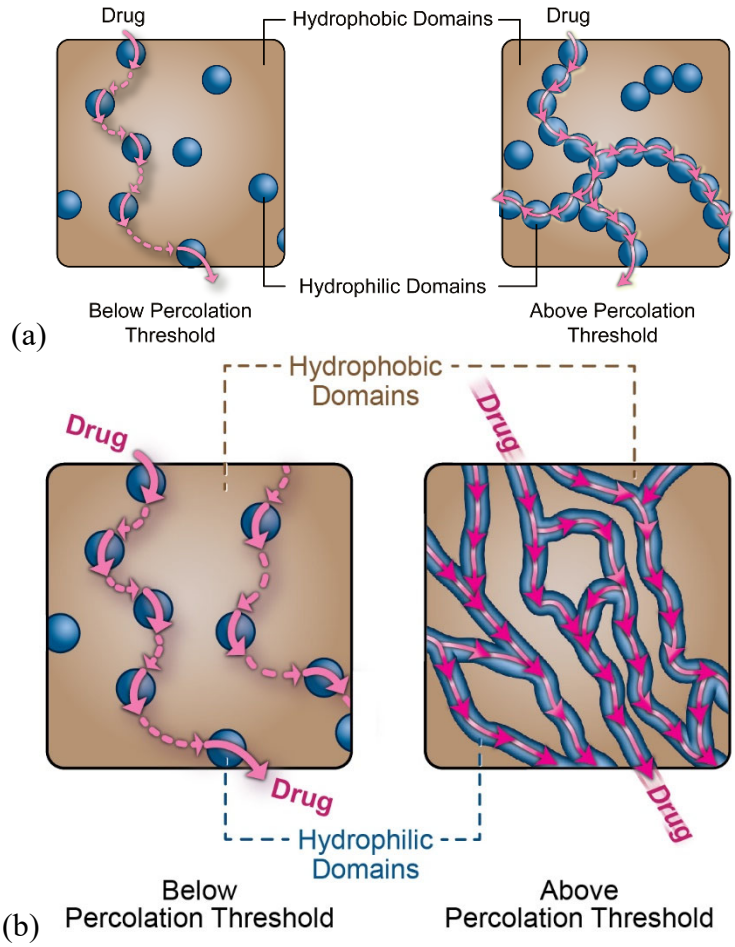


Figure 3.8: Conceptual illustration of mechanism of drug diffusion through polymer mixture below and above the percolation threshold. The cartoon depicts the hydrophobic domains as the continuous phase and the hydrophilic domains as the discrete phase. Above the percolation threshold, drug can diffuse within the polymer entirely through water-filled pores. (a) The cartoon as depicted in Lowinger et al. based on emtricitabine apparent permeability data. Adapted from [37], Elsevier, 2019 with permission. (b) The cartoon as revised based on the additional characterization data gathered in this study.

If a drug were to diffuse from one side of the membrane to the other, it would necessarily pass through regions of hydrophobic TPU. Therefore, its diffusion through hydrophobic TPU becomes the rate-limiting step to its overall diffusion through the

membrane. This microstructural feature also explains why there is a negligible difference in apparent permeability between pure hydrophobic TPU membranes and those composed of 25% (w/w) hydrophilic TPU across all drugs and ionization states investigated. The addition of 25% (w/w) hydrophilic TPU to the membrane does not change the inevitability that the drug must diffuse through regions of hydrophilic TPU.

We also observed evidence that a continuous network of hydrophilic TPU is present at compositions above the percolation threshold, as previously proposed in Figure 3.8a. We did not predict that the hydrophilic TPU domains would crystallize into a lamellar structure. In retrospect, however, the observation of crystalline domains is not surprising. Poly(ethylene oxide) (PEO), a constituent of the hydrophilic TPU copolymer, is known to crystallize into a semi-crystalline polymer at room temperature [54]. It has also been well established that crystallization of polymer chains follows a morphology where the chains fold back and forth to form lamellae with a thickness of 10-20 nm that will grow isotropically to form spherulites [55]. Wang et al. performed an interesting study to investigate the crystallization of PEO in a confined environment wherein the polymer was coextruded in alternating nanolayers with ethylene-co-acrylic acid [56]. Among other findings, they observed that when the thickness of the nanolayer was confined by another polymer phase, the PEO crystallized as single, high aspect ratio lamellae. Therefore, it may be expected that a mixed polymer system in which the hydrophilic PEO-containing TPU copolymer forms a continuous network but which is still constrained by a hydrophobic TPU polymer phase would form crystalline lamellae of 5-15 nm thickness as observed.

It is important to note that the images depicted in Figure 3.7 are of dry polymer membranes. The relevant environment for understanding the diffusion of drugs through

the membrane is an aqueous one where the polymer is hydrated. PEO is a water soluble polymer [57] and we would expect the crystalline PEO portions of the hydrophilic TPU that we observe in the images to dissolve when the polymer is hydrated, forming the water-filled pores. In other words, we would expect that water-filled pores would be present in the hydrated membrane where we observe crystalline lamellar regions in the dry AFM images. However, the hydrophilic TPU polymers swell when hydrated [36,37]. Consequently, we would expect the thickness of the lamellar phase to expand when the polymer hydrates. Since the images reveal that the 5-15 nm thick lamellae are very close (<5 nm) in proximity to each other, it is conceivable that multiple PEO lamellae coalesce when hydrated into a larger water-filled pore. This proposal helps to reconcile the dry AFM images with equivalent pore radius of 128 nm determined using FITC-dextran permeability measurements and equivalent pore analysis (Table 3.5).

The 50% (w/w) hydrophilic TPU image (Figure 3.7c) represents intermediate structural features to the features exhibited at those compositions directly below and above it. It is evident that hydrophilic TPU has begun to crystallize and exhibit a longer-range network. However, we can observe disruptions to the lamellar network at the 50% (w/w) hydrophilic TPU composition that we do not see at higher concentration TPU images. Based on these data, we would expect a drug to diffuse faster through the 50% (w/w) hydrophilic TPU membrane, but substantially slower than through the 55% (w/w) hydrophilic TPU membrane because it still must periodically diffuse through small hydrophobic TPU domains. Indeed, we observe this diffusion behavior with both emtricitabine (Figure 3.4) and metoprolol under a variety of ionization states (Figure 3.3a). The significant change in diffusion rate between 25%, 50%, and 55% (w/w) hydrophilic TPU is less apparent for unionized ibuprofen, but we propose this is because

unionized ibuprofen is significantly more hydrophobic than the other drug species and can diffuse through hydrophobic TPU domains at rates similar to its diffusion through water-filled pores.

### 3.5.3 Hydrated Membrane Microstructure Characterization

Although AFM imaging provides valuable insight into the microstructure of the TPU membranes, we sought an orthogonal approach to address two gaps. Firstly, while imaging can be a powerful tool to visualize structural changes to the membrane as TPU mixture composition changes, it is qualitative and is therefore inherently more subjective than a more quantitative technique. Secondly, the AFM membranes were imaged in the dry state and we made inferences about how they would behave in the hydrated state. By using an equivalent pore analysis approach, we were able to quantitatively characterize the TPU membranes in the hydrated state.

When determining the total pore area available for diffusion, we assumed that the pore length in the hydrated membrane was equivalent to the membrane thickness. That is, we assumed there is no tortuosity to the pores. Although there is certainly some tortuosity to the pore in reality, the extensive network suggested by the AFM images (Figure 3.7) suggests that tortuosity is low. Consequently, we believe that a reasonable approximation of the pore length is the membrane thickness.

The total pore area relative to the total membrane area (0.583%) described in Table 3.5 provides a quantitative measure of membrane porosity. Membrane porosity would typically be expressed as a fraction of the total membrane volume, rather than area, taken up by pores. However, the AFM images suggest that water-filled pores are distributed throughout the TPU membrane isotropically (Figure 3.7c-f). Since there is no

apparent preferred orientation to the pores, we can assume that the area fraction consumed by pores is equivalent to the volume fraction taken up by pores. By selecting a hydrophilic TPU composed of a lower soft segment content, with a lower extent of swelling, we would expect the total pore area relative to the total membrane area to decrease, constituting a mechanism to modulate drug release rate.

Table 3.5: Outcome of 75% (w/w) hydrophilic TPU membrane microstructure analysis using FITC-dextrans of varying nominal molecular weight.

| | |
|---|---|
| **Total pore area available for diffusion/pore length ($A_p$/dx)** | 0.898 cm |
| **Total pore area ($A_p$) assuming 100 µm pore length** | 0.00898 $cm^2$ |
| **Pore area relative to total membrane area** | 0.583% |
| **Equivalent number of pores ($N_p$)** | 1.14 x $10^7$ pores/$cm^2$ |
| **Equivalent pore radius ($r_p$)** | 128 nm |

The equivalent pore radius approximates the maximum size of a molecule that can diffuse through a homogeneous pore population but assumes that the molecule is spherical. Dextrans are known to exhibit a rod shape, more closely resembling an ellipsoid [58]. The free diffusion of rod-shaped solutes in a liquid medium has been found to correlate with its longer dimension. In contrast, the diffusion of rod-shaped solutes through polymers has been shown to correlate with its shorter dimension [59]. The diffusion of rod-shaped dextrans is expected to occur by entering the pore with the smaller axis of the dextran. Consequently, dextrans are not ideally suited for pore size

determination and the estimates of equivalent pore attributes described in this study represent only an upper end approximation of the microstructure.

However, the determined equivalent pore radius (128 nm) shown in Table 3.5 is substantially larger than the hydrodynamic radii of small and macromolecules. Armstrong et al. reported that a variety of therapeutic antibodies exhibited hydrodynamic radii in the range of 3-7 nm, with the largest macromolecules they studied having a hydrodynamic radius of approximately 25 nm. Therefore, despite any inaccuracies in the membrane microstructure caused by our assumptions, we would expect rate-controlling membranes composed of hydrophilic TPUs can release both small and large drug molecules.

## 3.6 CONCLUSION

As part of this investigation, we sought to more deeply understand the findings from our previous study. We examined the effect of drug physicochemical properties on their diffusion through rate-controlling membranes composed of TPU mixtures. We identified a substantial correlation between a drug's distribution coefficient and its apparent permeability through membranes at TPU mixture compositions below the percolation threshold. We believe this behavior broadly represents the relationship between drug properties and their release through EVA and silicone, the dominant materials used in commercial implants. In contrast, we observed a minimal effect of drug hydrophobicity on its apparent permeability through membranes at hydrophilic-rich TPU mixture compositions. Our finding suggests that implants with rate-controlling membranes composed of hydrophilic TPU will allow for the modulation of drug release

rate based on the swelling behavior of the selected TPU, largely irrespective of drug hydrophobicity.

We leveraged a nanoscale imaging approach to visualize changes to the dry membrane microstructure across the TPU mixture composition range. We found that the membrane images broadly reflected the conceptual microstructure that we proposed in our previous study. We observed a discrete phase of hydrophilic TPU dispersed in a continuous phase of hydrophobic TPU at TPU mixture compositions below the percolation threshold. We found that the PEO segments of the hydrophilic TPU crystallized into lamellar structures at TPU mixture compositions above the percolation threshold, which are expected to dissolve, swell, and coalesce into water-filled pores when the membrane is hydrated. Consequently, we can bolster our confidence in the conclusion that drug release through implants with rate-controlling membranes composed of hydrophilic TPU will not be sensitive to drug hydrophobicity.

Finally, we performed an equivalent pore analysis to determine the membrane pore area of 0.583% of the 75% (w/w) hydrophilic TPU membrane. We estimated the equivalent pore radius at 128 nm, importantly finding that rate-controlling membranes composed of hydrophilic TPU can release both small and macromolecule drugs through their water-filled pore mechanism. Future work should investigate the tunability of both small and large molecule drug diffusion rate by varying the soft segment content of hydrophilic poly(urethane) membranes.

## 3.7 REFERENCES

[1] R.I. Horwitz, S.M. Horwitz, Adherence to Treatment and Health Outcomes, Arch. Intern. Med. 153 (1993) 1863. doi:10.1001/archinte.1993.00410160017001.

[2] P.L. Canner, S.A. Forman, M.A. Prud'homme, K.G. Berge, J. Stamler, Influence of Adherence to Treatment and Response of Cholesterol on Mortality in the Coronary Drug Project, N. Engl. J. Med. 303 (1980) 1038–1041. doi:10.1056/NEJM198010303031804.

[3] P.A. Pizzo, K.J. Robichaud, B.K. Edwards, C. Schumaker, B.S. Kramer, A. Johnson, Oral antibiotic prophylaxis in patients with cancer: A double-blind randomized placebo-controlled trial, J. Pediatr. 102 (1983) 125–133. doi:10.1016/S0022-3476(83)80310-2.

[4] R. Fuller, H. Roth, S. Long, Compliance with disulfiram treatment of alcoholism, J. Chronic Dis. 36 (1983) 161–170. doi:10.1016/0021-9681(83)90090-5.

[5] R.I. Horwitz, C.M. Viscoli, R.M. Donaldson, C.J. Murray, D.F. Ransohoff, R.I. Horwitz, L. Berkman, S.M. Horwitz, D.F. Ransohoff, J. Sindelar, Treatment adherence and risk of death after a myocardial infarction, Lancet. 336 (1990) 542–545. doi:10.1016/0140-6736(90)92095-Y.

[6] C. Celum, J.M. Baeten, Tenofovir-based pre-exposure prophylaxis for HIV prevention: evolving evidence., Curr. Opin. Infect. Dis. 25 (2012) 51–7. doi:10.1097/QCO.0b013e32834ef5ef.

[7] N. Islam, E. Gladki, Dry powder inhalers (DPIs)—A review of device reliability and innovation, Int. J. Pharm. 360 (2008) 1–11. doi:10.1016/J.IJPHARM.2008.04.044.

[8] S. Delany-Moretlwe, C. Lombard, D. Baron, L.-G. Bekker, B. Nkala, K. Ahmed, M. Sebe, W. Brumskine, M. Nchabeleng, T. Palanee-Philips, J. Ntshangase, S. Sibiya, E. Smith, R. Panchia, L. Myer, J.L. Schwartz, M. Marzinke, L. Morris, E.R. Brown, G.F. Doncel, G. Gray, H. Rees, Tenofovir 1% vaginal gel for prevention of HIV-1 infection in women in South Africa (FACTS-001): a phase 3, randomised, double-blind, placebo-controlled trial., Lancet. Infect. Dis. 18 (2018) 1241–1250. doi:10.1016/S1473-3099(18)30428-6.

[9] T.O.. Dieben, F.J.M.. Roumen, D. Apter, Efficacy, cycle control, and user acceptability of a novel combined contraceptive vaginal ring, Obstet. Gynecol. 100 (2002) 585–593. doi:10.1016/S0029-7844(02)02124-5.

[10] L.L. Sabin, M. Bachman DeSilva, C.J. Gill, L. Zhong, T. Vian, W. Xie, F. Cheng, K. Xu, G. Lan, J.E. Haberer, D.R. Bangsberg, Y. Li, H. Lu, A.L. Gifford, Improving Adherence to Antiretroviral Therapy With Triggered Real-time Text Message Reminders: The China Adherence Through Technology Study., J. Acquir. Immune Defic. Syndr. 69 (2015) 551–9. doi:10.1097/QAI.0000000000000651.

[11] T. Peters-Strickland, L. Pestreich, A. Hatch, S. Rohatagi, R.A. Baker, J.P. Docherty, L. Markovtsova, P. Raja, P.J. Weiden, D.P. Walling, Usability of a

novel digital medicine system in adults with schizophrenia treated with sensor-embedded tablets of aripiprazole., Neuropsychiatr. Dis. Treat. 12 (2016) 2587–2594. doi:10.2147/NDT.S116029.

[12] H.B. Bosworth, J.N. Brown, S. Danus, L.L. Sanders, F. McCant, L.L. Zullig, M.K. Olsen, Evaluation of a packaging approach to improve cholesterol medication adherence., Am. J. Manag. Care. 23 (2017) e280–e286. http://www.ncbi.nlm.nih.gov/pubmed/29087166 (accessed March 28, 2019).

[13] J.H. Lin, Bisphosphonates: A review of their pharmacokinetic properties, Bone. 18 (1996) 75–85. doi:10.1016/8756-3282(95)00445-9.

[14] M. Markowitz, S.G. Sarafianos, 4′-Ethynyl-2-fluoro-2′-deoxyadenosine, MK-8591, Curr. Opin. HIV AIDS. 13 (2018) 294–299. doi:10.1097/COH.0000000000000467.

[15] D.A. Smith, K. Beaumont, T.S. Maurer, L. Di, Relevance of Half-Life in Drug Design, J. Med. Chem. 61 (2018) 4273–4282. doi:10.1021/acs.jmedchem.7b00969.

[16] I. Sivin, L. Wan, S. Ranta, F. Alvarez, V. Brache, D.R. Mishell, P. Darney, A. Biswas, S. Diaz, O. Kiriwat, M.P. Anant, C. Klaisle, M. Pavez, J. Schechter, Levonorgestrel concentrations during 7 years of continuous use of Jadelle contraceptive implants, Contraception. 64 (2001) 43–49. doi:10.1016/S0010-7824(01)00226-8.

[17] J. White, J. Bell, J.B. Saunders, P. Williamson, M. Makowska, A. Farquharson, K.L. Beebe, Open-label dose-finding trial of buprenorphine implants (Probuphine)® for treatment of heroin dependence, Drug Alcohol Depend. 103 (2009) 37–43. doi:10.1016/J.DRUGALCDEP.2009.03.008.

[18] S. Stewart, J. Domínguez-Robles, R. Donnelly, E. Larrañeta, S.A. Stewart, J. Domínguez-Robles, R.F. Donnelly, E. Larrañeta, Implantable Polymeric Drug Delivery Devices: Classification, Manufacture, Materials, and Clinical Applications, Polymers (Basel). 10 (2018) 1379. doi:10.3390/polym10121379.

[19] J. Siepmann, F. Siepmann, Mathematical modeling of drug delivery, Int. J. Pharm. 364 (2008) 328–343. doi:10.1016/j.ijpharm.2008.09.004.

[20] S. Palomba, A. Falbo, A. Di Cello, C. Materazzo, F. Zullo, Nexplanon: The new implant for long-term contraception. A comprehensive descriptive review, Gynecol. Endocrinol. 28 (2012) 710–721. doi:10.3109/09513590.2011.652247.

[21] S.H. Perry, P. Swamy, G.A. Preidis, A. Mwanyumba, N. Motsa, H.N. Sarero, Implementing the Jadelle implant for women living with HIV in a resource-limited setting, AIDS. 28 (2014) 791–793. doi:10.1097/QAD.0000000000000177.

[22] M. Gunawardana, M. Remedios-Chan, C.S. Miller, R. Fanter, F. Yang, M.A.

Marzinke, C.W. Hendrix, M. Beliveau, J.A. Moss, T.J. Smith, M.M. Baum, Pharmacokinetics of Long-Acting Tenofovir Alafenamide (GS-7340) Subdermal Implant for HIV Prophylaxis, Antimicrob. Agents Chemother. 59 (2015) 3913–3919. doi:10.1128/aac.00656-15.

[23] S.E. Barrett, R.S. Teller, S.P. Forster, L. Li, M.A. Mackey, D. Skomski, Z. Yang, K.L. Fillgrove, G.J. Doto, S.L. Wood, J. Lebron, J.A. Grobler, R.I. Sanchez, Z. Liu, B. Lu, T. Niu, L. Sun, M.E. Gindy, Extended Duration MK-8591-Eluting Implant as a Candidate for HIV Treatment and Prevention., Antimicrob. Agents Chemother. (2018) AAC.01058-18. doi:10.1128/AAC.01058-18.

[24] M. He, G. Yang, S. Zhang, X. Zhao, Y. Gao, Dissolving Microneedles Loaded With Etonogestrel Microcrystal Particles for Intradermal Sustained Delivery, J. Pharm. Sci. 107 (2018) 1037–1045. doi:10.1016/J.XPHS.2017.11.013.

[25] D. Bateson, K. McNamee, P. Briggs, Newer non-oral hormonal contraception., BMJ. 346 (2013) f341. doi:10.1136/bmj.f341.

[26] L. Xu, L. Li, J. Huang, S. Yu, J. Wang, N. Li, Determination of the lipophilicity (log Po/w) of organic compounds by microemulsion liquid chromatography, J. Pharm. Biomed. Anal. 102 (2015) 409–416. doi:10.1016/J.JPBA.2014.09.037.

[27] K. Krätschmer, Medicinal Chemistry In The Framework Of Hormonal And Non-Hormonal Contraception, Org. Med. Chem. Int. J. 3 (2017). doi:10.19080/OMCIJ.2017.03.555612.

[28] J.C. Wright, A.S. Hoffman, Historical Overview of Long Acting Injections and Implants, in: Long Act. Inject. Implant., Springer US, Boston, MA, 2012: pp. 11–24. doi:10.1007/978-1-4614-0554-2_2.

[29] J. Wang, V. Yadav, A.L. Smart, S. Tajiri, A.W. Basit, Stability of peptide drugs in the colon, Eur. J. Pharm. Sci. 78 (2015) 31–36. doi:10.1016/J.EJPS.2015.06.018.

[30] J.T. Clark, M.R. Clark, N.B. Shelke, T.J. Johnson, E.M. Smith, A.K. Andreasen, J.S. Nebeker, J. Fabian, D.R. Friend, P.F. Kiser, Engineering a Segmented Dual-Reservoir Polyurethane Intravaginal Ring for Simultaneous Prevention of HIV Transmission and Unwanted Pregnancy, PLoS One. 9 (2014) e88509. doi:10.1371/journal.pone.0088509.

[31] A.J. Coury, P.C. Slaikeu, P.T. Cahalan, K.B. Stokes, C.M. Hobot, Factors and Interactions Affecting the Performance of Polyurethane Elastomers in Medical Devices, J. Biomater. Appl. 3 (1988) 130–179. doi:10.1177/088532828800300202.

[32] M. Habash, G. Reid, Microbial Biofilms: Their Development and Significance for Medical Device-Related Infections, J. Clin. Pharmacol. 39 (1999) 887–898. doi:10.1177/00912709922008506.

[33] K. Stokes, R. McVenes, J.M. Anderson, Polyurethane Elastomer Biostability, J.

Biomater. Appl. 9 (1995) 321–354. doi:10.1177/088532829500900402.

[34] M.B. Lowinger, S.E. Barrett, F. Zhang, R.O. Williams, Sustained Release Drug Delivery Applications of Polyurethanes, Pharmaceutics. 10 (2018) 55. doi:10.3390/pharmaceutics10020055.

[35] Y. Ikeda, S. Kohjiya, S. Takesako, S. Yamashita, Polyurethane elastomer with PEO-PTMO-PEO soft segment for sustained release of drugs, Biomaterials. 11 (1990) 553–560. doi:10.1016/0142-9612(90)90077-4.

[36] G. Verstraete, J. Van Renterghem, P.J. Van Bockstal, S. Kasmi, B.G. De Geest, T. De Beer, J.P. Remon, C. Vervaet, Hydrophilic thermoplastic polyurethanes for the manufacturing of highly dosed oral sustained release matrices via hot melt extrusion and injection molding, Int. J. Pharm. 506 (2016) 214–221. doi:10.1016/J.IJPHARM.2016.04.057.

[37] M.B. Lowinger, Y. Su, X. Lu, R.O. Williams, F. Zhang, Can drug release rate from implants be tailored using poly(urethane) mixtures?, Int. J. Pharm. 557 (2019) 390–401. doi:10.1016/j.ijpharm.2018.11.067.

[38] J.K. Armstrong, R.B. Wenby, H.J. Meiselman, T.C. Fisher, The Hydrodynamic Radii of Macromolecules and Their Effect on Red Blood Cell Aggregation, Biophys. J. 87 (2004) 4259–4270. doi:10.1529/BIOPHYSJ.104.047746.

[39] R.P. Durbin, H. Frank, A.K. Soloman, Water Flow Through Frog Gastric Mucosa, J. Gen. Physiol. 39 (1956) 535–551. doi:10.1085/jgp.39.4.535.

[40] E.M. Renkin, Filtration, diffusion, and molecular sieving through porous cellulose membranes., J. Gen. Physiol. 38 (1954) 225–243. doi:10.1085/JGP.38.2.225.

[41] K.J. Kim, E.D. Crandall, Heteropore populations of bullfrog alveolar epithelium., J. Appl. Physiol. 54 (1983) 140–6. doi:10.1152/jappl.1983.54.1.140.

[42] L.C. Dong, A.S. Hoffman, Q. Yan, Macromolecular penetration through hydrogels, J. Biomater. Sci. Polym. 5 (1994) 473–484.

[43] Y. Matsukawa, V.H.L. Lee, E.D. Crandall, K.-J. Kim, Size-Dependent Dextran Transport across Rat Alveolar Epithelial Cell Monolayers, J. Pharm. Sci. 86 (1997) 305–309. doi:10.1021/JS960352X.

[44] J.S. Vrentas, J.L. Duda, Diffusion in polymer–solvent systems. II. A predictive theory for the dependence of diffusion coefficients on temperature, concentration, and molecular weight, J. Polym. Sci. Polym. Phys. Ed. 15 (1977) 417–439. doi:10.1002/pol.1977.180150303.

[45] K.F. Morris, C.S. Johnson, Diffusion-ordered two-dimensional nuclear magnetic resonance spectroscopy, J. Am. Chem. Soc. 114 (1992) 3139–3141. doi:10.1021/ja00034a071.

[46] D.A. Ivanov, Z. Amalou, S.N. Magonov, Real-time evolution of the lamellar organization of poly(ethylene terephthalate) during crystallization from the melt: High-temperature atomic force microscopy study, Macromolecules. 34 (2001) 8944–8952. doi:10.1021/ma010809b.

[47] P. Busch, D. Posselt, D.M. Smilgies, B. Rheinländer, F. Kremer, C.M. Papadakis, Lamellar diblock copolymer thin films investigated by tapping mode atomic force microscopy: Molar-mass dependence of surface ordering, Macromolecules. 36 (2003) 8717–8727. doi:10.1021/ma034375r.

[48] J.-J. Zhou, J.-G. Liu, S.-K. Yan, J.-Y. Dong, L. Li, C.-M. Chan, J.M. Schultz, Atomic force microscopy study of the lamellar growth of isotactic polypropylene, Polymer (Guildf). 46 (2005) 4077–4087. doi:10.1016/J.POLYMER.2005.03.047.

[49] M. Hombreiro-Pérez, J. Siepmann, C. Zinutti, A. Lamprecht, N. Ubrich, M. Hoffman, R. Bodmeier, P. Maincent, Non-degradable microparticles containing a hydrophilic and/or a lipophilic drug: preparation, characterization and drug release modeling, J. Control. Release. 88 (2003) 413–428. doi:10.1016/S0168-3659(03)00030-0.

[50] C. Hansch, J.E. Quinlan, G.L. Lawrence, Linear free-energy relationship between partition coefficients and the aqueous solubility of organic liquids, J. Org. Chem. 33 (1968) 347–350. doi:10.1021/jo01265a071.

[51] S.H. Yalkowsky, S.C. Valvani, Solubility and partitioning I: Solubility of nonelectrolytes in water, J. Pharm. Sci. 69 (1980) 912–922. doi:10.1002/jps.2600690814.

[52] M.Z. Southard, L.J. Dias, K.J. Himmelstein, V.J. Stella, Experimental Determinations of Diffusion Coefficients in Dilute Aqueous Solution Using the Method of Hydrodynamic Stability, Pharm. Res. 08 (1991) 1489–1494. doi:10.1023/A:1015886131198.

[53] C.R. Wilke, P. Chang, Correlation of diffusion coefficients in dilute solutions, AIChE J. 1 (1955) 264–270. doi:10.1002/aic.690010222.

[54] J.. Hay, M. Sabir, Crystallization kinetics of high polymers. Polyethylene oxide—Part II, Polymer (Guildf). 10 (1969) 203–211. doi:10.1016/0032-3861(69)90031-7.

[55] E. Baer, A. Hiltner, H.D. Keith, Hierarchical structure in polymeric materials., Science. 235 (1987) 1015–22. doi:10.1126/SCIENCE.3823866.

[56] H. Wang, J.K. Keum, A. Hiltner, E. Baer, B. Freeman, A. Rozanski, A. Galeski, Confined crystallization of polyethylene oxide in nanolayer assemblies, Science (80-. ). 323 (2009) 757–760. doi:10.1126/science.1164601.

[57] R. Kjellander, E. Florin, Water structure and changes in thermal stability of the system poly(ethylene oxide)–water, J. Chem. Soc. Faraday Trans. 1 Phys. Chem.

Condens. Phases. 77 (1981) 2053. doi:10.1039/f19817702053.

[58] C.H. van Os, M.D. de Jong, J.F.G. Slegers, Dimensions of polar pathways through rabbit gallbladder epithelium, J. Membr. Biol. 15 (1974) 363–382. doi:10.1007/BF01870095.

[59] W.R. Lieb, W.D. Stein, Implications of two different types of diffusion for biological membranes, Nat. New Biol. 234 (1971) 220–222. doi:10.1038/newbio234220a0.

# Chapter 4: Hydrophilic poly(urethanes) are an effective tool for gastric retention independent of drug release rate[4]

## 4.1 ABSTRACT

Acyclovir is a poorly permeable, short half-life drug with poor colonic absorption, and current conventional controlled release formulations are unable to decrease the frequency of administration. We designed acyclovir dosage forms to be administered less frequently by being retained in the stomach and releasing drug over an extended duration. We developed a conventional modified-release matrix tablet to sustain the release of acyclovir and surrounded it with a hydrophilic poly(urethane) layer. When hydrated, the porous poly(urethane) swells to a size near or beyond that of the relaxed pylorus diameter and does not affect drug release rate. We demonstrated that the formulation is retained in the stomach for extended durations as it slowly releases drug, allowing for similar AUC but delayed $t_{max}$ relative to a non-gastroretentive control tablet. Unlike many other gastroretentive formulations, this dosage form design decouples drug release rate from gastric retention time, allowing them to be modulated independently. It also effectively retains in the stomach regardless of prandial state, differentiating from other approaches. Our direct observation of excised rat stomachs allowed for a rigorous assessment of the impact of polymer swelling extent and prandial state on both the dosage form integrity and retention time.

[4] Submitted to Journal of Pharmaceutical Sciences. Michael Lowinger designed, executed, and performed the experiments, and wrote the manuscript.

## 4.2 INTRODUCTION

Pharmaceutical researchers have attempted gastric retention for decades as a technique to improve the pharmacokinetic (PK) properties of drugs with oral absorption challenges. Increasing the gastric residence time may be useful for drugs that are locally active in the stomach [1–4], have a narrow absorption window [5–8], are unstable in the intestinal environment [9], or which exhibit poor solubility at intestinal pH [10–12]. By virtue of increasing the overall gastrointestinal residence time, gastric retention may be used to develop an extended release drug product with reduced frequency of administration and improved patient adherence [13].

A key challenge in successfully achieving gastric retention relates to the physiological environment. The process of gastric emptying is determined by the interdigestive migrating myoelectric complex (MMC), which cycles through the stomach and small intestine every 1.5-2 hours [14]. Gastroretentive (GR) dosage forms aim to overcome the MMC process in which the stomach removes large, undigested material during Phase III [15]. The main approaches undertaken by researchers to retain a dosage form in the stomach can be generally grouped into floating, mucoadhesive, and expandable systems.

The design intent of floating systems is to achieve gastric retention by keeping the dosage form away from the pylorus. Such systems are characterized by their capacity to float in and over the gastric content due to their low density [16]. This approach, however, requires the presence of stomach contents on which the dosage form can float. Since water empties rapidly from the stomach, there is an implicit requirement for food to be present in order to obtain a long gastric retention time [15]. Indeed, several clinical studies investigating floating systems have identified a relationship between gastric

retention time and food intake, making it difficult to envision consistent success in the fasted state [1,17].

Since their introduction several decades ago, mucoadhesive systems have attracted research interest to extend gastric retention time [18]. Designed to adhere to the stomach mucosal membrane, these systems must be able to resist high gastric motility and continual renewal of the mucus lining [19]. Consequently, multiple studies investigating the utility of mucoadhesive systems were able to identify evidence of gastric retention under fasted conditions [20–22]. Some limited preclinical successes with mucoadhesive systems have been reported. Patil and Talele developed a mucoadhesive gastroretentive tablet of lafutidine containing xanthan gum [23]. They performed x-ray imaging on rabbits and determined that their tablet retained in the stomach for over 10 hours. Pandey et al. prepared a mucoadhesive patch of lercanidipine HCl, using a combination of Eudragit RS and RL [24]. They assessed mucoadhesion by performing an *ex vivo* study using rat stomach mucosa and confirmed in a rabbit PK study that their formulation substantially increased gastrointestinal residence time. However, in both studies, the dosage forms also swelled substantially, so the specific mechanism of gastric retention is not clear.

Expandable systems are designed to increase in size to dimensions greater than those of the pyloric sphincter, thereby physically preventing the dosage form emptying from the stomach. To allow for facile administration, the dosage forms must be easily swallowed and increase in size significantly once inside the stomach [25]. Unfolding systems are composed of elastomers that unfold in the stomach [26–28]. Swelling systems utilize polymers with extensive swelling characteristics upon hydration [29–32]. Several researchers have attempted to estimate the size of the relaxed pylorus, since these

systems must expand to a size greater than the pyloric diameter to achieve gastric retention. Keet used radiological imaging to measure the relaxed pyloric diameter in 10 normal subjects and found its size to be 11-19 mm across the individuals studied [33]. Munk et al. measured the resting pylorus in the presence of food and determined it to be 12.8 ± 7.0 mm [34]. Lalloo et al. proposed that a formulation should swell to >15-16 mm in order to retain in the stomach [15].

Although many approaches undertaken to develop gastroretentive formulations have not translated into clinically successful drug products, some have demonstrated success including Glumetza®, Proquin® XR, and Gralise® [13]. We chose to focus on Gralise® as a comparator, which is a once daily tablet of gabapentin intended to retain in the stomach for extended durations. Gralise® tablets contain poly(ethylene oxide) (PEO) and hydroxypropyl methylcellulose, which swell when hydrated and form a matrix to control the drug release rate. Chen et al. reported that when compared with an immediate release gabapentin product, Gralise® exhibited a longer time ($t_{max}$) to reach a lower peak plasma concentration ($C_{max}$) [35]. To the extent that its formulation plays a role in stomach retention, the same polymers are used to swell the tablet and modulate drug release, such that these two attributes cannot be decoupled.

Thermoplastic poly(urethanes) (TPUs) have been applied to implanted medical devices for decades [36–38]. There has also been a substantial amount of research performed on the use of poly(urethanes) to deliver drugs orally [39–43]. Claeys et al. studied the impact of dicarboxylic acids on the release behavior of melt extruded and injection molded hydrophobic poly(urethane) tablets containing diprophylline [44]. Verstraete et al. followed up on that work by investigating the ability of hydrophilic poly(urethanes) to modify the release of several model drugs from tablets without the

need for a third component [45]. These hydrophilic TPUs, where the soft segment is PEO, are water insoluble yet have been shown to swell in water proportional to the PEO content in the copolymer [46]. We have recently studied the underlying mechanism of drug transport through hydrophilic poly(urethanes) and demonstrated that a pore network is formed when the polymer is hydrated [47]. We also found that the diffusion of small molecule drugs through the hydrophilic TPU pore network is relatively fast and insensitive to drug physicochemical properties. The properties of hydrophilic TPU may be suitable for gastric retention, whereby the substantial swelling of the polymer physically prevents passing through the pylorus while the pore network allows for drug release at a rate dictated by other attributes of the dosage form.

Acyclovir is a guanosine-analogue antiviral drug used to treat herpes-simplex and varicella-zoster virus infections [48]. It is available to be administered as an oral tablet, a topical cream, an ophthalmic ointment, and as an intravenous injection [49]. Despite its relatively high water solubility (1.82 mg/mL), acyclovir exhibits poor oral bioavailability of only 15-20% [48,50]. The drug's poor absorption behavior is likely driven by its low intestinal permeability, leading to high administered doses [51]. Moreover, acyclovir exhibits a short elimination half-life of 2-3 hours, resulting in the need for patients to take tablets as often as five times per day [48]. The high frequency of administration may present adherence challenges as long term administration of acyclovir (6 months or longer) is required in patients with relapsing herpes-simplex infection [52]. The drug is predominantly absorbed from the upper gastrointestinal tract, making it unlikely for conventional sustained release formulations to effectively reduce frequency of administration [53]. However, acyclovir's poor colonic absorption and short half-life make it a suitable candidate for a gastroretentive formulation approach, which has the

potential to reduce the frequency of administration. Indeed, others have tried various gastroretentive approaches to improve the pharmacokinetics of this drug [54–57].

We sought to develop a dosage form of acyclovir that could be administered less frequently by being retained in the stomach and releasing drug over a 6-12 hour time period. Our approach was to develop a conventional controlled release matrix tablet to sustain the release of acyclovir over the 6-12 hour time period and surround the matrix tablet with an outer layer composed of hydrophilic TPU. When the tablet is hydrated, the hydrophilic TPU layer swells beyond the size of the relaxed pylorus, providing a robust mechanism for gastric retention. We hypothesized that formulating acyclovir in such a dosage form will retain the tablet in the stomach as it slowly releases drug, allowing for similar area under the curve (AUC) but delayed $t_{max}$ relative to an immediate release control. Unlike many other gastroretentive formulations, this dosage form design decouples drug release rate from gastric retention time, allowing them to be modulated independently. We tested our hypothesis by conducting rat studies in which the stomach retention behavior of the dosage form was directly observed, in addition to comparing the pharmacokinetics of a control formulation to our gastroretentive dosage form.

## 4.3 MATERIALS AND METHODS

### 4.3.1 Materials

Acyclovir was purchased from Carbosynth Limited (Berkshire, UK). Hydrophilic poly(urethanes) Pathway™ PY-PT60DE500 and PY-PT60DE2000 and hydrophobic poly(urethane) Pathway™ PY-PT60DE were obtained from Lubrizol (Cleveland, OH). Microcrystalline cellulose Avicel® PH-102, hydroxypropyl methylcellulose (HPMC) grades K4M and K100M, and croscarmellose sodium were acquired from Dow (Midland,

MI). Lactose 316 was purchased from Kerry (Tralee, Ireland). Magnesium stearate was purchased from Mallinckrodt (Staines-upon-Thames, UK). Size 9 hard gelatin capsules were obtained from Torpac (Fairfield, NJ). Gabapentin drug substance was purchased from Sigma-Aldrich (St. Louis, MO). Gralise® 300 mg potency tablets were acquired from Assertio Therapeutics (Newark, CA). 0.1N hydrochloric acid (HCl) solution was purchased from Fisher (Hampton, NH). Acetonitrile and water were of HPLC grade. All other chemicals and reagents were of ACS grade or better.

### 4.3.2 Methods

#### *4.3.2.1 Dosage Form Preparation and Characterization*

Physical blends were weighed according to the compositions described in

Table 4.1 and Table 4.2 for acyclovir immediate release (IR) and controlled release (CR) formulations, respectively. The only compositional difference between the immediate and controlled release formulations was the addition of 20% (w/w) hydroxypropyl methylcellulose (HPMC) K4M to the controlled release formulation. The composition of the minitablet CR formulation used for rat studies is shown in Table 4.3. The only compositional difference between the large tablet and the minitablet controlled release formulation compositions is the grade of HPMC, changed from K4M to K100M. This change reflects the increased surface area of minitablets, necessitating a higher viscosity polymer to obtain similar drug release rate.

All components except magnesium stearate were added to glass bottles and mixed for 10 minutes using a Glen Mills Turbula mixer (Clifton, NJ). Magnesium stearate was screened through a 60 mesh sieve, added to the glass bottle, and blended for an additional

2 minutes. Blends were compressed with a Roland Research Devices compaction simulator (Ewing, NJ) using 17.02 x 6.73 mm tooling from Elizabeth Carbide (McKeesport, PA) for the large immediate release and controlled release tablets to prepare 200 mg potency tablets. The controlled release minitablets were compressed using 1.5 mm diameter 18-tip tooling from Elizabeth Carbide to prepare 1 mg potency minitablets. The large immediate release tablets were compressed with a 15 kN force to a hardness of 29 kP. The large controlled release tablets were compressed with a 12 kN force to a hardness of 20 kP, while the controlled release minitablets were compressed with a 12 kN force.

Table 4.1: Core tablet composition for immediate release acyclovir formulation.

| Component | Composition (% w/w) | Weight/Tablet (mg) |
|---|---|---|
| Acyclovir | 30% | 200 |
| Microcrystalline Cellulose, Avicel® PH102 | 33% | 220 |
| Lactose 316 | 33% | 220 |
| Croscarmellose sodium | 3% | 20.0 |
| Magnesium stearate | 1% | 6.70 |

Table 4.2: Core tablet composition for controlled release acyclovir matrix formulation.

| Component | Composition (% w/w) | Weight/Tablet (mg) |
|---|---|---|
| Acyclovir | 30% | 200 |
| Microcrystalline Cellulose, Avicel® PH102 | 23% | 154 |
| Lactose 316 | 23% | 153 |
| Hydroxypropyl methylcellulose K4M | 20% | 133 |
| Croscarmellose sodium | 3% | 20.0 |
| Magnesium stearate | 1% | 6.70 |

Table 4.3: Core tablet composition for minitablet controlled release acyclovir matrix formulation.

| Component | Composition (% w/w) | Weight/Tablet (mg) |
|---|---|---|
| Acyclovir | 30% | 200 |
| Microcrystalline Cellulose, Avicel® PH102 | 23% | 154 |
| Lactose 316 | 23% | 153 |
| Hydroxypropyl methylcellulose K100M | 20% | 133 |
| Croscarmellose sodium | 3% | 20.0 |
| Magnesium stearate | 1% | 6.70 |

Poly(urethane) films with two different swelling extents were prepared in different ways. The greater swelling (100% TPU2000) film was prepared by drying PY-PT60DE2000 polymer pellets overnight in a vacuum oven set to 40°C with 200 mbar absolute pressure, followed by compression at 700 lbf on an Automated Carver Press (Wabash, IN) between two poly(tetrafluoroethylene)-coated sheets at 180°C for a 5 minute dwell time. The film was then cooled for at least 15 minutes in a 5°C refrigerator. The lesser swelling (75% TPU500) film was prepared according to a procedure described elsewhere [58]. Briefly, it was manufactured using a Leistritz ZSE 18 twin-screw extruder (Somerville, NJ). The two polymers (PY-PT60DE500 and PY-PT60DE) were added using separate K-Tron feeders (Sewell, NJ). The film composition was determined by controlling the ratio of the feed rates into the extruder. The end of the extruder featured a $0.02 \times 6$ inch sheet die and the extrudate was fed into a Leistritz 3-roll film stack, temperature controlled to 15 °C.

Each large tablet was sandwiched between two polymer films on a hot plate set to 100°C. In the case of minitablets, two minitablets were sandwiched between the polymer films. Once a seal was formed, the tablet was tumbled on the 100°C hot plate to smooth

the edges. In the case of minitablets, the minitablets with a TPU layer were inserted into size 9 hard gelatin capsules to facilitate rat dosing.

Tablet dissolution was performed using a Hanson (Chatsworth, CA) USP dissolution apparatus type II. Each dissolution vessel was filled with 500 mL of 0.1N HCl, temperature controlled to 37°C, and the paddles were stirred at 75 rpm. Three 200 mg potency acyclovir matrix tablets and three 300 mg potency Gralise® tablets were added separately to each dissolution vessel. Acyclovir concentration was measured using ultraviolet (UV) absorbance with a Pion (Billerica, MA) Rainbow™ fiber optic system equipped with a deuterium lamp and UV dip probes. Gabapentin concentration was measured by taking aliquots, centrifuging them at 8000 rpm for 10 minutes, and transferring the supernatant to an HPLC. The gabapentin samples were analyzed using an Agilent (Santa Clara, CA) high performance liquid chromatography apparatus, coupled to a UV spectrophotometer. The chromatography used a Sigma-Aldrich Supelco (St. Louis, MO) Ascentis Express $C_{18}$ reverse phase column with a 4.6 mm inner diameter, 100 mm length, and 2.7 μm silica particle size. The mobile phase consisted of a gradient with mixtures of 0.1% (v/v) phosphoric acid and acetonitrile. Over the course of the 6 minute run time, the mobile phase composition shifted from 5% acetonitrile to 95% acetonitrile.

Tablet swelling was measured by soaking the dosage form in 0.1N HCl, removing the dosage form at each time point, and measuring the dimensions using a caliper. The dosage form was then returned to the hydrochloric acid solution.

#### *4.3.2.2 Rat Gastric Retention Study*

In order to assess the capability of our formulations to retain in the stomach for extended durations, we performed an *in vivo* gastric retention study in 10-week old female Sprague-Dawley rats (CD(SD) rats, Charles River Laboratories, Raleigh, NC). The study was conducted according to an approved institutional animal care and use committee (IACUC) protocol at the University of Texas at Austin (protocol number AUP-2019-00153). Animals were housed on a reversed 12-hour light cycle (lights on a 6 AM), and food and water were provided *ad libitum* unless otherwise described. One half of the rats were fasted starting 6 hours prior to dosage form administration and throughout the duration of the study, although they had free access to water. To reduce stress in the fasted animals, fasting was introduced in 2-4 hour increments over 4 days leading up to the study until a maximum 12-hour fasting period was achieved. On the day of the experiment, rats in the fasted group were transferred to a fresh cage 6 hours and 2 hours prior to dosing in order to minimize coprophagy during the study. Each rat received an oral administration of a gelatin capsule containing the greater swelling formulation, the lesser swelling formulation, or a non-swelling control formulation containing only acyclovir minitablets. Rat gastric contents were examined at 3, 6, 9, and 24 hours after dosage form administration. At each time point, three rats were sacrificed, and their stomachs were immediately excised, opened using a longitudinal incision, and investigated for the presence and disposition of the dosage form.

#### *4.3.2.3 Rat Pharmacokinetic Study*

In addition to the gastric retention study, we sought to investigate how our gastroretentive formulation affected drug release in an animal model. A rat pharmacokinetic study was performed according to an approved IACUC protocol at

Pharmaron Beijing Co., Ltd. (protocol number PH-DMPK-TEX-19-001), in which PK properties of the greater swelling formulation and the non-swelling control formulation in male Sprague-Dawley rats were compared. Three rats each were administered a 1.2 mg acyclovir dose of either formulation. The rats were given free access to food and water throughout the duration of the study. Blood samples were taken at 0.25, 0.5, 1, 2, 3, 6, 9, 24, and 36 hours after dosing. The bioanalytical assay was performed using a Shimadzu (Kyoto, Japan) high performance liquid chromatography apparatus, coupled to an AB Sciex (Framingham, MA) API 5500 LC-MS/MS mass spectrometer. The chromatography used a Waters (Milford, MA) XSelect HSS T3 $C_{18}$ reverse phase column with a 2.1 mm inner diameter, 50 mm length, and 2.5 μm silica particle size. The mobile phase consisted of a gradient with mixtures of 0.1% (v/v) formic acid and acetonitrile. Over the course of the 2 minute run time, the mobile phase composition shifted from 5% acetonitrile to 95% acetonitrile.

## 4.4 RESULTS

### 4.4.1 Dosage Form Characterization

We sought to develop an acyclovir matrix tablet that generally mimicked the drug release profile of gabapentin from Gralise®. Specifically, we aimed to achieve a tablet release profile where approximately 80% of drug is released at 9 hours with approximately 100% released by 24 hours. As shown in Figure 4.1, we developed an acyclovir matrix tablet formulation that closely matches the release profile of Gralise®. Our acyclovir formulation releases approximately 80% of the drug in 9 hours and approximately 100% of the drug is released by 24 hours.

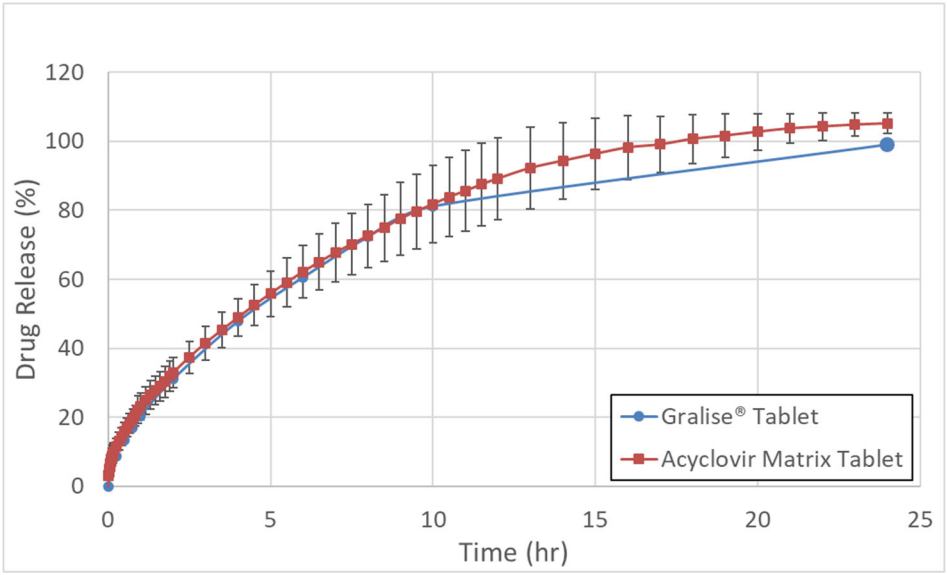


Figure 4.1: Mean concentration over time (N = 3 ± SD) of Gralise® tablets overlaid with matrix acyclovir tablets.

Since our acyclovir gastroretentive tablet design includes a matrix tablet surrounded by a hydrophilic TPU outer layer, we sought to understand the effect of the TPU layer itself on drug release. Figure 4.2a compares the dissolution behavior of an acyclovir immediate release tablet without any TPU outer layer to the same immediate release tablet with a greater swelling 100% TPU2000 outer layer. While the immediate release tablet without any TPU outer layer releases acyclovir rapidly with >80% released in 1.5 minutes, the tablet with a 100% TPU2000 outer layer exhibits substantially slower release. By performing a linear regression on the linear portion of the dissolution curve between 1 and 2 hours ($r^2$ = 0.99), we estimate an approximate release rate through the 100% TPU2000 outer layer of 2.6 µg/mL/hr.

(a)

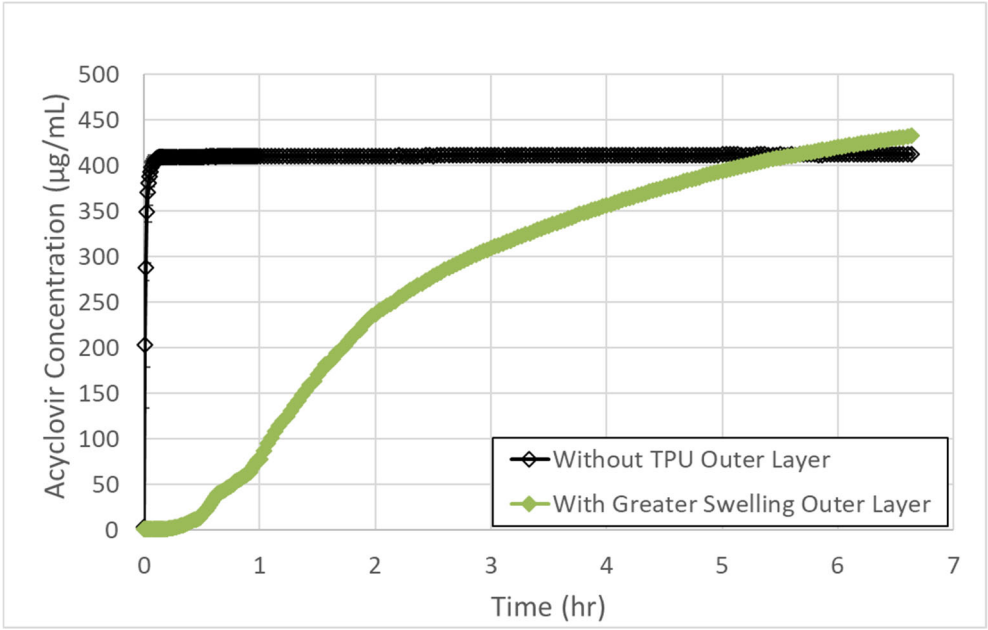


(b)

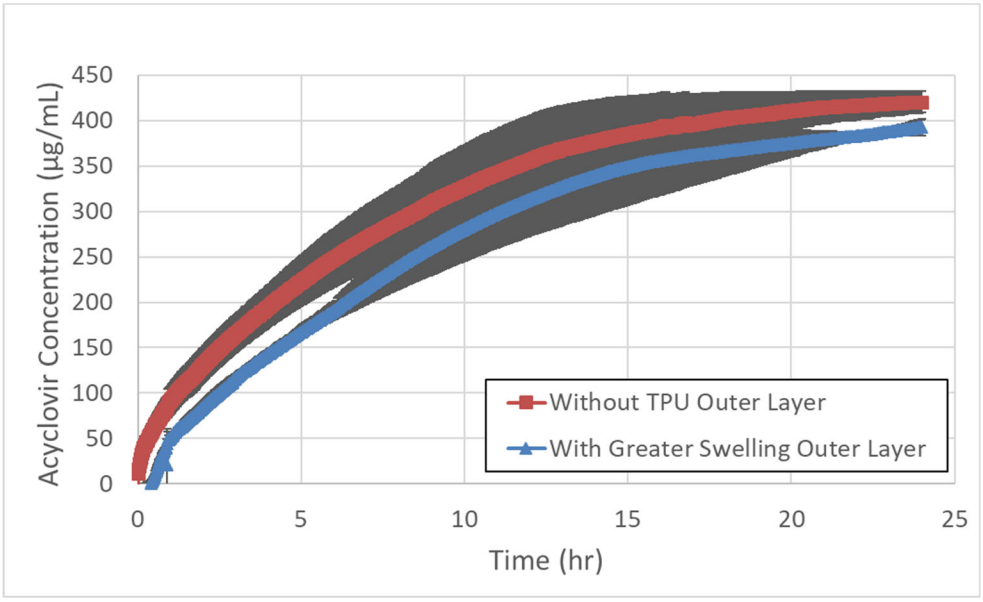


Figure 4.2: Mean concentration over time (N = 3 ± SD) of (a) immediate release and (b) controlled release acyclovir tablets with and without a greater swelling 100% TPU2000 outer layer.

Figure 4.2b shows the dissolution profile of the acyclovir controlled release matrix tablet without a TPU outer layer compared with the same tablet surrounded by a 100% TPU2000 outer layer. We performed a linear regression on the linear portion of both dissolution curves between 1.5 and 6.5 hours ($r^2$ = 0.99) and estimated that the release rates of both formulations are approximately identical at 0.46 µg/mL/hr. The only difference between the two dissolution curves shown in Figure 4.2b is an approximate 30-minute delay in release associated with the tablet surrounded by the TPU outer layer.

Figure 4.3 overlays the dissolution profiles of the same acyclovir matrix tablet without a TPU outer layer, with a greater swelling 100% TPU2000 outer layer, and with a lesser swelling 75% TPU500 outer layer. All three formulations exhibit similar drug release profiles over the 24-hour time course, suggesting that drug release rate can be decoupled from the absence, presence, or type of TPU outer layer used.

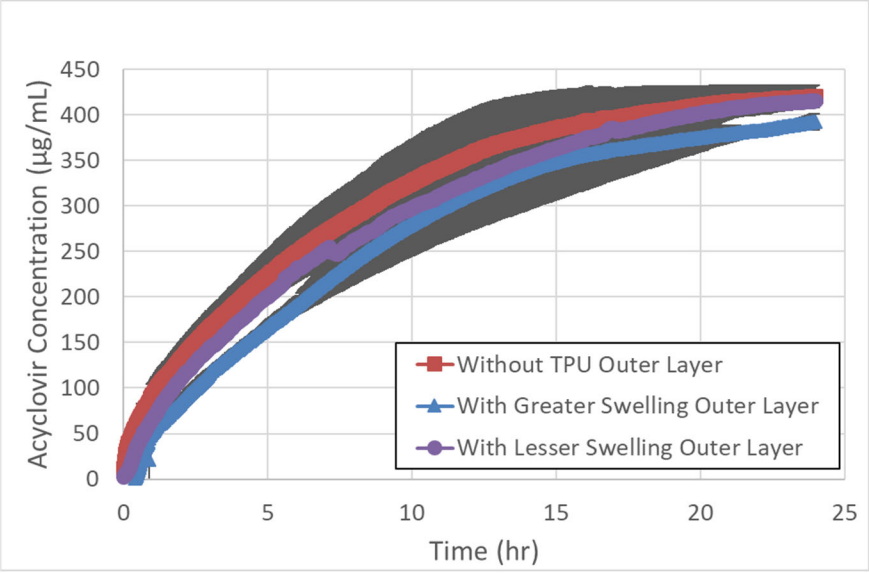


Figure 4.3: Mean concentration over time (N = 3 ± SD) of acyclovir controlled release tablets with no TPU outer layer, a greater swelling outer layer, and lesser swelling outer layer.

Since expandable dosage forms retain in the stomach by increasing their size to dimensions unable to pass through the pylorus, we investigated the swelling behavior of Gralise® as a benchmark. As described in Table 4.4, the tablet length, width, and thickness expanded approximately 30%, 20%, and 50%, respectively. Notably, the two largest dimensions of the fully swollen tablet are approximately 21 mm and 12 mm.

Table 4.4: Swelling behavior of a Gralise® tablet after soaking in 0.1N hydrochloric acid for varying lengths of time.

| Time (hr) | Length (mm) | Width (mm) | Thickness (mm) | % Change Length | % Change Width | % Change Thickness |
|---|---|---|---|---|---|---|
| 0 | 16.2 | 10.2 | 6.9 | --- | --- | --- |
| 0.25 | 17.3 | 10.5 | 7.4 | 7% | 3% | 7% |
| 0.5 | 17.9 | 11.5 | 7.9 | 10% | 13% | 14% |
| 0.75 | 17.9 | 11.8 | 7.8 | 10% | 16% | 13% |
| 1 | 18.2 | 12.2 | 8 | 12% | 20% | 16% |
| 2 | 18.6 | 12.5 | 9.3 | 15% | 23% | 35% |
| 4 | 18.9 | 12.4 | 10.8 | 17% | 22% | 57% |
| 6 | 19.8 | 12.1 | 10 | 22% | 19% | 45% |
| 8 | 20.2 | 12 | 10.2 | 25% | 18% | 48% |
| 10 | 20.9 | 11.9 | 10.4 | 29% | 17% | 51% |

Table 4.5 shows the swelling kinetics of acyclovir matrix tablets surrounded by greater swelling 100% TPU2000 and lesser swelling 75% TPU500 outer layers. The dry tablet width and thickness are similar to Gralise®, but they swell considerably more when soaked in 0.1N HCl. The greater swelling formulation achieves a hydrated length of 49 mm, a width 27 mm, and a thickness of 14 mm. The lesser swelling formulation attains a hydrated length of 35 mm, a width of 17 mm, and a thickness of 13 mm.

Table 4.5: Swelling behavior of controlled release acyclovir GR tablets with greater swelling and lesser swelling outer layers. Relative size to pylorus column indicates whether at least 2 dimensions are smaller than, similar to, or larger than the estimated human pylorus diameter.

| Time (hr) | Greater Swelling Outer Layer | | | | Lesser Swelling Outer Layer | | | |
|---|---|---|---|---|---|---|---|---|
| | Length (mm) | Width (mm) | Thickness (mm) | Relative Size to Pylorus | Length (mm) | Width (mm) | Thickness (mm) | Relative Size to Pylorus |
| 0 | 20.8 | 10.5 | 6.1 | Smaller | 19.7 | 8.1 | 6.2 | Smaller |
| 0.5 | 33.0 | 20.4 | 20.4 | Similar | 33.1 | 15.0 | 9.2 | Similar |
| 2 | 47.0 | 26.7 | 11.9 | Larger | 34.9 | 14.0 | 13.4 | Similar |
| 3 | 48.5 | 28.4 | 12.7 | Larger | 35.3 | 16.2 | 11.0 | Similar |
| 6 | 48.9 | 28.4 | 11.3 | Larger | 34.7 | 14.2 | 12.5 | Similar |
| 8 | 49.4 | 27.4 | 14.2 | Larger | 35.4 | 16.6 | 12.6 | Similar |

Our *in vivo* studies required scaling down of the acyclovir GR formulation to a scale suitable for rat consumption. Consequently, acyclovir matrix minitablets were encapsulated in an outer layer of either greater swelling 100% TPU2000 or lesser swelling 75% TPU500 and inserted into size 9 hard gelatin capsules. Table 4.6 describes the swelling behavior of both dosage forms in 0.1N HCl. The rat pylorus was previously estimated to be 2-3 mm in diameter, therefore we aimed to design formulations for which at least two of the dimensions swelled greater than 3 mm [59].

Table 4.6: Swelling behavior of minitablet controlled release acyclovir GR rat dosage forms with greater swelling and lesser swelling outer layers. Relative size to pylorus column indicates whether at least 2 dimensions are smaller than, similar to, or larger than the estimated rat pylorus diameter.

| Time (hr) | Greater Swelling Outer Layer | | | | Lesser Swelling Outer Layer | | | |
|---|---|---|---|---|---|---|---|---|
| | Length (mm) | Width (mm) | Thickness (mm) | Relative Size to Pylorus | Length (mm) | Width (mm) | Thickness (mm) | Relative Size to Pylorus |
| 0 | 8.6 | 2.5 | 2.5 | Similar | 8.3 | 2.5 | 2.5 | Similar |
| 0.5 | 17.1 | 6.3 | 6.3 | Larger | 14.2 | 4.4 | 4.4 | Similar |
| 2 | 18.0 | 6.2 | 6.2 | Larger | 13.5 | 3.2 | 3.6 | Similar |
| 3 | 19.0 | 5.1 | 5.6 | Larger | 12.8 | 3.9 | 3.5 | Similar |
| 6 | 19.6 | 6.4 | 5.1 | Larger | 13.3 | 4.0 | 3.4 | Similar |
| 8 | 19.0 | 6.2 | 5.0 | Larger | 13.0 | 4.0 | 3.5 | Similar |

### 4.4.2 Rat Gastric Retention Study

We investigated the ability of our GR dosage forms to retain in the stomach by administering the formulations to rats and, at specific time points, sacrificing them and inspecting their stomach contents. Table 4.7 summarizes the observations of stomach retention for the two GR formulations of varying swelling extent and a non-swelling control in the fasted and fed states. Representative pictures of the excised stomach and isolated dosage form for each formulation, prandial state, and time point are provided in Appendix C:. Two animals were removed from the study due to dosing error (i.e., potential release of capsule in mouth, which led to chewing or expelling the dosage form from the mouth in the cage). Consequently, we denoted these observations with a N/A in the table and excluded them from subsequent analysis. We summarized the findings at each time point and prandial state by reporting the percent of rats for which the dosage form was retained in the stomach. Notably, both GR formulations retain in the rat

stomach for extended durations, whereas the non-swelling control does not retain in the stomach at 6 hours.

Table 4.7: Summary of dosage form retention in each rat during gastric retention study. N/M indicates that the replicate was not measured. N/A means not applicable and indicates that we were unable to verify that the rat swallowed the capsule, resulting in the exclusion of that data point from the analysis.

| Formulation | Prandial State | Time Point (hr) | Dosage Form Retained in Stomach | | | |
|---|---|---|---|---|---|---|
| | | | Replicate 1 | Replicate 2 | Replicate 3 | % Retained |
| Greater Swelling | Fed | 3 | Yes | Yes | Yes | 100% |
| Greater Swelling | Fed | 6 | Yes | Yes | Yes | 100% |
| Greater Swelling | Fed | 9 | Yes | Yes | Yes | 100% |
| Greater Swelling | Fed | 24 | No | No | No | 0% |
| Lesser Swelling | Fed | 3 | N/A | Yes | Yes | 100% |
| Lesser Swelling | Fed | 6 | Yes | Yes | Yes | 100% |
| Lesser Swelling | Fed | 9 | Yes | Yes | No | 67% |
| Lesser Swelling | Fed | 24 | No | Yes | No | 33% |
| Negative Control | Fed | 6 | No | No | N/M | 0% |
| Greater Swelling | Fasted | 3 | Yes | Yes | Yes | 100% |
| Greater Swelling | Fasted | 6 | N/A | Yes | Yes | 100% |
| Greater Swelling | Fasted | 9 | No | No | No | 0% |
| Greater Swelling | Fasted | 24 | No | No | No | 0% |
| Lesser Swelling | Fasted | 3 | Yes | Yes | Yes | 100% |
| Lesser Swelling | Fasted | 6 | No | No | No | 0% |
| Lesser Swelling | Fasted | 9 | No | No | No | 0% |
| Lesser Swelling | Fasted | 24 | No | No | Yes | 33% |
| Negative Control | Fasted | 6 | No | No | N/M | 0% |

Figure 4.4 allows for the comparison of the GR formulations across time and prandial state. The greater swelling formulation exhibited better retention behavior in both the fasted and fed states than the lesser swelling formulation. In the fasted state, the lesser swelling formulation retained at 3 hours in all rats, however it did not retain in the

stomach at 6 hours and beyond. In contrast, the greater swelling formulation retained at 6 hours in all rats and did not retain in the stomach at 9 hours and beyond. In the fed state, the greater swelling formulation retained in all rats through 9 hours after dosage administration, yet the lesser swelling formulation only retained in 2 out of 3 rats at the 9-hour time point. The greater swelling formulation had emptied the stomach by 24 hours in both the fasted and fed states. However, the lesser swelling formulation retained in the stomach of 1 of 3 rats in both the fasted and fed states.

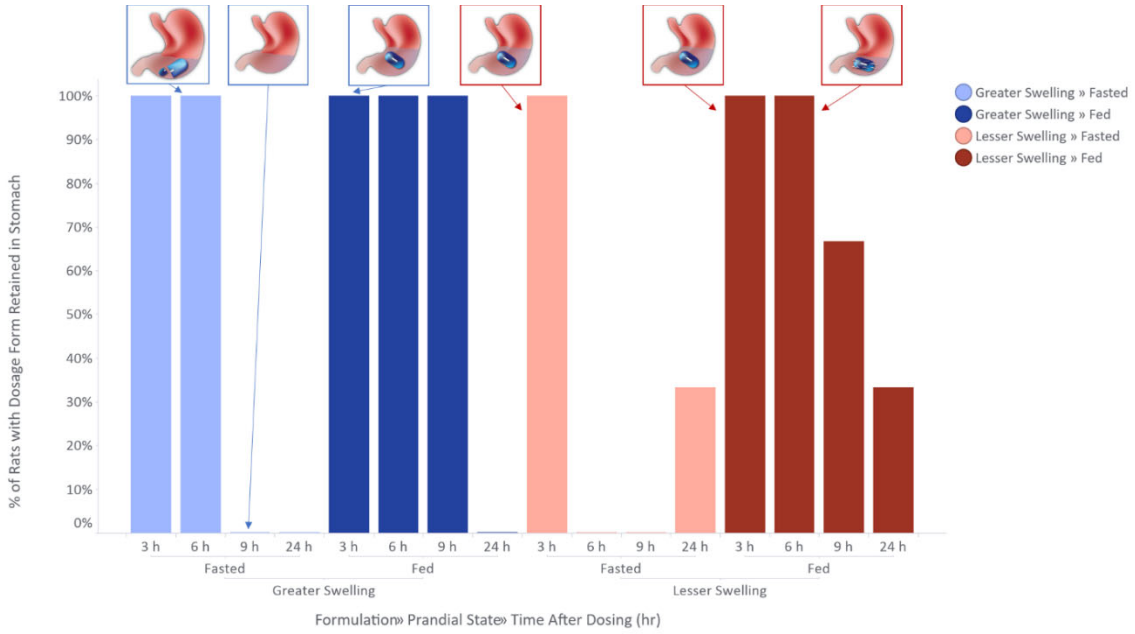


Figure 4.4: Summary of dosage form retention during gastric retention study. The data are presented as the percent of total rats studied at the particular time point and prandial state for which a dosage form was observed to be retained in the stomach.

Among the observations where the dosage form was retained in the rat stomach, we also recorded whether it remained largely intact compared to a reference standard soaking in 0.1N HCl in a scintillation vial. Figure 4.5 describes the dosage form integrity

over time for different formulations and prandial states. The data are presented as the percent of rats with the dosage form largely intact in the stomach out of the instances in which the dosage form was retained. Therefore, individual observations in which no dosage form was retained in the stomach are excluded from this analysis. Although neither formulation remains intact in all observed rats, the lesser swelling formulation tends to maintain integrity over the greater swelling formulation in both the fasted and fed states. Additionally, each formulation is more likely to remain intact in the rat stomach in the fasted state than in the fed state. Finally, the greater swelling formulation is no longer intact in the rat stomach by 9 hours in both prandial states, whereas the lesser swelling formulation largely remains intact when it is retained in the stomach.

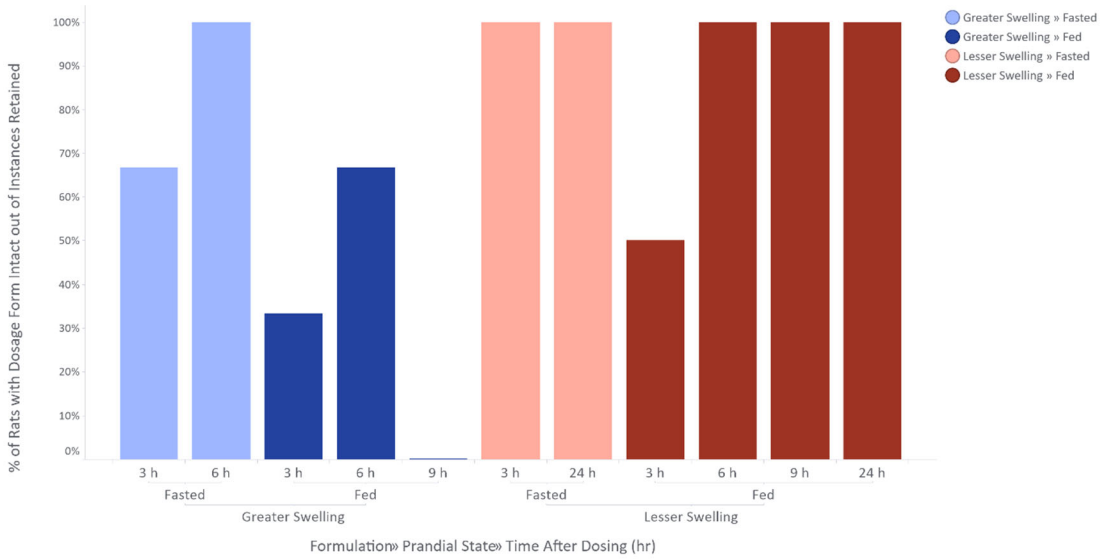


Figure 4.5: Summary of dosage form integrity during gastric retention study. The data are presented as the percent of total rats studied at the particular time point and prandial state for which a dosage form was observed to be intact among those rats which retained the dosage form.

### 4.4.3 Rat pharmacokinetic study

We sought to verify that the controlled release matrix tablet surrounded by a TPU outer layer would result in a gastroretentive dosage form that slowly released drug over the course of multiple hours. Consequently, we measured the pharmacokinetic properties of our greater swelling formulation and the non-swelling control in rats. Figure 4.6 shows the plasma concentration as a function of time for the two formulations. The data show that the greater swelling formulation exhibits a substantially delayed $t_{max}$ compared with the non-swelling control. The key pharmacokinetic parameters are described in Table 4.8, illustrating that the area under the curve (AUC) of the two formulations are comparable, with the greater swelling formulation achieving 75% the AUC of the non-swelling control formulation.

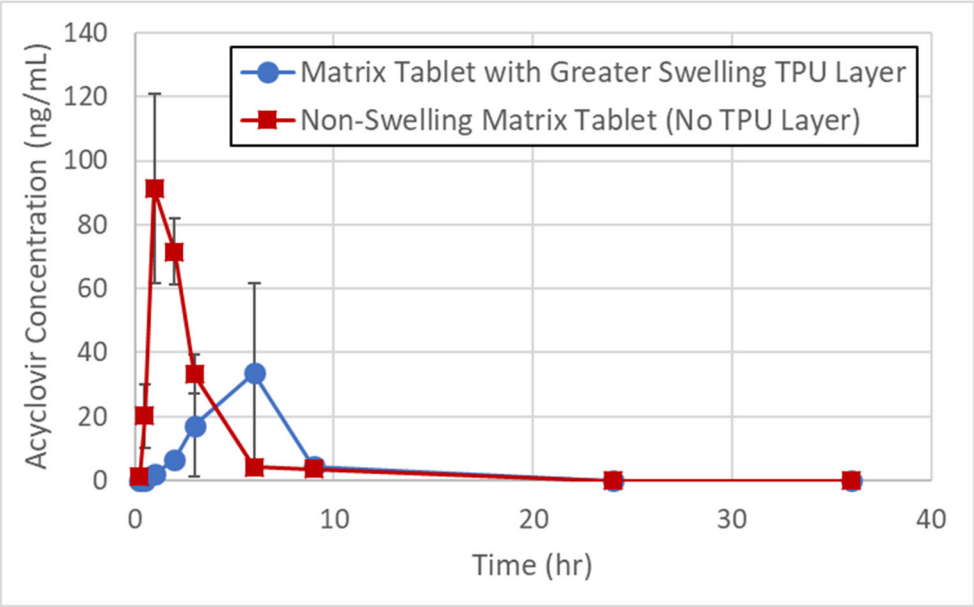


Figure 4.6: Mean pharmacokinetic profile (N = 3 ± SD) of acyclovir formulations administered to rats.

Table 4.8: Key acyclovir mean pharmacokinetic parameters (N = 3 ± SD) from the rat study comparing the plasma concentration-time profiles of the greater swelling formulation and the non-swelling control formulation.

| **Formulation** | Non-Swelling Control | Greater swelling |
|---|---|---|
| **$AUC_{0\text{-}36hr}$ (h*ng/mL)** | 245.5 ± 27.10 | 184.5 ± 154.2 |
| **Relative AUC** | – | 75% |
| **$C_{max}$ (ng/mL)** | 92.07 ± 28.28 | 35.50 ± 24.87 |
| **$t_{max}$ (hr)** | 1.33 ± 0.577 | 4.67 ± 2.31 |

## 4.5 DISCUSSION

We sought to develop a gastroretentive dosage form that differentiates from others [60–67] in that it can decouple drug release rate from gastric retention properties. Our dosage form design separates the two properties by relying on the matrix tablet formulation composition to determine drug release behavior and emphasizes the swelling behavior of the hydrophilic TPU outer layer in order to retain in the stomach. In this study, we analyzed each of the two major design components of the dosage form by comparing an immediate release acyclovir tablet to one surrounded by the TPU outer layer and by comparing a controlled release matrix tablet without a TPU layer to one surrounded by the TPU outer layer.

Although we observed in Figure 4.2a that an IR acyclovir tablet releases within a few minutes, the IR tablet with TPU outer layer slows the release of acyclovir. This finding aligns with a previous study showing that drug diffusion through a hydrophilic TPU membrane was constrained but relatively rapid [47]. However, the drug diffusion rate through the TPU outer layer (2.6 µg/mL/hr) is substantially faster than the CR acyclovir matrix tablet release rate (0.46 µg/mL/hr) shown in Figure 4.2b. The dissolution behavior of our CR acyclovir matrix tablet is representative of a release rate

that one would expect for a typical once daily controlled release tablet, as illustrated by the comparison to Gralise® in Figure 4.1. Since drug release rate through the TPU outer layer is greater than 5 times its expected release rate from a typical once daily matrix tablet, we believe that the matrix tablet will generally be the determinant of drug release rate from the dosage form. Our data further support this hypothesis, given that the CR acyclovir matrix tablet surrounded by the TPU outer layer exhibits approximately the same release rate as the CR acyclovir matrix tablet without a TPU outer layer (Figure 4.2b). We attribute the 30-minute lag time between the two dissolution curves to the hydration time of hydrophilic TPU polymer prior to the formation of a continuous pore network. Consequently, we have demonstrated a dosage form design that effectively decouples the duration of gastric retention from the rate of drug release from the tablet.

Elements of our dosage form design approach have been investigated by other researchers. Deshpande et al. reported on the development of a gastroretentive delivery system in which a core tablet is surrounded by an outer polymer layer [31]. The general design strategy is similar to ours, however there are several key differences. Their design relies on the core tablet to swell, whereas the polymer layer functions only as a permeable membrane that promotes gelling and tensile strength. Therefore, their dosage form does not decouple drug release from swelling behavior, making it challenging to develop a dosage form that swells substantially while maintaining slow drug release. In addition, investigators have extensively studied the role of superporous hydrogel composites for gastric retention [68–70]. Although they have synthesized their own polymers, their approach is similar to ours in that they rely on rapid and extensive swelling, in addition to mechanical strength, of the polymer hydrogels to retain in the stomach. However, their studies have shown that the hydrogel layer slows drug release significantly more than the

core tablet itself. Therefore, the approach has not yet been shown to fully decouple swelling behavior and release rate.

Sufficient expansion in at least two dimensions is required to retain the dosage form in the stomach. The expanded length necessary to avoid emptying from the stomach as part of the MMC has been widely debated. The estimate provided by Munk et al. of 12.8 ± 7.0 mm implies that 67% of the population has a relaxed pylorus diameter ranging between 5.8 mm and 19.8 mm, suggesting a broad distribution of sizes [34]. We found that the two largest dimensions of swollen Gralise® are 21 and 12 mm (Table 4.5), which suggests that either the pylorus estimates are inaccurate or that the delivery mechanism of Gralise® is not expandable gastric retention. Furthermore, the product's Food and Drug Administration (FDA) Center for Drug Evaluation and Research Cross Discipline Team Leader Review indicates that the reviewers questioned if the product should be classified as an extended-release product [71]. While the FDA's specific rationale has been redacted, it is reported that Gralise® takes advantage of changes to the MMC cycle in the fed state, where Phase III contractions are significantly less than in the fasted state [35]. For example, a clinical study comparing the effect of fasted, low-fat, and high-fat prandial states on the pharmacokinetics of Gralise® found that the geometric mean $t_{max}$ increased from 3.5 hr (fasted) to 6.0 hr (low-fat fed) to 9.0 hr (high-fat fed) [72]. Consequently, it remains unclear what role the swelling of Gralise® plays in its gastric retention, and it is possible that the 12 mm hydrated dimension is insufficient to retain the tablet for extended durations.

We developed two GR formulations based on the same design approach, using the same matrix tablet composition, but surrounding it with two different hydrophilic TPU polymers, such that they each swelled to a different extent. As described by Table 4.5,

the greater swelling dosage form expands to a size well beyond pylorus diameter estimates in two dimensions, whereas the lesser swelling dosage form expands to a size where the second largest dimension is in the approximate range of the relaxed pylorus diameter. The GR dosage forms used for the rat studies were intended to mimic the human dosage forms and exhibit similar swelling behavior. The rat relaxed pylorus diameter has been estimated at 2-3 mm [59]. As illustrated in Table 4.6, the greater swelling dosage form using in rat studies expands to much larger than 3 mm in all dimensions, whereas the lesser swelling dosage form used in rat studies expands to approximately the same estimated size as the rat pylorus.

It is worth noting that our reported dimensions reflect the expanded dosage form size unconstrained by gastric forces. Since the dosage form is realistically under stress from gastric forces, and because it is unclear what dosage form strength is necessary to ensure stomach retention, it was necessary to investigate the *in vivo* performance of our formulations. There is no ideal animal model for the human gastrointestinal tract, with each animal's gastrointestinal attributes exhibiting both similarities and differences to humans [73]. Although dogs are routinely used to assess the performance of formulation technologies, they exhibit some key differences with humans that may limit their ability to model gastroretentive formulation performance in humans. Gastric emptying time is comparable between humans and dogs in the fasted state, but extended gastric residence time has been observed under fed conditions with small non-disintegrating dosage forms ranging from 5-13.3 hours in dogs compared with 2.6-4.8 hours in humans [74]. Additionally, the substantially shorter intestinal transit time in dogs contrasted with humans (111 ± 17 min in dogs *vs* 238 ± 14 min in humans) may result in underprediction of the performance of controlled release formulations in humans [75]. Finally, dogs

exhibit 6-fold greater gastric forces than humans in the fasted state and 4-fold greater gastric forces than humans in the fed state [76]. A GR formulation whose retention mechanism is dependent on having sufficient strength to withstand gastric forces may not be retained in a canine stomach whereas it could easily be retained in a human stomach.

In contrast to dogs, rats exhibit comparable intestinal transit times to humans (2.6-3.3 hours in rats vs 3.5-4.5 hours in humans) [77]. Although fasted rats exhibit approximately 10-fold lower gastric forces than fasted humans, fed state rats exhibit comparable gastric forces to humans [76]. However, one area where rats do not model humans substantially better than dogs is with respect to gastric emptying time. In a study investigating the gastrointestinal transit time of pellets in rats, Tuleu et al. found that approximately 50% of the stomach contents were still present after 3 hours and they observed that it took 6 hours following food intake for >90% of the stomach contents to empty [77]. We incorporated this difference into our study design by extending the time points out beyond what one would typically investigate for a human gastroretentive formulation. We examined the stomach contents of the rats out to longer than 9 hours to ensure sufficient gastric retention, rather than the 4-6 hours we might anticipate for a human GR formulation. Similarly, the presence of our non-swelling control formulation was observed at 6 hours for comparison to our GR dosage forms, rather than at 3-4 hours we might have done for a human GR formulation.

Both GR formulations of varying TPU swelling extent retained in the rat stomach for extended durations, whereas the non-swelling control formulation was consistently absent from the stomach at the 6 hour time point investigated (Table 4.7). This suggests that gastric retention may be possible for expandable dosage forms in which two dimensions are not substantially greater than the pylorus diameter, like Gralise®.

However, we did observe differentiation between formulations and prandial states with regard to retention time (Figure 4.4). The greater swelling formulation was retained for a longer duration than the lesser swelling formulation in both the fasted and fed states. It is possible that the retention time of GR dosage forms that expand to sizes within the range of the pylorus diameter is related to the timing of the MMC Phase III wave, as has been proposed for Gralise® [67]. In contrast, the gastric retention times of dosage forms that expand to a size substantially larger than the relaxed pylorus diameter, such as our greater swelling formulation, are less sensitive to MMC waves.

Interestingly, each formulation was retained in the stomach for a longer duration in the fed state than in the fasted state. This phenomenon may be due to delayed gastric emptying in the fed state, however we would expect emptying from the rat stomach to be complete by 9 hours even in the fed state [77]. Better gastric retention in the fed state is also consistent with the Gralise® behavior, where the investigators relied on lower gastric forces during the fed state MMC Phase III wave than in the fasted state [67]. We would expect lower gastric forces to result in extended stomach retention.

We verified that the gastric retention of our dosage form results in delayed $t_{max}$ and similar AUC compared with the control formulation by conducting a pharmacokinetic study (Figure 4.6). Acyclovir is poorly permeable and has limited absorption in the lower gastrointestinal tract [51,53]. Consequently, one would expect that a conventional controlled release formulation designed to slowly release drug as it travels through the gastrointestinal tract may exhibit delayed $t_{max}$ but with a reduced AUC compared with an immediate release reference. Although our control formulation contains high molecular weight hydroxypropyl methylcellulose polymer, we found it to only slow drug release when the minitablets were surrounded by TPU. When the

minitablets were freely dispersed in dissolution media, they exhibited immediate release behavior, likely due to the high surface area of individual minitablets. Consequently, our control formulation exhibited immediate release behavior. As shown in Table 4.8, our greater swelling formulation exhibits a significantly delayed $t_{max}$, but with similar AUC to the control formulation. We propose that this outcome is possible because we have effectively retained the dosage form in the rat stomach for an extended duration as it slowly released drug.

Although the greater swelling formulation was more often retained in the stomach, we found that the lesser swelling formulation remained intact more often (Figure 4.5). While the polymer films used for the two formulations exhibit similar rigidity in the dry state, the volume of the 100% TPU2000 polymer used in the greater swelling formulation contains substantially more water when hydrated (Table 4.6). Consequently, the greater swelling formulation is substantially softer than the lesser swelling formulation, which may explain why it is less likely to remain intact after being subjected to gastric forces for extended lengths of time. Better dosage form integrity of the lesser swelling formulation may result in more consistent drug release rates than the greater swelling formulation, highlighting that there may be an optimal set of polymer properties between swelling extent and strength.

We observed that the fasted state resulted in greater dosage form integrity over that in the fed state, regardless of the formulation (Figure 4.5). Changes in stomach pH between prandial states are unlikely to drive changes in dosage form integrity, as the polymer is nonionic [58]. Given that gastric forces are expected to be lower in intensity in the fed state, we found these results to be counterintuitive. However, we hypothesize

that food particles prevalent in the stomach of fed state animals may act as milling media, breaking apart the dosage form over time.

A key design aspect of our GR dosage form was that, despite targeting gastric retention for extended durations, it should exit the stomach by 24 hours. If it were to be retained in the GI tract for especially longer durations, there would be an increased risk of gastrointestinal obstruction, as has been observed in a range of instances including ingestible electronic devices [78], percutaneous feeding tubes [79], and intragastric balloons for weight loss [80]. Therefore, we sought to avoid this risk by designing the dosage form to retain for extended durations, but less than 24 hours. As shown in Figure 4.4, the greater swelling formulation was successfully cleared from the stomach by 24 hours for all rats in both the fasted and fed states. The lesser swelling formulation remained in the stomach of one out of three rats at the 24 hour time point for both the fasted and fed states. Since the greater swelling formulation is softer, its mechanical properties may be responsible for its tendency to clear the stomach by 24 hours more consistently.

## 4.6 CONCLUSION

We designed dosage forms of acyclovir that could be administered less frequently by being retained in the stomach and releasing drug over an extended time period. We approached the challenge by developing a conventional controlled release matrix tablet to sustain the release of acyclovir over the target time duration and surrounding the matrix tablet with an outer layer composed of hydrophilic TPU that does not substantially contribute to controlled release of the drug. When the tablet is hydrated, the hydrophilic TPU layer swells to a size near or beyond the relaxed pylorus diameter. We

demonstrated that formulating acyclovir in such a dosage form will retain the tablet in the stomach for extended durations in both the fasted and fed states as it slowly releases drug, allowing for similar AUC but delayed $t_{max}$ relative to a non-gastroretentive control. Unlike many other gastroretentive formulations, this dosage form design decouples drug release rate from gastric retention time, allowing the two parameters to be modulated independently based on the needs of a particular product. Our direct observation of the dosage form retention and disposition in the stomach allowed for a high confidence assessment of the impact of polymer swelling extent and prandial state on both the dosage form integrity and retention time. Future work will focus on developing predictive mechanical tests intended to simulate the gastric forces imparted on the dosage form over time in a way that may avoid the need for *in vivo* testing to assess gastric retention behavior.

## 4.7 REFERENCES


[1] M. Oth, M. Franz, J. Timmermans, A. Möes, The Bilayer Floating Capsule: A Stomach-Directed Drug Delivery System for Misoprostol, Pharm. Res. 09 (1992) 298–302. doi:10.1023/A:1015870314340.

[2] J.L. Fabregas, J. Claramunt, J. Cucala, R. Pous, A. Siles, "In-Vitro" Testing of an Antacid Formulation with Prolonged Gastric Residence Time (Almagate Flot-Coat®), Drug Dev. Ind. Pharm. 20 (1994) 1199–1212. doi:10.3109/03639049409038361.

[3] A.K. Hilton, P.B. Deasy, In vitro and in vivo evaluation of an oral sustained-release floating dosage form of amoxycillin trihydrate, Int. J. Pharm. 86 (1992) 79–88. doi:10.1016/0378-5173(92)90033-X.

[4] L. Whitehead, J.H. Collett, J.T. Fell, Amoxycillin release from a floating dosage form based on alginates, Int. J. Pharm. 210 (2000) 45–49. doi:10.1016/S0378-5173(00)00567-6.

[5] A. Hoffman, D. Stepensky, E. Lavy, S. Eyal, E. Klausner, M. Friedman, Pharmacokinetic and pharmacodynamic aspects of gastroretentive dosage forms,

Int. J. Pharm. 277 (2004) 141–153. doi:10.1016/J.IJPHARM.2003.09.047.

[6] M. Ichikawa, T. Kato, M. Kawahara, S. Watanabe, M. Kayano, A New Multiple-Unit Oral Floating Dosage System. II: In Vivo Evaluation of Floating and Sustained-Release Characteristics with p-Aminobenzoic Acid and Isosorbide Dinitrate as Model Drugs, J. Pharm. Sci. 80 (1991) 1153–1156. doi:10.1002/JPS.2600801212.

[7] N. Özdemir, S. Ordu, Y. Özkan, Studies of Floating Dosage Forms of Furosemide: In Vitro and In Vivo Evaluations of Bilayer Tablet Formulations, Drug Dev. Ind. Pharm. 26 (2000) 857–866. doi:10.1081/DDC-100101309.

[8] G. Levy, W.J. Jusko, Factors Affecting the Absorption of Riboflavin in Man, J. Pharm. Sci. 55 (1966) 285–289. doi:10.1002/JPS.2600550305.

[9] R.S. Matharu, N.M. Sanghavi, Novel drug delivery system for captopril, Drug Dev. Ind. Pharm. 18 (1992) 1567–1574. doi:10.3109/03639049209040859.

[10] P.R. Sheth, J. Tossounian, The Hydrodynamically Balanced System (Hbs$^{TM}$): A Novel Drug Delivery System for Oral Use, Drug Dev. Ind. Pharm. 10 (1984) 313–339. doi:10.3109/03639048409064653.

[11] G.-L. Chen, W.-H. Hao, In Vitro Performance of Floating Sustained-Release Capsule of Verapamil, Drug Dev. Ind. Pharm. 24 (1998) 1067–1072. doi:10.3109/03639049809089950.

[12] K.S. Soppimath, A.R. Kulkarni, T.M. Aminabhavi, Development of Hollow Microspheres as Floating Controlled-Release Systems for Cardiovascular Drugs: Preparation and Release Characteristics, Drug Dev. Ind. Pharm. 27 (2001) 507–515. doi:10.1081/DDC-100105175.

[13] B. Berner, V.E. Cowles, Case studies in swelling polymeric gastric retentive tablets, Expert Opin. Drug Deliv. 3 (2006) 541–548. doi:10.1517/17425247.3.4.541.

[14] H. Minami, R.W. Mccallum, The Physiology and Pathophysiology of Gastric Emptying in Humans, Gastroenterology. 86 (1984) 1592–1610. doi:10.1016/S0016-5085(84)80178-X.

[15] A.K. Lalloo, E.L. McConnell, L. Jin, R. Elkes, C. Seiler, Y. Wu, Decoupling the role of image size and calorie intake on gastric retention of swelling-based gastric retentive formulations: Pre-screening in the dog model, Int. J. Pharm. 431 (2012) 90–100. doi:10.1016/J.IJPHARM.2012.04.044.

[16] L. Whitehead, J.T. Fell, J.H. Collett, H.L. Sharma, A.-M. Smith, Floating dosage forms: an in vivo study demonstrating prolonged gastric retention, J. Control. Release. 55 (1998) 3–12. doi:10.1016/S0168-3659(97)00266-6.

[17] S. Desai, S. Bolton, A Floating Controlled-Release Drug Delivery System: In

Vitro-in Vivo Evaluation, Pharm. Res. 10 (1993) 1321–1325. doi:10.1023/A:1018921830385.

[18] K. Park, J.R. Robinson, Bioadhesive polymers as platforms for oral-controlled drug delivery: method to study bioadhesion, Int. J. Pharm. 19 (1984) 107–127. doi:10.1016/0378-5173(84)90154-6.

[19] P.L. Bardonnet, V. Faivre, W.J. Pugh, J.C. Piffaretti, F. Falson, Gastroretentive dosage forms: Overview and special case of Helicobacter pylori, J. Control. Release. 111 (2006) 1–18. doi:10.1016/J.JCONREL.2005.10.031.

[20] R. Khosla, S.S. Davis, The effect of polycarbophil on the gastric emptying of pellets, J. Pharm. Pharmacol. 39 (1987) 47–49. doi:10.1111/j.2042-7158.1987.tb07161.x.

[21] D. Harris, J.T. Fell, H.L. Sharma, D.C. Taylor, GI transit of potential bioadhesive formulations in man: A scintigraphic study, J. Control. Release. 12 (1990) 45–53. doi:10.1016/0168-3659(90)90182-S.

[22] S.J. Jackson, D. Bush, A.C. Perkins, Comparative scintigraphic assessment of the intragastric distribution and residence of cholestyramine, Carbopol 934P and sucralfate, Int. J. Pharm. 212 (2001) 55–62. doi:10.1016/S0378-5173(00)00600-1.

[23] S. Patil, G.S. Talele, Gastroretentive mucoadhesive tablet of lafutidine for controlled release and enhanced bioavailability, Drug Deliv. 22 (2015) 312–319. doi:10.3109/10717544.2013.877099.

[24] S. Pandey, P. Jirwankar, S. Mehta, S. Pandit, P. Tripathi, A. Patil, Formulation and Evaluation of Bilayered Gastroretentable Mucoadhesive Patch for Stomach-Specific Drug Delivery, (n.d.). https://www.ingentaconnect.com/content/ben/cdd/2013/00000010/00000004/art00002# (accessed August 26, 2019).

[25] F. Schneider, M. Koziolek, W. Weitschies, In Vitro and In Vivo Test Methods for the Evaluation of Gastroretentive Dosage Forms, Pharmaceutics. 11 (2019) 416. doi:10.3390/pharmaceutics11080416.

[26] E.A. Klausner, E. Lavy, D. Stepensky, M. Friedman, A. Hoffman, Novel Gastroretentive Dosage Forms: Evaluation of Gastroretentivity and Its Effect on Riboflavin Absorption in Dogs, Pharm. Res. 19 (2002) 1516–1523. doi:10.1023/A:1020412817716.

[27] S. Zhang, A.M. Bellinger, D.L. Glettig, R. Barman, Y.-A.L. Lee, J. Zhu, C. Cleveland, V.A. Montgomery, L. Gu, L.D. Nash, D.J. Maitland, R. Langer, G. Traverso, A pH-responsive supramolecular polymer gel as an enteric elastomer for use in gastric devices, Nat. Mater. 14 (2015) 1065–1071. doi:10.1038/nmat4355.

[28] A.M. Bellinger, M. Jafari, T.M. Grant, S. Zhang, H.C. Slater, E.A. Wenger, S. Mo,

Y.-A.L. Lee, H. Mazdiyasni, L. Kogan, R. Barman, C. Cleveland, L. Booth, T. Bensel, D. Minahan, H.M. Hurowitz, T. Tai, J. Daily, B. Nikolic, L. Wood, P.A. Eckhoff, R. Langer, G. Traverso, Oral, ultra-long-lasting drug delivery: Application toward malaria elimination goals., Sci. Transl. Med. 8 (2016) 365ra157. doi:10.1126/scitranslmed.aag2374.

[29] H. Sugihara, Y. Matsui, H. Takeuchi, I. Wilding, A. Connor, K. Abe, A. Nishiura, Development of a gastric retentive system as a sustained-release formulation of pranlukast hydrate and its subsequent in vivo verification in human studies, Eur. J. Pharm. Sci. 53 (2014) 62–68. doi:10.1016/J.EJPS.2013.11.018.

[30] M.D. Chavanpatil, P. Jain, S. Chaudhari, R. Shear, P.R. Vavia, Novel sustained release, swellable and bioadhesive gastroretentive drug delivery system for ofloxacin, Int. J. Pharm. 316 (2006) 86–92. doi:10.1016/J.IJPHARM.2006.02.038.

[31] A.A. Deshpande, N.H. Shah, C.T. Rhodes, W. Malick, Development of a Novel Controlled-Release System for Gastric Retention, Pharm. Res. 14 (1997) 815–819. doi:10.1023/A:1012171010492.

[32] W.S.W. Shalaby, W.E. Blevins, K. Park, In vitro and in vivo studies of enzyme-digestible hydrogels for oral drug delivery, J. Control. Release. 19 (1992) 131–144. doi:10.1016/0168-3659(92)90071-X.

[33] A.D. Keet, Diameter of the pyloric aperture in relation to the contraction of the canalis egestorius, Acta Radiol. 57 (1962) 31–44. doi:10.3109/00016926209171725.

[34] J.F. Munk, R.M. Gannaway, M. Hoare, A.G. Johnson, Direct measurement of pyloric diameter and tone in man and their response to cholecystokinin, in: Gastrointest. Motil. Heal. Dis., Springer Netherlands, Dordrecht, 1978: pp. 349–359. doi:10.1007/978-94-017-4389-1_38.

[35] C. Chen, C.-H. (Sara) Han, M. Sweeney, V.E. Cowles, Pharmacokinetics, Efficacy, and Tolerability of a Once-Daily Gastroretentive Dosage Form of Gabapentin for the Treatment of Postherpetic Neuralgia, J. Pharm. Sci. 102 (2013) 1155–1164. doi:10.1002/JPS.23467.

[36] A.J. Coury, P.C. Slaikeu, P.T. Cahalan, K.B. Stokes, C.M. Hobot, Factors and Interactions Affecting the Performance of Polyurethane Elastomers in Medical Devices, J. Biomater. Appl. 3 (1988) 130–179. doi:10.1177/088532828800300202.

[37] K. Stokes, R. McVenes, J.M. Anderson, Polyurethane Elastomer Biostability, J. Biomater. Appl. 9 (1995) 321–354. doi:10.1177/088532829500900402.

[38] M. Habash, G. Reid, Microbial Biofilms: Their Development and Significance for Medical Device-Related Infections, J. Clin. Pharmacol. 39 (1999) 887–898. doi:10.1177/00912709922008506.

[39] M.A. Hussain, R.C. DiLuccio, E. Shefter, Hollow Fibers as an Oral Sustained-Release Delivery System, Pharm. Res. 06 (1989) 49–52. doi:10.1023/A:1015847618671.

[40] T. Yamaoka, Y. Makita, H. Sasatani, S.-I. Kim, Y. Kimura, Linear type azo-containing polyurethane as drug-coating material for colon-specific delivery: its properties, degradation behavior, and utilization for drug formulation, J. Control. Release. 66 (2000) 187–197. doi:10.1016/S0168-3659(99)00270-9.

[41] A. Bhattacharyya, P. Mukhopadhyay, P.P. Kundu, Synthesis of a novel pH-sensitive polyurethane-alginate blend with poly(ethylene terephthalate) waste for the oral delivery of protein, J. Appl. Polym. Sci. 131 (2014) n/a-n/a. doi:10.1002/app.40650.

[42] M.R. Nabid, I. Omrani, Facile preparation of pH-responsive polyurethane nanocarrier for oral delivery, Mater. Sci. Eng. C. 69 (2016) 532–537. doi:10.1016/J.MSEC.2016.07.017.

[43] L. Polo Fonseca, R.B. Trinca, M.I. Felisberti, Amphiphilic polyurethane hydrogels as smart carriers for acidic hydrophobic drugs, Int. J. Pharm. 546 (2018) 106–114. doi:10.1016/J.IJPHARM.2018.05.034.

[44] B. Claeys, S. De Bruyn, L. Hansen, T. De Beer, J.P. Remon, C. Vervaet, Release characteristics of polyurethane tablets containing dicarboxylic acids as release modifiers – a case study with diprophylline, Int. J. Pharm. 477 (2014) 244–250. doi:10.1016/J.IJPHARM.2014.10.046.

[45] G. Verstraete, J. Van Renterghem, P.J. Van Bockstal, S. Kasmi, B.G. De Geest, T. De Beer, J.P. Remon, C. Vervaet, Hydrophilic thermoplastic polyurethanes for the manufacturing of highly dosed oral sustained release matrices via hot melt extrusion and injection molding, Int. J. Pharm. 506 (2016) 214–221. doi:10.1016/J.IJPHARM.2016.04.057.

[46] M.B. Lowinger, S.E. Barrett, F. Zhang, R.O. Williams, Sustained Release Drug Delivery Applications of Polyurethanes, Pharmaceutics. 10 (2018) 55. doi:10.3390/pharmaceutics10020055.

[47] M.B. Lowinger, J.D. Ormes, Y. Su, J.H. Small, R.O. Williams, F. Zhang, How broadly can poly(urethane)-based implants be applied to drugs of varied properties?, Int. J. Pharm. 568 (2019) 118550. doi:10.1016/J.IJPHARM.2019.118550.

[48] H.H. Balfour, Antiviral Drugs, N. Engl. J. Med. 340 (1999) 1255–1268. doi:10.1056/NEJM199904223401608.

[49] G. Bruni, M. Maietta, L. Maggi, P. Mustarelli, C. Ferrara, V. Berbenni, C. Milanese, A. Girella, A. Marini, Preparation and Physicochemical Characterization of Acyclovir Cocrystals with Improved Dissolution Properties, J. Pharm. Sci. 102

(2013) 4079–4086. doi:10.1002/JPS.23721.

[50] W. Zielenkiewicz, B. Golankiewicz, G.L. Perlovich, M. Koźbiał, Aqueous Solubilities, Infinite Dilution Activity Coefficients and Octanol–Water Partition Coefficients of Tricyclic Analogs of Acyclovir, J. Solution Chem. 28 (1999) 731–745. doi:10.1023/A:1021720128725.

[51] P. Shah, V. Jogani, P. Mishra, A.K. Mishra, T. Bagchi, A. Misra, In Vitro Assessment of Acyclovir Permeation Across Cell Monolayers in the Presence of Absorption Enhancers, Drug Dev. Ind. Pharm. 34 (2008) 279–288. doi:10.1080/03639040701655952.

[52] M. Ruhnek-Forsbeck, E. Sandström, B. Andersoon, G. Eriksson, K. Hersle, G.-B. Lövhagen, H. Mobacken, L. Hillström, L. Svensson, Treatment of recurrent genital herpes simplex infections with oral acyclovir, J. Antimicrob. Chemother. 16 (1985) 621–628. doi:10.1093/jac/16.5.621.

[53] G. Park, Z. Shao, A.K. Mitra, Acyclovir Permeation Enhancement Across Intestinal and Nasal Mucosae by Bile Salt-Acylcarnitine Mixed Micelles, Pharm. Res. 09 (1992) 1262–1267. doi:10.1023/A:1015845031488.

[54] S. Dhaliwal, S. Jain, H.P. Singh, A.K. Tiwary, Mucoadhesive Microspheres for Gastroretentive Delivery of Acyclovir: In Vitro and In Vivo Evaluation, AAPS J. 10 (2008) 322. doi:10.1208/s12248-008-9039-2.

[55] H. Liu, W. Pan, P. Ke, Y. Dong, L. Ji, Preparation and evaluation of a novel gastric mucoadhesive sustained-release acyclovir microsphere, Drug Dev. Ind. Pharm. 36 (2010) 1098–1105. doi:10.3109/03639041003677780.

[56] S.S. El Gamal, V.F. Naggar, A.N. Allam, Optimization of acyclovir oral tablets based on gastroretention technology: Factorial design analysis and physicochemical characterization studies, Drug Dev. Ind. Pharm. 37 (2011) 855–867. doi:10.3109/03639045.2010.546404.

[57] R. Ruiz-Caro, M. Gago-Guillan, F.J. Otero-Espinar, M.D. Veiga, Mucoadhesive Tablets for Controlled Release of Acyclovir, Chem. Pharm. Bull. 60 (2012) 1249–1257. doi:10.1248/cpb.c12-00324.

[58] M.B. Lowinger, Y. Su, X. Lu, R.O. Williams, F. Zhang, Can drug release rate from implants be tailored using poly(urethane) mixtures?, Int. J. Pharm. 557 (2019) 390–401. doi:10.1016/j.ijpharm.2018.11.067.

[59] S.-F. Jang, B.A. Goins, W.T. Phillips, C. Santoyo, A. Rice-Ficht, J.T. McConville, Size discrimination in rat and mouse gastric emptying, Biopharm. Drug Dispos. 34 (2013) 107–124. doi:10.1002/bdd.1828.

[60] B.S. Dave, A.F. Amin, M.M. Patel, Gastroretentive drug delivery system of ranitidine hydrochloride: Formulation and in vitro evaluation, AAPS

PharmSciTech. 5 (2004) 77–82. doi:10.1208/pt050234.

[61] M. Chavanpatil, P. Jain, S. Chaudhari, R. Shear, P. Vavia, Development of sustained release gastroretentive drug delivery system for ofloxacin: In vitro and in vivo evaluation, Int. J. Pharm. 304 (2005) 178–184. doi:10.1016/J.IJPHARM.2005.08.009.

[62] Q. Liu, R. Fassihi, Zero-order delivery of a highly soluble, low dose drug alfuzosin hydrochloride via gastro-retentive system, Int. J. Pharm. 348 (2008) 27–34. doi:10.1016/J.IJPHARM.2007.07.009.

[63] R.A.K. Arza, C.S.R. Gonugunta, P.R. Veerareddy, Formulation and Evaluation of Swellable and Floating Gastroretentive Ciprofloxacin Hydrochloride Tablets, AAPS PharmSciTech. 10 (2009) 220–226. doi:10.1208/s12249-009-9200-y.

[64] S.C. Jagdale, A.J. Agavekar, S. V. Pandya, B.S. Kuchekar, A.R. Chabukswar, Formulation and Evaluation of Gastroretentive Drug Delivery System of Propranolol Hydrochloride, AAPS PharmSciTech. 10 (2009) 1071. doi:10.1208/s12249-009-9300-8.

[65] R.-N. Chen, H.-O. Ho, C.-Y. Yu, M.-T. Sheu, Development of swelling/floating gastroretentive drug delivery system based on a combination of hydroxyethyl cellulose and sodium carboxymethyl cellulose for Losartan and its clinical relevance in healthy volunteers with CYP2C9 polymorphism, Eur. J. Pharm. Sci. 39 (2010) 82–89. doi:10.1016/J.EJPS.2009.10.015.

[66] C. Murphy, V. Pillay, Y.E. Choonara, L.C. du Toit, V.M.K. Ndesendo, N. Chirwa, P. Kumar, Optimization of a Dual Mechanism Gastrofloatable and Gastroadhesive Delivery System for Narrow Absorption Window Drugs, AAPS PharmSciTech. 13 (2012) 1–15. doi:10.1208/s12249-011-9711-1.

[67] Y.-C. Chen, H.-O. Ho, T.-Y. Lee, M.-T. Sheu, Physical characterizations and sustained release profiling of gastroretentive drug delivery systems with improved floating and swelling capabilities, Int. J. Pharm. 441 (2013) 162–169. doi:10.1016/J.IJPHARM.2012.12.002.

[68] J. Chen, W.E. Blevins, H. Park, K. Park, Gastric retention properties of superporous hydrogel composites, J. Control. Release. 64 (2000) 39–51. doi:10.1016/S0168-3659(99)00139-X.

[69] H. Park, K. Park, D. Kim, Preparation and swelling behavior of chitosan-based superporous hydrogels for gastric retention application, J. Biomed. Mater. Res. Part A. 76A (2006) 144–150. doi:10.1002/jbm.a.30533.

[70] H. Omidian, K. Park, J.G. Rocca, Recent developments in superporous hydrogels, J. Pharm. Pharmacol. 59 (2007) 317–327. doi:10.1211/jpp.59.3.0001.

[71] E. Fields, Application Number: 022544Orig1s000 Cross Discipline Team Leader

Review, 2010. https://www.accessdata.fda.gov/drugsatfda_docs/nda/2011/022544Orig1s000CrossR.pdf.

[72] C. Chen, V.E. Cowles, E. Hou, Pharmacokinetics of Gabapentin in a Novel Gastric-Retentive Extended-Release Formulation: Comparison With an Immediate-Release Formulation and Effect of Dose Escalation and Food, J. Clin. Pharmacol. 51 (2011) 346–358. doi:10.1177/0091270010368411.

[73] T.T. Kararli, Comparison of the gastrointestinal anatomy, physiology, and biochemistry of humans and commonly used laboratory animals, Biopharm. Drug Dispos. 16 (1995) 351–380. doi:10.1002/bdd.2510160502.

[74] S.S. Davis, E.A. Wilding, I.R. Wilding, Gastrointestinal transit of a matrix tablet formulation: comparison of canine and human data, Int. J. Pharm. 94 (1993) 235–238. doi:10.1016/0378-5173(93)90029-F.

[75] J.B. Dressman, Comparison of Canine and Human Gastrointestinal Physiology, Pharm. Res. 03 (1986) 123–131. doi:10.1023/A:1016353705970.

[76] B. Laulicht, A. Tripathi, V. Schlageter, P. Kucera, E. Mathiowitz, Understanding gastric forces calculated from high-resolution pill tracking., Proc. Natl. Acad. Sci. U. S. A. 107 (2010) 8201–6. doi:10.1073/pnas.1002292107.

[77] C. Tuleu, C. Andrieux, P. Boy, J.. Chaumeil, Gastrointestinal transit of pellets in rats: effect of size and density, Int. J. Pharm. 180 (1999) 123–131. doi:10.1016/S0378-5173(98)00400-1.

[78] A.S. Cheifetz, A.A. Kornbluth, P. Legnani, I. Schmelkin, A. Brown, S. Lichtiger, B.S. Lewis, The risk of retention of the capsule endoscope in patients with known or suspected Crohn's disease., Am. J. Gastroenterol. 101 (2006) 2218–22. doi:10.1111/j.1572-0241.2006.00761.x.

[79] R. McGovern, J.S. Barkin, R.I. Goldberg, R.S. Phillips, Duodenal obstruction: a complication of percutaneous endoscopic gastrostomy tube migration., Am. J. Gastroenterol. 85 (1990) 1037–8. http://www.ncbi.nlm.nih.gov/pubmed/2197857 (accessed October 11, 2019).

[80] P. Trande, A. Mussetto, V.G. Mirante, E. De Martinis, G. Olivetti, R.L. Conigliaro, E.A. De Micheli, Efficacy, Tolerance and Safety of New Intragastric Air-Filled Balloon (Heliosphere BAG) for Obesity: the Experience of 17 Cases, Obes. Surg. 20 (2010) 1227–1230. doi:10.1007/s11695-008-9786-2.

# Appendix A: Supplementary Information to Chapter 2

## A.1 Polymer Film Fabrication Details

As part of the study described in Chapter 2, we varied the independent extrusion parameters (barrel temperature profile, screw speed, screw profile, and feed rates) in order to affect dependent process parameters, as shown in Table A.1. Mixture composition was calculated by dividing the feed rate of the hydrophilic thermoplastic poly(urethane) (TPU) by the total feed rate. Melt temperature was measured directly by a flush-mounted thermocouple at the die adapter. Specific mechanical energy was calculated by dividing the measured screw motor power draw by the total feed rate. Estimated breakthrough time is a measure of residence time. Briefly, we added color-dyed poly(ethylene) pellets to the extruder feed port while the process was running at steady state and recorded the time until the appearance of color was observed at the die. Thus, breakthrough time represents the leading edge of the residence time distribution. Breakthrough time was measured at several key runs. It was found to vary only with screw profile and total feed rate (not temperature or screw speed). Therefore, breakthrough time for most runs was estimated based on measurements of other runs using the same screw profile and total feed rate.

Table A.1: Independent process parameters studied on Leistritz 18 mm twin-screw extruder, along with corresponding dependent process parameters that are used to assess impact on mixing and release.

| **Process Independent Parameters** | | | | | | **Process Dependent Parameters** | | | |
|---|---|---|---|---|---|---|---|---|---|
| Hydrophobic TPU Feed Rate (kg/hr) | Hydrophilic TPU Feed Rate (kg/hr) | Screw Profile | Temp Profile | Screw Speed (rpm) | Power Draw (kW) | Mixture Composition (% w/w Hydrophilic) | Melt Temp (°C) | Estimated Breakthrough Time (sec) | Specific Mechanical Energy (kW*hr/kg) |
| 3.015 | 0 | A | A | 200 | 0.6 | 0.00% | 193 | 116 | 0.20 |
| 5.547 | 0.368 | B | B | 350 | 1.3 | 6.22% | 176 | 46 | 0.22 |
| 5.643 | 0.393 | A | A | 400 | 1.4 | 6.51% | 213 | 116 | 0.23 |
| 5.241 | 0.733 | A | A | 400 | 1.4 | 12.27% | 212 | 116 | 0.23 |
| 5.253 | 0.741 | B | B | 350 | 1.2 | 12.36% | 175 | 46 | 0.20 |
| 4.494 | 1.473 | B | B | 300 | 1.2 | 24.69% | 173 | 46 | 0.20 |
| 4.461 | 1.476 | A | B | 444 | 1.8 | 24.86% | 172 | 116 | 0.30 |
| 2.214 | 0.736 | A | B | 200 | 0.8 | 24.95% | 170 | 116 | 0.27 |
| 2.229 | 0.743 | A | A | 200 | 0.6 | 25.00% | 203 | 116 | 0.20 |
| 3.009 | 2.999 | A | B | 400 | 1.7 | 49.92% | 171 | 116 | 0.28 |
| 1.467 | 1.466 | A | A | 400 | 1.6 | 49.98% | 176 | 108 | 0.55 |
| 2.973 | 2.986 | B | B | 300 | 1.1 | 50.11% | 172 | 46 | 0.18 |
| 1.485 | 1.503 | A | B | 200 | 0.7 | 50.30% | 167 | 116 | 0.23 |
| 1.473 | 1.526 | A | A | 200 | 0.6 | 50.88% | 179 | 116 | 0.20 |
| 1.401 | 1.62 | B | B | 140 | 0.9 | 53.62% | 165 | 127 | 0.30 |
| 1.407 | 1.656 | A | B | 600 | 2.2 | 54.06% | 166 | 83 | 0.72 |
| 1.356 | 1.637 | B | B | 160 | 0.9 | 54.69% | 165 | 127 | 0.30 |
| 1.353 | 1.656 | A | A | 400 | 1.5 | 55.03% | 176 | 108 | 0.50 |
| 1.239 | 1.792 | B | B | 160 | 0.9 | 59.12% | 164 | 127 | 0.30 |
| 1.209 | 1.781 | A | A | 400 | 1.4 | 59.57% | 175 | 108 | 0.47 |
| 1.182 | 1.814 | A | B | 600 | 2.3 | 60.55% | 173 | 83 | 0.77 |
| 1.071 | 1.914 | B | B | 160 | 0.8 | 64.12% | 163 | 127 | 0.27 |
| 1.065 | 1.932 | A | A | 400 | 1.4 | 64.46% | 175 | 108 | 0.47 |
| 1.047 | 1.971 | A | B | 600 | 2.2 | 65.31% | 166 | 83 | 0.73 |
| 0.915 | 2.068 | A | A | 400 | 1.4 | 69.33% | 175 | 108 | 0.47 |
| 0.909 | 2.102 | A | B | 600 | 2.3 | 69.81% | 166 | 83 | 0.76 |
| 0.897 | 2.076 | B | B | 160 | 0.8 | 69.83% | 164 | 127 | 0.27 |
| 0.756 | 2.239 | A | A | 400 | 1.4 | 74.76% | 175 | 108 | 0.47 |
| 0.753 | 2.243 | A | A | 200 | 0.5 | 74.87% | 179 | 116 | 0.17 |
| 1.494 | 4.482 | A | B | 350 | 1.5 | 75.00% | 171 | 116 | 0.25 |
| 0 | 2.992 | A | A | 200 | 0.5 | 100.00% | 178 | 116 | 0.17 |

## A.2 SOLID-STATE NUCLEAR MAGNETIC RESONANCE DETAILS

Most previous studies of pharmaceutical dispersions have used $^{13}C$-detected relaxation time measurements for making use of the resolved carbon peak of the active pharmaceutical ingredient and polymer. In this study, the hydrophilic and hydrophobic TPU polymers exhibit fully overlapped carbon peaks as shown in Figure A.1. Therefore, we established a $^{1}H$-detected method for efficiently evaluating the miscibility of the two polymer components, as described in section 2.3.2.2. An example is illustrated in Figure A.2. $^{1}H$ ssNMR spectra of extruded pure hydrophobic TPU, pure hydrophilic TPU, and a mixture (50.11% hydrophilic content) are shown in the left column of A, B, and C, respectively. The $^{1}H$ spectrum of the TPU mixture sample can be deconvoluted to two components by utilizing the weight percentages (i.e., 49.89% and 50.11% for hydrophobic and hydrophilic TPUs, respectively).

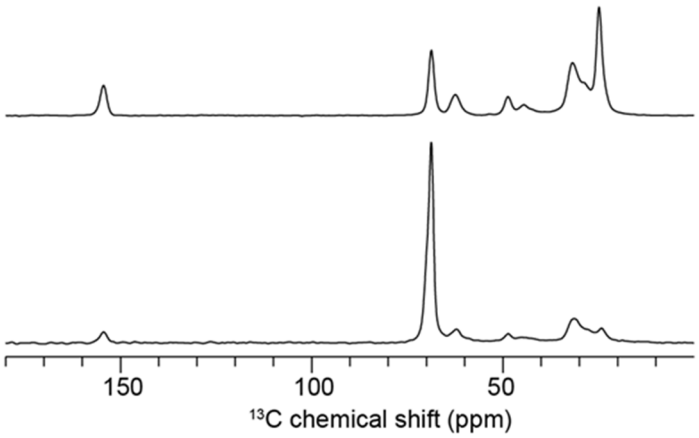


Figure A.1: $^{13}C$ nuclear magnetic resonance spectra of the hydrophilic (top) and hydrophobic (bottom) TPUs.

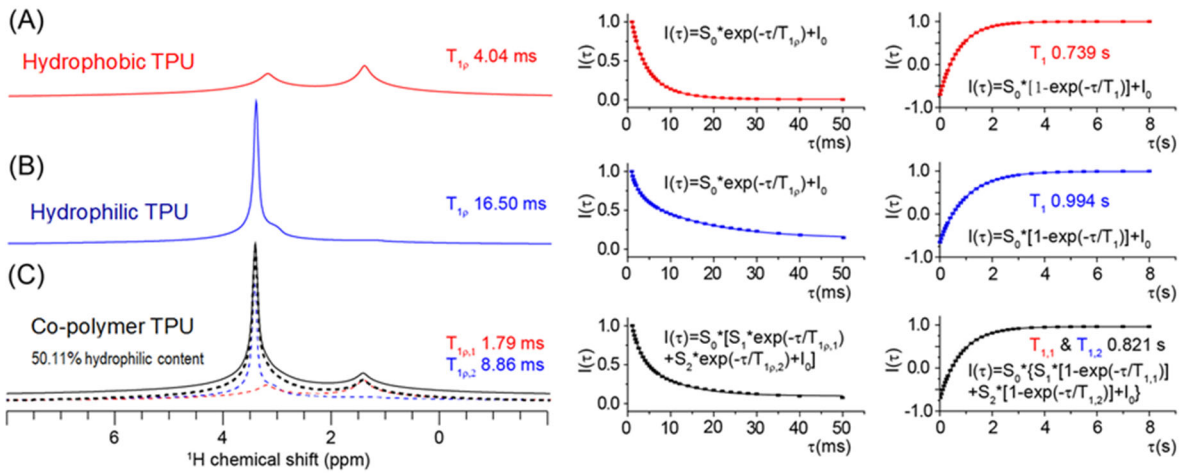


Figure A.2: $^{1}H$ spectra (left column) of extruded hydrophobic TPU (A), hydrophilic TPU (B), and TPU mixture with 50.11% (w/w) hydrophilic TPU (C), and their corresponding relaxation curves of $T_1$ (right column) and $T_{1\rho}$ (middle column). The decovoluted pure hydrophobic (red and dashed) and pure hydrophilic (blue and dashed) components, and their added spectrum (black dashed), are shown in C, which matches well with the spectrum of the TPU mixtures.

# Appendix B: Supplementary Information to Chapter 3

## B.1 Drug Apparent Permeability Measurement through Membranes

As part of the study described in Chapter 3, we measured drug apparent permeability through polymer membranes. A polymer membrane of each sample was cut using a hammer-driven hole punch and placed into a membrane holder. The membrane holder was positioned between identical donor and acceptor glass chambers. Cross-type magnetic stir bars were used to ensure good mixing within the chamber. The drug solution was intended to model the core of the reservoir implant, while the polymer film was intended to model the rate-controlling membrane of the implant. A drug solution in a buffer of defined pH was added to the donor chamber, while pure buffer was added to the acceptor chamber. Ultraviolet absorbance was measured in the acceptor chamber using a Pion Rainbow™ fiber optic system (Billerica, MA) equipped with a deuterium lamp and UV dip probes. Figure B.1, Figure B.2, and Figure B.3 show representative concentration data as a function of time for emtricitabine, metoprolol, and ibuprofen, respectively.

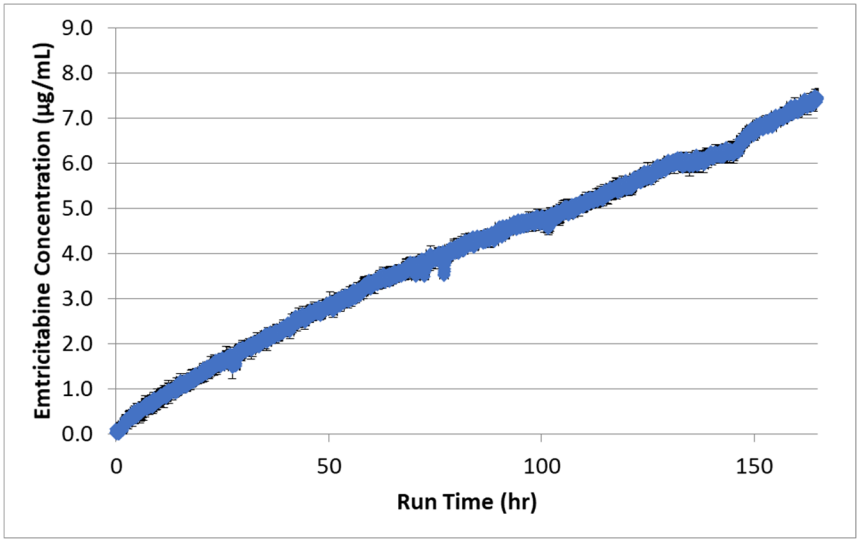


Figure B.1: Emtricitabine concentration (N = 3 ± SD) in a diffusion cell receptor chamber as a function of run time through a 100% hydrophobic poly(urethane) membrane. The donor concentration in the diffusion cell was 1000 µg/mL. The steady-state diffusion rate was used to determine membrane permeability.

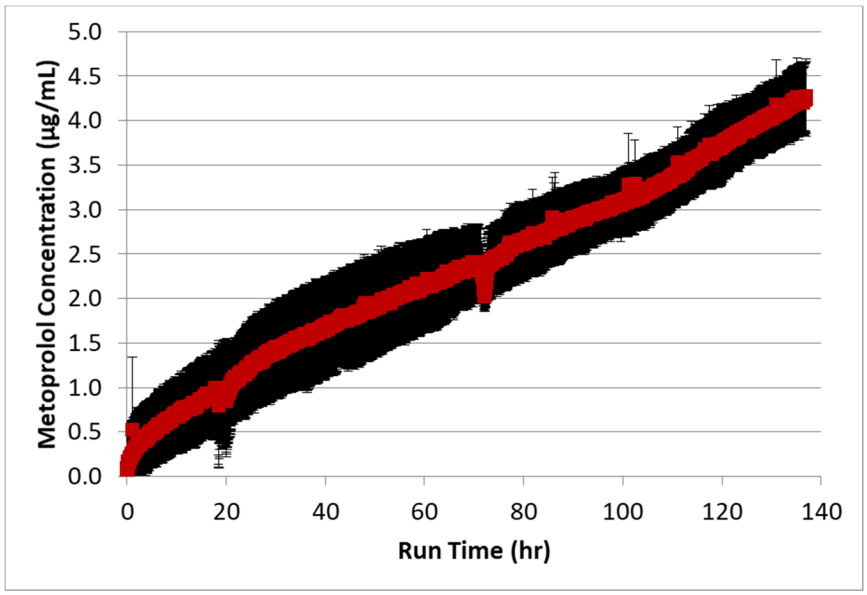


Figure B.2: Metoprolol concentration (N = 3 ± SD) in a diffusion cell receptor chamber as a function of run time through a 100% hydrophobic poly(urethane) membrane. The donor concentration in the diffusion cell was 400 µg/mL. The steady-state diffusion rate was used to determine membrane permeability.

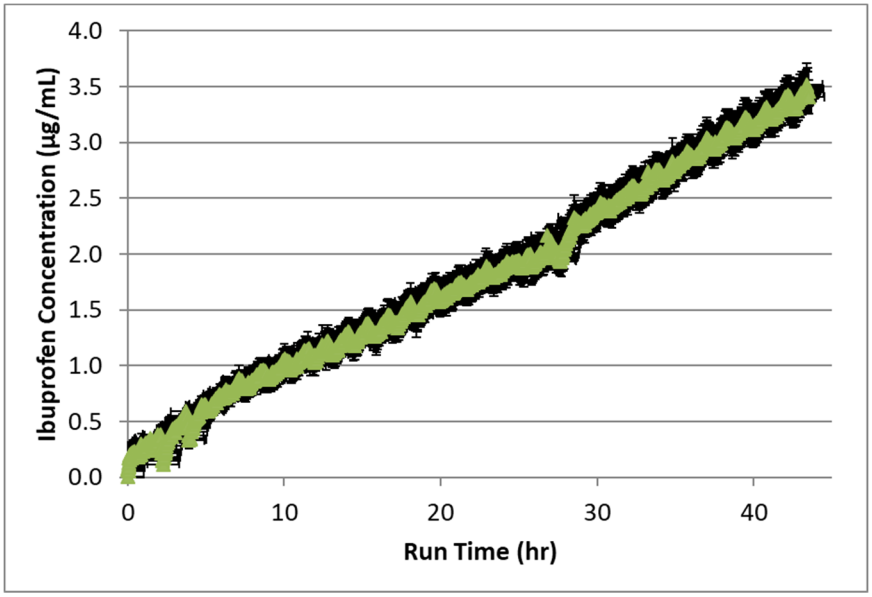


Figure B.3: Ibuprofen concentration (N = 3 ± SD) in a diffusion cell receptor chamber as a function of run time through a 100% hydrophobic poly(urethane) membrane. The donor concentration in the diffusion cell was 11.8 µg/mL. The steady-state diffusion rate was used to determine membrane permeability.

# Appendix C: Supplementary Information to Chapter 4

## C.1 Rat Gastric Retention Study

We investigated the ability of our GR dosage forms to retain in the stomach by administering the formulations to rats and, at specific time points, sacrificing them and inspecting their stomach contents. Representative pictures of the excised stomach and isolated dosage form for each formulation, prandial state, and time point are provided in

(a) 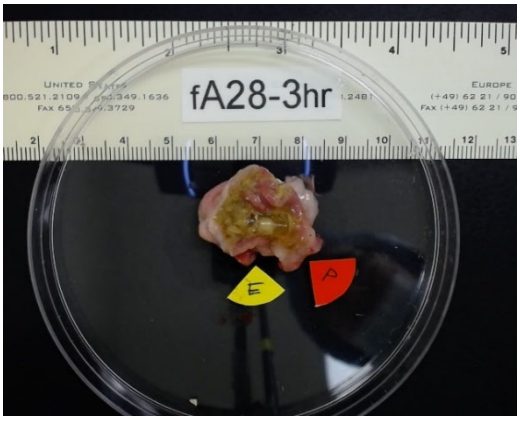

(b) 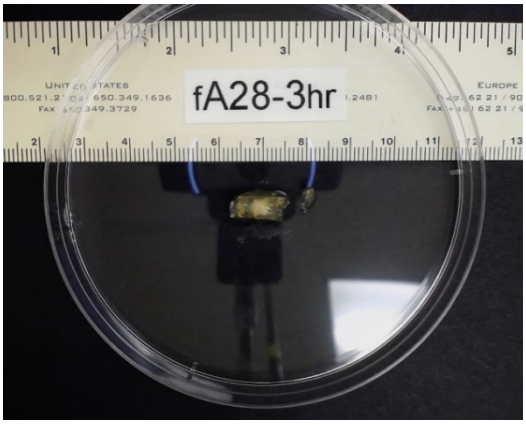


Figure C.1: Representative excised stomach (a) and isolated dosage form (b) from a fasted rat administered the greater swelling GR formulation and sacrificed 3 hours following dosing. Measurements are provided in cm. The yellow "E" indicates where the esophagus is located and the red "P" indicates where the pylorus is located.

(a) 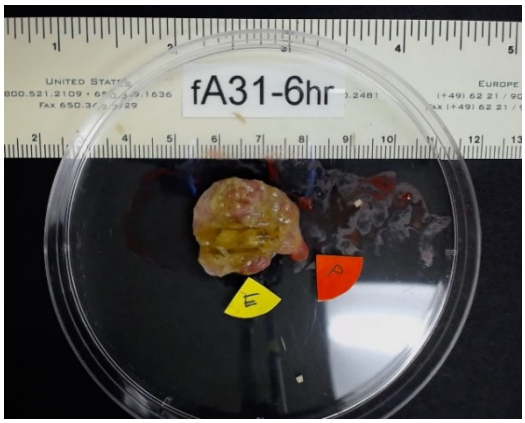

(b) 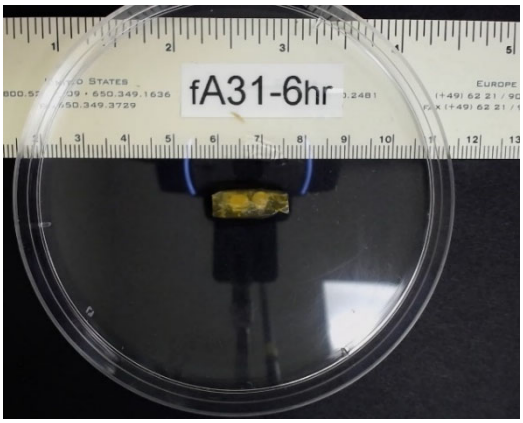


Figure C.2: Representative excised stomach (a) and isolated dosage form (b) from a fasted rat administered the greater swelling GR formulation and sacrificed 6 hours following dosing. Measurements are provided in cm. The yellow "E" indicates where the esophagus is located and the red "P" indicates where the pylorus is located.

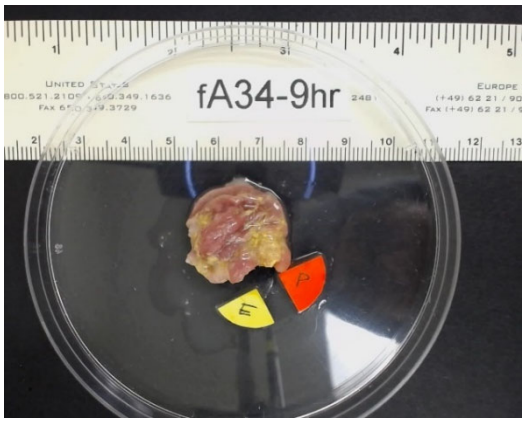


Figure C.3: Representative excised stomach from a fasted rat administered the greater swelling GR formulation and sacrificed 9 hours following dosing. No dosage form was found. Measurements are provided in cm. The yellow "E" indicates where the esophagus is located and the red "P" indicates where the pylorus is located.

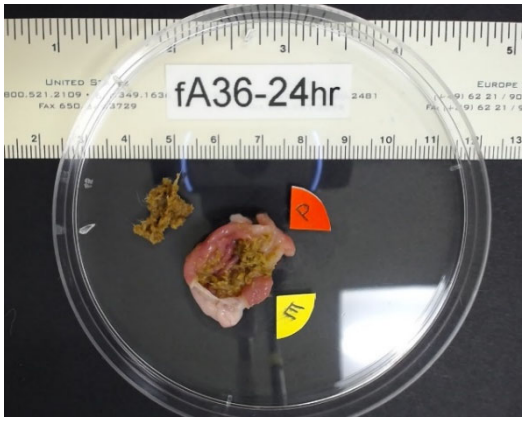


Figure C.4: Representative excised stomach from a fasted rat administered the greater swelling GR formulation and sacrificed 24 hours following dosing. No dosage form was found. Measurements are provided in cm. The yellow "E" indicates where the esophagus is located and the red "P" indicates where the pylorus is located.

(a) 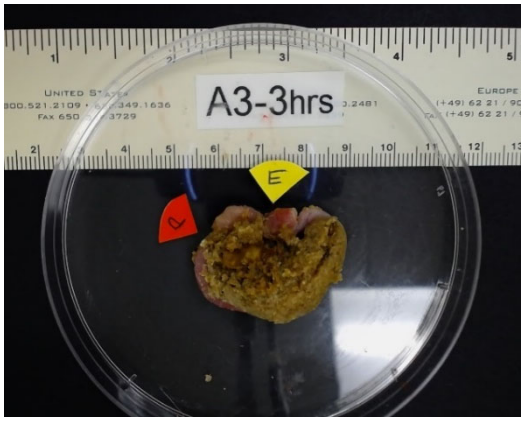

(b) 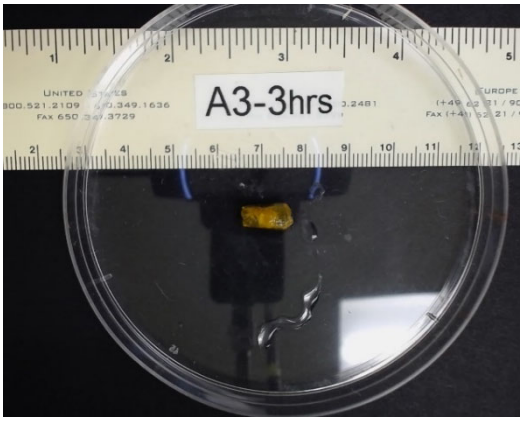


Figure C.5: Representative excised stomach (a) and isolated dosage form (b) from a fed rat administered the greater swelling GR formulation and sacrificed 3 hours following dosing. Measurements are provided in cm. The yellow "E" indicates where the esophagus is located and the red "P" indicates where the pylorus is located.

(a) 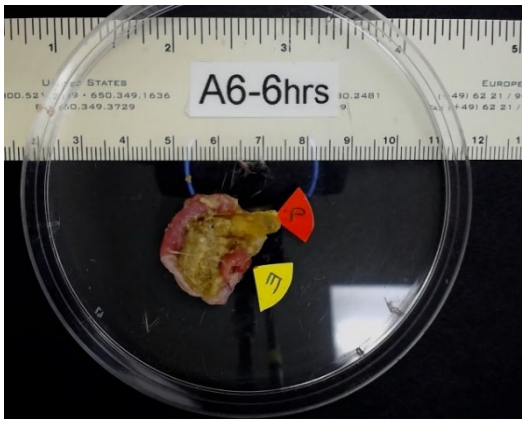

(b) 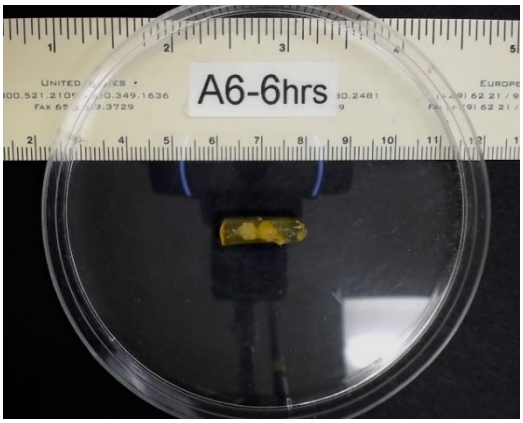


Figure C.6: Representative excised stomach (a) and isolated dosage form (b) from a fed rat administered the greater swelling GR formulation and sacrificed 6 hours following dosing. Measurements are provided in cm. The yellow "E" indicates where the esophagus is located and the red "P" indicates where the pylorus is located.

(a) 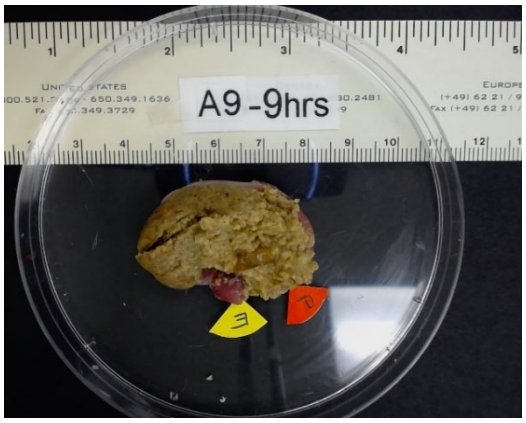

(b) 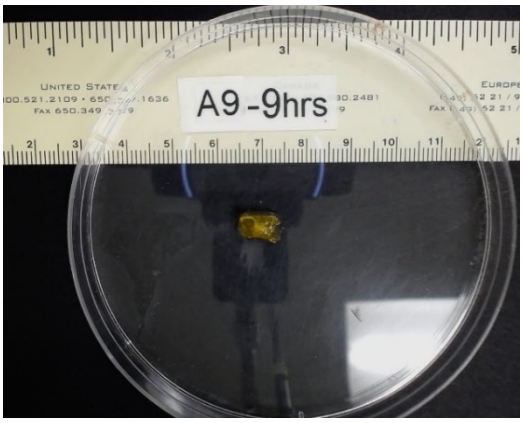


Figure C.7: Representative excised stomach (a) and isolated dosage form (b) from a fed rat administered the greater swelling GR formulation and sacrificed 9 hours following dosing. Measurements are provided in cm. The yellow "E" indicates where the esophagus is located and the red "P" indicates where the pylorus is located.

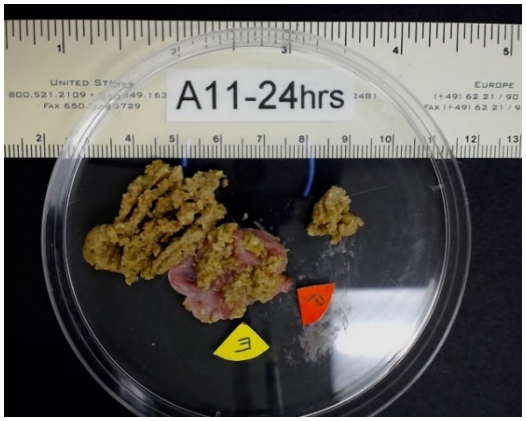


Figure C.8: Representative excised stomach from a fed rat administered the greater swelling GR formulation and sacrificed 24 hours following dosing. No dosage form was found. Measurements are provided in cm. The yellow "E" indicates where the esophagus is located and the red "P" indicates where the pylorus is located.

(a) 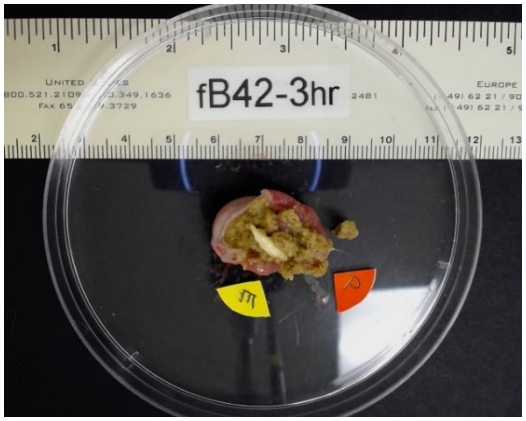


(b) 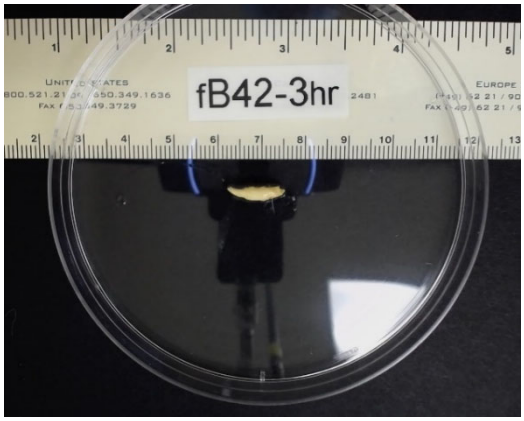


Figure C.9: Representative excised stomach (a) and isolated dosage form (b) from a fasted rat administered the less swelling GR formulation and sacrificed 3 hours following dosing. Measurements are provided in cm. The yellow "E" indicates where the esophagus is located and the red "P" indicates where the pylorus is located.

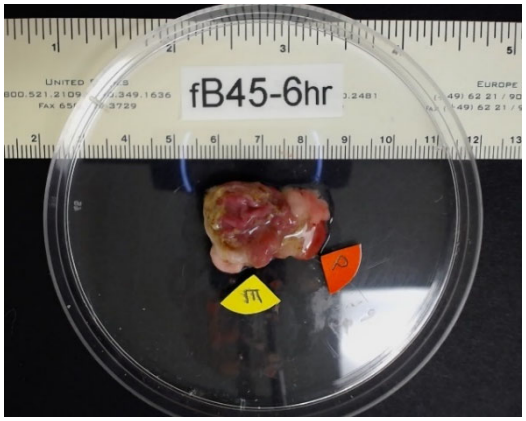


Figure C.10: Representative excised stomach from a fasted rat administered the less swelling GR formulation and sacrificed 6 hours following dosing. No dosage form was found. Measurements are provided in cm. The yellow "E" indicates where the esophagus is located and the red "P" indicates where the pylorus is located.

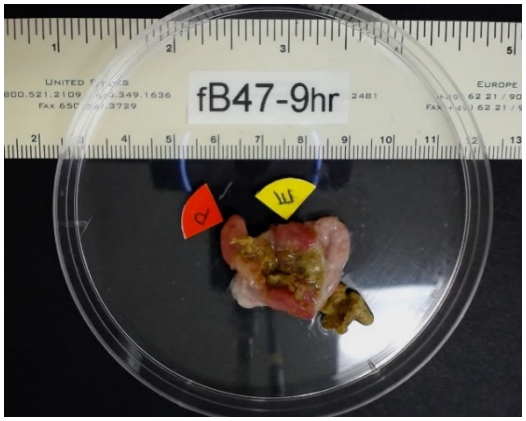


Figure C.11: Representative excised stomach from a fasted rat administered the less swelling GR formulation and sacrificed 9 hours following dosing. No dosage form was found. Measurements are provided in cm. The yellow "E" indicates where the esophagus is located and the red "P" indicates where the pylorus is located.

(a) 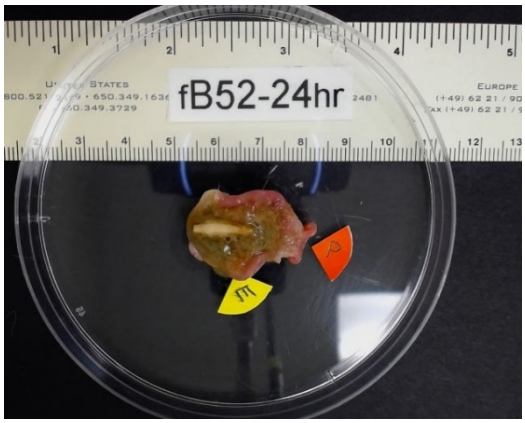

(b) 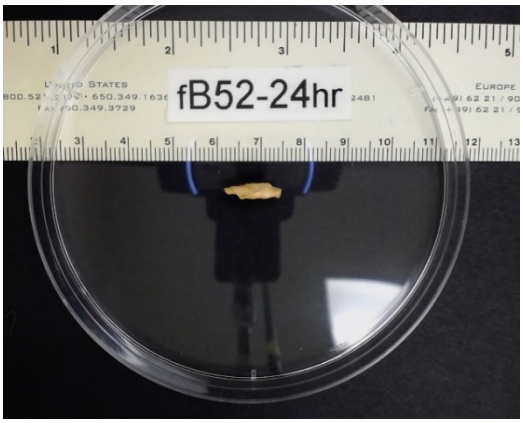


Figure C.12: Representative excised stomach (a) and isolated dosage form (b) from a fasted rat administered the less swelling GR formulation and sacrificed 24 hours following dosing. Measurements are provided in cm. The yellow "E" indicates where the esophagus is located and the red "P" indicates where the pylorus is located.

(a) 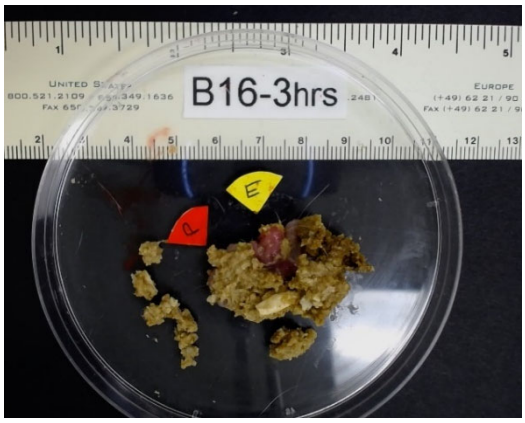

(b) 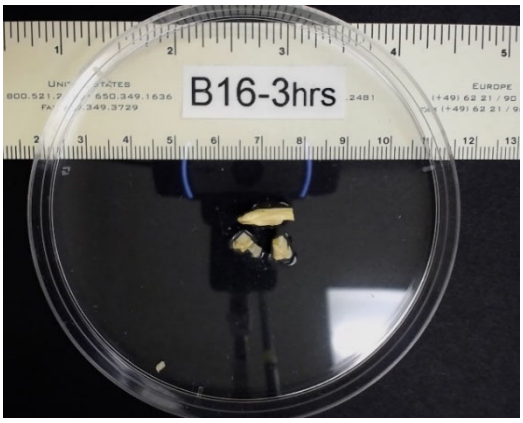


Figure C.13: Representative excised stomach (a) and isolated dosage form (b) from a fed rat administered the less swelling GR formulation and sacrificed 3 hours following dosing. Measurements are provided in cm. The yellow "E" indicates where the esophagus is located and the red "P" indicates where the pylorus is located.

(a) 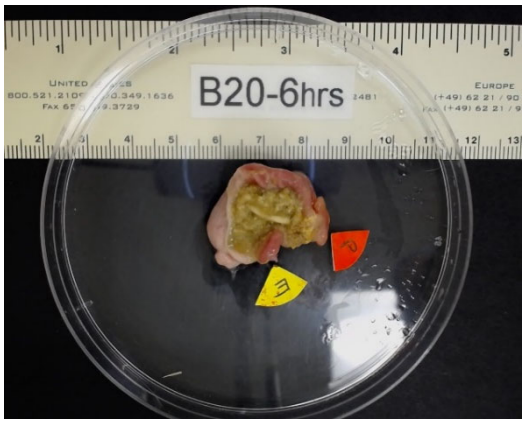

(b) 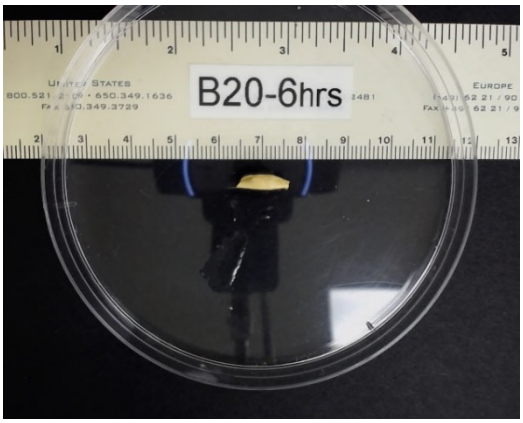


Figure C.14: Representative excised stomach (a) and isolated dosage form (b) from a fed rat administered the less swelling GR formulation and sacrificed 6 hours following dosing. Measurements are provided in cm. The yellow "E" indicates where the esophagus is located and the red "P" indicates where the pylorus is located.

(a) 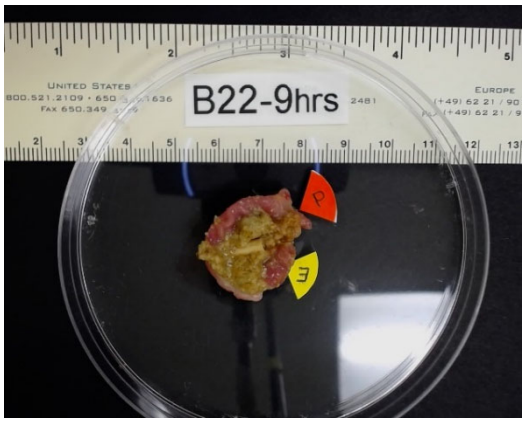

(b) 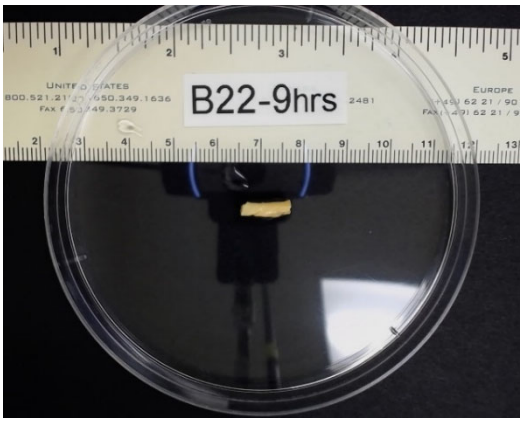


Figure C.15: Representative excised stomach (a) and isolated dosage form (b) from a fed rat administered the less swelling GR formulation and sacrificed 9 hours following dosing. Measurements are provided in cm. The yellow "E" indicates where the esophagus is located and the red "P" indicates where the pylorus is located.

(a) 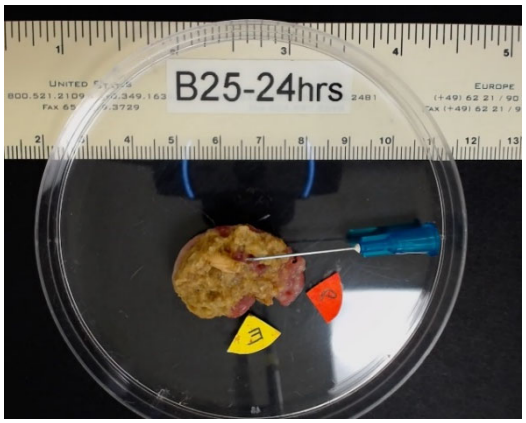

(b) 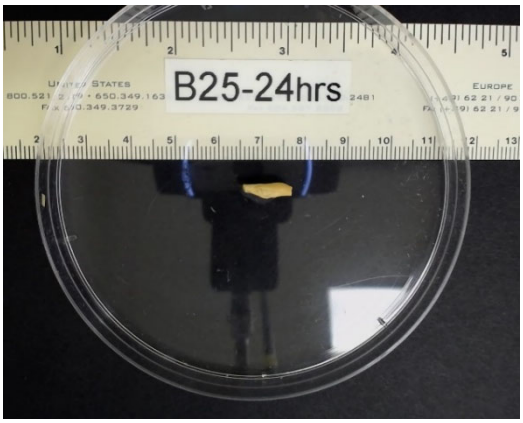


Figure C.16: Representative excised stomach (a) and isolated dosage form (b) from a fed rat administered the less swelling GR formulation and sacrificed 24 hours following dosing. Measurements are provided in cm. The yellow "E" indicates where the esophagus is located and the red "P" indicates where the pylorus is located.

## C.2 Mechanical Testing of Gastroretentive Dosage Forms

### C.2.1 Introduction

During our study described in Chapter 4, our reported dosage form dimensions reflect the expanded dosage form size unconstrained by gastric forces. Since the dosage form is realistically under stress from gastric forces, we performed mechanical testing on the dosage forms to assess its strength under stress. Sufficient strength in at least two dimensions is required to prevent deformation of the expanded dosage form such that it may be emptied as part of the MMC. However, the reported forces that gastroretentive formulations encounter in the stomach are varied. Moreover, although much research efforts has been dedicated to simulating gastric forces *in vitro*, the vast majority of the work has been focused on studying the effect of gastric forces on drug release behavior rather than on stomach retention [1–7]. Vassallo et al. coupled a load cell to a balloon catheter to monitor load and observed 22.0 ± 2.8 N of cumulative load during gastric

emptying of solids over 2 hours [8]. Kamba et al. attempted to estimate the gastric forces on a tablet by preparing tablets of defined crushing strength, dosing them to healthy subjects, and observing whether the tablets were destroyed by the stomach indicated by the release of drug [9]. They observed all tablets with a crushing strength of 1.5 N were crushed, but tablets with a crushing strength of 1.89 N were crushed by the stomachs of only 2 of 5 subjects. Tablets with a crushing strength of 3.04 N were not crushed by the stomachs of any subject investigated. Marciani et al. prepared 12.7 mm diameter agar gel beads with fracture strengths ranging from 0.15-0.90 N and assessed their time to breakage by measuring their gastric residence time residence time in humans using magnetic resonance imaging [10]. They found that all beads were eventually cleared from the stomach, but that those with a strength >0.65 N exhibited longer residence time.

Cassilly et al. measured the pressure, among other parameters, encountered by a SmartPill recording device as it passed through the human gastrointestinal tract [11]. They observed peak pressures around 200 mm Hg associated with Phase III of the MMC, which can be estimated at 85 N force given the dimensions of the SmartPill. Their work was recapitulated by Parkman and Jones using the SmartPill and they reported similar peak pressure values [12]. Laulicht et al. utilized a Hall array sensor technology to track the position and orientation of magnetic pills, which were then used to make force calculations [13]. They reported a maximum gastric motive force of 3014 dynes, which is approximately 0.03 N. A peak gastric force variance of 0.03 – 85 N is dramatic and speaks to the uncertainty in these estimations. For example, most studies assume that the entire surface area of their chosen probe (i.e., balloon, tablet, pill, etc.) is in contact with the stomach tissue when force is imparted, but this is almost certainly a poor assumption.

As previously described, multiple publications describe human stomach forces of varying levels, including varying orders of magnitude. Researchers also propose varying *in vitro* tests to assess retention of a dosage form in the stomach, although most publications related to gastric forces focus on their effects on drug dissolution, rather than on deformation/size changes relevant to stomach retention. Consequently, we found no clear consensus on the most relevant *in vitro* test to assess gastric retention or what success criteria would be for such a test. Therefore, we sought to compare *in vivo* gastric retention observations in rats to the data from *in vitro* tests, identifying suitable *in vitro* gastric retention test and success criteria.

### C.2.2 Methods

We developed two different mechanical tests using an Instron (Norwood, MA) 5544 Tensile/Compressive Machine and custom-made three-dimensional printed poly(lactic acid) parts. Our "normal" mechanical test used a custom-made three-dimensional printed funnel with an upper diameter of 27.5 mm and a lower diameter of 20 mm, as shown in Figure C.17a. The funnel height was 10.5 mm, whereas the overall fixture raised the funnel portion higher from the surface and was 68.5 mm. The probe attached to the Instron crosshead was a 15.9 mm diameter cylinder. The hydrated dosage form was placed in the funnel after soaking in 0.1N HCl for a specific duration, oriented such that the smaller dimension was perpendicular to the funnel opening, as shown in Figure C.17a. The crosshead and probe approach the tablet as a normal force at a displacement rate of 10 mm/sec. The test is meant to represent the normal force required for the dosage form to push through an orifice representing the relaxed pyloric sphincter.

Our “compression” mechanical test used a custom-made three-dimensional printed container and probe. The container was 62 mm long, 16 mm wide, and 36 mm high, as shown in Figure C.17b. The narrow width ensures that the dosage form is oriented on its side. The probe attached to the Instron is 55 mm long, 12 mm wide, and 35 mm high. The hydrated dosage form was placed in the container after soaking in 0.1N HCl for a specific duration. The crosshead and probe approach the tablet as a normal force at a displacement rate of 10 mm/sec. The test is meant to represent the compressive peristaltic forces of the stomach.

(a) 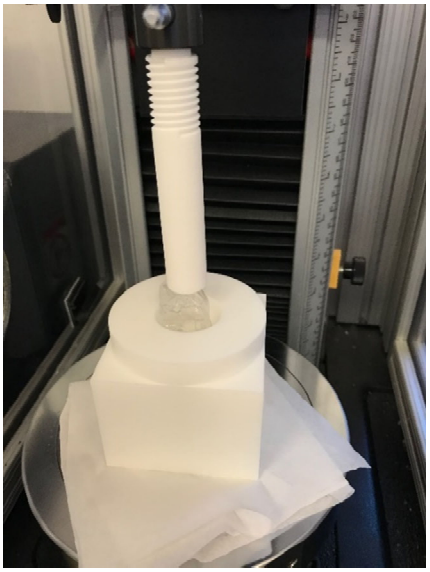 (b) 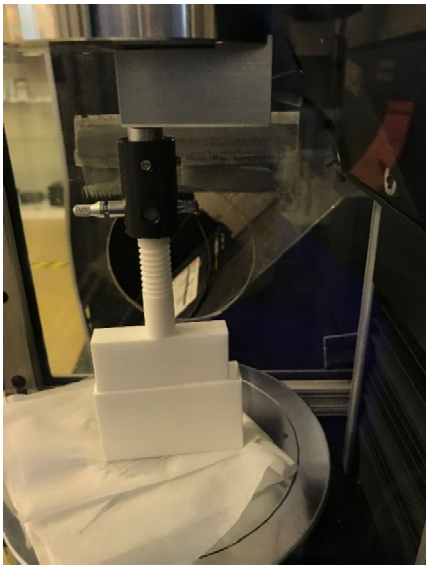

Figure C.17: Normal (a) and compression (b) mechanical test components.

### C.2.3 Results and Discussion

The curves of force as a function of displacement for the normal and compression mechanical tests of the greater swelling formulation are shown in Figure C.18 after 1 hour of soaking, Figure C.19 after 3 hours of soaking, and Figure C.20 after 6 hours of

soaking. In each figure, the red horizontal line corresponds to the 0.03 N maximum force threshold described by Laulicht et al. [13]. The green vertical line related to the compression mechanical test and represents a displacement of 17 mm from the top of the container, representing a 20 mm relaxed pylorus diameter. We observed a substantial softening of the polymer layer between 1 and 3 hours, as measured by the force-displacement curve of both the normal and compression mechanical tests. However, we observed no substantial change in the force required to displace the dosage form from 3 to 6 hours using that test. At all time points, we found that the force required to push the dosage form through the funnel orifice of the normal mechanical test was substantially greater than 0.03 N (from 0.5 N to >2 N). Similarly, we found that the force required to compress the dosage form to less than 20 mm in width exceeded 0.03 N at all time points, although it required less than 0.3 N.

The curves of force as a function of displacement for the compression mechanical tests of the lesser swelling formulation after 1 hour, 3 hours, and 6 hours of soaking in 0.1N HCl are shown in Figure C.21. The normal mechanical test was not possible for this dosage form because the shorter dimension was less than 20 mm for all swollen samples and the dosage form falls through the funnel immediately. Similar to the previous figures, the red horizontal line corresponds to the 0.03 N maximum force threshold described by Laulicht et al [13]. The green vertical line related to the compression mechanical test and represents a displacement of 17 mm from the top of the container, representing a 20 mm relaxed pylorus diameter. We observed a similar trend to the greater swelling formulation of polymer layer softening, with less force required to displace the dosage form. However, there were no recordable forces exerted on the probe well beyond the 20 mm threshold represented by the green vertical line.

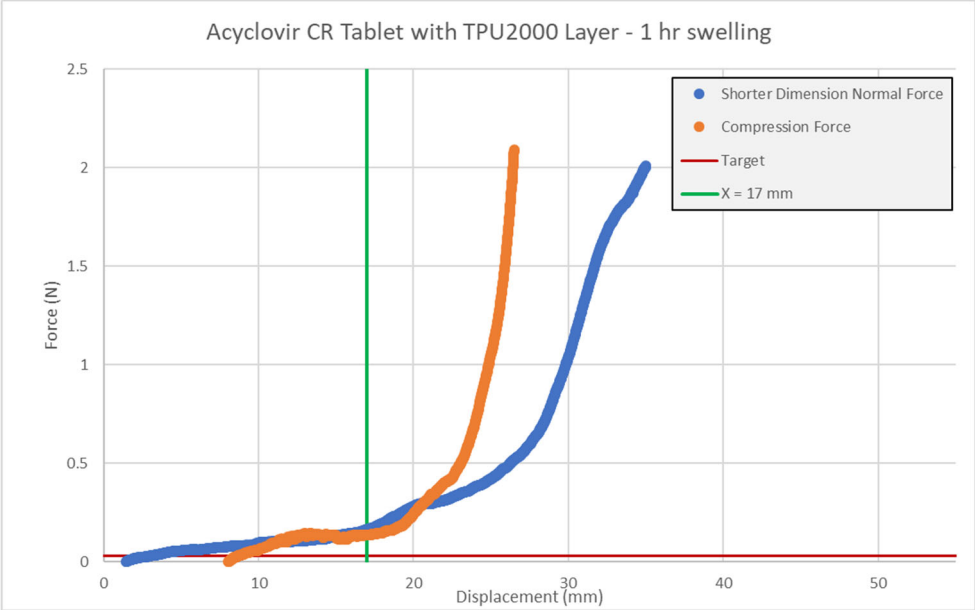


Figure C.18: Normal and compression mechanical tests on the greater swelling (100% TPU2000) dosage form after 1 hour soaking in 0.1N HCl.

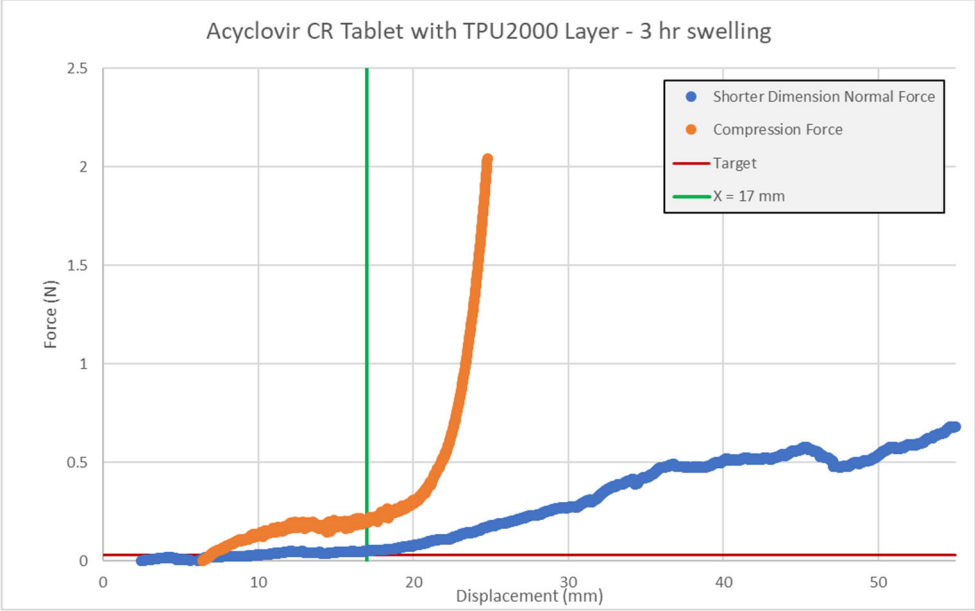


Figure C.19: Normal and compression mechanical tests on the greater swelling (100% TPU2000) dosage form after 3 hours soaking in 0.1N HCl.

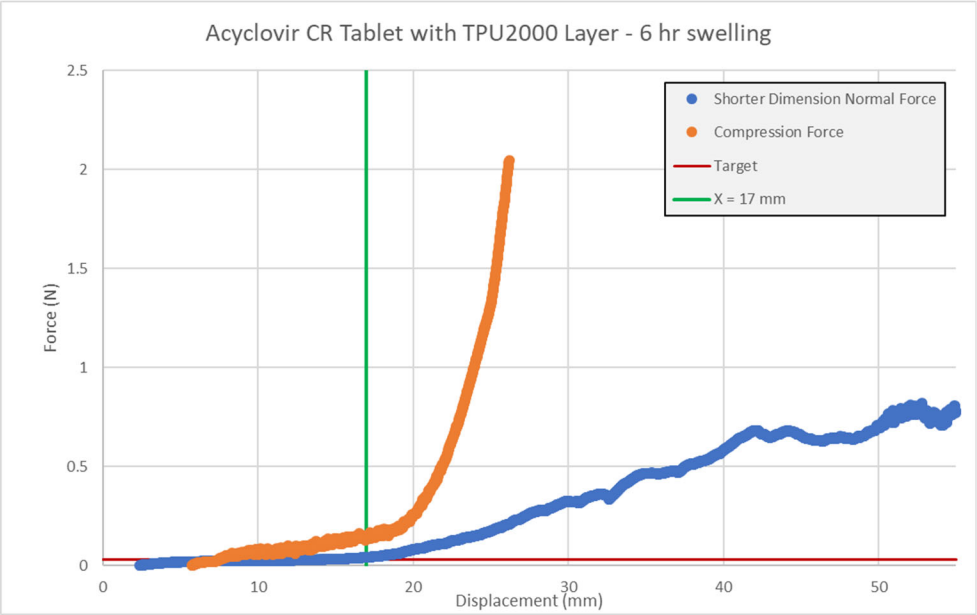


Figure C.20: Normal and compression mechanical tests on the greater swelling (100% TPU2000) dosage form after 6 hours soaking in 0.1N HCl.

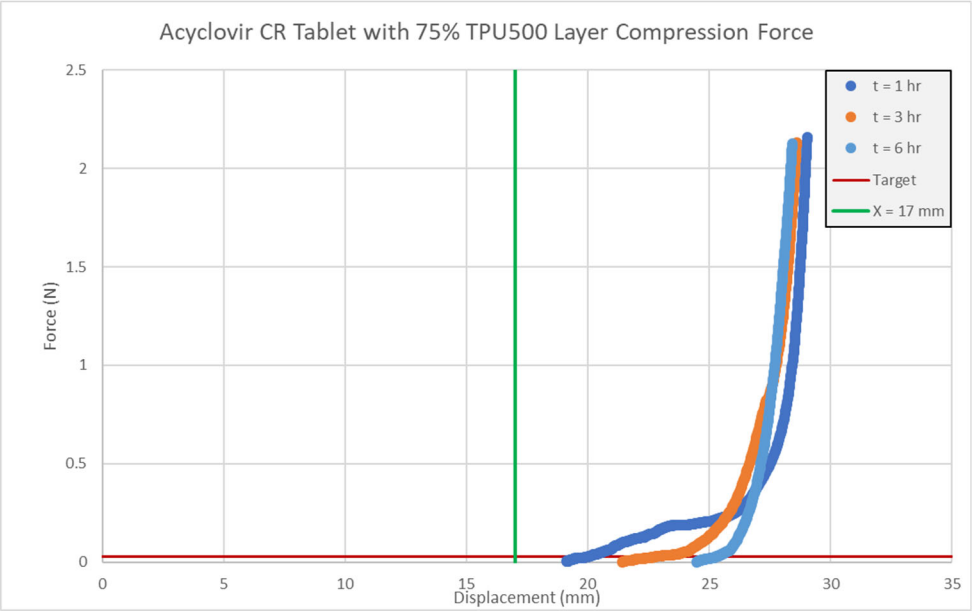


Figure C.21: Compression mechanical test on the lesser swelling (75% TPU500) dosage form after 1, 3, and 6 hours of soaking in 0.1N HCl.

### C.2.4 Conclusion

We developed two mechanical tests intended to simulate mechanical forces in the stomach. The normal mechanical test is less physiologically relevant to the mode of gastric forces that a dosage form encounters, however it is a more well-defined test. The compression mechanical test is closer to the peristaltic motions of the stomach, but potentially less reproducible. Ultimately, we were unable to effectively correlate our mechanical test data to the rat gastric retention study data. Although the two formulations retained to different extents in the rat gastric retention study, it is possible that there was insufficient differentiation to properly develop an *in vitro-in vivo* correlation. Future work will focus on the development of alternative mechanical tests that may better represent the forces a gastroretentive dosage form encounters in the stomach.

## C.3 REFERENCES


[1] F. Kong, R.P. Singh, A Human Gastric Simulator (HGS) to Study Food Digestion in Human Stomach, J. Food Sci. 75 (2010) E627–E635. doi:10.1111/j.1750-3841.2010.01856.x.

[2] G. Garbacz, S. Klein, W. Weitschies, A biorelevant dissolution stress test device – background and experiences, Expert Opin. Drug Deliv. 7 (2010) 1251–1261. doi:10.1517/17425247.2010.527943.

[3] M. Vardakou, A. Mercuri, S.A. Barker, D.Q.M. Craig, R.M. Faulks, M.S.J. Wickham, Achieving Antral Grinding Forces in Biorelevant In Vitro Models: Comparing the USP Dissolution Apparatus II and the Dynamic Gastric Model with Human In Vivo Data, AAPS PharmSciTech. 12 (2011) 620–626. doi:10.1208/s12249-011-9616-z.

[4] M. Koziolek, G. Garbacz, M. Neumann, W. Weitschies, Simulating the Postprandial Stomach: Biorelevant Test Methods for the Estimation of Intragastric Drug Dissolution, Mol. Pharm. 10 (2013) 2211–2221. doi:10.1021/mp300607e.

[5] M. Koziolek, K. Görke, M. Neumann, G. Garbacz, W. Weitschies, Development

of a bio-relevant dissolution test device simulating mechanical aspects present in the fed stomach, Eur. J. Pharm. Sci. 57 (2014) 250–256. doi:10.1016/J.EJPS.2013.09.004.

[6] E.S. Kostewicz, B. Abrahamsson, M. Brewster, J. Brouwers, J. Butler, S. Carlert, P.A. Dickinson, J. Dressman, R. Holm, S. Klein, J. Mann, M. McAllister, M. Minekus, U. Muenster, A. Müllertz, M. Verwei, M. Vertzoni, W. Weitschies, P. Augustijns, In vitro models for the prediction of in vivo performance of oral dosage forms, Eur. J. Pharm. Sci. 57 (2014) 342–366. doi:10.1016/J.EJPS.2013.08.024.

[7] F. Schneider, M. Hoppe, M. Koziolek, W. Weitschies, Influence of Postprandial Intragastric Pressures on Drug Release from Gastroretentive Dosage Forms, AAPS PharmSciTech. 19 (2018) 2843–2850. doi:10.1208/s12249-018-1022-3.

[8] M.J. Vassallo, M. Camilleri, C.M. Prather, R.B. Hanson, G.M. Thomforde, Measurement of axial forces during emptying from the human stomach., Am. J. Physiol. 263 (1992) G230-9. doi:10.1152/ajpgi.1992.263.2.G230.

[9] M. Kamba, Y. Seta, A. Kusai, M. Ikeda, K. Nishimura, A unique dosage form to evaluate the mechanical destructive force in the gastrointestinal tract, Int. J. Pharm. 208 (2000) 61–70. doi:10.1016/S0378-5173(00)00552-4.

[10] L. Marciani, P.A. Gowland, A. Fillery-Travis, P. Manoj, J. Wright, A. Smith, P. Young, R. Moore, R.C. Spiller, Assessment of antral grinding of a model solid meal with echo-planar imaging, Am. J. Physiol. Liver Physiol. 280 (2001) G844–G849. doi:10.1152/ajpgi.2001.280.5.G844.

[11] D. Cassilly, S. Kantor, L.C. Knight, A.H. Maurer, R.S. Fisher, J. Semler, H.P. Parkman, Gastric emptying of a non-digestible solid: assessment with simultaneous SmartPill pH and pressure capsule, antroduodenal manometry, gastric emptying scintigraphy, Neurogastroenterol. Motil. 20 (2008) 311–319. doi:10.1111/j.1365-2982.2007.01061.x.

[12] H.P. Parkman, M.P. Jones, Tests of Gastric Neuromuscular Function, Gastroenterology. 136 (2009) 1526–1543. doi:10.1053/J.GASTRO.2009.02.039.

[13] B. Laulicht, A. Tripathi, V. Schlageter, P. Kucera, E. Mathiowitz, Understanding gastric forces calculated from high-resolution pill tracking., Proc. Natl. Acad. Sci. U. S. A. 107 (2010) 8201–6. doi:10.1073/pnas.1002292107.

# Bibliography


G.A. Abraham, P.M. Frontini, T.R. Cuadrado, Physical and mechanical behavior of sterilized biomedical segmented polyurethanes, J. Appl. Polym. Sci. 65 (1997) 1193–1203. https://doi.org/10.1002/(SICI)1097-4628(19970808)65:6<1193::AID-APP15>3.0.CO;2-V.

M. Ahmed, G. Punshon, A. Darbyshire, A.M. Seifalian, Effects of sterilization treatments on bulk and surface properties of nanocomposite biomaterials, J. Biomed. Mater. Res. Part B Appl. Biomater. 101 (2013) 1182–1190. https://doi.org/10.1002/jbm.b.32928.

T.O. Ahn, I.S. Choi, H.M. Jeong, K. Cho, Thermal and mechanical properties of thermoplastic polyurethane elastomers from different polymerization methods, Polym. Int. 31 (1993) 329–333. https://doi.org/10.1002/pi.4990310404.

A. Almeida, L. Brabant, F. Siepmann, T. De Beer, W. Bouquet, L. Van Hoorebeke, J. Siepmann, J.P. Remon, C. Vervaet, Sustained release from hot-melt extruded matrices based on ethylene vinyl acetate and polyethylene oxide, Eur. J. Pharm. Biopharm. 82 (2012) 526–533. https://doi.org/10.1016/J.EJPB.2012.08.008.

K. Amighi, A.J. Moës, Evaluation of Thermal and Film Forming Properties of Acrylic Aqueous Polymer Dispersion Blends: Application to the Formulation of Sustained-Release Film Coated Theophylline Pellets, Drug Dev. Ind. Pharm. 21 (1995) 2355–2369. https://doi.org/10.3109/03639049509070874.

J.M. Anderson, A. Hiltner, M.J. Wiggins, M.A. Schubert, T.O. Collier, W.J. Kao, A.B. Mathur, Recent advances in biomedical polyurethane biostability and biodegradation, Polym. Int. 46 (1998) 163–171. https://doi.org/10.1002/(SICI)1097-0126(199807)46:3<163::AID-PI972>3.0.CO;2-9.

J.M. Anderson, A. Rodriguez, D.T. Chang, Foreign body reaction to biomaterials, Semin. Immunol. 20 (2008) 86–100. https://doi.org/10.1016/j.smim.2007.11.004.

D.Y. Arifin, L.Y. Lee, C.-H. Wang, Mathematical modeling and simulation of drug release from microspheres: Implications to drug delivery systems, Adv. Drug Deliv. Rev. 58 (2006) 1274–1325. https://doi.org/10.1016/j.addr.2006.09.007.

J.K. Armstrong, R.B. Wenby, H.J. Meiselman, T.C. Fisher, The Hydrodynamic Radii of Macromolecules and Their Effect on Red Blood Cell Aggregation, Biophys. J. 87 (2004) 4259–4270. https://doi.org/10.1529/BIOPHYSJ.104.047746.

R.A.K. Arza, C.S.R. Gonugunta, P.R. Veerareddy, Formulation and Evaluation of Swellable and Floating Gastroretentive Ciprofloxacin Hydrochloride Tablets, AAPS PharmSciTech. 10 (2009) 220–226. https://doi.org/10.1208/s12249-009-

9200-y.

Y. Aso, S. Yoshioka, T. Miyazaki, T. Kawanishi, K. Tanaka, S. Kitamura, A. Takakura, T. Hayashi, N. Muranushi, Miscibility of Nifedipine and Hydrophilic Polymers as Measured by 1H-NMR Spin–Lattice Relaxation, Chem. Pharm. Bull. (Tokyo). 55 (2007) 1227–1231. https://doi.org/10.1248/cpb.55.1227.

ASTM International, ASTM D2240-15e1, Standard Test Method for Rubber Property—Durometer Hardness, in: ASTM Stand., West Conshohocken, PA, 2015. https://doi.org/10.1520/D2240-15E01.

A. Avdeef, Physicochemical Profiling (Solubility, Permeability and Charge State), Curr. Top. Med. Chem. 1 (2001) 277–351. https://doi.org/10.2174/1568026013395100.

E. Baer, A. Hiltner, H.D. Keith, Hierarchical structure in polymeric materials., Science. 235 (1987) 1015–22. https://doi.org/10.1126/SCIENCE.3823866.

L. Baert, G. van 't Klooster, W. Dries, M. François, A. Wouters, E. Basstanie, K. Iterbeke, F. Stappers, P. Stevens, L. Schueller, P. Van Remoortere, G. Kraus, P. Wigerinck, J. Rosier, Development of a long-acting injectable formulation with nanoparticles of rilpivirine (TMC278) for HIV treatment, Eur. J. Pharm. Biopharm. 72 (2009) 502–508. https://doi.org/10.1016/J.EJPB.2009.03.006.

H.H. Balfour, Antiviral Drugs, N. Engl. J. Med. 340 (1999) 1255–1268. https://doi.org/10.1056/NEJM199904223401608.

P.L. Bardonnet, V. Faivre, W.J. Pugh, J.C. Piffaretti, F. Falson, Gastroretentive dosage forms: Overview and special case of Helicobacter pylori, J. Control. Release. 111 (2006) 1–18. https://doi.org/10.1016/J.JCONREL.2005.10.031.

S.E. Barrett, R.S. Teller, S.P. Forster, L. Li, M.A. Mackey, D. Skomski, Z. Yang, K.L. Fillgrove, G.J. Doto, S.L. Wood, J. Lebron, J.A. Grobler, R.I. Sanchez, Z. Liu, B. Lu, T. Niu, L. Sun, M.E. Gindy, Extended Duration MK-8591-Eluting Implant as a Candidate for HIV Treatment and Prevention., Antimicrob. Agents Chemother. (2018) AAC.01058-18. https://doi.org/10.1128/AAC.01058-18.

G.L. Bas, The Molecular Volumes of Liquid Chemical Compounds, from the Point of View of Kopp, Longmans, Green, 1915. https://books.google.com/books?id=6FUuAQAAIAAJ.

P. Basak, B. Adhikari, I. Banerjee, T.K. Maiti, Sustained release of antibiotic from polyurethane coated implant materials, J. Mater. Sci. Mater. Med. 20 (2009) 213–221. https://doi.org/10.1007/s10856-008-3521-3.

D. Bateson, K. McNamee, P. Briggs, Newer non-oral hormonal contraception., BMJ. 346 (2013) f341. https://doi.org/10.1136/bmj.f341.

M.M. Baum, I. Butkyavichene, J. Gilman, S. Kennedy, E. Kopin, A.M. Malone, C.

Nguyen, T.J. Smith, D.R. Friend, M.R. Clark, J.A. Moss, An intravaginal ring for the simultaneous delivery of multiple drugs., J. Pharm. Sci. 101 (2012) 2833–43. https://doi.org/10.1002/jps.23208.

F. Bauss, R.G. Russell, Ibandronate in osteoporosis: preclinical data and rationale for intermittent dosing, Osteoporos. Int. 15 (2004) 423–433. https://doi.org/10.1007/s00198-004-1612-7.

O. Bayer, Das Di-Isocyanat-Polyadditionsverfahren (Polyurethane), Angew. Chemie. 59 (1947) 257–272. https://doi.org/10.1002/ange.19470590901.

A.M. Bellinger, M. Jafari, T.M. Grant, S. Zhang, H.C. Slater, E.A. Wenger, S. Mo, Y.-A.L. Lee, H. Mazdiyasni, L. Kogan, R. Barman, C. Cleveland, L. Booth, T. Bensel, D. Minahan, H.M. Hurowitz, T. Tai, J. Daily, B. Nikolic, L. Wood, P.A. Eckhoff, R. Langer, G. Traverso, Oral, ultra-long-lasting drug delivery: Application toward malaria elimination goals., Sci. Transl. Med. 8 (2016) 365ra157. https://doi.org/10.1126/scitranslmed.aag2374.

B. Berner, V.E. Cowles, Case studies in swelling polymeric gastric retentive tablets, Expert Opin. Drug Deliv. 3 (2006) 541–548. https://doi.org/10.1517/17425247.3.4.541.

A. Bhattacharyya, P. Mukhopadhyay, P.P. Kundu, Synthesis of a novel pH-sensitive polyurethane-alginate blend with poly(ethylene terephthalate) waste for the oral delivery of protein, J. Appl. Polym. Sci. 131 (2014) n/a-n/a. https://doi.org/10.1002/app.40650.

R. Bodmeier, O. Paeratakul, Theophylline Tablets Coated with Aqueous Latexes Containing Dispersed Pore Formers, J. Pharm. Sci. 79 (1990) 925–928. https://doi.org/10.1002/jps.2600791017.

J.W. Boretos, W.S. Pierce, Segmented polyurethane: A polyether polymer. An initial evalution for biomedical applications, J. Biomed. Mater. Res. 2 (1968) 121–130. https://doi.org/10.1002/jbm.820020109.

H.B. Bosworth, J.N. Brown, S. Danus, L.L. Sanders, F. McCant, L.L. Zullig, M.K. Olsen, Evaluation of a packaging approach to improve cholesterol medication adherence., Am. J. Manag. Care. 23 (2017) e280–e286. http://www.ncbi.nlm.nih.gov/pubmed/29087166 (accessed March 28, 2019).

W. Bounds, A. Szarewski, D. Lowe, J. Guillebaud, Preliminary report of unexpected local reactions to a progestogen-releasing contraceptive vaginal ring, Eur. J. Obstet. Gynecol. Reprod. Biol. 48 (1993) 123–125. https://doi.org/10.1016/0028-2243(93)90252-8.

J. Breitenbach, Melt extrusion: from process to drug delivery technology, Eur. J. Pharm. Biopharm. 54 (2002) 107–117. https://doi.org/10.1016/S0939-6411(02)00061-9.

G. Bruni, M. Maietta, L. Maggi, P. Mustarelli, C. Ferrara, V. Berbenni, C. Milanese, A. Girella, A. Marini, Preparation and Physicochemical Characterization of Acyclovir Cocrystals with Improved Dissolution Properties, J. Pharm. Sci. 102 (2013) 4079–4086. https://doi.org/10.1002/JPS.23721.

P. Busch, D. Posselt, D.M. Smilgies, B. Rheinländer, F. Kremer, C.M. Papadakis, Lamellar diblock copolymer thin films investigated by tapping mode atomic force microscopy: Molar-mass dependence of surface ordering, Macromolecules. 36 (2003) 8717–8727. https://doi.org/10.1021/ma034375r.

P.L. Canner, S.A. Forman, M.A. Prud'homme, K.G. Berge, J. Stamler, Influence of Adherence to Treatment and Response of Cholesterol on Mortality in the Coronary Drug Project, N. Engl. J. Med. 303 (1980) 1038–1041. https://doi.org/10.1056/NEJM198010303031804.

D. Cassilly, S. Kantor, L.C. Knight, A.H. Maurer, R.S. Fisher, J. Semler, H.P. Parkman, Gastric emptying of a non-digestible solid: assessment with simultaneous SmartPill pH and pressure capsule, antroduodenal manometry, gastric emptying scintigraphy, Neurogastroenterol. Motil. 20 (2008) 311–319. https://doi.org/10.1111/j.1365-2982.2007.01061.x.

C. Celum, J.M. Baeten, Tenofovir-based pre-exposure prophylaxis for HIV prevention: evolving evidence., Curr. Opin. Infect. Dis. 25 (2012) 51–7. https://doi.org/10.1097/QCO.0b013e32834ef5ef.

M. Chavanpatil, P. Jain, S. Chaudhari, R. Shear, P. Vavia, Development of sustained release gastroretentive drug delivery system for ofloxacin: In vitro and in vivo evaluation, Int. J. Pharm. 304 (2005) 178–184. https://doi.org/10.1016/J.IJPHARM.2005.08.009.

M.D. Chavanpatil, P. Jain, S. Chaudhari, R. Shear, P.R. Vavia, Novel sustained release, swellable and bioadhesive gastroretentive drug delivery system for ofloxacin, Int. J. Pharm. 316 (2006) 86–92. https://doi.org/10.1016/J.IJPHARM.2006.02.038.

A.S. Cheifetz, A.A. Kornbluth, P. Legnani, I. Schmelkin, A. Brown, S. Lichtiger, B.S. Lewis, The risk of retention of the capsule endoscope in patients with known or suspected Crohn's disease., Am. J. Gastroenterol. 101 (2006) 2218–22. https://doi.org/10.1111/j.1572-0241.2006.00761.x.

C. Chen, V.E. Cowles, E. Hou, Pharmacokinetics of Gabapentin in a Novel Gastric-Retentive Extended-Release Formulation: Comparison With an Immediate-Release Formulation and Effect of Dose Escalation and Food, J. Clin. Pharmacol. 51 (2011) 346–358. https://doi.org/10.1177/0091270010368411.

C. Chen, C.-H. (Sara) Han, M. Sweeney, V.E. Cowles, Pharmacokinetics, Efficacy, and Tolerability of a Once-Daily Gastroretentive Dosage Form of Gabapentin for

the Treatment of Postherpetic Neuralgia, J. Pharm. Sci. 102 (2013) 1155–1164. https://doi.org/10.1002/JPS.23467.

G.-L. Chen, W.-H. Hao, In Vitro Performance of Floating Sustained-Release Capsule of Verapamil, Drug Dev. Ind. Pharm. 24 (1998) 1067–1072. https://doi.org/10.3109/03639049809089950.

J. Chen, W.E. Blevins, H. Park, K. Park, Gastric retention properties of superporous hydrogel composites, J. Control. Release. 64 (2000) 39–51. https://doi.org/10.1016/S0168-3659(99)00139-X.

R.-N. Chen, H.-O. Ho, C.-Y. Yu, M.-T. Sheu, Development of swelling/floating gastroretentive drug delivery system based on a combination of hydroxyethyl cellulose and sodium carboxymethyl cellulose for Losartan and its clinical relevance in healthy volunteers with CYP2C9 polymorphism, Eur. J. Pharm. Sci. 39 (2010) 82–89. https://doi.org/10.1016/J.EJPS.2009.10.015.

X. Chen, W. Liu, Y. Zhao, L. Jiang, H. Xu, X. Yang, Preparation and characterization of PEG-modified polyurethane pressure-sensitive adhesives for transdermal drug delivery, Drug Dev. Ind. Pharm. 35 (2009) 704–711. https://doi.org/10.1080/03639040802512235.

Y.-C. Chen, H.-O. Ho, T.-Y. Lee, M.-T. Sheu, Physical characterizations and sustained release profiling of gastroretentive drug delivery systems with improved floating and swelling capabilities, Int. J. Pharm. 441 (2013) 162–169. https://doi.org/10.1016/J.IJPHARM.2012.12.002.

J.Y. Cherng, T.Y. Hou, M.F. Shih, H. Talsma, W.E. Hennink, Polyurethane-based drug delivery systems, Int. J. Pharm. 450 (2013) 145–162. https://doi.org/10.1016/j.ijpharm.2013.04.063.

E.M. Christenson, M. Dadsetan, M. Wiggins, J.M. Anderson, A. Hiltner, Poly(carbonate urethane) and poly(ether urethane) biodegradation: In vivo studies, J. Biomed. Mater. Res. Part A. 69A (2004) 407–416. https://doi.org/10.1002/jbm.a.30002.

B. Claeys, S. De Bruyn, L. Hansen, T. De Beer, J.P. Remon, C. Vervaet, Release characteristics of polyurethane tablets containing dicarboxylic acids as release modifiers – a case study with diprophylline, Int. J. Pharm. 477 (2014) 244–250. https://doi.org/10.1016/J.IJPHARM.2014.10.046.

B. Claeys, A. Vervaeck, X.K.D. Hillewaere, S. Possemiers, L. Hansen, T. De Beer, J.P. Remon, C. Vervaet, Thermoplastic polyurethanes for the manufacturing of highly dosed oral sustained release matrices via hot melt extrusion and injection molding, Eur. J. Pharm. Biopharm. 90 (2015) 44–52. https://doi.org/10.1016/J.EJPB.2014.11.003.

J.T. Clark, M.R. Clark, N.B. Shelke, T.J. Johnson, E.M. Smith, A.K. Andreasen, J.S.

Nebeker, J. Fabian, D.R. Friend, P.F. Kiser, Engineering a Segmented Dual-Reservoir Polyurethane Intravaginal Ring for Simultaneous Prevention of HIV Transmission and Unwanted Pregnancy, PLoS One. 9 (2014) e88509. https://doi.org/10.1371/journal.pone.0088509.

J.T. Clark, T.J. Johnson, M.R. Clark, J.S. Nebeker, J. Fabian, A.L. Tuitupou, S. Ponnapalli, E.M. Smith, D.R. Friend, P.F. Kiser, Quantitative evaluation of a hydrophilic matrix intravaginal ring for the sustained delivery of tenofovir, J. Control. Release. 163 (2012) 240–248. https://doi.org/10.1016/J.JCONREL.2012.08.033.

M.R. Clark, T.J. Johnson, R.T. McCabe, J.T. Clark, A. Tuitupou, H. Elgendy, D.R. Friend, P.F. Kiser, A hot-melt extruded intravaginal ring for the sustained delivery of the antiretroviral microbicide UC781., J. Pharm. Sci. 101 (2012) 576–87. https://doi.org/10.1002/jps.22781.

A.J. Claxton, J. Cramer, C. Pierce, A systematic review of the associations between dose regimens and medication compliance., Clin. Ther. 23 (2001) 1296–310. http://www.ncbi.nlm.nih.gov/pubmed/11558866 (accessed September 4, 2018).

G. Di Colo, Controlled drug release from implantable matrices based on hydrophobia polymers, Biomaterials. 13 (1992) 850–856. https://doi.org/10.1016/0142-9612(92)90178-Q.

S.L. Cooper, J. Guan, Advances in Polyurethane Biomaterials, Woodhead Publishing, Cambridge, MA, USA, 2016. https://doi.org/10.1016/C2014-0-04143-3.

J.M. Cortez, R. Quintero, J.A. Moss, M. Beliveau, T.J. Smith, M.M. Baum, Pharmacokinetics of injectable, long-acting nevirapine for HIV prophylaxis in breastfeeding infants., Antimicrob. Agents Chemother. 59 (2015) 59–66. https://doi.org/10.1128/AAC.03906-14.

L.C. Costantini, The Development of ProNeura Technology for the Treatment of Addictions, in: Opiate Recept. Antagon., Humana Press, Totowa, NJ, 2009: pp. 689–708. https://doi.org/10.1007/978-1-59745-197-0_37.

A.J. Coury, P.C. Slaikeu, P.T. Cahalan, K.B. Stokes, C.M. Hobot, Factors and Interactions Affecting the Performance of Polyurethane Elastomers in Medical Devices, J. Biomater. Appl. 3 (1988) 130–179. https://doi.org/10.1177/088532828800300202.

J. Crank, The mathematics of diffusion, 2d ed, Clarendon Press, Oxford, [Eng], 1979.

C.J. Crnich, J.A. Halfmann, W.C. Crone, D.G. Maki, BS, W.C. Crone, P. and D.G. Maki, MD, The Effects of Prolonged Ethanol Exposure on the Mechanical Properties of Polyurethane and Silicone Catheters Used for Intravascular Access, Infect. Control Hosp. Epidemiol. 26 (2005) 708–714. https://doi.org/10.1086/502607.

B.S. Dave, A.F. Amin, M.M. Patel, Gastroretentive drug delivery system of ranitidine hydrochloride: Formulation and in vitro evaluation, AAPS PharmSciTech. 5 (2004) 77–82. https://doi.org/10.1208/pt050234.

S.S. Davis, E.A. Wilding, I.R. Wilding, Gastrointestinal transit of a matrix tablet formulation: comparison of canine and human data, Int. J. Pharm. 94 (1993) 235–238. https://doi.org/10.1016/0378-5173(93)90029-F.

S. Delany-Moretlwe, C. Lombard, D. Baron, L.-G. Bekker, B. Nkala, K. Ahmed, M. Sebe, W. Brumskine, M. Nchabeleng, T. Palanee-Philips, J. Ntshangase, S. Sibiya, E. Smith, R. Panchia, L. Myer, J.L. Schwartz, M. Marzinke, L. Morris, E.R. Brown, G.F. Doncel, G. Gray, H. Rees, Tenofovir 1% vaginal gel for prevention of HIV-1 infection in women in South Africa (FACTS-001): a phase 3, randomised, double-blind, placebo-controlled trial., Lancet. Infect. Dis. 18 (2018) 1241–1250. https://doi.org/10.1016/S1473-3099(18)30428-6.

S. Desai, S. Bolton, A Floating Controlled-Release Drug Delivery System: In Vitro-in Vivo Evaluation, Pharm. Res. 10 (1993) 1321–1325. https://doi.org/10.1023/A:1018921830385.

A.A. Deshpande, N.H. Shah, C.T. Rhodes, W. Malick, Development of a Novel Controlled-Release System for Gastric Retention, Pharm. Res. 14 (1997) 815–819. https://doi.org/10.1023/A:1012171010492.

S. Dhaliwal, S. Jain, H.P. Singh, A.K. Tiwary, Mucoadhesive Microspheres for Gastroretentive Delivery of Acyclovir: In Vitro and In Vivo Evaluation, AAPS J. 10 (2008) 322. https://doi.org/10.1208/s12248-008-9039-2.

G. DiBattista, H.W.I. Peerlings, W. Kaufhold, Aliphatic TPUs for light-stable applications, Rubber World. 227 (2003) 39–42.

T.O.. Dieben, F.J.M.. Roumen, D. Apter, Efficacy, cycle control, and user acceptability of a novel combined contraceptive vaginal ring, Obstet. Gynecol. 100 (2002) 585–593. https://doi.org/10.1016/S0029-7844(02)02124-5.

T. Dinh, R. Sparer, S. Lyu, K. Dang, C. Hobot, Active agent delivery systems including a miscible polymer blend, medical devices, and methods, US20050064005A1, 2003.

G. Donelli, I. Francolini, V. Ruggeri, E. Guaglianone, L. D'Ilario, A. Piozzi, Pore formers promoted release of an antifungal drug from functionalized polyurethanes to inhibit Candida colonization, J. Appl. Microbiol. 100 (2006) 615–622. https://doi.org/10.1111/j.1365-2672.2005.02801.x.

L.C. Dong, A.S. Hoffman, Q. Yan, Macromolecular penetration through hydrogels, J. Biomater. Sci. Polym. 5 (1994) 473–484.

J.B. Dressman, Comparison of Canine and Human Gastrointestinal Physiology,

Pharm. Res. 03 (1986) 123–131. https://doi.org/10.1023/A:1016353705970.

R.P. Durbin, H. Frank, A.K. Soloman, Water Flow Through Frog Gastric Mucosa, J. Gen. Physiol. 39 (1956) 535–551. https://doi.org/10.1085/jgp.39.4.535.

H.-W. Engels, H.-G. Pirkl, R. Albers, R.W. Albach, J. Krause, A. Hoffmann, H. Casselmann, J. Dormish, Polyurethanes: Versatile Materials and Sustainable Problem Solvers for Today's Challenges, Angew. Chemie Int. Ed. 52 (2013) 9422–9441. https://doi.org/10.1002/anie.201302766.

J.L. Fabregas, J. Claramunt, J. Cucala, R. Pous, A. Siles, "In-Vitro" Testing of an Antacid Formulation with Prolonged Gastric Residence Time (Almagate Flot-Coat®), Drug Dev. Ind. Pharm. 20 (1994) 1199–1212. https://doi.org/10.3109/03639049409038361.

E. Fields, Application Number: 022544Orig1s000 Cross Discipline Team Leader Review, 2010. https://www.accessdata.fda.gov/drugsatfda_docs/nda/2011/022544Orig1s000CrossR.pdf.

D.R. Friend, J.T. Clark, P.F. Kiser, M.R. Clark, Multipurpose prevention technologies: Products in development, Antiviral Res. 100 (2013) S39–S47. https://doi.org/10.1016/J.ANTIVIRAL.2013.09.030.

M.A. Frohoff-Hülsmann, A. Schmitz, B.C. Lippold, Aqueous ethyl cellulose dispersions containing plasticizers of different water solubility and hydroxypropyl methylcellulose as coating material for diffusion pellets: I. Drug release rates from coated pellets, Int. J. Pharm. 177 (1999) 69–82. https://doi.org/10.1016/S0378-5173(98)00327-5.

R. Fuller, H. Roth, S. Long, Compliance with disulfiram treatment of alcoholism, J. Chronic Dis. 36 (1983) 161–170. https://doi.org/10.1016/0021-9681(83)90090-5.

S.S. El Gamal, V.F. Naggar, A.N. Allam, Optimization of acyclovir oral tablets based on gastroretention technology: Factorial design analysis and physicochemical characterization studies, Drug Dev. Ind. Pharm. 37 (2011) 855–867. https://doi.org/10.3109/03639045.2010.546404.

G. Garbacz, S. Klein, W. Weitschies, A biorelevant dissolution stress test device – background and experiences, Expert Opin. Drug Deliv. 7 (2010) 1251–1261. https://doi.org/10.1517/17425247.2010.527943.

E.J. Garboczi, K.A. Snyder, J.F. Douglas, M.F. Thorpe, Geometrical percolation threshold of overlapping ellipsoids, Phys. Rev. E. 52 (1995) 819–828. https://doi.org/10.1103/PhysRevE.52.819.

M. Gisslén, V. Svedhem, L. Lindborg, L. Flamholc, H. Norrgren, S. Wendahl, M. Axelsson, A. Sönnerborg, Sweden, the first country to achieve the Joint

United Nations Programme on HIV/AIDS (UNAIDS)/World Health Organization (WHO) 90-90-90 continuum of HIV care targets, HIV Med. 18 (2017) 305–307. https://doi.org/10.1111/hiv.12431.

A. Go¨pferich, R. Langer, Modeling monomer release from bioerodible polymers, J. Control. Release. 33 (1995) 55–69. https://doi.org/10.1016/0168-3659(94)00064-2.

S. Gogolewski, Selected topics in biomedical polyurethanes. A review, Colloid Polym. Sci. 267 (1989) 757–785. https://doi.org/10.1007/BF01410115.

P. Gonzalez-Tello, F. Camacho, G. Blazquez, Density and Viscosity of Concentrated Aqueous Solutions of Polyethylene Glycol, J. Chem. Eng. Data. 39 (1994) 611–614. https://doi.org/10.1021/je00015a050.

K. Gorna, S. Gogolewski, Preparation, degradation, and calcification of biodegradable polyurethane foams for bone graft substitutes, J. Biomed. Mater. Res. 67A (2003) 813–827. https://doi.org/10.1002/jbm.a.10148.

K. Gorna, S. Gogolewski, The effect of gamma radiation on molecular stability and mechanical properties of biodegradable polyurethanes for medical applications, Polym. Degrad. Stab. 79 (2003) 465–474. https://doi.org/10.1016/S0141-3910(02)00362-2.

P.A. Gunatillake, D.J. Martin, G.F. Meijs, S.J. McCarthy, R. Adhikari, Designing Biostable Polyurethane Elastomers for Biomedical Implants, Aust. J. Chem. 56 (2003) 545–557. https://doi.org/10.1071/ch02168.

M. Gunawardana, M. Remedios-Chan, C.S. Miller, R. Fanter, F. Yang, M.A. Marzinke, C.W. Hendrix, M. Beliveau, J.A. Moss, T.J. Smith, M.M. Baum, Pharmacokinetics of Long-Acting Tenofovir Alafenamide (GS-7340) Subdermal Implant for HIV Prophylaxis, Antimicrob. Agents Chemother. 59 (2015) 3913–3919. https://doi.org/10.1128/aac.00656-15.

Q. Guo, P.T. Knight, P.T. Mather, Tailored drug release from biodegradable stent coatings based on hybrid polyurethanes, J. Control. Release. 137 (2009) 224–233. https://doi.org/10.1016/J.JCONREL.2009.04.016.

K.M. Gupta, S.M. Pearce, A.E. Poursaid, H.A. Aliyar, P.A. Tresco, M.A. Mitchnik, P.F. Kiser, Polyurethane Intravaginal Ring for Controlled Delivery of Dapivirine, a Nonnucleoside Reverse Transcriptase Inhibitor of HIV-1, J. Pharm. Sci. 97 (2008) 4228–4239. https://doi.org/10.1002/jps.21331.

M. Habash, G. Reid, Microbial Biofilms: Their Development and Significance for Medical Device-Related Infections, J. Clin. Pharmacol. 39 (1999) 887–898. https://doi.org/10.1177/00912709922008506.

A.E. Hafeman, B. Li, T. Yoshii, K. Zienkiewicz, J.M. Davidson, S.A. Guelcher,

Injectable Biodegradable Polyurethane Scaffolds with Release of Platelet-derived Growth Factor for Tissue Repair and Regeneration, Pharm. Res. 25 (2008) 2387–2399. https://doi.org/10.1007/s11095-008-9618-z.

A.E. Hafeman, K.J. Zienkiewicz, E. Carney, B. Litzner, C. Stratton, J.C. Wenke, S.A. Guelcher, Local Delivery of Tobramycin from Injectable Biodegradable Polyurethane Scaffolds, J. Biomater. Sci. Polym. Ed. 21 (2010) 95–112. https://doi.org/10.1163/156856209X410256.

M. Hanada, S. V. Jermain, X. Lu, Y. Su, R.O. Williams, Predicting physical stability of ternary amorphous solid dispersions using specific mechanical energy in a hot melt extrusion process, Int. J. Pharm. 548 (2018) 571–585. https://doi.org/10.1016/J.IJPHARM.2018.07.029.

C. Hansch, J.E. Quinlan, G.L. Lawrence, Linear free-energy relationship between partition coefficients and the aqueous solubility of organic liquids, J. Org. Chem. 33 (1968) 347–350. https://doi.org/10.1021/jo01265a071.

D. Harris, J.T. Fell, H.L. Sharma, D.C. Taylor, GI transit of potential bioadhesive formulations in man: A scintigraphic study, J. Control. Release. 12 (1990) 45–53. https://doi.org/10.1016/0168-3659(90)90182-S.

J.. Hay, M. Sabir, Crystallization kinetics of high polymers. Polyethylene oxide—Part II, Polymer (Guildf). 10 (1969) 203–211. https://doi.org/10.1016/0032-3861(69)90031-7.

M. He, G. Yang, S. Zhang, X. Zhao, Y. Gao, Dissolving Microneedles Loaded With Etonogestrel Microcrystal Particles for Intradermal Sustained Delivery, J. Pharm. Sci. 107 (2018) 1037–1045. https://doi.org/10.1016/J.XPHS.2017.11.013.

T. Higuchi, Mechanism of sustained-action medication. Theoretical analysis of rate of release of solid drugs dispersed in solid matrices, J. Pharm. Sci. 52 (1963) 1145–1149. https://doi.org/10.1002/jps.2600521210.

T. Higuchi, Mechanism of sustained-action medication. Theoretical analysis of rate of release of solid drugs dispersed in solid matrices, J. Pharm. Sci. 52 (1963) 1145–1149. https://doi.org/10.1002/jps.2600521210.

A.K. Hilton, P.B. Deasy, In vitro and in vivo evaluation of an oral sustained-release floating dosage form of amoxycillin trihydrate, Int. J. Pharm. 86 (1992) 79–88. https://doi.org/10.1016/0378-5173(92)90033-X.

A. Hoffman, D. Stepensky, E. Lavy, S. Eyal, E. Klausner, M. Friedman, Pharmacokinetic and pharmacodynamic aspects of gastroretentive dosage forms, Int. J. Pharm. 277 (2004) 141–153. https://doi.org/10.1016/J.IJPHARM.2003.09.047.

M. Hombreiro-Pérez, J. Siepmann, C. Zinutti, A. Lamprecht, N. Ubrich, M. Hoffman, R.

Bodmeier, P. Maincent, Non-degradable microparticles containing a hydrophilic and/or a lipophilic drug: preparation, characterization and drug release modeling, J. Control. Release. 88 (2003) 413–428. https://doi.org/10.1016/S0168-3659(03)00030-0.

M. Hombreiro-Pérez, J. Siepmann, C. Zinutti, A. Lamprecht, N. Ubrich, M. Hoffman, R. Bodmeier, P. Maincent, Non-degradable microparticles containing a hydrophilic and/or a lipophilic drug: preparation, characterization and drug release modeling, J. Control. Release. 88 (2003) 413–428. https://doi.org/10.1016/S0168-3659(03)00030-0.

R.I. Horwitz, S.M. Horwitz, Adherence to Treatment and Health Outcomes, Arch. Intern. Med. 153 (1993) 1863. https://doi.org/10.1001/archinte.1993.00410160017001.

R.I. Horwitz, C.M. Viscoli, R.M. Donaldson, C.J. Murray, D.F. Ransohoff, R.I. Horwitz, L. Berkman, S.M. Horwitz, D.F. Ransohoff, J. Sindelar, Treatment adherence and risk of death after a myocardial infarction, Lancet. 336 (1990) 542–545. https://doi.org/10.1016/0140-6736(90)92095-Y.

T.T.-P. Hsu, R. Langer, Polymers for the controlled release of macromolecules: Effect of molecular weight of ethylene-vinyl acetate copolymer, J. Biomed. Mater. Res. 19 (1985) 445–460. https://doi.org/10.1002/jbm.820190409.

M.A. Hussain, R.C. DiLuccio, E. Shefter, Hollow Fibers as an Oral Sustained-Release Delivery System, Pharm. Res. 06 (1989) 49–52. https://doi.org/10.1023/A:1015847618671.

M. Ichikawa, T. Kato, M. Kawahara, S. Watanabe, M. Kayano, A New Multiple-Unit Oral Floating Dosage System. II: In Vivo Evaluation of Floating and Sustained-Release Characteristics with p-Aminobenzoic Acid and Isosorbide Dinitrate as Model Drugs, J. Pharm. Sci. 80 (1991) 1153–1156. https://doi.org/10.1002/JPS.2600801212.

Y. Ikeda, S. Kohjiya, S. Takesako, S. Yamashita, Polyurethane elastomer with PEO-PTMO-PEO soft segment for sustained release of drugs, Biomaterials. 11 (1990) 553–560. https://doi.org/10.1016/0142-9612(90)90077-4.

Y. Ikeda, S. Kohjiya, S. Takesako, S. Yamashita, Polyurethane elastomer with PEO-PTMO-PEO soft segment for sustained release of drugs, Biomaterials. 11 (1990) 553–560. https://doi.org/10.1016/0142-9612(90)90077-4.

M. Irfan, A.R. Ahmed, K. Kolter, R. Bodmeier, A. Dashevskiy, Curing mechanism of flexible aqueous polymeric coatings, Eur. J. Pharm. Biopharm. 115 (2017) 186–196. https://doi.org/10.1016/J.EJPB.2017.02.012.

L. Irusta, M.J. Fernandez-Berridi, Aromatic poly(ester–urethanes): effect of the polyol molecular weight on the photochemical behaviour, Polymer (Guildf). 41 (2000)

3297–3302. https://doi.org/10.1016/S0032-3861(99)00548-0.

N. Islam, E. Gladki, Dry powder inhalers (DPIs)—A review of device reliability and innovation, Int. J. Pharm. 360 (2008) 1–11. https://doi.org/10.1016/J.IJPHARM.2008.04.044.

ISO, ISO 8009 Mechanical contraceptives — Reusable natural and silicone rubber contraceptive diaphragms — Requirements and tests, ISO Stand. 2014 (2014). www.iso.org (accessed February 27, 2018).

D.A. Ivanov, Z. Amalou, S.N. Magonov, Real-time evolution of the lamellar organization of poly(ethylene terephthalate) during crystallization from the melt: High-temperature atomic force microscopy study, Macromolecules. 34 (2001) 8944–8952. https://doi.org/10.1021/ma010809b.

E. Jabbari, M. Khakpour, Morphology of and release behavior from porous polyurethane microspheres, Biomaterials. 21 (2000) 2073–2079. https://doi.org/10.1016/S0142-9612(00)00135-6.

S.J. Jackson, D. Bush, A.C. Perkins, Comparative scintigraphic assessment of the intragastric distribution and residence of cholestyramine, Carbopol 934P and sucralfate, Int. J. Pharm. 212 (2001) 55–62. https://doi.org/10.1016/S0378-5173(00)00600-1.

S.C. Jagdale, A.J. Agavekar, S. V. Pandya, B.S. Kuchekar, A.R. Chabukswar, Formulation and Evaluation of Gastroretentive Drug Delivery System of Propranolol Hydrochloride, AAPS PharmSciTech. 10 (2009) 1071. https://doi.org/10.1208/s12249-009-9300-8.

S.-F. Jang, B.A. Goins, W.T. Phillips, C. Santoyo, A. Rice-Ficht, J.T. McConville, Size discrimination in rat and mouse gastric emptying, Biopharm. Drug Dispos. 34 (2013) 107–124. https://doi.org/10.1002/bdd.1828.

T.J. Johnson, M.R. Clark, T.H. Albright, J.S. Nebeker, A.L. Tuitupou, J.T. Clark, J. Fabian, R.T. McCabe, N. Chandra, G.F. Doncel, D.R. Friend, P.F. Kiser, A 90-day tenofovir reservoir intravaginal ring for mucosal HIV prophylaxis., Antimicrob. Agents Chemother. 56 (2012) 6272–83. https://doi.org/10.1128/AAC.01431-12.

T.J. Johnson, K.M. Gupta, J. Fabian, T.H. Albright, P.F. Kiser, Segmented polyurethane intravaginal rings for the sustained combined delivery of antiretroviral agents dapivirine and tenofovir, Eur. J. Pharm. Sci. 39 (2010) 203–212. https://doi.org/10.1016/J.EJPS.2009.11.007.

K. Kääriä, A. Hirvonen, H. Norppa, P. Piirilä, H. Vainio, C. Rosenberg, Exposure to 4,4′-methylenediphenyl diisocyanate (MDI) during moulding of rigid polyurethane foam: determination of airborne MDI and urinary 4,4′-methylenedianiline (MDA), Analyst. 126 (2001) 476–479. https://doi.org/10.1039/B009549O.

M. Kamba, Y. Seta, A. Kusai, M. Ikeda, K. Nishimura, A unique dosage form to evaluate the mechanical destructive force in the gastrointestinal tract, Int. J. Pharm. 208 (2000) 61–70. https://doi.org/10.1016/S0378-5173(00)00552-4.

J.M. Kane, M. Eerdekens, J.-P. Lindenmayer, S.J. Keith, M. Lesem, K. Karcher, Long-Acting Injectable Risperidone: Efficacy and Safety of the First Long-Acting Atypical Antipsychotic, Am. J. Psychiatry. 160 (2003) 1125–1132. https://doi.org/10.1176/appi.ajp.160.6.1125.

T.T. Kararli, Comparison of the gastrointestinal anatomy, physiology, and biochemistry of humans and commonly used laboratory animals, Biopharm. Drug Dispos. 16 (1995) 351–380. https://doi.org/10.1002/bdd.2510160502.

M. Kaur, K.M. Gupta, A.E. Poursaid, P. Karra, A. Mahalingam, H.A. Aliyar, P.F. Kiser, Engineering a degradable polyurethane intravaginal ring for sustained delivery of dapivirine, Drug Deliv. Transl. Res. 1 (2011) 223–237. https://doi.org/10.1007/s13346-011-0027-1.

A.D. Keet, Diameter of the pyloric aperture in relation to the contraction of the canalis egestorius, Acta Radiol. 57 (1962) 31–44. https://doi.org/10.3109/00016926209171725.

M.J. Keller, P.M. Mesquita, M.A. Marzinke, R. Teller, L. Espinoza, J.M. Atrio, Y. Lo, B. Frank, S. Srinivasan, D.N. Fredricks, L. Rabe, P.L. Anderson, C.W. Hendrix, P.F. Kiser, B.C. Herold, A phase 1 randomized placebo-controlled safety and pharmacokinetic trial of a tenofovir disoproxil fumarate vaginal ring., AIDS. 30 (2016) 743–51. https://doi.org/10.1097/QAD.0000000000000979.

M.Z.I. Khan, Ž. Prebeg, N. Kurjaković, A pH-dependent colon targeted oral drug delivery system using methacrylic acid copolymers: I. Manipulation of drug release using Eudragit® L100-55 and Eudragit® S100 combinations, J. Control. Release. 58 (1999) 215–222. https://doi.org/10.1016/S0168-3659(98)00151-5.

R. Khosla, S.S. Davis, The effect of polycarbophil on the gastric emptying of pellets, J. Pharm. Pharmacol. 39 (1987) 47–49. https://doi.org/10.1111/j.2042-7158.1987.tb07161.x.

J.-E. Kim, S.-R. Kim, S.-H. Lee, C.-H. Lee, D.-D. Kim, The effect of pore formers on the controlled release of cefadroxil from a polyurethane matrix, Int. J. Pharm. 201 (2000) 29–36. https://doi.org/10.1016/S0378-5173(00)00388-4.

K.J. Kim, E.D. Crandall, Heteropore populations of bullfrog alveolar epithelium., J. Appl. Physiol. 54 (1983) 140–6. https://doi.org/10.1152/jappl.1983.54.1.140.

A.R. Kirtane, O. Abouzid, D. Minahan, T. Bensel, A.L. Hill, C. Selinger, A. Bershteyn, M. Craig, S.S. Mo, H. Mazdiyasni, C. Cleveland, J. Rogner, Y.-A.L. Lee, L. Booth, F. Javid, S.J. Wu, T. Grant, A.M. Bellinger, B. Nikolic, A. Hayward, L. Wood, P.A. Eckhoff, M.A. Nowak, R. Langer, G. Traverso, Development of an

oral once-weekly drug delivery system for HIV antiretroviral therapy, Nat. Commun. 9 (2018) 2. https://doi.org/10.1038/s41467-017-02294-6.

R. Kjellander, E. Florin, Water structure and changes in thermal stability of the system poly(ethylene oxide)–water, J. Chem. Soc. Faraday Trans. 1 Phys. Chem. Condens. Phases. 77 (1981) 2053. https://doi.org/10.1039/f19817702053.

E.A. Klausner, E. Lavy, D. Stepensky, M. Friedman, A. Hoffman, Novel Gastroretentive Dosage Forms: Evaluation of Gastroretentivity and Its Effect on Riboflavin Absorption in Dogs, Pharm. Res. 19 (2002) 1516–1523. https://doi.org/10.1023/A:1020412817716.

L.W. Kleiner, R.M. Gale, R.G. Berggren, G.T. Tong, G. Chen, K.E. Dionne, P.R. Houston, Rate controlling membranes for controlled drug delivery devices, US6375978B1, 1997. https://patents.google.com/patent/US6375978B1/en (accessed September 17, 2018).

S. Koetsawang, J. Gao, U. Krishna, A. Cuadros, G.I. Dhall, R. Wyss, J.R. la Puenta, A.T.L. Andrade, T. Khan, E.S. Kononova, J.P. Lawson, U. Parekh, M. Elstein, V. Hingorani, N. Wang, Z. Yao, B.-M. Landgren, R. Boukhris, L. Lo, S. Boccard, D. Machin, A. Pinol, P.J. Rowe, Microdose intravaginal levonorgestrel contraception: A multicentre clinical trial, Contraception. 41 (1990) 125–141. https://doi.org/10.1016/0010-7824(90)90142-I.

F. Kong, R.P. Singh, A Human Gastric Simulator (HGS) to Study Food Digestion in Human Stomach, J. Food Sci. 75 (2010) E627–E635. https://doi.org/10.1111/j.1750-3841.2010.01856.x.

Y. Kong, J.N. Hay, The measurement of the crystallinity of polymers by DSC, Polymer (Guildf). 43 (2002) 3873–3878. https://doi.org/10.1016/S0032-3861(02)00235-5.

E.S. Kostewicz, B. Abrahamsson, M. Brewster, J. Brouwers, J. Butler, S. Carlert, P.A. Dickinson, J. Dressman, R. Holm, S. Klein, J. Mann, M. McAllister, M. Minekus, U. Muenster, A. Müllertz, M. Verwei, M. Vertzoni, W. Weitschies, P. Augustijns, In vitro models for the prediction of in vivo performance of oral dosage forms, Eur. J. Pharm. Sci. 57 (2014) 342–366. https://doi.org/10.1016/J.EJPS.2013.08.024.

M. Koziolek, G. Garbacz, M. Neumann, W. Weitschies, Simulating the Postprandial Stomach: Biorelevant Test Methods for the Estimation of Intragastric Drug Dissolution, Mol. Pharm. 10 (2013) 2211–2221. https://doi.org/10.1021/mp300607e.

M. Koziolek, K. Görke, M. Neumann, G. Garbacz, W. Weitschies, Development of a bio-relevant dissolution test device simulating mechanical aspects present in the fed stomach, Eur. J. Pharm. Sci. 57 (2014) 250–256.

https://doi.org/10.1016/J.EJPS.2013.09.004.

K. Krätschmer, Medicinal Chemistry In The Framework Of Hormonal And Non-Hormonal Contraception, Org. Med. Chem. Int. J. 3 (2017). https://doi.org/10.19080/OMCIJ.2017.03.555612.

H.R. Kricheldorf, R.P. Quirk, G. Holden, Thermoplastic elastomers, Hanser Gardner Publications, Munich, Germany, 2004.

R.P. Kusy, Influence of particle size ratio on the continuity of aggregates, J. Appl. Phys. 48 (1977) 5301–5305. https://doi.org/10.1063/1.323560.

J.A.. van Laarhoven, M.A.. Kruft, H. Vromans, In vitro release properties of etonogestrel and ethinyl estradiol from a contraceptive vaginal ring, Int. J. Pharm. 232 (2002) 163–173. https://doi.org/10.1016/S0378-5173(01)00900-0.

A.K. Lalloo, E.L. McConnell, L. Jin, R. Elkes, C. Seiler, Y. Wu, Decoupling the role of image size and calorie intake on gastric retention of swelling-based gastric retentive formulations: Pre-screening in the dog model, Int. J. Pharm. 431 (2012) 90–100. https://doi.org/10.1016/J.IJPHARM.2012.04.044.

N.M.K. Lamba, K.A. Woodhouse, S.L. Cooper, Polyurethanes in biomedical applications, CRC press, Boca Raton, FL, USA, 1997.

R. LANGER, J. FOLKMAN, Polymers for the sustained release of proteins and other macromolecules, Nature. 263 (1976) 797–800. https://doi.org/10.1038/263797a0.

R. Langer, N. Peppas, Chemical and Physical Structure of Polymers as Carriers for Controlled Release of Bioactive Agents: A Review, J. Macromol. Sci. Part C. 23 (1983) 61–126. https://doi.org/10.1080/07366578308079439.

B. Laulicht, A. Tripathi, V. Schlageter, P. Kucera, E. Mathiowitz, Understanding gastric forces calculated from high-resolution pill tracking., Proc. Natl. Acad. Sci. U. S. A. 107 (2010) 8201–6. https://doi.org/10.1073/pnas.1002292107.

J. Lazarus, M. Pagliery, L. Lachman, Factors Influencing the Release of a Drug from a Prolonged-Action Matrix, J. Pharm. Sci. 53 (1964) 798–802. https://doi.org/10.1002/jps.2600530722.

F. Lecomte, J. Siepmann, M. Walther, R.. MacRae, R. Bodmeier, Blends of enteric and GIT-insoluble polymers used for film coating: physicochemical characterization and drug release patterns, J. Control. Release. 89 (2003) 457–471. https://doi.org/10.1016/S0168-3659(03)00155-X.

F. Lecomte, J. Siepmann, M. Walther, R.J. MacRae, R. Bodmeier, Polymer Blends Used for the Coating of Multiparticulates: Comparison of Aqueous and Organic Coating Techniques, Pharm. Res. 21 (2004) 882–890. https://doi.org/10.1023/B:PHAM.0000026443.71935.cb.

G. Levy, W.J. Jusko, Factors Affecting the Absorption of Riboflavin in Man, J. Pharm. Sci. 55 (1966) 285–289. https://doi.org/10.1002/JPS.2600550305.

B. Li, K. V. Brown, J.C. Wenke, S.A. Guelcher, Sustained release of vancomycin from polyurethane scaffolds inhibits infection of bone wounds in a rat femoral segmental defect model, J. Control. Release. 145 (2010) 221–230. https://doi.org/10.1016/J.JCONREL.2010.04.002.

B. Li, T. Yoshii, A.E. Hafeman, J.S. Nyman, J.C. Wenke, S.A. Guelcher, The effects of rhBMP-2 released from biodegradable polyurethane/microsphere composite scaffolds on new bone formation in rat femora, Biomaterials. 30 (2009) 6768–6779. https://doi.org/10.1016/J.BIOMATERIALS.2009.08.038.

W.R. Lieb, W.D. Stein, Implications of two different types of diffusion for biological membranes, Nat. New Biol. 234 (1971) 220–222. https://doi.org/10.1038/newbio234220a0.

J.H. Lin, Bisphosphonates: A review of their pharmacokinetic properties, Bone. 18 (1996) 75–85. https://doi.org/10.1016/8756-3282(95)00445-9.

T. Lindholm, B.-Å. Lindholm, M. Niskanen, J. Koskiniemi, Polysorbate 20 as a drug release regulator in ethyl cellulose film coatings, J. Pharm. Pharmacol. 38 (1986) 686–688. https://doi.org/10.1111/j.2042-7158.1986.tb03110.x.

H. Liu, W. Pan, P. Ke, Y. Dong, L. Ji, Preparation and evaluation of a novel gastric mucoadhesive sustained-release acyclovir microsphere, Drug Dev. Ind. Pharm. 36 (2010) 1098–1105. https://doi.org/10.3109/03639041003677780.

H. Liu, P. Wang, X. Zhang, F. Shen, C.G. Gogos, Effects of extrusion process parameters on the dissolution behavior of indomethacin in Eudragit® E PO solid dispersions, Int. J. Pharm. 383 (2010) 161–169. https://doi.org/10.1016/J.IJPHARM.2009.09.003.

Q. Liu, R. Fassihi, Zero-order delivery of a highly soluble, low dose drug alfuzosin hydrochloride via gastro-retentive system, Int. J. Pharm. 348 (2008) 27–34. https://doi.org/10.1016/J.IJPHARM.2007.07.009.

M.B. Lowinger, S.E. Barrett, F. Zhang, R.O. Williams, Sustained Release Drug Delivery Applications of Polyurethanes, Pharmaceutics. 10 (2018) 55. https://doi.org/10.3390/pharmaceutics10020055.

M.B. Lowinger, J.D. Ormes, Y. Su, J.H. Small, R.O. Williams, F. Zhang, How broadly can poly(urethane)-based implants be applied to drugs of varied properties?, Int. J. Pharm. 568 (2019) 118550. https://doi.org/10.1016/J.IJPHARM.2019.118550.

M.B. Lowinger, Y. Su, X. Lu, R.O. Williams, F. Zhang, Can drug release rate from implants be tailored using poly(urethane) mixtures?, Int. J. Pharm. 557 (2019) 390–401. https://doi.org/10.1016/j.ijpharm.2018.11.067.

S.J. Lue, D.-T. Lee, J.-Y. Chen, C.-H. Chiu, C.-C. Hu, Y.C. Jean, J.-Y. Lai, Diffusivity enhancement of water vapor in poly(vinyl alcohol)–fumed silica nano-composite membranes: Correlation with polymer crystallinity and free-volume properties, J. Memb. Sci. 325 (2008) 831–839. https://doi.org/10.1016/J.MEMSCI.2008.09.015.

S.-P. Lyu, R. Sparer, C. Hobot, K. Dang, Adjusting drug diffusivity using miscible polymer blends, J. Control. Release. 102 (2005) 679–687. https://doi.org/10.1016/J.JCONREL.2004.11.007.

L. Marciani, P.A. Gowland, A. Fillery-Travis, P. Manoj, J. Wright, A. Smith, P. Young, R. Moore, R.C. Spiller, Assessment of antral grinding of a model solid meal with echo-planar imaging, Am. J. Physiol. Liver Physiol. 280 (2001) G844–G849. https://doi.org/10.1152/ajpgi.2001.280.5.G844.

M. Markowitz, S.G. Sarafianos, 4′-Ethynyl-2-fluoro-2′-deoxyadenosine, MK-8591, Curr. Opin. HIV AIDS. 13 (2018) 294–299. https://doi.org/10.1097/COH.0000000000000467.

A. Martinelli, L. D'Ilario, I. Francolini, A. Piozzi, Water state effect on drug release from an antibiotic loaded polyurethane matrix containing albumin nanoparticles, Int. J. Pharm. 407 (2011) 197–206. https://doi.org/10.1016/J.IJPHARM.2011.01.029.

L.K. Massey, The effects of sterilization methods on plastics and elastomers : the definitive user's guide and databook, William Andrew Pub, Norwich, NY, USA, 2005.

R.S. Matharu, N.M. Sanghavi, Novel drug delivery system for captopril, Drug Dev. Ind. Pharm. 18 (1992) 1567–1574. https://doi.org/10.3109/03639049209040859.

Y. Matsukawa, V.H.L. Lee, E.D. Crandall, K.-J. Kim, Size-Dependent Dextran Transport across Rat Alveolar Epithelial Cell Monolayers, J. Pharm. Sci. 86 (1997) 305–309. https://doi.org/10.1021/JS960352X.

R. McGovern, J.S. Barkin, R.I. Goldberg, R.S. Phillips, Duodenal obstruction: a complication of percutaneous endoscopic gastrostomy tube migration., Am. J. Gastroenterol. 85 (1990) 1037–8. http://www.ncbi.nlm.nih.gov/pubmed/2197857 (accessed October 11, 2019).

M.A. Mensink, M.J. Nethercott, W.L.J. Hinrichs, K. van der Voort Maarschalk, H.W. Frijlink, E.J. Munson, M.J. Pikal, Influence of Miscibility of Protein-Sugar Lyophilizates on Their Storage Stability, AAPS J. 18 (2016) 1225–1232. https://doi.org/10.1208/s12248-016-9937-7.

P.M.M. Mesquita, R. Rastogi, T.J. Segarra, R.S. Teller, N.M. Torres, A.M. Huber, P.F. Kiser, B.C. Herold, Intravaginal ring delivery of tenofovir disoproxil fumarate

for prevention of HIV and herpes simplex virus infection, J. Antimicrob. Chemother. 67 (2012) 1730–1738. https://doi.org/10.1093/jac/dks097.

H. Minami, R.W. Mccallum, The Physiology and Pathophysiology of Gastric Emptying in Humans, Gastroenterology. 86 (1984) 1592–1610. https://doi.org/10.1016/S0016-5085(84)80178-X.

K.K. Mohanty, J.M. Ottino, H.T. Davis, Reaction and transport in disordered composite media: Introduction of percolation concepts, Chem. Eng. Sci. 37 (1982) 905–924. https://doi.org/10.1016/0009-2509(82)80179-6.

K.F. Morris, C.S. Johnson, Diffusion-ordered two-dimensional nuclear magnetic resonance spectroscopy, J. Am. Chem. Soc. 114 (1992) 3139–3141. https://doi.org/10.1021/ja00034a071.

K. Morrow Guthrie, S. Vargas, J.G. Shaw, R.K. Rosen, J.J. van den Berg, P.F. Kiser, K. Buckheit, D. Bregman, L. Thompson, K. Jensen, T. Johnson, R.W. Buckheit, The Promise of Intravaginal Rings for Prevention: User Perceptions of Biomechanical Properties and Implications for Prevention Product Development, PLoS One. 10 (2015) e0145642. https://doi.org/10.1371/journal.pone.0145642.

S.A.L. Moura, L.D.C. Lima, S.P. Andrade, A. Da Silva-Cunha Junior, R.L. Órefice, E. Ayres, G.R. Da Silva, Local Drug Delivery System: Inhibition of Inflammatory Angiogenesis in a Murine Sponge Model by Dexamethasone-Loaded Polyurethane Implants, J. Pharm. Sci. 100 (2011) 2886–2895. https://doi.org/10.1002/jps.22497.

T.M.. Mulders, T.O.. Dieben, Use of the novel combined contraceptive vaginal ring NuvaRing for ovulation inhibition, Fertil. Steril. 75 (2001) 865–870. https://doi.org/10.1016/S0015-0282(01)01689-2.

J.F. Munk, R.M. Gannaway, M. Hoare, A.G. Johnson, Direct measurement of pyloric diameter and tone in man and their response to cholecystokinin, in: Gastrointest. Motil. Heal. Dis., Springer Netherlands, Dordrecht, 1978: pp. 349–359. https://doi.org/10.1007/978-94-017-4389-1_38.

C. Murphy, V. Pillay, Y.E. Choonara, L.C. du Toit, V.M.K. Ndesendo, N. Chirwa, P. Kumar, Optimization of a Dual Mechanism Gastrofloatable and Gastroadhesive Delivery System for Narrow Absorption Window Drugs, AAPS PharmSciTech. 13 (2012) 1–15. https://doi.org/10.1208/s12249-011-9711-1.

M.R. Nabid, I. Omrani, Facile preparation of pH-responsive polyurethane nanocarrier for oral delivery, Mater. Sci. Eng. C. 69 (2016) 532–537. https://doi.org/10.1016/J.MSEC.2016.07.017.

J.B. Nachega, M. Hislop, D.W. Dowdy, R.E. Chaisson, L. Regensberg, G. Maartens, Adherence to Nonnucleoside Reverse Transcriptase Inhibitor–Based HIV Therapy and Virologic Outcomes, Ann. Intern. Med. 146 (2007) 564. https://doi.org/10.7326/0003-4819-146-8-200704170-00007.

J.B. Nachega, V.C. Marconi, G.U. van Zyl, E.M. Gardner, W. Preiser, S.Y. Hong, E.J. Mills, R. Gross, HIV treatment adherence, drug resistance, virologic failure: evolving concepts., Infect. Disord. Drug Targets. 11 (2011) 167–74. http://www.ncbi.nlm.nih.gov/pubmed/21406048 (accessed September 4, 2018).

S. Narisawa, M. Nagata, C. Danyoshi, H. Yoshino, K. Murata, Y. Hirakawa, K. Noda, An Organic Acid-Induced Sigmoidal Release System for Oral Controlled-Release Preparations, Pharm. Res. 11 (1994) 111–116. https://doi.org/10.1023/A:1018910114436.

L.E. Nielsen, Models for the Permeability of Filled Polymer Systems, J. Macromol. Sci. Part A - Chem. 1 (1967) 929–942. https://doi.org/10.1080/10601326708053745.

H. Omidian, K. Park, J.G. Rocca, Recent developments in superporous hydrogels, J. Pharm. Pharmacol. 59 (2007) 317–327. https://doi.org/10.1211/jpp.59.3.0001.

C.H. van Os, M.D. de Jong, J.F.G. Slegers, Dimensions of polar pathways through rabbit gallbladder epithelium, J. Membr. Biol. 15 (1974) 363–382. https://doi.org/10.1007/BF01870095.

M. Oth, M. Franz, J. Timmermans, A. Möes, The Bilayer Floating Capsule: A Stomach-Directed Drug Delivery System for Misoprostol, Pharm. Res. 09 (1992) 298–302. https://doi.org/10.1023/A:1015870314340.

N. Özdemir, S. Ordu, Y. Özkan, Studies of Floating Dosage Forms of Furosemide: In Vitro and In Vivo Evaluations of Bilayer Tablet Formulations, Drug Dev. Ind. Pharm. 26 (2000) 857–866. https://doi.org/10.1081/DDC-100101309.

S. Palomba, A. Falbo, A. Di Cello, C. Materazzo, F. Zullo, Nexplanon: The new implant for long-term contraception. A comprehensive descriptive review, Gynecol. Endocrinol. 28 (2012) 710–721. https://doi.org/10.3109/09513590.2011.652247.

S. Pandey, P. Jirwankar, S. Mehta, S. Pandit, P. Tripathi, A. Patil, Formulation and Evaluation of Bilayered Gastroretentable Mucoadhesive Patch for Stomach-Specific Drug Delivery, (n.d.). https://www.ingentaconnect.com/content/ben/cdd/2013/00000010/00000004/art00002# (accessed August 26, 2019).

G. Park, Z. Shao, A.K. Mitra, Acyclovir Permeation Enhancement Across Intestinal and Nasal Mucosae by Bile Salt-Acylcarnitine Mixed Micelles, Pharm. Res. 09 (1992) 1262–1267. https://doi.org/10.1023/A:1015845031488.

H. Park, K. Park, D. Kim, Preparation and swelling behavior of chitosan-based superporous hydrogels for gastric retention application, J. Biomed. Mater. Res. Part A. 76A (2006) 144–150. https://doi.org/10.1002/jbm.a.30533.

K. Park, J.R. Robinson, Bioadhesive polymers as platforms for oral-controlled drug delivery: method to study bioadhesion, Int. J. Pharm. 19 (1984) 107–127.

https://doi.org/10.1016/0378-5173(84)90154-6.

H.P. Parkman, M.P. Jones, Tests of Gastric Neuromuscular Function, Gastroenterology. 136 (2009) 1526–1543. https://doi.org/10.1053/J.GASTRO.2009.02.039.

R.A. Patel, L.R. Bucalo, Implantable polymeric device for sustained release of buprenorphine, US7736665B2, 2002. https://patents.google.com/patent/US20040033250A1/en?assignee=titan+pharmaceuticals&oq=titan+pharmaceuticals (accessed September 17, 2018).

S. Patil, G.S. Talele, Gastroretentive mucoadhesive tablet of lafutidine for controlled release and enhanced bioavailability, Drug Deliv. 22 (2015) 312–319. https://doi.org/10.3109/10717544.2013.877099.

S.H. Perry, P. Swamy, G.A. Preidis, A. Mwanyumba, N. Motsa, H.N. Sarero, Implementing the Jadelle implant for women living with HIV in a resource-limited setting, AIDS. 28 (2014) 791–793. https://doi.org/10.1097/QAD.0000000000000177.

T. Peters-Strickland, L. Pestreich, A. Hatch, S. Rohatagi, R.A. Baker, J.P. Docherty, L. Markovtsova, P. Raja, P.J. Weiden, D.P. Walling, Usability of a novel digital medicine system in adults with schizophrenia treated with sensor-embedded tablets of aripiprazole., Neuropsychiatr. Dis. Treat. 12 (2016) 2587–2594. https://doi.org/10.2147/NDT.S116029.

P.A. Pizzo, K.J. Robichaud, B.K. Edwards, C. Schumaker, B.S. Kramer, A. Johnson, Oral antibiotic prophylaxis in patients with cancer: A double-blind randomized placebo-controlled trial, J. Pediatr. 102 (1983) 125–133. https://doi.org/10.1016/S0022-3476(83)80310-2.

L. Polo Fonseca, R.B. Trinca, M.I. Felisberti, Amphiphilic polyurethane hydrogels as smart carriers for acidic hydrophobic drugs, Int. J. Pharm. 546 (2018) 106–114. https://doi.org/10.1016/J.IJPHARM.2018.05.034.

H.S. Purohit, J.D. Ormes, S. Saboo, Y. Su, M.S. Lamm, A.K.P. Mann, L.S. Taylor, Insights into Nano- and Micron-Scale Phase Separation in Amorphous Solid Dispersions Using Fluorescence-Based Techniques in Combination with Solid State Nuclear Magnetic Resonance Spectroscopy, Pharm. Res. 34 (2017) 1364–1377. https://doi.org/10.1007/s11095-017-2145-z.

T.T. Reddy, M. Hadano, A. Takahara, Controlled Release of Model Drug from Biodegradable Segmented Polyurethane Ureas: Morphological and Structural Features, Macromol. Symp. 242 (2006) 241–249. https://doi.org/10.1002/masy.200651033.

E.M. Renkin, Filtration, diffusion, and molecular sieving through porous cellulose membranes., J. Gen. Physiol. 38 (1954) 225–243.

https://doi.org/10.1085/JGP.38.2.225.

P.L. Ritger, N.A. Peppas, A simple equation for description of solute release II. Fickian and anomalous release from swellable devices, J. Control. Release. 5 (1987) 37–42. https://doi.org/10.1016/0168-3659(87)90035-6.

J. Rosenblatt, I. Raad, Antimicrobial catheters, US20160074560A1, 2013. https://patents.google.com/patent/US20160074560A1/en?q=polyurethane&q=tecophilic&q=tecoflex&q=blends&oq=polyurethane+tecophilic+tecoflex+blends (accessed September 17, 2018).

M. Ruhnek-Forsbeck, E. Sandström, B. Andersoon, G. Eriksson, K. Hersle, G.-B. Lövhagen, H. Mobacken, L. Hillström, L. Svensson, Treatment of recurrent genital herpes simplex infections with oral acyclovir, J. Antimicrob. Chemother. 16 (1985) 621–628. https://doi.org/10.1093/jac/16.5.621.

R. Ruiz-Caro, M. Gago-Guillan, F.J. Otero-Espinar, M.D. Veiga, Mucoadhesive Tablets for Controlled Release of Acyclovir, Chem. Pharm. Bull. 60 (2012) 1249–1257. https://doi.org/10.1248/cpb.c12-00324.

J. Rychlý, A. Lattuati-Derieux, B. Lavédrine, L. Matisová-Rychlá, M. Malíková, K. Csomorová, I. Janigová, Assessing the progress of degradation in polyurethanes by chemiluminescence and thermal analysis. II. Flexible polyether- and polyester-type polyurethane foams, Polym. Degrad. Stab. 96 (2011) 462–469. https://doi.org/10.1016/j.polymdegradstab.2011.01.012.

B. Saad, T.D. Hirt, M. Welti, G.K. Uhlschmid, P. Neuenschwander, U.W. Suter, Development of degradable polyesterurethanes for medical applications: In vitro and in vivo evaluations, J. Biomed. Mater. Res. 36 (1997) 65–74. https://doi.org/10.1002/(SICI)1097-4636(199707)36:1<65::AID-JBM8>3.0.CO;2-J.

L.L. Sabin, M. Bachman DeSilva, C.J. Gill, L. Zhong, T. Vian, W. Xie, F. Cheng, K. Xu, G. Lan, J.E. Haberer, D.R. Bangsberg, Y. Li, H. Lu, A.L. Gifford, Improving Adherence to Antiretroviral Therapy With Triggered Real-time Text Message Reminders: The China Adherence Through Technology Study., J. Acquir. Immune Defic. Syndr. 69 (2015) 551–9. https://doi.org/10.1097/QAI.0000000000000651.

A.L. Sarode, H. Sandhu, N. Shah, W. Malick, H. Zia, Hot melt extrusion (HME) for amorphous solid dispersions: Predictive tools for processing and impact of drug–polymer interactions on supersaturation, Eur. J. Pharm. Sci. 48 (2013) 371–384. https://doi.org/10.1016/J.EJPS.2012.12.012.

D. Sauer, A.B. Watts, L.B. Coots, W.C. Zheng, J.W. McGinity, Influence of polymeric subcoats on the drug release properties of tablets powder-coated with pre-plasticized Eudragit® L 100-55, Int. J. Pharm. 367 (2009) 20–28. https://doi.org/10.1016/J.IJPHARM.2008.09.020.

C. Schneider, R. Langer, D. Loveday, D. Hair, Applications of ethylene vinyl acetate copolymers (EVA) in drug delivery systems, J. Control. Release. 262 (2017) 284–295. https://doi.org/10.1016/J.JCONREL.2017.08.004.

F. Schneider, M. Hoppe, M. Koziolek, W. Weitschies, Influence of Postprandial Intragastric Pressures on Drug Release from Gastroretentive Dosage Forms, AAPS PharmSciTech. 19 (2018) 2843–2850. https://doi.org/10.1208/s12249-018-1022-3.

F. Schneider, M. Koziolek, W. Weitschies, In Vitro and In Vivo Test Methods for the Evaluation of Gastroretentive Dosage Forms, Pharmaceutics. 11 (2019) 416. https://doi.org/10.3390/pharmaceutics11080416.

E. Seo, K. Na, Polyurethane membrane with porous surface for controlled drug release in drug eluting stent, Biomater. Res. 18 (2014) 15. https://doi.org/10.1186/2055-7124-18-15.

P. Shah, V. Jogani, P. Mishra, A.K. Mishra, T. Bagchi, A. Misra, In Vitro Assessment of Acyclovir Permeation Across Cell Monolayers in the Presence of Absorption Enhancers, Drug Dev. Ind. Pharm. 34 (2008) 279–288. https://doi.org/10.1080/03639040701655952.

W.S.W. Shalaby, W.E. Blevins, K. Park, In vitro and in vivo studies of enzyme-digestible hydrogels for oral drug delivery, J. Control. Release. 19 (1992) 131–144. https://doi.org/10.1016/0168-3659(92)90071-X.

P.R. Sheth, J. Tossounian, The Hydrodynamically Balanced System (Hbs$^{TM}$): A Novel Drug Delivery System for Oral Use, Drug Dev. Ind. Pharm. 10 (1984) 313–339. https://doi.org/10.3109/03639048409064653.

M. Shoaib, A. Bahadur, S. Iqbal, M.S.U. Rahman, S. Ahmed, G. Shabir, M.A. Javaid, Relationship of hard segment concentration in polyurethane-urea elastomers with mechanical, thermal and drug release properties, J. Drug Deliv. Sci. Technol. 37 (2017) 88–96. https://doi.org/10.1016/J.JDDST.2016.12.003.

F. Siepmann, A. Hoffmann, B. Leclercq, B. Carlin, J. Siepmann, How to adjust desired drug release patterns from ethylcellulose-coated dosage forms, J. Control. Release. 119 (2007) 182–189. https://doi.org/10.1016/J.JCONREL.2007.02.003.

F. Siepmann, J. Siepmann, M. Walther, R.J. MacRae, R. Bodmeier, Blends of aqueous polymer dispersions used for pellet coating: Importance of the particle size, J. Control. Release. 105 (2005) 226–239. https://doi.org/10.1016/J.JCONREL.2005.03.028.

F. Siepmann, J. Siepmann, M. Walther, R.J. MacRae, R. Bodmeier, Polymer blends for controlled release coatings, J. Control. Release. 125 (2008) 1–15. https://doi.org/10.1016/J.JCONREL.2007.09.012.

J. Siepmann, N.A. Peppas, Hydrophilic Matrices for Controlled Drug Delivery: An

Improved Mathematical Model to Predict the Resulting Drug Release Kinetics (the "sequential Layer" Model), Pharm. Res. 17 (2000) 1290–1298. https://doi.org/10.1023/A:1026455822595.

J. Siepmann, F. Siepmann, Mathematical modeling of drug delivery, Int. J. Pharm. 364 (2008) 328–343. https://doi.org/10.1016/j.ijpharm.2008.09.004.

A. Simmons, J. Hyvarinen, L. Poole-Warren, The effect of sterilisation on a poly(dimethylsiloxane)/poly(hexamethylene oxide) mixed macrodiol-based polyurethane elastomer, Biomaterials. 27 (2006) 4484–4497. https://doi.org/10.1016/J.BIOMATERIALS.2006.04.017.

I. Sivin, L. Wan, S. Ranta, F. Alvarez, V. Brache, D.R. Mishell, P. Darney, A. Biswas, S. Diaz, O. Kiriwat, M.P. Anant, C. Klaisle, M. Pavez, J. Schechter, Levonorgestrel concentrations during 7 years of continuous use of Jadelle contraceptive implants, Contraception. 64 (2001) 43–49. https://doi.org/10.1016/S0010-7824(01)00226-8.

D.A. Smith, K. Beaumont, T.S. Maurer, L. Di, Relevance of Half-Life in Drug Design, J. Med. Chem. 61 (2018) 4273–4282. https://doi.org/10.1021/acs.jmedchem.7b00969.

J.M. Smith, R. Rastogi, R.S. Teller, P. Srinivasan, P.M.M. Mesquita, U. Nagaraja, J.M. McNicholl, R.M. Hendry, C.T. Dinh, A. Martin, B.C. Herold, P.F. Kiser, Intravaginal ring eluting tenofovir disoproxil fumarate completely protects macaques from multiple vaginal simian-HIV challenges., Proc. Natl. Acad. Sci. U. S. A. 110 (2013) 16145–50. https://doi.org/10.1073/pnas.1311355110.

J.M. Smith, P. Srinivasan, R.S. Teller, Y. Lo, C.T. Dinh, P.F. Kiser, B.C. Herold, Tenofovir disoproxil fumarate intravaginal ring protects high-dose depot medroxyprogesterone acetate-treated macaques from multiple SHIV exposures., J. Acquir. Immune Defic. Syndr. 68 (2015) 1–5. https://doi.org/10.1097/QAI.0000000000000402.

K.S. Soppimath, A.R. Kulkarni, T.M. Aminabhavi, Development of Hollow Microspheres as Floating Controlled-Release Systems for Cardiovascular Drugs: Preparation and Release Characteristics, Drug Dev. Ind. Pharm. 27 (2001) 507–515. https://doi.org/10.1081/DDC-100105175.

M.Z. Southard, L.J. Dias, K.J. Himmelstein, V.J. Stella, Experimental Determinations of Diffusion Coefficients in Dilute Aqueous Solution Using the Method of Hydrodynamic Stability, Pharm. Res. 08 (1991) 1489–1494. https://doi.org/10.1023/A:1015886131198.

W.R. Spreen, D.A. Margolis, J.C. Pottage, Jr., Long-acting injectable antiretrovirals for HIV treatment and prevention., Curr. Opin. HIV AIDS. 8 (2013) 565–71. https://doi.org/10.1097/COH.0000000000000002.

K. Sreenivasan, Effect of blending methyl ?-cyclodextrin on the release of hydrophobic hydrocortisone into water from polyurethane, J. Appl. Polym. Sci. 81 (2001) 520–522. https://doi.org/10.1002/app.1466.

S. Stewart, J. Domínguez-Robles, R. Donnelly, E. Larrañeta, S.A. Stewart, J. Domínguez-Robles, R.F. Donnelly, E. Larrañeta, Implantable Polymeric Drug Delivery Devices: Classification, Manufacture, Materials, and Clinical Applications, Polymers (Basel). 10 (2018) 1379. https://doi.org/10.3390/polym10121379.

K. Stokes, R. McVenes, J.M. Anderson, Polyurethane Elastomer Biostability, J. Biomater. Appl. 9 (1995) 321–354. https://doi.org/10.1177/088532829500900402.

H. Sugihara, Y. Matsui, H. Takeuchi, I. Wilding, A. Connor, K. Abe, A. Nishiura, Development of a gastric retentive system as a sustained-release formulation of pranlukast hydrate and its subsequent in vivo verification in human studies, Eur. J. Pharm. Sci. 53 (2014) 62–68. https://doi.org/10.1016/J.EJPS.2013.11.018.

M. Szycher, A.A. Siciliano, An Assessment of 2,4 TDA Formation from Surgitek Polyurethane Foam under Simulated Physiological Conditions, J. Biomater. Appl. 5 (1991) 323–336. https://doi.org/10.1177/088532829100500404.

P. Tallury, N. Alimohammadi, S. Kalachandra, Poly(ethylene-co-vinyl acetate) copolymer matrix for delivery of chlorhexidine and acyclovir drugs for use in the oral environment: effect of drug combination, copolymer composition and coating on the drug release rate., Dent. Mater. 23 (2007) 404–9. https://doi.org/10.1016/j.dental.2006.02.011.

R.S. Teller, D.C. Malaspina, R. Rastogi, J.T. Clark, I. Szleifer, P.F. Kiser, Controlling the hydration rate of a hydrophilic matrix in the core of an intravaginal ring determines antiretroviral release, J. Control. Release. 224 (2016) 176–183. https://doi.org/10.1016/J.JCONREL.2015.12.035.

D.G. Thompson, J.C. Osborn, E.M. Kober, J.R. Schoonover, Effects of hydrolysis-induced molecular weight changes on the phase separation of a polyester polyurethane, Polym. Degrad. Stab. 91 (2006) 3360–3370. https://doi.org/10.1016/j.polymdegradstab.2006.05.019.

C.J. Timmer, T.M.T. Mulders, Pharmacokinetics of Etonogestrel and Ethinylestradiol Released from a Combined Contraceptive Vaginal Ring, Clin. Pharmacokinet. 39 (2000) 233–242. https://doi.org/10.2165/00003088-200039030-00005.

P. Trande, A. Mussetto, V.G. Mirante, E. De Martinis, G. Olivetti, R.L. Conigliaro, E.A. De Micheli, Efficacy, Tolerance and Safety of New Intragastric Air-Filled Balloon (Heliosphere BAG) for Obesity: the Experience of 17 Cases, Obes. Surg. 20 (2010) 1227–1230. https://doi.org/10.1007/s11695-008-9786-2.

Y.L. Traore, Y. Chen, A.-M. Bernier, E.A. Ho, Impact of Hydroxychloroquine-Loaded Polyurethane Intravaginal Rings on Lactobacilli., Antimicrob. Agents Chemother. 59 (2015) 7680–6. https://doi.org/10.1128/AAC.01819-15.

C. Trezza, S.L. Ford, W. Spreen, R. Pan, S. Piscitelli, Formulation and pharmacology of long-acting cabotegravir., Curr. Opin. HIV AIDS. 10 (2015) 239–45. https://doi.org/10.1097/COH.0000000000000168.

C. Tuleu, C. Andrieux, P. Boy, J.. Chaumeil, Gastrointestinal transit of pellets in rats: effect of size and density, Int. J. Pharm. 180 (1999) 123–131. https://doi.org/10.1016/S0378-5173(98)00400-1.

S.R. Ugaonkar, J.T. Clark, L.B. English, T.J. Johnson, K.W. Buckheit, R.J. Bahde, D.H. Appella, R.W. Buckheit, P.F. Kiser, An Intravaginal Ring for the Simultaneous Delivery of an HIV-1 Maturation Inhibitor and Reverse-Transcriptase Inhibitor for Prophylaxis of HIV Transmission., J. Pharm. Sci. 104 (2015) 3426–39. https://doi.org/10.1002/jps.24551.

M. Vardakou, A. Mercuri, S.A. Barker, D.Q.M. Craig, R.M. Faulks, M.S.J. Wickham, Achieving Antral Grinding Forces in Biorelevant In Vitro Models: Comparing the USP Dissolution Apparatus II and the Dynamic Gastric Model with Human In Vivo Data, AAPS PharmSciTech. 12 (2011) 620–626. https://doi.org/10.1208/s12249-011-9616-z.

M.J. Vassallo, M. Camilleri, C.M. Prather, R.B. Hanson, G.M. Thomforde, Measurement of axial forces during emptying from the human stomach., Am. J. Physiol. 263 (1992) G230-9. https://doi.org/10.1152/ajpgi.1992.263.2.G230.

J.-M. Vergnaud, Controlled drug release of oral dosage forms, CRC Press, Boca Raton, FL, USA, 1993.

P. Vermette, H.J. Griesser, G. Laroche, R. editors Guidoin, Biomedical applications of polyurethanes, Landes Bioscience, Georgetown, TX, USA, 2001. https://publications.csiro.au/rpr/pub?list=BRO&pid=procite:fb236b1d-fec9-46ef-a84d-6b9f75888af5 (accessed February 20, 2018).

G. Verstraete, J. Van Renterghem, P.J. Van Bockstal, S. Kasmi, B.G. De Geest, T. De Beer, J.P. Remon, C. Vervaet, Hydrophilic thermoplastic polyurethanes for the manufacturing of highly dosed oral sustained release matrices via hot melt extrusion and injection molding, Int. J. Pharm. 506 (2016) 214–221. https://doi.org/10.1016/J.IJPHARM.2016.04.057.

G. Verstraete, L. Vandenbussche, S. Kasmi, L. Nuhn, D. Brouckaert, J. Van Renterghem, W. Grymonpré, V. Vanhoorne, T. Coenye, B.G. De Geest, T. De Beer, J.P. Remon, C. Vervaet, Thermoplastic polyurethane-based intravaginal rings for prophylaxis and treatment of (recurrent) bacterial vaginosis, Int. J. Pharm. 529 (2017) 218–226. https://doi.org/10.1016/J.IJPHARM.2017.06.076.

J.S. Vrentas, J.L. Duda, Diffusion in polymer—solvent systems. I. Reexamination of the free-volume theory, J. Polym. Sci. Polym. Phys. Ed. 15 (1977) 403–416. https://doi.org/10.1002/pol.1977.180150302.

J.S. Vrentas, J.L. Duda, Diffusion in polymer–solvent systems. II. A predictive theory for the dependence of diffusion coefficients on temperature, concentration, and molecular weight, J. Polym. Sci. Polym. Phys. Ed. 15 (1977) 417–439. https://doi.org/10.1002/pol.1977.180150303.

A. Wang, H. Gao, Y. Sun, Y. Sun, Y.-W. Yang, G. Wu, Y. Wang, Y. Fan, J. Ma, Temperature- and pH-responsive nanoparticles of biocompatible polyurethanes for doxorubicin delivery, Int. J. Pharm. 441 (2013) 30–39. https://doi.org/10.1016/J.IJPHARM.2012.12.021.

H. Wang, J.K. Keum, A. Hiltner, E. Baer, B. Freeman, A. Rozanski, A. Galeski, Confined crystallization of polyethylene oxide in nanolayer assemblies, Science (80-. ). 323 (2009) 757–760. https://doi.org/10.1126/science.1164601.

J. Wang, V. Yadav, A.L. Smart, S. Tajiri, A.W. Basit, Stability of peptide drugs in the colon, Eur. J. Pharm. Sci. 78 (2015) 31–36. https://doi.org/10.1016/J.EJPS.2015.06.018.

J. White, J. Bell, J.B. Saunders, P. Williamson, M. Makowska, A. Farquharson, K.L. Beebe, Open-label dose-finding trial of buprenorphine implants (Probuphine)® for treatment of heroin dependence, Drug Alcohol Depend. 103 (2009) 37–43. https://doi.org/10.1016/J.DRUGALCDEP.2009.03.008.

L. Whitehead, J.H. Collett, J.T. Fell, Amoxycillin release from a floating dosage form based on alginates, Int. J. Pharm. 210 (2000) 45–49. https://doi.org/10.1016/S0378-5173(00)00567-6.

L. Whitehead, J.T. Fell, J.H. Collett, H.L. Sharma, A.-M. Smith, Floating dosage forms: an in vivo study demonstrating prolonged gastric retention, J. Control. Release. 55 (1998) 3–12. https://doi.org/10.1016/S0168-3659(97)00266-6.

M.J. Wiggins, B. Wilkoff, J.M. Anderson, A. Hiltner, Biodegradation of polyether polyurethane inner insulation in bipolar pacemaker leads, J. Biomed. Mater. Res. 58 (2001) 302–307. https://doi.org/10.1002/1097-4636(2001)58:3<302::AID-JBM1021>3.0.CO;2-Y.

C.R. Wilke, P. Chang, Correlation of diffusion coefficients in dilute solutions, AIChE J. 1 (1955) 264–270. https://doi.org/10.1002/aic.690010222.

J.C. Wright, A.S. Hoffman, Historical Overview of Long Acting Injections and Implants, in: Long Act. Inject. Implant., Springer US, Boston, MA, 2012: pp. 11–24. https://doi.org/10.1007/978-1-4614-0554-2_2.

R.-R. Wu, H.-M. Kao, J.-C. Chiang, E.. Woo, Solid-state NMR studies on phase

behavior and motional mobility in binary blends of polystyrene and poly(cyclohexyl methacrylate), Polymer (Guildf). 43 (2002) 171–176. https://doi.org/10.1016/S0032-3861(01)00570-5.

L. Xu, L. Li, J. Huang, S. Yu, J. Wang, N. Li, Determination of the lipophilicity (log Po/w) of organic compounds by microemulsion liquid chromatography, J. Pharm. Biomed. Anal. 102 (2015) 409–416. https://doi.org/10.1016/J.JPBA.2014.09.037.

S.H. Yalkowsky, S.C. Valvani, Solubility and partitioning I: Solubility of nonelectrolytes in water, J. Pharm. Sci. 69 (1980) 912–922. https://doi.org/10.1002/jps.2600690814.

T. Yamaoka, Y. Makita, H. Sasatani, S.-I. Kim, Y. Kimura, Linear type azo-containing polyurethane as drug-coating material for colon-specific delivery: its properties, degradation behavior, and utilization for drug formulation, J. Control. Release. 66 (2000) 187–197. https://doi.org/10.1016/S0168-3659(99)00270-9.

F. Yang, Y. Su, J. Zhang, J. DiNunzio, A. Leone, C. Huang, C.D. Brown, Rheology Guided Rational Selection of Processing Temperature To Prepare Copovidone–Nifedipine Amorphous Solid Dispersions via Hot Melt Extrusion (HME), Mol. Pharm. 13 (2016) 3494–3505. https://doi.org/10.1021/acs.molpharmaceut.6b00516.

H. Yasuda, C.E. Lamaze, L.D. Ikenberry, Permeability of solutes through hydrated polymer membranes. Part I. Diffusion of sodium chloride, Die Makromol. Chemie. 118 (1968) 19–35. https://doi.org/10.1002/macp.1968.021180102.

E. Yilgör, E. Burgaz, E. Yurtsever, İ. Yilgör, Comparison of hydrogen bonding in polydimethylsiloxane and polyether based urethane and urea copolymers, Polymer (Guildf). 41 (2000) 849–857. https://doi.org/10.1016/S0032-3861(99)00245-1.

J. Yu, F. Lin, P. Lin, Y. Gao, M.L. Becker, Phenylalanine-Based Poly(ester urea): Synthesis, Characterization, and *in vitro* Degradation, Macromolecules. 47 (2014) 121–129. https://doi.org/10.1021/ma401752b.

X. Yuan, D. Sperger, E.J. Munson, Investigating Miscibility and Molecular Mobility of Nifedipine-PVP Amorphous Solid Dispersions Using Solid-State NMR Spectroscopy, Mol. Pharm. 11 (2014) 329–337. https://doi.org/10.1021/mp400498n.

S. Zhang, A.M. Bellinger, D.L. Glettig, R. Barman, Y.-A.L. Lee, J. Zhu, C. Cleveland, V.A. Montgomery, L. Gu, L.D. Nash, D.J. Maitland, R. Langer, G. Traverso, A pH-responsive supramolecular polymer gel as an enteric elastomer for use in gastric devices, Nat. Mater. 14 (2015) 1065–1071. https://doi.org/10.1038/nmat4355.

J.-J. Zhou, J.-G. Liu, S.-K. Yan, J.-Y. Dong, L. Li, C.-M. Chan, J.M. Schultz, Atomic

force microscopy study of the lamellar growth of isotactic polypropylene, Polymer (Guildf). 46 (2005) 4077–4087. https://doi.org/10.1016/J.POLYMER.2005.03.047.

L. Zhou, D. Liang, X. He, J. Li, H. Tan, J. Li, Q. Fu, Q. Gu, The degradation and biocompatibility of pH-sensitive biodegradable polyurethanes for intracellular multifunctional antitumor drug delivery, Biomaterials. 33 (2012) 2734–2745. https://doi.org/10.1016/J.BIOMATERIALS.2011.11.009.

W. Zielenkiewicz, B. Golankiewicz, G.L. Perlovich, M. Koźbiał, Aqueous Solubilities, Infinite Dilution Activity Coefficients and Octanol–Water Partition Coefficients of Tricyclic Analogs of Acyclovir, J. Solution Chem. 28 (1999) 731–745. https://doi.org/10.1023/A:1021720128725.

K.B.H. Zolnierek, M.R. Dimatteo, Physician communication and patient adherence to treatment: a meta-analysis., Med. Care. 47 (2009) 826–34. https://doi.org/10.1097/MLR.0b013e31819a5acc.